

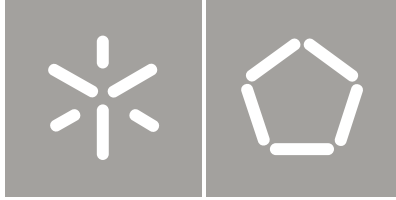


Universidade do Minho
Escola de Engenharia

Isabel Maria Dias Cabral

**Dynamic Light Filters:
Smart Materials Applied to Textile Design**

Isabel Maria Dias Cabral
**Dynamic Light Filters:
Smart Materials Applied to Textile Design**



Universidade do Minho

Escola de Engenharia

Isabel Maria Dias Cabral

**Dynamic Light Filters:
Smart Materials Applied to Textile Design**

Tese de Doutoramento
Engenharia Têxtil

Trabalho efectuado sob a orientação de
Professor Doutor António Pedro Souto
Professora Doutora Linda Worbin

DECLARAÇÃO

Nome: Isabel Maria Dias Cabral

Título da tese: Dynamic Light Filters: Smart Materials Applied to Textile Design

Orientador(es): Professor Doutor António Pedro Souto e Professora Doutora Linda Worbin

Ano de conclusão: 2017

Designação do Doutoramento: Engenharia Têxtil

É AUTORIZADA A REPRODUÇÃO PARCIAL DESTA TESE ,APENAS PARA EFEITOS DE INVESTIGAÇÃO, MEDIANTE DECLARAÇÃO ESCRITA DO INTERESSADO, QUE A TAL SE COMPROMETE;

Universidade do Minho, 31/10/2017

Assinatura: Isabel Maria Dias Cabral

STATEMENT OF INTEGRITY

I hereby declare having conducted my thesis with integrity. I confirm that I have not used plagiarism or any form of falsification of results in the process of the thesis elaboration.

I further declare that I have fully acknowledged the Code of Ethical Conduct of the University of Minho.

University of Minho, 31 / 10 / 2017

Full name: Isabel Maria Dias Cabral

Signature: Isabel Maria Dias Cabral

Acknowledgements

Many people have accompanied me and contributed to this PhD journey, all of whom I am grateful for.

I would like to thank my supervisor, Professor Pedro Souto for his guidance and friendship, sharing his wisdom and giving me continuous encouragement through this process. Thank you.

I also thank to my supervisor, Linda Worbin for her support and creativeness during this experience. Thanks for your time and inspiring discussions.

I would like to extend my thanks to other professors in the University of Minho, particularly to Professor Helder Carvalho and Professor Joana Cunha, for their support.

Thank you to my department colleagues and laboratory technicians with a special thanks to Joaquim Jorge Peixoto and Anabela Pereira for their camaraderie and commitment in providing a good and positive environment that helped me working through. To Cristiano Silva, for his collaboration developing the electronic and programing components of the research prototypes.

I wish to thank to my family and friends for their motivation, for being always present and giving me the strength to finish this chapter of my life. Special thanks to Lara Soares, Daniela Tomás, Sofia Sequeira, Catarina Miranda, and my dear brother Manuel Cabral.

To my parents, who have always encouraged me to follow my motivations and dreams. Thank you mom and dad.

To Mario for sharing, and for being who you are.

Thanks to the Foundation for Science and Technology (FCT), Portugal for the Ph.D. Grant SFRH/BD/87196/2012.

I also acknowledge Smart Textiles Design Lab for their support in the prototypes development.

Abstract

Smart textiles are able to interact with the environment and perform dynamic changes over time. Introducing new sensing and reactive qualities to conventional textiles' functions and expressions, smart textiles brings forth innovative potential for the design of responsive environments.

Variation of artificial light intensity and tone are commonly achieved by acting upon the light source. The ability to sense and react of smart textiles creates possibilities to change the incident light that passes through them – light transmittance – to design dynamic light scenarios and perform as *Dynamic Light Filters*.

This research studied colour change and shape memory textiles in interaction with light. The objectives were to develop integration processes of thermochromic pigments in textile substrates that change colour according to a predefined colour ratio, from similar to different and the inverse; develop a workflow setup to design and manufacture shape memory textiles in which dynamic behaviour achieves predefined geometric morphologies, changing shape with layer number variation; study resistive heating activation of thermo-responsive textiles with metal-based conductive materials and explore and discuss dynamic qualities of thermo-responsive textiles behaviour based on selected design variables that affect resistive heating and textile thermal expansion and also the dynamic relationship between colour, shape and light in the expressions of change.

The results attained have proposed systematic processes of paste recipe formulation of thermochromic and conventional pigments; outlined a process to develop shape memory textiles based on origami morphologies with one or two different morphologies, based on a bias mechanism; and demonstrated the influence of a set of variables in the dynamic qualities and expressions of change, designing thermo-responsive textile behaviour and creating dynamic and interactive lighting.

Resumo

Os têxteis inteligentes têm a capacidade de interagir com o meio envolvente e realizar mudanças dinâmicas ao longo do tempo. Introduzindo novas qualidades sensoriais e reativas às funções e expressões dos têxteis convencionais, os têxteis inteligentes surgem como um potencial inovador para o design de ambientes interativos.

A variação da intensidade e cor da luz artificial é normalmente obtida agindo sobre a fonte de luz. A capacidade de sentir e reagir dos têxteis inteligentes cria possibilidades para variar a luz incidente que passa por eles – transmitância de luz – para desenhar cenários de luz dinâmica agindo como *Filtros de luz dinâmica*.

Esta investigação estudou têxteis de mudança de cor e de memória de forma em interação com a luz. Os seus principais objetivos foram desenvolver processos de integração de pigmentos termocromáticos em substratos têxteis, que mudam de cor de acordo com uma relação de cores predefinida, de semelhante para distinto e o seu inverso; desenvolver uma metodologia processual para desenhar e produzir têxteis de memória de forma cujo comportamento dinâmico assume morfologias geométricas predefinidas, mudando de forma variação de número de camadas; Estudar o aquecimento resistivo de materiais condutores de base metálica para a ativação de têxteis de resposta térmica e explorar e discutir as qualidades dinâmicas do comportamento de resposta térmica com base num conjunto de variáveis que influenciam o aquecimento resistivo, a expansão térmica no têxtil e também a relação dinâmica entre a cor, forma e luz nas expressões de mudança.

Os resultados alcançados propuseram processos sistemáticos na formulação de receita de pastas de pigmentos termocromáticos e convencionais; Delinearam um processo para desenvolver têxteis de memória de forma com base em morfologia de origami com uma ou duas morfologias de mudança de forma, através de um mecanismo duplo; E demonstraram a influência do conjunto de variáveis nas qualidades dinâmicas e expressões de mudança, desenhando o comportamento dos têxteis de resposta térmica, criando iluminação dinâmica interativa.

Table of contents

Acknowledgements	iii
Abstract	v
Resumo	vi
Table of contents	vii
List of Abbreviations	xii
List of figures	xiii
List of tables	xvii
CHAPTER 1. INTRODUCTION.....	1
1.1 Motivation.....	2
1.2 Background to this thesis	3
1.3 Objectives	5
1.4 Structure of the thesis	6
1.5 References	7
CHAPTER 2. LITERATURE REVIEW.....	9
2.1 Introduction	10
2.2 Colour Change Materials.....	11
2.2.1 Thermochromism	12
2.2.2 Thermochromic leuco dyes	12
2.2.3 Thermochromic textiles.....	16
2.3 Shape Memory Materials.....	21
2.3.1 Shape Memory Alloys.....	21
2.3.2 Nickel Titanium Shape Memory Alloy.....	23
2.3.3 Shape Memory Textiles	25
2.4 Conductive Materials.....	29
2.4.1 Fabrication technologies of conductive textiles	30
2.4.2 Conductive textiles	32

2.5 Light.....	35
2.5.1 Qualitative lighting design.....	36
2.5.2 Lighting in design, arts and architecture	37
2.6 Summary.....	39
2.7 References	40
CHAPTER 3. MATERIALS AND METHODS	49
3.1 Introduction	50
3.2 Materials	50
3.2.1 Textile Materials.....	50
3.2.2 Pigments	51
3.2.3 Binders.....	51
3.2.4 Finishing agents.....	51
3.2.5 Dyes.....	51
3.2.7 Conductive threads	52
3.3 Equipment and Methods	53
3.3.1 Screen printing table.....	53
3.3.2 Dyeing machine.....	53
3.3.2 Coating table	53
3.3.4 Furnace	54
3.3.5 Looms	54
3.3.6 Lux meter	55
3.3.7 Spectrophotometer	55
3.3.9 Linitest	55
3.3.10 Accelerated Weathering Tester QUV (AWT)	56
3.3.11 Power supply.....	56
3.3.12 Infrared (IR) camera.....	56
3.3.13 Dynamometer.....	56
3.3.14 Viscometer	57
3.3.15 Thickness gauge.....	57
3.4 References	57
CHAPTER 4. THERMOCHROMIC TEXTILES	58
4.1 Colour	59
4.2 Introduction to the Experimental Work	65

4.3 Experimental 1 – Thermochromic Textiles and Light Transmittance	66
4.3.1 Materials and Methods.....	66
4.3.2 Results and Discussion	68
4.4 Experimental 2 – Colour ratio: from different colours to similar ones.....	72
4.4.1 Materials and Methods.....	73
4.4.2 Results and Discussion	74
4.5 Experimental 3 – Colour ratio: from similar colours to different ones.....	79
4.5.1 Materials and Methods.....	79
4.5.2 Results and Discussion	82
4.6 Experimental 4 – Rub, wash and light fastness.....	93
4.6.1 Materials and Methods.....	94
4.6.2 Results and Discussion	94
4.7 Conclusions.....	96
4.8 References	98
CHAPTER 5. SHAPE MEMORY TEXTILES	101
5.1 Shape.....	102
5.2 Introduction to the Experimental Work	106
5.3 Experimental 1: Textile Morphology and Light Transmittance	107
5.3.1 Materials and Methods.....	108
5.3.2 Results and Discussion	109
5.4 Experimental 2: Nitinol Shape Set	111
5.4.1 Materials and Methods.....	111
5.4.2 Results and Discussion	112
5.5 Experimental 3: Study Samples of Origami Base Folds.....	112
5.5.1 Materials and Methods.....	113
5.5.2 Results and Discussion	114
5.6 Experimental 4: SquarTwists Pattern Sample.....	116
5.6.1 Materials and Methods.....	116
5.6.2 Electrical Activation	118
5.6.3 Results and Discussion	121
5.7 Experimental 5: Finishing Processes.....	122
5.7.1 Materials and Methods.....	123
5.7.2 Results and Discussion	124

5.8 Experimental 6: Effect of finishing processes in shape change	126
5.8.1 Materials and Methods.....	126
5.8.2 Results and Discussion	127
5.9 Experimental 7: Two Shapes Behaviour	128
5.9.1 Materials and Methods.....	129
5.9.2 Results and Discussion	129
5.10 Experimental 8: Nitinol integration based on the crease axis	130
5.10.1 Materials and Methods.....	130
5.10.2 Results and Discussion	133
5.11 Experimental 9: Nitinol angles and Textile angles.....	134
5.11.1 Materials and Methods.....	134
5.11.2 Results and Discussion	135
5.12 Experimental 10: Shape change and samples scale.....	138
5.12.1 Materials and Methods.....	138
5.12.2 Results and Discussion	139
5.13 Conclusions.....	141
5.14 References	142
CHAPTER 6. ELECTROCONDUCTIVE TEXTILES.....	145
6.1 Conductive Materials Catalogue.....	146
6.2. Introduction to the Experimental Work	146
6.3 Experimental 1: Conductive Threads	147
6.3.1 Materials and Methods.....	147
6.3.2 Results and Discussion	149
6.4 Experimental 2: Conductive Pigments.....	154
6.4.1 Materials and Methods.....	155
6.4.2 Results and Discussion	156
6.5 Conductive material selection.....	157
6.6. Conclusions.....	158
6.7 References	160
CHAPTER 7. DESIGN RESEARCH: DYNAMIC LIGHT FILTERS.....	162
7.1 Introduction	163

7.2 Exploring textile dynamic behaviour	165
7.2.1 Colour Change.....	166
7.2.2 Shape Change	178
7.2.3 Discussion	184
7.3 Exploring textiles and light.....	186
7.3.1 Textile and light transmittance.....	187
7.3.2 Colour, shape and light.....	189
7.3.3 Discussion	196
7.4 Research prototype I: Narratives of Winter Daylight	196
7.4.1 Textile behaviour and light.....	199
7.4.2 Colour, shape and light responsive environments	204
7.5 Research prototype II: Dialogues	207
7.5.1 Textile behaviour and dynamic lighting	211
7.5.2 Colour, shape and light responsive environments	215
7.6 References	219
 CHAPTER 8. FINAL CONCLUSIONS AND FUTURE WORK	 220
 APPENDICES.....	 224
APPENDIX A	225
APPENDIX B	228
APPENDIX C	231
APPENDIX D	236

List of Abbreviations

A	Austenite
Af	Austenite finish
As	Austenite start
CO	Cotton
TC	Thermochromic
M	Martensite
Mf	Martensite finish
Ms	Martensite start
PES	Polyester
SMM	Shape Memory Materials
SMA	Shape Memory Alloys
SME	Shape Memory Effect

List of Figures

Figure 1. Colour change example of TC pigments combination with different activation temperatures (TCyellow and TCblue). 13

Figure 2. Colour change example of TC and conventional pigment combination..... 14

Figure 3. Example of TC pigment gradual colours change. 14

Figure 4. Example of gradual colour change with TC pigments combination. 15

Figure 5. Shape memory phase transitions. 22

Figure 6. CIE L*a*b* colour space. 64

Figure 7. Dyeing programs applied for disperse and reactive dyes (left and right, respectively). 67

Figure 8. Light transmittance variation with samples A, B, C, D and E. 68

Figure 9. Light transmittance variation with samples E, F and G. 69

Figure 10. Light transmittance variation with samples H, I and J. 71

Figure 11. Base framework of screen printed samples, below and above 27°C. 74

Figure 12. Framework of samples with different TC and conventional pigments' concentrations, below and above 27°C. 75

Figure 13. K, L, M and N samples, below and above 27°C. 76

Figure 14. K, O and P samples, below and above 27°C. 77

Figure 15. Light transmittance variation with samples K, O and P. 78

Figure 16. Sample: from different to similar colours ratio. 79

Figure 17. Samples with different concentrations of conventional pigments (1st row) and TC pigments (2nd row). 82

Figure 18. TC pattern samples and conventional pigment samples. 84

Figure 19. Samples Q, Q1 and Q2, respectively. 86

Figure 20. Spectral curves of samples Q, Q1 and Q2, below 27°C. 87

Figure 21. Colour of samples Q, Q1 and Q2 in light transmittance, below and above 27°C. 87

Figure 22. Light transmittance variation with samples Q, Q1 and Q2. 87

Figure 23. Sample: from similar to different colour ratio. 88

Figure 24. Samples R, R1.0, R2.0 and R3.0, below 27°C. 89

Figure 25. Samples R, R1.1, R2.1 and R3.1, below 27°C. 91

Figure 26. Samples R, R1, R2 and R3, below 27°C. 91

Figure 27. Spectral curves of samples R, R1, R2 and R3, below 27°C. 92

Figure 28. Study prototype section, below and above 27°C. 93

Figure 29. Study prototype section, under two different artificial light sources. 93

Figure 30. Klein transformations (Nefs, 2008). 102

Figure 31. Gestalt laws: similarity, proximity, good continuation, closure, common fate and synchrony. 103

Figure 32. Waterbomb and Squaretwist crease pattern (left and right, respectively). 108

Figure 33. Pile-up of textiles from one to six layers (left to right, respectively). 109

Figure 34. Study model waterbomb fold based: folded (left) and unfolded (centre and right). 110

Figure 35. Study model squaretwist fold based: folded (left) and unfolded (centre and right). 110

Figure 36. Nitinol die setup. 111

Figure 37. Angle values attained throughout 5 cycle tests for each Nitinol wire, with heat treatment during 15 minutes. Upper row to lower row: 0,2; 0,3 and 0,5mm diameter. 112

Figure 38. Waterbomb model open and close (left and centre); SMA shapes (right). 113

Figure 39. Squaretwist model open and close (left and centre); SMA shapes (right).....	113
Figure 40. Waterbomb dies (left); Squaretwist dies (right).....	114
Figure 41. Waterbomb samples during thermal activation (1st row 0,2 mm wire sample, 2nd 0,3 mm and 3rd 0,5 mm).....	115
Figure 42. Squaretwist samples during thermal activation (1st row 0,2 mm wire sample; 2nd 0,3 mm and 3rd 0,5 mm).....	115
Figure 43. Layer number variation per areas: squaretwist (left), vertical tabs fold up (centre) and colour subtitles (right).	117
Figure 44. Sample crease pattern.....	117
Figure 45. Nitinol wires' shape (left); Nitinol dies' shape (right).....	118
Figure 46. Thermal images of Nitinol wire number 3 during voltage variation.....	119
Figure 47. Circuit diagram with "N" representing the Nitinol wires.....	120
Figure 48. Arduino code.....	120
Figure 49. Prototype before activation (left); activated (middle) and paper model (right).	121
Figure 50. Thermal images of Nitinol number 9 and 10, being activated.	122
Figure 51. Schematic of the samples' geometry.....	123
Figure 52. Samples before activation and activated.....	127
Figure 53. Sample before and after treatment during sequential activation.	128
Figure 54. Diagram of Nitinol alloys configuration	129
Figure 55. Sample deformed (left); 1st Actuator group activated (centre) and 2nd Actuator group activated (right).	129
Figure 56. Squaretwist crease pattern (left) and model folded (right).	131
Figure 57. Sample S6 A crease pattern (left) and Nitinol wire geometries (right).	131
Figure 58. Sample S6 B crease pattern (left) and Nitinol geometries (right).	132
Figure 59. Sample S6 C crease pattern (left) and Nitinol geometries (right).	132
Figure 60. Samples behaviour comparison: S6A, S6B and S6C.	133
Figure 61. Crease pattern samples S6 D, F and G (left), S6 E (right).	135
Figure 62. Study samples with different memorized angles and alloys' spacing.....	136
Figure 63. Samples behaviour comparison: S6A, D and E.....	137
Figure 64. Samples behaviour comparison: S6 D, F e G.	137
Figure 65. Crease pattern of S12 sample (left) and S18 sample (right).....	139
Figure 66. Samples scale S6G, S12 and S18.	139
Figure 67. Samples behaviour comparison: S6G, S12 and S18.....	140
Figure 68. S18 sample behaviour in horizontal and vertical positioning.	140
Figure 69. Schematic of the conductive threads integration in sample A woven structure.....	147
Figure 70. Schematic of the conductive threads integration in sample B woven structure.....	148
Figure 71. Sample A: front view from CT5 to CT11 (left); perspective top side (right, top) and perspective back side (right, bottom).....	149
Figure 72. Results of test conducted with conductive thread number 1 (CT1).	151
Figure 73. Results attained with CT5, CT4 and CT13, in the 3 rd stage of power supply defined (45'').....	151
Figure 74. Results attained with CT15, 26 and 27, in the 3 rd stage of power supply defined (45'').....	152
Figure 75. CT16 results in the 3 rd stage of power supply defined (45'').....	153
Figure 76. Results attained with CT9 and CT20, in the 3 rd stage of power supply defined (45'').....	153
Figure 77. Sample B results with CT9, 13, 15 and 26 in the 2 nd stage of power supply defined (1').....	154

Figure 78. Electrical resistance and IR images of samples C and D, with 1,5 V power supply.....	156
Figure 79. Magnifying glass photo and IR image of C1 and D1, after being folded.	157
Figure 80. Conductive pigment sample front and back view before power supply (top left and top right, respectively) and during power supply (bottom).	157
Figure 81. Conductive threads list.	161
Figure 82. Test A1 setup.....	167
Figure 83. Test A1 results.	167
Figure 84. Test A2 setup.....	168
Figure 85. Test A2 results.	169
Figure 86. Test B setup.	171
Figure 87. Test B results.	171
Figure 88. Test C setup.	172
Figure 89. Test C results.	173
Figure 90. Test D setup.	175
Figure 91. Test D results.	175
Figure 92. Test E setup.	176
Figure 93. Test E results.	177
Figure 94. Test F setup.	178
Figure 95. Test F results.	179
Figure 96. Test G setup.....	180
Figure 97. Test G results.....	181
Figure 98. Test H setup.	181
Figure 99. Test H results.....	182
Figure 100. Test I setup.	183
Figure 101. Test I results.	184
Figure 102. Textile stiffness variation in textile origami.	187
Figure 103. Textile origami with and without creases.	188
Figure 104. Light transmittance patterns.	189
Figure 105. Squar twist textile above three light structures: LEDs module (left), LEDs stripe (centre) and woven POFs (right)..	189
Figure 106. Sample Y without and with light transmittance.	190
Figure 107. Colour change (1 st to 3 rd image) and colour return (3 rd to 5 th image) in light transmittance.	191
Figure 108. Frames of colour change sequences.	193
Figure 109. Frames of shape change sequences.	194
Figure 110. Exploring dynamic light and movement through manual shape change.....	195
Figure 111. Photos record from 6 a.m. to 6 p.m.....	196
Figure 112. Conceptual bar of luminosities and colours.	197
Figure 113. Prototype layout folded (left), pleat fold crease pattern and pleat unit folded (right).....	198
Figure 114. Fold down to fold up in colourized state (1st to 2nd image) and colour change in fold up state (2nd to 3rd image).	200
Figure 115. Prototype fold down and fold up activation.	200

Figure 116. Prototype without and with colour change activation in fold up state (left and right, respectively).	202
Figure 117. Colour samples below and above 27°C, without and with light transmittance.....	202
Figure 118. Photos and IR images during colour change.....	203
Figure 119. Interaction diagram.	204
Figure 120. Activation sequence setup.	205
Figure 121. Prototype geometric layout.	207
Figure 122. Prototype folded pattern.	208
Figure 123. M3 folded pattern (left) and crease pattern (right).	209
Figure 124. Colour studies with folded samples in light transmittance, below and above 27°C (left and right, respectively).....	209
Figure 125. Colour and pattern studies.....	210
Figure 126. <i>Dialogues</i> prototype.....	211
Figure 127. Prototype section in colorized state (left) and changing colour (right).	212
Figure 128. Colour change activation with areas with complete decolourization.	212
Figure 129. Colour change linear patterns.	213
Figure 130. Shape change in a dark colour squaretwist.	214
Figure 131. Colour change during shape change activation.....	214
Figure 132. Shape change	214
Figure 133. Prototype and light reflection at left, front and right perspectives, respectively.	216
Figure 134. Light reflection of the colour change pattern.....	216
Figure 135. Gradual colour and pattern changes.	217
Figure 136. Dynamic colour and pattern expressions.	217

List of Tables

Table 1. Conductive threads' list.....	52
Table 2. Description of samples A to J.....	67
Table 3. Mean values of light intensities with samples A to G.....	70
Table 4. Colour coordinates and CIELAB differences of samples A to G, above 27°C.....	70
Table 5. Mean values of light intensities with samples H, I and J.....	71
Table 6. Samples' colour coordinates below and above 27°C and CIELAB differences between heated samples and respective conventional colourant substrate.....	72
Table 7. Colour coordinates and CIELAB differences of K, L, M and N samples, above 27°C.....	76
Table 8. Colour coordinates and CIELAB differences of samples K, O and P, above 27°C.....	77
Table 9. Mean values of light intensities with samples K, O and P.....	78
Table 10. Samples' description and respective paste recipes.....	83
Table 11. Samples' colour coordinates and CIELAB differences.....	84
Table 12. Paste recipes of samples Q, Q1 and Q2.....	86
Table 13. Colour coordinates of samples Q, Q1 and Q2, below 27°C.....	86
Table 14. Mean values of light intensities with samples Q, Q1 and Q2.....	88
Table 15. Description of R, R1, R2 and R3 samples and respective paste recipes.....	89
Table 16. Samples R, R1, R2 and R3 colour coordinates and CIELAB differences, below 27°C.....	90
Table 17. Samples' paste recipes adjustments.....	90
Table 18. Samples' colour coordinates and CIELAB differences, below 27°C.....	91
Table 19. R, R1, R2 and R3 colour coordinates and CIELAB differences, below 27°C.....	91
Table 20. Staining grade in dry and wet rub fastness tests.....	95
Table 21. Staining grade in wash fastness tests.....	95
Table 22. CIELAB colour differences in light fastness tests.....	96
Table 23. Mean values of light intensities.....	109
Table 24. Mean values of light intensities.....	110
Table 25. Mean values of electrical current and maximum temperatures attained.....	119
Table 26. Mean values of light intensity.....	122
Table 27. Description of samples' materials and finishing processes.....	124
Table 28. Breaking strength and elongation values.....	125
Table 29. Samples thickness and weight.....	125
Table 30. List of the conductive threads (CT) integrated in the woven substrate.....	148
Table 31. Description of conductive pigment samples C and F.....	155

INTRODUCTION

CHAPTER 1

CHAPTER 1. INTRODUCTION

1.1 Motivation

Textiles have been a prominent interface with our environment and a prime example of innovation-driven developments. Among diverse possibilities, textiles have been applied for sun shading and to transform wind into motion energy. They provide enhanced qualities for high-performance applications, such as lighter and stronger architectural structures, protective professional clothing and biocompatible implants. They are at the basis of technological advances, namely materials processing and computing-based technologies and are able to sense and dynamically react to external stimuli (McQuaid, 2005; Quinn, 2010; Keetley, 2016).

Emerging sensing and reacting capabilities are imparted to textiles by means of smart materials and enabling conductive and electronic technologies (Koncar, 2016). Introducing new qualities to conventional textiles functions and expressions, smart textiles have been opening up vast potential for the creation of dynamic and interactive applications (Kirstein, 2013; Pailes-Friedman, 2016).

Through the perspective of seamless integration of technology into our environment, smart textiles are able to involve physical and immaterial dimensions, promoting added functionality and interaction between individuals and their surroundings (Bonnemaison and Macy, 2007; Schneegass and Amft, 2017). In interior spaces, variation of artificial light intensity and tone are commonly achieved by acting upon the light source. The emergent sensing and reacting behaviour of smart textiles present the potential to transform the incident light that passes through them – light transmittance (Yot, 2011) – to design dynamic lighting scenarios and perform as *Dynamic Light Filters*.

The interplay of textiles and light is designed through the textile properties and dynamic qualities. In this research, interaction of textiles and light transmittance is explored through colour and shape changing behaviour. Thermochromic (TC) leuco dyes are a class of colour change materials that through thermal stimulus change their visual characteristics reversibly (Addington and Schodek, 2005). As dark colours absorb a greater intensity of the visible light spectrum than lighter colours (Descottes and Ramos, 2011), TC textiles affect the light that passes through them, when they are below or above their activation temperature. Furthermore, different amounts of textile layers also interfere in light transmittance, depending on the light absorbed. With shape memory materials (SMMs), defined by their ability to change from a

temporary to a memorized shape (Otsuka and Wayman, 1998), it is possible to develop textiles that perform morphological variations with variable layer number.

This research proposes to study integration processes of colour change and shape memory materials in textile substrates to vary the textiles' optical characteristics and change light transmittance. Thermal variation that activates the textile changes aimed of being developed through resistive heating of conductive materials, which are also integrated in the substrate. Through the *Dynamic Light Filters* concept, this research proposes to explore and discuss dynamic qualities of textile colour and shape and their interaction with light.

1.2 Background to this thesis

Driven by scientific and technological developments, smart materials' ability to sense and react to an external stimulus have been gaining increased interest for textile research and applications, namely in biomedical, military, fashion and communication fields. Moreover, textiles can also combine electronic and computation capabilities, introducing adaptive qualities to the textiles (Mattila, 2006; Langenhove, 2015).

Design and development of smart textiles encompasses competences in diverse domains and presents new challenges. They require technical and creative understanding of the materials' properties, behaviour and process possibilities as a material system disassociated to their active qualities. In parallel, smart textiles also demand a rethinking of conventional design variables and methodologies, given the novelty that dynamic and interactive dimensions introduce (Worbin, 2010; Vallgård, 2014; Mossé, 2016).

TC leuco dyes can perform reversible colour change, fading away above their activation temperature and returning to the predefined colour below it. Able to be mixed with TC pigments with the same or different activation temperatures and also with conventional pigments, instead of a gradual transition to colourless, the heat variation achieves different possibilities in the colour change performance. Due to the lack of affinity and water insolubility, TC pigments are combined with appropriate binders and commonly applied to textiles through screen printing processes (Christie, 2013; Chowdhury et al., 2014). To combine the TC pigments and conventional pigments in the paste, empirical processes are conducted, being a time-consuming and skilled process with particular limitations when a colour or colour palette is intended.

Through diverse conceptual and technical perspectives, TC projects and research examples include experiments on colour change effects, heating methods, relationships between the printed pattern, the pigments combined and the heating elements and combination with other colour change materials.

Thermo-responsive shape memory alloys (SMAs) are metal compounds capable of converting thermal energy into mechanical energy, commonly generating motion and force (Rao et al., 2015). To display this effect, the alloys require an annealing process to memorize the shape they assume when exposed to their activation temperature. The heat treatment required to shape set the alloys has to be conducted at temperatures significantly higher than those supported by textile fibres. In this sense, they must be processed prior to their integration in the textile substrate (Stylios, 2006; Laschuk and Souto, 2008; Ugur, 2013).

Comprising various processes such as spun, weaving and knitting, as well as diverse applications, research in this area highlights important considerations to develop shape memory textiles, including the low strain properties of the alloys, the importance of the processing parameters for the SMAs shape transfer to the host structure as well as the limitations found when memorizing two-way behaviour in the alloy (Vili, 2007; Dyer, 2010; Cianchetti, 2013). The shape change within the SMA projects studied fulfils changes in the textile texture, volume, rolling up and forward and backward movement.

Defined by the ability to conduct electrical current, conductive materials are a key topic in smart textiles field, as they enable the transfer of energy or data and impart textiles with electronic functionalities (Storey, 2009; Eichhoff et al., 2013). Electrical conductivity can be conferred to textiles at fibre or filament level, threads, substrates and applied finishings. Conductive materials development have been providing a wide range of ready made metal-based materials with increasingly textile-like mechanical and tactile properties (Kirstein, 2013; Koncar, 2016).

Working with thermo-responsive textiles, conductive materials enable the electrical activation of colour and shape behaviour, according to their electrical and expressive properties as well as the thermal conductivity of the textile structure. In this research the integration of conductive materials in textiles with the objective to produce thermal variation of the TC pigments. SMAs are conductive materials and shape change activation aimed to be performed through resistive heating properties.

In addition, the use of conductive materials encompasses the development of joining processes to enable the connection between the materials and also with other components such as power supply. Permanent or

reversible connections can be conducted by different processes namely soldering and crimping or the use of pinheads and metal eyelets (Locher, 2013; Mecnika et al., 2015).

Smart textiles design comprises of a synergetic relationship of the textiles tangible and immaterial aspects, in respect to the potential qualities of the dynamic and interactive behaviour. Considering time and movement as critical variables that smart textiles introduce, they also entail new perspectives and alternative methods to understand how to work with temporal forms in textiles (Redström, 2010; Mossé, 2016). With thermo-responsive textiles, heat is a main dynamic variable to explore design possibilities of textile colour and shape behaviour and in this research context, the creation of dynamic lighting.

1.3 Objectives

This research focuses on integration processes of smart materials in textile substrates and the design potential of smart textiles behaviour to transform incident light that passes through them.

The research objectives are:

- The study and development of systematic processes of paste recipe formulation with TC and conventional pigments to screen-print textiles with defined colour change ratios from similar to different with temperature increase and the inverse;
- The study and development of a workflow setup to design and manufacture shape memory woven textiles in which dynamic behaviour achieves predefined geometric morphologies;
- The study of integration processes of metal-based conductive materials in woven substrates and the analysis of their electrical and expressive qualities for resistive heating activation of thermo-responsive textiles.
- The study of design possibilities of light transmittance variation through textile chromic behaviour with defined colour ratios and shape change behaviour with variable layer number;
- The exploring and discussion of dynamic qualities of thermo-responsive textiles behaviour based on selected design variables that affect resistive heating and textile thermal expansion and also the dynamic relationship between colour, shape and light in the expressions of change.

1.4 Structure of the thesis

This chapter introduced the subject of smart materials and *Dynamic Light Filters* concept, presenting the research motivation, background and objectives.

Chapter 2 provides a review of the literature relevant to this research. The first section presents an introduction of the research field and is followed by three sections divided into colour change materials, shape memory materials and conductive materials subjects. Each section reviews the materials' properties and behaviour, developing technologies for their integration in textile substrates and relevant applications, with particular focus in textile design. The fifth section discusses light and qualitative lighting concepts and presents an overview of lighting in design, arts and architecture, giving insight into textiles interaction with light.

Chapter 3 describes the materials, equipment and methods applied during the experimental work conducted.

Chapters 4, 5 and 6 discuss the materials research developed with TC, SMA and conductive materials.

Chapter 4 introduces discussion on fundamental aspects of colour, colour theory and colourimetry; presents the preliminary analysis on textile chromic behaviour and light transmittance variation; and describes the research and development of systematic processes to create TC textiles with defined colour ratios. In addition, the study of rub, wash and light fastness properties of the TC and conventional pigments used is presented.

Chapter 5 introduces base concepts associated with shape, shape-changing interfaces and origami structures; presents the preliminary analysis of light transmittance variation through textile layers number; and describes the research conducted on shape memory textiles according to predefined geometric morphologies. The experimental work presented comprises of Nitinol annealing processes, their integration in woven substrates to develop shape memory textiles with one and two shapes behaviour, electrical activation of shape change and finishing processes. An analysis of the shape change behaviour of samples developed during the processes is also presented.

Chapter 6 describes the experimental studies developed with conductive threads and pigments, including integration of the materials in textile substrates and their properties for resistive heating of TC textiles. In

this chapter, data documentation developed to communicate the technical and expressive findings is also discussed.

Chapter 7 presents the practice-based design research developed to explore dynamic qualities of colour and shape thermo-responsive textiles and their interaction with light. The research program presented comprises of two main experimental studies on textile behaviour and dynamic light, followed by the development and discussion of two research prototypes that proposed to explore expressive possibilities of colour, shape and light performances through different intensity levels of change.

Chapter 8 presents the final conclusions of the research and discusses future work.

1.5 References

- ADDINGTON, M. & SCHODEK, D. 2005. *Smart materials and new technologies*, Amsterdam, Architectural Press.
- BONNEMAISON, S. & MACY, C. 2007. Introduction. *In: BONNEMAISON, S. & MACY, C. (eds.) Responsive textile environments*. Halifax, N.S.: TUNS Press.
- CHOWDHURY, M. A., JOSHI, M. & BUTOLA, B. S. 2014. Photochromic and Thermochromic Colorants in Textile Applications. *Journal of Engineered Fabrics & Fibers*, 9(1), 107-123.
- CHRISTIE, R. M. 2013. Chromic materials for technical textile applications. *In: L., G. M. (ed.) Advances in the dyeing and finishing of technical textiles*. Oxford: Woodhead Publishing.
- CIANCHETTI, M. 2013. Fundamentals on the Use of Shape Memory Alloys in Soft Robotics. *Interdisciplinary Mechatronics*. John Wiley & Sons, Inc., 227-254.
- DESCOTTES, H. & RAMOS, C. E. 2011. *Architectural lighting: designing with light and space*, New York, Princeton Architectural Press.
- DYER, P. E. 2010. *Dynamic control of active textiles: the integration of nickel-titanium shape memory alloys and the manipulation of woven structures*. PhD Thesis, University of Brighton.
- EICHHOFF, J., HEHL, A., JOCKENHOEVEL, S. & GRIES, T. 2013. Textile fabrication technologies for embedding electronic functions into fibres, yarns and fabrics. *In: KIRSTEIN, T. (ed.) Multidisciplinary know-how for smart textiles developers*. Oxford: Woodhead Publishing.
- KEETLEY, S. 2016. *Designing with smart textiles*, London, Bloomsbury.
- KIRSTEIN, T. 2013. The future of smart-textiles development: new enabling technologies, commercialization and market trends. *In: KIRSTEIN, T. (ed.) Multidisciplinary know-how for smart textiles developers*. Oxford: Woodhead Publishing.
- KONCAR, V. 2016. Introduction to smart textiles and their applications. *In: KONCAR, V. (ed.) Smart textiles and their applications*. Amsterdam: Woodhead Publishing.
- LANGENHOVE, L. V. 2015. Smart Textiles: Past, Present, and Future. *In: TAO, X. (ed.) Handbook of Smart Textiles*. Singapore: Springer.
- LASCHUK, T. & SOUTO, A. P. Incorporation of SMA technologies in fashion underwear apparel. Ambience 08, 2-3 June 2008 2008. 215-218.
- LOCHER, I. 2013. Joining technologies for smart textiles. *In: KIRSTEIN, T. (ed.) Multidisciplinary know-how for smart textiles developers*. Oxford: Woodhead Publishing.

- MATTILA, H. R. 2006. Intelligent textiles and clothing – a part of our intelligent ambience. *In: MATTILA, H. (ed.) Intelligent textiles and clothing*. Cambridge: Woodhead Publishing.
- MCQUAID, M. 2005. *Extreme textiles: designing for high performance*, New York, Smithsonian Cooper-Hewitt, National Design Museum.
- MECNIKA, V., SCHEULEN, K., ANDERSON, C., HÖRR, M. & BRECKENFELDER, C. 2015. Joining technologies for electronic textiles. *In: DIAS, T. (ed.) Electronic Textiles*. Cambridge: Elsevier Science & Technology.
- MOSSÉ, A. 2016. Self-actuated textiles, interconnectivity, and the design of the home as a more sustainable timescape. *In: SCHNEIDERMAN, D. & WINTON, A. (eds.) Textile technology and design: from interior space to outer space*. New York: Bloomsbury Academic.
- OTSUKA, K. & WAYMAN, C. M. 1998. *Shape memory materials*, Cambridge, Cambridge University Press.
- PAILES-FRIEDMAN, R. 2016. *Smart textiles for designers: inventing the future of fabrics*, London, Laurence King Publishing.
- QUINN, B. 2010. *Textile futures: fashion, design and technology*, Oxford, Berg.
- RAO, A., SRINIVASA, A. R. & REDDY, J. N. 2015. *Design of Shape Memory Alloy (SMA) Actuators*, Cham, Springer International Publishing.
- REDSTRÖM, J. 2010. On technology as material in design. *In: REDSTRÖM, M., REDSTRÖM, J. & MAZÉ, R. (eds.) IT+Textiles*. Borås: The Interactive Institute and the Swedish School of Textiles.
- SCHNEEGASS, S. & AMFT, O. 2017. Introduction to Smart Textiles. *In: SCHNEEGASS, S. & AMFT, O. (eds.) Smart Textiles: Fundamentals, Design, and Interaction*. Cham: Springer International Publishing, 1-15.
- STOREY, N. 2009. *Electronics: a systems approach*, Harlow, Pearson Education Limited.
- STYLIOS, G. K. 2006. Engineering textile and clothing aesthetics using shape changing materials. *In: MATTILA, H. R. (ed.) Intelligent textiles and clothing*. Cambridge: Woodhead, 165-190.
- UGUR, S. 2013. *Wearing Embodied Emotions: A Practice Based Design Research on Wearable Technology*, Springer Publishing Company, Incorporated.
- VALLGÅRDA, A. 2014. Giving form to computational things: developing a practice of interaction design *Personal and Ubiquitous Computing*, 18(3), 577-592.
- VILI, Y. Y. F. C. 2007. Investigating Smart Textiles Based on Shape Memory Materials. *Textile Research Journal*, 77, 290-300.
- WORBIN, L. 2010. *Designing dynamic textile patterns*. Doctoral Thesis, University of Borås.
- YOT, R. 2011. *Light for visual artists: understanding & using light in art & design*, London, Laurence King.

LITERATURE REVIEW

CHAPTER 2

CHAPTER 2. LITERATURE REVIEW

This chapter provides a literature review of colour change materials, shape memory materials and conductive materials. For each group, the review presents an introduction of the materials' properties and behaviour, developing technologies for their integration in textile substrates and relevant applications, with particular focus in textile design. Moreover light phenomenon is discussed, giving insight to qualitative lighting concepts and textiles interaction with light.

2.1 Introduction

Emergent materials and technologies originated by scientific and technological advances have been providing new means to extend textiles' traditional properties and functions (Quinn, 2010; Kirstein, 2013; Pailles-Friedman, 2016). Smart materials exhibit the ability to sense and react reversibly to an external stimulus, such as thermal, mechanical or electrical and when integrated in textile substrates, embed them with intrinsic dynamic and interactive behaviour. For example, thermochromic textiles change colour upon temperature variation and, through the same stimulus, shape memory textiles can change shape (Tao, 2001; Kettley, 2016; Koncar, 2016).

Smart textiles' sensor and actuator behaviour can also combine data processing, communication and power supply functions, enabled by increased progress of textile-based conductive materials and electronics miniaturization that impart textiles with electronic and computation capabilities. This innovative character is commonly classified as very smart, describing the textile ability of sensing, reacting and adapting (Mattila, 2006; Langenhove, 2015; Schneegass and Amft, 2017).

Characterized by interdisciplinary convergence, research and development of smart textiles combine knowledge and competence from materials science, electronics, textile engineering, textile design, interaction design, etc. Towards performance feasibility of textiles, collaborative research seeks to embed and explore functional and interactive dimensions in an unobtrusive way, so that textile intrinsic properties or designed expressions are not significantly compromised, for example stretching, recovery, draping, shearing or handling (Zysset et al., 2013; Stoppa and Chiolerio, 2014; Kumar and Vigneswaran, 2016).

The perspective of seamless technology integration is transversal to diverse fields. The 'ubiquitous computing' concept, introduced by Marc Weiser in the late 1980's, envisioned that "The most profound technologies are those that disappear. They weave themselves into the fabric of everyday life until they are indistinguishable from it" (Weiser, 1991). Whereas technology is embedded into our environment (Ambient

Intelligence), occurring through continuous interconnections (Pervasive Computing) or regarding to clothing and accessories (Wearable Electronics), the main aims rely on built-in active performances able to enhance welfare, intellect, creativity and communication, also stimulating sensory and emotional fulfilment (Baurley, 2005; Ko et al., 2005; Aarts and Wichert, 2009; Schneegass and Amft, 2017).

Textiles as a pervasive and soft interface for new technologies and interactive performances, challenge our concept of textiles, commonly associated with passive functionality, as well as the way we may use or interact with them (Frumkin and Weiss, 2012; Pailles-Friedman, 2016). In parallel, smart textiles also add new parameters to design research and practice. Design reactive and adaptive qualities in textiles, requires technical and creative understanding of the materials behaviour, process possibilities in respect to smart textiles' physical materialization disassociated to their behaviour framework, as well as a rethinking of conventional design variables and methodologies given the novelty that dynamic and interactive dimensions introduce (Worbin, 2010; Vallgård, 2014; Mossé, 2016).

The following sections present an overview of materials' properties, integration processes, innovative design potential and challenges, in respect to the topics of particular relevance in this research – colour change materials, shape memory alloys and conductive materials. Furthermore, an introduction of light principles and interaction of textiles and light is presented.

2.2 Colour Change Materials

Colour change materials are defined by the ability of changing colour in response to an external stimulus (Addington and Schodek, 2005). This behaviour, also referred as chromic or chromogenic, is usually reversible and involves a variation of the substances microstructure or electronic state, affecting their optical properties – absorptance, reflectance or scattering – thus, being observed as colour change (Talvenma, 2006; Bamfield and Hutchings, 2010; Salaün, 2016).

The chromic behaviour is classified according to the stimulus that induces the change. The most extensively researched materials are: thermochromics, photochromics, ionochromics, electrochromics and solvatochromics, which respond to heat, light, ions, electric current and solvents, respectively. There are also chromic materials sensitive to imposed stress and/or deformations (mechanochromics), chemical changes (chemochromics), variations in magnetic field (magnetochemochromics), presence of pathogens (biochromics), among others (Bamfield and Hutchings, 2010; Christie, 2013; Ferrara and Bengisu, 2014).

Colour change materials present the opportunity to explore sensing and reacting qualities in design-driven innovations. Relevant applications have been found in fields such as ophthalmics, thermometry, electronics and biomedicine (Christie, 2013). In textiles, this phenomenon is more recent, but increasing research and outcomes reflect the interest and potentialities of chromatic dynamic behaviour.

2.2.1 Thermochromism

Thermochromism refers to the process by which the colour change effect is induced through a thermal stimulus (Day, 1963; Schwartz, 2002). Diverse temperature-dependent materials have been documented, however the suitability for textile application relies on encapsulated organic substances (Bamfield and Hutchings, 2010; Durasevic, 2016). TC microencapsulation processes date from 1970s and involve the coating of small particles or droplets of the chromic compounds to create a capsule or shell, which provides a level of protection from environmental influences (Talvenma, 2006; Chowdhury et al., 2013; Salaün, 2016).

The main types of TC systems used in textiles are the leuco dyes and liquid crystals (Aitken et al., 1996; Ferrara and Bengisu, 2014). TC Leuco dye systems exhibit a reversible colour-change from coloured to colourless with temperature increase, a behaviour that is based on chemical changes in the molecular rearrangement of the particles (Bamfield and Hutchings, 2010; Salaün, 2016). TC Liquid crystals show different colours at a temperature range, which result from a change in their orientational structure, causing a selective reflection of specific wavelengths of light. In this case a dark background is required, in order to absorb the incident light and the reflected colours be fully observed (Talvenma, 2006; Christie, 2013).

Taking into consideration the objective to study light transmittance variation through colour change, TC leuco dyes present the possibility to perform greater differences between darker and lighter colours than liquid crystals, which require a permanent dark background for the chromic effect be perceived. Thus, leuco dyes system was selected to be address in this research.

2.2.2 Thermochromic leuco dyes

A colour former, a colour developer and a co-solvent compose the TC leuco dyes and the entire/complete system is contained at each microcapsule. Colour former leuco dyes are electron donating and their reaction with the colour developer (electron-accepting) determines the colourization of the compound, which occurs at a temperature below the melting point of the co-solvent, thus being in solid state. When the co-solvent melts at a higher temperature, it causes a dissociation of the colour former and colour developer,

resulting in the microcapsule decolourization state (Seeboth and Löttsch, 2008; Bamfield and Hutchings, 2010).

The described formulation allows the selection of the TC pigment colour at the lower temperature, across a range of colours and the predefinition of the pigments' activation temperature according to the co-solvent melting point, usually between -15 and 65°C (Seeboth and Löttsch, 2013). Although TC systems can be formulated with custom-made characteristics, they are commercial available in dispersion (also called slurry) or powder forms with standard colours such as orange, red, magenta, blue and black. Activation temperature values vary according to the pigments' brand, being the most common classes approximately 7, 15, 27, 31, 41 and 47°C.

Each TC leuco dye is confined to a variation from a colour to colourless state at a defined activation temperature, although, it is possible to expand the colours palette and the chromic effect, by mixing TC pigments with the same or different activation temperatures and/or by combining TC with conventional pigments, according to the defined binder type.

Mixtures of TC systems with different activation temperatures, present more than two colour stages with temperature variation. For example if a TC yellow is combined with a TC blue, which presents a higher activation temperature, the colour observed in the cool state of both TC systems is the result of the colours addition, thus green (also depending on the pigments concentration combined). When the colour of the TC pigment with the lowest activation temperature fades (TC yellow), it is possible to observe the pigment colour which co-solvent is in solid state – blue. Above the temperature that both pigments are colourless, the substrate colour is perceived. Figure 1 depicts the example described for temperature increase. The inverse colour change process is applied for temperature decrease.

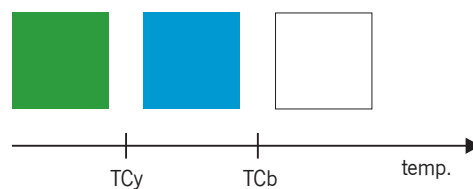


Figure 1. Colour change example of TC pigments combination with different activation temperatures (TCyellow and TCblue).

The combination of TC with conventional pigments attains a change from one colour to another. If a TC pigment blue is combined with a conventional pigment yellow, below the activation temperature of the TC pigment handled, the colour observed is the addition of the TC and conventional pigment colours – green. Above it, the TC pigment colour fades away and the conventional pigment colour is perceived – yellow, as illustrated in Figure 2.

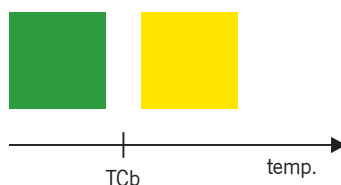


Figure 2. Colour change example of TC and conventional pigment combination.

Figure 1 and Figure 2 depict the colour change effect in independent states, to describe the base behaviour of TC colours and pigments combination with temperature variation. However, these materials perform a gradual behaviour of colour change. When TC leuco dyes are exposed to their activation temperature there is not an abrupt transition, rather, they transit through colour nuances in a temperature interval, as illustrated in Figure 3 (Nilsson et al., 2011).

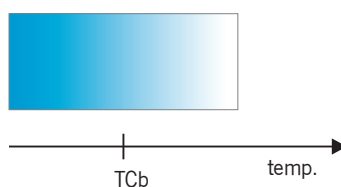


Figure 3. Example of TC pigment gradual colours change.

Studies on TC leuco dyes colourimetric properties have been carried out focusing on the gradual colour change as a function of temperature. Heating systems with controlled temperature were used, such as a hot stage or a full cover water block, combined with a spectrophotometer for a quantitative evaluation of colour at determined temperatures during heating and cooling. Results highlight that with temperature increase, colour starts to change slightly before the labelled activation temperature of the pigments handled and finishes at higher temperatures, describing the gradual behaviour in a temperature interval with small differences among pigments' colours and brands (Kulčar et al., 2010; Ibrahim, 2012).

When TC pigments with the same activation temperature are combined, the slight differences in the pigments' activation temperature can be observed by the appearance of new colour shades in the main chromic effect (Christie et al., 2007; Nilsson et al., 2011). For example, a mixture of TC blue and TC yellow with the same labelled temperature of activation, would be expected to perform a gradual change between green and colourless on heating. However, if the TC blue presents a slightly higher activation temperature than TC yellow, a blue shade can be observed between the predominant green nuance and the colourless state of both pigments, as depicted in Figure 4 left. If the TC yellow has the slightly higher activation temperature, the same occurs with the yellow nuance, Figure 4 right.



Figure 4. Example of gradual colour change with TC pigments combination.

This chromic behaviour reveals the possibility to design complex colour changes, where each TC pigment colour added to a mixture can create an increase of colour or shade in the main chromic effect (Nilsson et al., 2011). While this performance can be compared to the combination of TC pigments with labelled different activation temperatures, the colour transitions attain different expressions. With TC pigments of different activation temperatures the fading of each pigment occurs at distinct times, whereas with the similar temperature activation there is an overlap interval of the colour change trajectories and doesn't require large temperature ranges to be observed.

Studies with colour measurements on screen-printed TC leuco dyes have also found that colour trajectory attained during heating is different than during cooling. Commonly, a specific colour lightness requires a lower temperature to be obtained in the colourizing process than when decolourizing. Thus, the gradual colour change is not merely characterized as a function of temperature but also depends on the thermal history, effect defined as colour hysteresis (Kulčar et al., 2010; Kulčar et al., 2011; Ibrahim, 2012).

Furthermore, diverse authors have also reported that the TC decolourization process is not complete, even at high temperatures. Through observation and colour measurements, different results were attained across TC pigments' brands. Kulčar et al. (2010) observed a yellow shade above the activation temperature of the pigments handled, differing from the substrate colour used. The possible causes discussed rely on a potential incomplete transparency of the leuco dye compound, light scattering the microcapsules' shell and/or blue light absorption of the binder (Kulčar et al., 2012). Ibrahim (2012) and Cabral and Souto (2014) observed a residual colour in the colourless state, according to each TC pigment colour, which can also indicate an incomplete dissociation of the colour former and developer in the microcapsules. The shades remained in TC colourless state can present implications in the colour change effect, being an important parameter to take in consideration particularly when specific colours are to be designed.

TC leuco dyes lifespan depends mostly upon the external conditions at which the materials are exposed to, rather than the number of times they are activated. Colour fastness properties refer to the resistance of coloured substances to remain stable under specific conditions (Aspland, 1998). TC materials usually present poor stability to UV light and reasonable wash and rub fastness properties. Besides, they also show

propensity to degrade when exposed to high temperatures (commonly referred above 140°C) and aggressive solvents (Talvenma, 2006; Friškovec et al., 2013; Ferrara and Bengisu, 2014). Ibrahim (2012) have researched the possibility to improve TC leuco dyes light fastness through the use of UV absorbers, hindered amine light stabilisers and antioxidants. Non-phenolic UV absorbers attained enhanced light stability, although TC daylight exposure for long periods of time demonstrated to be still limited.

2.2.3 Thermochromic textiles

Early TC textiles were developed in the late 1980s, of which are examples: Sway®, a multicolour fabric presented by Toray Industries Inc. where activation temperatures were defined for specific end-uses such as ski-wear (11-19°C), women's clothing (13-22°C) and window shades (24-32°C); and Hypercolor, a clothing line manufactured by Generra Sportwear, which heat-sensitive t-shirts became well known (Rhodes, 1991; Rijavec and Bračko, 2007). However, these examples have shown short lifespan and limited information was published in regards to their development. It was at the beginning of twenty-first century that ready-made TC materials began to be more easily accessed and thus, more systematically explored and researched in textile applications (Ferrara and Bengisu, 2014).

Thermochromic microcapsules were not initially developed for textile applications and present a lack of affinity and water insolubility. Thus, TC dispersion or powder form are commonly applied to textile substrates as pigments combined with appropriate binders, through printing processes (Christie, 2013; Chowdhury et al., 2014). Screen printing has been the most approached technique, presenting great versatility for the study and manufacturing of TC colour effects and patterns, also allowing the combination with other printing materials. Furthermore, screen printing also represents lower material waste in comparison to other techniques, which is an important consideration for sustainable reasons and given the expense of TC colourants in relation to conventional ones.

In this regard, great advantages are foreseen with inkjet printing, but is not a feasible process yet due to the TC microcapsule size and dispersion in the solution (Ibrahim, 2012). Christie, Shah and Wardman have conducted an experimental study with inkjet printing on cotton by microfiltration of the TC pigments before printing, having still observed the tendency of the TC microcapsules to clog the print heads (Ledendal, 2015).

Dyeing processes with TC materials have been limited so far due to their water insolubility. Addressing this issue, a dyeing method was patented in 1992, comprising of a process to treat textile cellulose fibres with a cationic compound, followed by the immersion in a dispersion with TC and high polymer compound and

further treatment with a binder addition. No applications with this technique have been reported (Masayasu et al., 1992). Recently, Matsui Chromicolor® developed the 'Aqualite Coloring System', enabling a water-based TC paste with clear dilutant and thinners to be dyed on cotton (Matsui, n.d.). This new TC material opens up emergent possibilities to explore colour change effects not just on the textile surface, but also into fabrics, yarns and fibres.

So far, few researchers have reported the incorporation of TC materials directly into fibres production. Rubacha (2007) developed a process of TC cellulose fibres based on wet spinning from concentrated solvents of cellulose with TC leuco dyes. The developed fibres presented a chromic effect, but their physical and mechanical properties were low, which the author suggests that smaller TC microcapsules and narrower range of size distribution would improve them. Ibrahim (2012) has incorporated TC in powder form into different polymers by screw extrusion. He created colour change filaments of polypropylene (PP), ethylene vinyl acetate (EVA) and linear low-density polyethylene (LLDPE), which also attained low mechanical properties.

The study of TC materials integration processes is an important subject to explore colour change effects and through printing, diverse techniques have been addressed. The interrelation of chromic behaviour with how pigments are combined and printed, as well as how thermal variation is introduced, has been catching special attention of researchers and designers with the objective to explore the potential of these materials to design interactive surfaces.

TC and conventional pigments can be combined in the same paste or overlapped individually during the printing process. In both cases, the combination possibilities are limitless considering the pigments' number, type and colours mixed or overlapped, concentrations and activation temperature of the TC pigments handled. While some of these parameters are associated to familiar processes when working with conventional colourants, the temporal and interactive dimensions of TC pigments changes how one is used to work with subtractive colour mixtures.

Linda Worbin conducted a practice-based design research focused on dynamic textile patterns, with emphasis on chromic textiles. Through a series of design examples, she explored new dynamic qualities that these smart materials introduce to textiles and textile design (Worbin, 2010). In Graffiti Cloth project, Worbin studied dynamic chromic palettes with TC and conventional pigments, applied through overprinting and raster techniques. The set of screen-printed samples created a 'colour map' of chromic possibilities with the pigments and raster scales combined. The researcher described the mixing process with TC pigments as more laborious and slower than with conventional pigments, due to the involvement of a

heating phase to analyse colours in TC colourless state and nuances between transitions and the definition of possible adjustments. Furthermore, the process was also compared to mixing for three colours, the colour of the TC pigment, conventional pigment and pigments overlapping.

The use of raster techniques allows the variation of colour strength without changing the pigments' concentration in the paste and it is also applied for the halftone overprinting with CMYK separation. Celine Marcq explored this technique with TC pigments, to create an image reproduction with dynamic multicolours. The designer also incorporated a dichroic smart film in the substrate backside, that changes colour when observed by different angles or moving the textile, thus adding a new variable in the creation of colour change effects (Marcq, 2014).

Furthermore, TC pigments have also been studied in combination with other chromic materials. Sara Robertson research included studies of colour change effects with textiles screen-printed with TC leuco dyes and coated with TC liquid crystals. The use of both TC systems, with different activation and threshold temperatures, lead to a broad chromatic palette and colour change transitions through temperature variation (Robertson, 2011). In the project Aqua chameleon swimming suit developed by Yun Ding, thermo, photo and hydrochromic pigments were applied through overlapping of different geometric and floral printing patterns, which enabled the creation of temporary expressions, according to the stimulus exposed: temperature, UV light and water (Collet, 2007).

Zane Berzina investigated the use of TC leuco dyes with other microencapsulated materials. Focused on the human skin as a metaphor to develop sensing and reacting surfaces, the author combined TC pigments, aroma microcapsules and phase change materials in a wallpaper that when touched displayed: visual response by colour change, olfactory response by releasing aroma and thermal variation according to the stored heat (Berzina, 2004).

Textile colour and pattern change can encompass diverse relations between forms composed by the printed pattern and the behaviour of the pigments and colours applied. In *Rather boring*, Worbin designed a textile pattern composed by aligned small forms printed with TC and conventional pigments of the same grey colour. When the textile is heated, TC forms fade away and a message is revealed corresponding to the conventional pigments' pattern. The researcher highlights that the two pigments prints require an alignment with high precision, so before the textile is heated the regular pattern composition don't present differences, also alluding for the challenge to achieve colour similarities for each pigment type (Worbin, 2010). The difficulty to reproduce specific colours with TC pigments is also discussed by Kulčar et al. (2012), referring it as an advantage for anti-counterfeit applications.

In addition to the TC pigments combination and printing possibilities, the heat generation source is also an important consideration during TC textiles design, as an intrinsic parameter of the chromic behaviour and in respect to the relations between printed and heated patterns. According to the way the heating source(s) activates the changes, Worbin (2010) distinguishes chromic dynamic patterns as direct or reported. Direct patterns account for colour change as a direct response to the thermal stimulus. Reported patterns involve the use of conductive and electronic components, which are programmed to induce temperature variation through resistive heating of conductive materials.

In direct patterns, transitions between TC pigments colourized and colourless states occur, in some degree, independently of pre-defined decisions of the designer, for example in which areas and when the textile is heated. In *Do Pattern* (Worbin, 2010), cups with different three-dimensional shapes at the base were designed so that when filled with hot liquids interact with a tablecloth screen printed with TC and conventional pigments. The dynamic pattern depends on the action of the user, being co-author of the textile expressions by the way the cups are (re)placed on top of the TC textile and for how long they are kept at the same place. Other examples explore visual gestural or body print experiences, such as *Swamp Stool* by NunoErin and *Bed linens* by Jürgen Mayer (Quinn, 2010); monitoring of body or breath temperature such as the thermochromic flu Mask by Marjan Kooroshnia (Kooroshnia, 2011) ; and interaction with ambient temperature, which Marie Ledendal investigated through TC textiles exposition to sunlight (Ledendal, 2015).

In reported patterns, sequences of activation are programmed to perform thermal variation of the conductive materials, that can be triggered through a specific stimulus or continuously run over time. Maggie Orth conducted early investigations in electronic textiles and explored the expressive potential of chromic displays through TC pigments screen printed in fabrics, woven with conductive threads (McQuaid, 2005). In Orths' project *Blip*, the textile changes from monochromic black tones in the cold state to bright colours in the heated state when programmed to occur in different areas at different periods of time (Orth, 2010). Joanna Berzowska also used conductive threads to explore relations between the TC pigments pattern and the physical configuration of the electric circuit, woven in a Jacquard loom. Her interest in textiles dynamic behaviour relied on the potential of soft responsive computation for "personal expression and playful exploration" (Berzowska, 2004; Berzowska, 2005).

Furthermore, direct and reported patterns can also be addressed simultaneously. Kärt Ojavee and Eszter Ozsvald created *SymbiosisS*, a part of a collection of TC felt interfaces that when touched, changes colour in response to the temperature of the human body and activates embedded electronics with tactile

capacitive sensing, triggering gradual changes of a predefined conductive pattern (Ojavee and Ozsvald, 2012; Ferrara and Bengisu, 2014) .

The stimulus that triggers the activation of colour change can also assign different purposes, where textile expressions (colour and pattern) can be linked to specific information. For example in Fabrication Bag project by Landin and Worbin (2005), the colour of a bag dot pattern changes from dull to colourful, for a visual and expressive alert that the bag user received a text message or a call; in Warning Signs, by Ngo and Lam (2010), a sweater pattern is revealed through colour change, to communicate the presence of high levels of carbon monoxide.

The selection of the conductive materials' type, integration processes in the textile substrate and activation definition has a significant effect on the dynamic textile behaviour and expressions. This topic will be further discussed in section 2.4.

Through diverse conceptual and technical perspectives, the presented projects discuss TC textiles simultaneously as a physical structure and a system of interactions. Inherent dynamic possibilities and development processes, lead to important findings and knowledge in order to design with chromic materials and textiles. From the understanding of these materials behaviour and interrelations with printing techniques, dynamic colour effects and heating stimulus, less emphasis has been placed on how to combine TC and conventional pigments through systematic processes. This topic is omitted in some studies or referred to as an empirical process involving trial and error paste combinations with direct observation and comparison between samples. The work developed in this research encompassed systematic processes. Other approaches such as in the Graffiti Cloth project (Worbin, 2010), developed a collection of colour swatches that through defined characteristics of the pigments, colours, concentrations and printing methods applied, build up a visual tool for colour change analysis, chromatics selection and elaboration techniques.

Furthermore, the intrinsic behaviour of TC pigments in response to heat entails complex relations between TC pigments activation temperature(s) selected, solutions to induce thermal variation, where and when the changes occur, which expressions and the stimulus that triggers it (reported patterns). These are important parameters to consider in the design of chromic textile behaviour and to explore new possibilities with this interactive material.

2.3 Shape Memory Materials

Shape Memory Materials are a class of stimuli-responsive materials with the ability to change from a temporary to a memorized shape (Otsuka and Wayman, 1998). Their unique behaviour and properties hold great potential for applications where shape change across sensing and actuation capabilities are required and have been gaining increased attention in textile design and engineering domain (Sun et al., 2012; LExcellent, 2013).

The shape change performance of SMMs lies in a phase transformation induced by an external stimulus, after having been deformed to a temporary shape, they respond to an input by returning to a pre-programmed physical geometry. Thermal energy is the most common SMMs' sensing stimulus, meaning that they are activated at a critical temperature, also known as reverse transformation temperature (Otsuka and Kakeshita 2002). Moreover, there are also SMMs that respond to stress, magnetic or electric field, pH-value, UV light and water (Huang et al., 2005; Lendlein et al., 2005; Yeduru, 2013).

The ability to perform shape change behaviour has been found in certain alloys, polymers, gels and ceramics which is called Shape Memory Effect (SME) (Tao, 2001; Honkala, 2006). The materials' types considered more suitable to be integrated in textile substrates are the Shape Memory Alloys (SMAs) and Shape Memory Polymers (SMPs), in particular in wire and monofilament form. Numerous researchers have examined and characterized their properties and both materials present diverse advantages and limitations to take into consideration in each application requirements. SMPs are reported as having high shape deformability and recoverability, and being more economic and flexible than SMAs. However, SMAs offer superior mechanical and recovery strengths as well as time response (Hu, 2007; Dyer, 2010; Huang et al., 2010; Hu and Meng, 2011; Sun et al., 2012; Jani et al., 2014; Gök et al., 2015).

In this research, higher actuation forces are a crucial parameter considering the objective to integrate SMMs in textile substrates to indirectly transfer the SME to the host structure, within predefined morphologies. Therefore, the materials chosen to study were the SMAs.

2.3.1 Shape Memory Alloys

Thermo-responsive SMAs are metal compounds capable of converting thermal energy into mechanical energy, commonly generating motion and force. As illustrated in Figure 5, their behaviour is based on two reversible phase transitions named: Austenite (A) at high temperature phase, also called parent phase; and Martensite (M) at low temperature phase, each one presenting different crystal structures and consequently

different properties (Honkala, 2006). When a SMA is deformed at M phase and temperature increases, it begins to transit to A phase at austenitic start temperature (A_s), completing the transformation at austenitic finish temperature (A_f). There is a transformation of the alloy crystal structure that becomes cubic, after which the alloy returns to its memorized shape. By decreasing the temperature, the reverse transformation starts to occur at martensitic start temperature (M_s) and the process is concluded at martensitic finish temperature (M_f). There is no shape change due to this transformation. When M_f temperature is attained, the alloy is ductile and can be deformed. In this phase, if a shape transformation by external forces occurs, the alloy passes from twinned martensite to detwinned martensitic state (Humbbeck, 2009; Adiguzel, 2015; Rao et al., 2015).

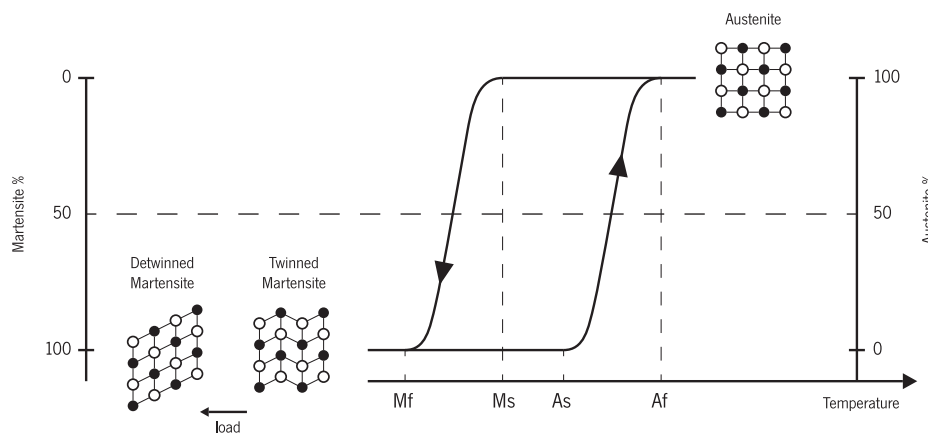


Figure 5. Shape memory phase transitions.

The process described it is known as the one-way memory effect, the alloy is able to memorize the shape that recovers at A_f temperature. However, it is also possible to program the alloy to perform two-ways memory effect: one activated at high temperature and another at low temperature. Thus, external forces are not required to perform the shape change upon cooling the material from A to M phases (Boussu and Petitniot, 2006; Hesselbach, 2007; Cianchetti, 2013).

The difference between the transition temperatures when heating and cooling defines the hysteresis of the process. This can be an important parameter for materials' selection in regards to small hysteresis performing faster actuation and larger hysteresis retaining the pre-programmed shape for a longer period (Honkala, 2006; Liu, 2010).

SMA's also present behaviour called superelasticity or pseudoelasticity. This property is observed when, without any temperature change, the alloy is able to return to its original shape after a mechanical strain has been applied and is then withdrawn (Kumar and Lagoudas, 2008; Cho, 2010).

Moreover, SMAs also demonstrate high damping capacities in comparison with other materials. They are able to reduce mechanical vibration or to absorb shocks, as a result of the high internal frictions exhibited during phase transformation and in the M phase (Boussu and Petitniot, 2006).

2.3.2 Nickel Titanium Shape Memory Alloy

Since the SME was first observed in a gold-cadmium (AuCd) alloy, in 1932 by Chang and Read, several SMAs have been developed (Otsuka and Wayman, 1998). Among different alloys' compositions, the SMA which has gained more attention is Nitinol, a nickel and titanium (NiTi) alloy, discovered by Buehler and co-workers in 1963, called NITINOL in honour of its discovery at the Naval Ordnance Laboratory (NOL) (Kumar and Lagoudas, 2008)

This alloy presents increased properties in relation to other SMAs and research in this area has led to a great variety of applications. Available with diverse transition temperatures and forms (wire, tube, strip and sheet), Nitinol exhibits strong SME, pseudoelastic behaviour, high damping capacity as well as high resistance to corrosion and abrasion. It is non-toxic, biocompatible and it is less expensive than other SMAs (Honkala, 2006; Ritter, 2007; Elahinia, 2016). Due to the characteristics cited and taking into consideration the objective to integrate SMAs in textile substrates, Nitinol wire was the alloy selected to be addressed in this research.

The most common Nitinol proportion is near-equiatomic, approximately 49% nickel by weight, but can be altered in order to attain specific properties. An increase in nickel by up to 1%, decreases the transformation temperature and increase the yield strength in the A phase. The combination of Nitinol with small quantities of other elements is also mentioned to customize specific properties, such as copper (Cu) and iron (Fe) to reduce hysteresis and niobium (Nb) to increase As temperature (Boussu and Petitniot, 2006). Although the mechanical properties of Nitinol SMAs are primarily defined by its composition, thermo-mechanical treatments, ageing after solution treatment, thermal cycling and processing techniques are also reported as interfering in the alloy characteristics (Zheng et al., 2004; Hartl and Lagoudas, 2008; Nurveren et al., 2008; Rao et al., 2015)

To memorize the shape that the Nitinol recovers to when exposed to their transformation temperature, it requires to be shape set by an annealing process at high temperatures. Previous to the heat treatment, the alloy has to be fixed in the desired shape in a die or fixture, with the wire ends constrained. The die is placed in a furnace at high temperature during a certain period of time, followed by rapid cooling. As temperature and time parameters depend upon the wire diameter and the mass of the die, without the

existence of an accurate guidance for their definition, several authors suggest that experimentation is required (Hesselbach, 2007; Liu et al., 2008; Rao et al., 2015). However, the common temperature recommended range between 400 and 550°C and duration should take into consideration that long periods of time can interfere in the alloys' properties, Rao et al. (2015) suggest between 5 and 30 minutes.

The process described, refers to the one-way memory effect. The annealing treatment for two-ways memory effect is more complex and involves several thermo-mechanical cycles along a specific loading path (Hesselbach, 2007; LExcellent, 2013). These repeated cycles significantly influence the alloys' microstructure and consequently their behaviour: the recovered strain reduces up to 2%; there is a decrease of the transformation forces; and the memory can be lost with a slight overheating (Wan and Stylios, 2007; Rottiers et al., 2011; Cianchetti, 2013).

During the heat treatment processes, Nitinol acquires an oxide layer that can influence corrosion resistance, joining ability besides other properties. Diverse surface modification processes can be applied to customize their qualities to the application requirements. The removal of these oxides can be developed by mechanical or electro-polishing, chemical etching, sandblasting, passivation and slurry ID cleaning (Shabalovskaya et al., 2008; Memry, n.d.-c; NDC, n.d.). Moreover, it is also possible to impart the alloy with another materials' layer, through coating and plating finishings (Memry, n.d.-c).

The oxide formations can also affect the Nitinol electrical resistance. Resistive heating (or Joule effect) is a method widely used to induce the alloys' thermal activation and, when the alloys are joined together or to other materials without a proper surface modification, the oxide can cause electrical resistance issues in the connection areas (Rao et al., 2015). Several authors have also researched Nitinol electrical resistance, in regards to its variation upon different phase transitions (Wu et al., 2000; Novák et al., 2008; Song et al., 2011).

Joining Nitinol components together or with other materials in a reliable way has a significant role for SMA applications. Taking into consideration each application, the reported methods include: mechanical techniques as crimping or swaging; soldering using preferentially silver bearing solders combined with aggressive flux; welding through TIG, laser, e-beam, resistance or plasma techniques; and adhesives, cyanoacrylates or epoxies (Šalej et al., 2011; Lah et al., 2016; Memry, n.d.-a)

Furthermore, Nitinol alloys are commercially available within different specifications. For textile integration, Nitinol wires with round sections are the most commonly used, comprising of different thicknesses, variation temperatures, surface finishes and states such as: cold work or as drawn, straight and spring

shape annealed (Memry, n.d.-b). It is also possible to purchase Nitinol with a pre-memorized behaviour of contraction and relaxation. This alloy, under the trade name FLEXINOL®, it is known as muscle wire (Dynalloy, n.d.).

2.3.3 Shape Memory Textiles

SMA's material and behaviour properties challenge new perspectives towards innovative and reliable applications, as well as revealing potential to supersede other materials and technologies in specific functions such as traditional hydraulic, pneumatic and motor actuators (Lawson, 2016). Over the past decades, SMA's have been implemented in technical domains, namely automotive, aerospace, robotics and biomedical. More recently, they have become an exponent of research and development in textiles where, besides functional possibilities, they also explore enhanced aesthetics and interactions.

Earlier developments in shape memory textiles have focused on functional protective clothing. In the late nineties, an intelligent suit for firefighters was developed, incorporating Nitinol springs placed in between two fabric layers whose shape change creates an insulating air layer (Congalton, 1999). The application of pseudoelastic and damping effect of SMA's has also been studied in ballistics, GEMTEX have been researching woven substrates of Nitinol combined with different materials such as high tenacity polyethylene (PE) and aramids to improve high-speed impact resistance (Boussu and Petitniot, 2006).

SMA's have also found application in women's brassieres. Nitinol underwire inserted in bra pads provide increased comfort in comparison with conventional steel underwires, due the lower elastic modulus and by resisting to permanent deformation (Wu and Schetky, 2000).

In 2000, Leenders explored the shape change behaviour by stitching SMA wires pre-programmed with different shapes in woven textiles. The effects achieved by shrinking, creasing or rolling were applied on certain areas of shirts and jackets, creating change in size and texture (Leenders, 2000).

Oricalco fabric, developed in 2001 by Corpo Nove through its spin-off firm Grado Zero Espace, was the first example of Nitinol integration in a woven textile substrate. It was used to manufacture a shirt that in response to heat, recovered its original shape, having the rolled up sleeves acquire a new size according to their pre-programmed geometry (Quinn, 2010; Grado Zero Espace, n.d.).

The fashion designer Hussein Chalayan, known as one of the pioneers of merging technology with fashion, presented a shape memory dress in his *Before Minus Now*, Spring/Summer 2000 collection. The dress

with SMA stitched in its skirt, instead of being stimulated with thermal radiation, is heated with electrical current that produces the phase transformation and therefore changes the skirt volume (Lee, 2005)

Design research studio XS Labs also developed shape memory garments activated electrically. In 2005, they have experimented to pre-program Nitinol in different configurations, such as curves and zigzags. However, they found that with coil or spring shape a greater performance was attained (Berzowska and Coelho, 2005). On the Vilkas dress, the Nitinol was stitched on cotton and the SME caused the fabric to wrinkle, thus revealing the wearer's knee. The Kukkia dress has felt and silk flowers with Nitinol stitched to each petal to achieve an open and closed effect. Later, they developed the Skorpions collection to explore anthropomorphic qualities in garments through textile movement. The Nitinol was hand-stitched and embroidered to perform aesthetic experiences (Berzowska et al., 2007; Seymour, 2008).

Coelho (2008) also relied on SMA incorporation with felt. Focusing on human-computer interactions and the shape change properties, he developed interfaces that study topological, textural and permeable transformations and researched how to use form transformation as a tool for communication and expression (Coelho and Zigelbaum, 2011)

In 2008/2009, Schäth developed Emotion: Outsourcing, a shape-shifting garment that addresses the wearer's senses and feelings via SMA and integrated sensors. By the jacket hood changes, the author intended to make the wearer aware of mood variation (Seymour, 2010).

Regarding yarn spinning with SMA and following integration on textile structures, Chan et al. (2002) conducted research focused on aesthetics and design. They have produced a variety of yarns with pre-programmed SMA as a core element, wrapped with conventional fibres. They found that the twist level and rollers' speed were important parameters to be optimized in order to avoid SMA protruding from the yarn and reducing SME constraints. Initial experiments using the yarns for knitting, exposed limitations due to the lack of extensibility of the SMA yarn and propensity to deform when knitted. Better results were achieved introducing SMA yarn formations in selected areas of the knitted structure (Winchester and Stylios, 2003). Tests aiming at weaving, with SMA yarns in the weft, revealed yarn end breaking when tension was too tight or slack. Samples were developed with SMA yarn formation with coil shapes, floating on the surface. A range of textures and sculptured woven and knitted fabrics were designed (Stylios, 2006; Vili, 2007).

Wan and Stylios (2007) have conducted experiments on the annealing process of Nitinol wire, for one-way and two-ways memory effect and their integration in woven structures. They have verified that the effect of

repeated treatment cycles for two-ways shape change have significantly decreased the amount of the alloys' recoverable strain. Additionally, they suggest the implementation of a bias mechanism in the textiles, to overcome this limitation.

Concerning experiments with SMA placed between two layers of fabric, Laschuk and Souto (2008) have developed SMA bras, which in near contact with skin recover their memorized shape. They have produced bra pads with knitted Nitinol and cotton yarn. Conventional yarn was applied in order to provide a better processability. After heat treatment, using a ceramic die, the cotton materials burn and are removed from the samples, resulting in 100% SMA structures. They also developed woven pads; however, in this case, it was not necessary to include textile fibres into the process. The woven samples achieved better performance (Laschuk, 2008).

Dyer (2010) alludes to the integration of Nitinol in woven fabrics. His research focused on the influence of textile yarn, woven structure, cloth set and Nitinol selection in the mechanical shape transfer and interfacial relationships. Results have demonstrated that lighter and tighter structures attain greater shape transfer than heavier or looser samples and plain weave samples with high density of threads required a higher loading to initiate the removal of Nitinol from the textile structure. The slippage phenomena was also studied by Vasile et al. (2010) and results demonstrate lower friction levels in samples with lower number of picks/cm and relatively high yarn diameter.

A SMA Velcro system was developed in 2011, presenting Nitinol hook fasteners on the male strip. Through electrical activation the hooks open and close when they cool down, providing a silent Velcro system (Vokoun et al., 2011).

Techno Naturology, a hybrid word that combines nature and technology, was the concept that Elaine Ling addressed in her investigation. Focusing on hybrid materialization, through diverse techniques such as weaving, laser-cutting and laminated surfaces, she studied and applied natural and man-made responsive materials, namely wood, SMAs and SMPs. Ling's collections achieved mimicked tectonic movements in response to changes in temperature and moisture, reflecting the micro behaviour of how nature becomes evident (Dieffenbacher, 2013).

Michalak and Krucińska (2015) have researched the two-ways memory effect to develop a controllable heat insulation textile. The Nitinol was annealed in spring spirals shape that changed their length when activated and when cooled down. The process was patented (Michalak et al., 2013). The Nitinol actuators were

placed in between a conductive nonwoven inner layer and 2 non-conductive outer layers, attaining an interlayer width increase of approximately 2,5mm.

Lah et al. (2016) have researched the two-ways memory effect in a knitted structure. After producing a 100% Nitinol (0,2mm) hand weft knitted, the annealing process began with the prototype mounted in a half-sphere form, placed in a furnace at 500°C for 30 minutes and air-cooled to a temperature below 22°C for 20 minutes. The prototype was then mounted in a flat form and annealed at 75°C for 10 minutes and again cooled at below 22°C for 20 minutes. The authors mentioned that this process was repeated more than 10 times, attaining the two-ways shape memory. As in Michalak et al., this research does not allude for the Nitinol recovered strains and transformation forces within the activation cycles.

The projects discussed address diverse approaches regarding SME training, integration of SMAs in textiles substrates and activation method. The materials' systems studied are diverse and comprise different concepts, processes and product applications, attaining milestones in shape memory textiles development.

The researchers also share common issues. The Nitinol shape set undergoes a thermo-mechanical process that can be optimized for one-way or two-ways shape memory. However, the repeated cycles necessary to impart the alloy to memorize two shapes, is reported to decrease the alloys' shape change properties and a bias mechanism is suggested as an alternative for the development of two shapes actuation (Hesselbach, 2007; Wan and Stylios, 2007; Rottiers et al., 2011; Cianchetti, 2013; Elahinia, 2016). Furthermore, SMAs memorize their shape at considerably higher temperatures than those supported by textile fibres. In this sense, they must be processed prior to their integration in fabric manufacturing, if a 100% SMA textile is not the goal (Stylios, 2006; Laschuk and Souto, 2008; Ugur, 2013).

Another aspect is related to the fact that textiles require a certain amount of stretch in the yarns to be processed. The low strain properties of SMAs represent a challenge when the material is to be spun, woven or knitted. Textile structures' characteristics and materials interaction can also constrain the SME, reducing the ability to perform the shape change (Chan et al., 2002; Stylios, 2006; Vili, 2007; Jani et al., 2014). In woven structures, a greater number of interlacings between the Nitinol and perpendicular warp threads has improved control and integration of Nitinol in the textile (Dyer, 2010). The ability of the SMA wire to be pulled out from the host structure was also highlighted and, besides greater resistance was found in samples with higher weft density, they still show tendency to easily slide (Dyer, 2010; Vasile et al., 2010).

Concerning the activation methods, different approaches have been taken. As a thermo-responsive material, Nitinol alloys can assume their pre-programmed shape by a direct response to ambient

temperature or thermal radiation from nearby bodies (Leenders, 2000; Grado Zero Espace, n.d.; Laschuk and Souto, 2008). As a conductive material, it is also possible to activate the Nitinol alloys through resistive heating. By this process, the shape change can be programmed and can have integrated sensors in order to explore SME in response to diverse stimuli that activate SMA heating (Lee, 2005; Berzowska et al., 2007; Seymour, 2010; Vokoun et al., 2011). The SME analysed within the projects fulfils changes in textile texture, volume, contractions and creasing, rolling up and forward and backward movement.

2.4 Conductive Materials

Defined by the ability to conduct electrical current, conductive materials are a key topic in smart textiles field, as they enable to transfer energy or data and impart textiles with electronic functionalities (Storey, 2009; Eichhoff et al., 2013). Cutting-edge potentials of fibre-based materials and products embedded with technology and added functionalities are also intertwined with great challenges. Functional feasibility of materials and devices that were traditionally rigid and heavy, combined with processability and comfort demands of soft and flexible textile structures have been great concerns, in parallel to wear and washing stability (Dias and Ratnayake, 2015; Kumar and Vigneswaran, 2016).

Enhanced means for conductive textiles development have undergone crucial advances, namely the emergence of conductive materials with increasingly textile-like mechanical and tactile properties. (Kirstein, 2013; Koncar, 2016). As on-going research into new enabling technologies is moving forward to more seamless and unobtrusive integration of electronics into textiles, creative approaches are also exploring and unfolding new textile futures as interactive surfaces of our daily life (Pailes-Friedman, 2016; Schneegass and Amft, 2017).

Conductive textiles applications hold a wide range of performances and electrical conductivity requirements, for example surfaces with low conductivity are applied for antistatic purposes, whereas for signal transmission, high conductivity is desired (Schwarz and Langenhove, 2013; Zeng et al., 2014). Encompassing diverse electrical mechanical and visual properties, conductive material selection is an important consideration for conductive textiles development including their manufacturing, functional and expressive capabilities (Tao and Koncar, 2016; Varga, 2017).

Electrical current that passes through a conductive material is defined by the flow of electrical charges, which are commonly carried through electrons. To generate this motion, an electrical voltage is applied between two points of the conductor, creating a potential difference that forces the charges to flow. In

addition, conductive materials present different resistance levels to the flow of electrical current depending on their properties and dimensions (Storey, 2009; Schwarz and Langenhove, 2013).

Ohm's law expresses this relation mathematically, where for a defined voltage (V) applied, the electrical current (I) that flows through the conductor is directly proportional to its electrical resistance (R):

$$V = I \times R$$

Accordingly, low resistance materials are highly conductive, whereas high resistance results in lower conductivity. The unit of electrical current is Ampere (A), being 1 A approximately 6242×10^{18} electrons (1 Coulomb) per second passing through a point in the conductor. Voltage is measured in Volt (V) and electrical resistance in Ohm (Ω).

Electrical conductivity is conferred to textiles by means of metals, intrinsically conductive polymers (ICP) and carbon-based materials. Metals or alloys present high levels of electrical conductivity, although they have low elasticity and are heavier than conventional textile fibres. Common metals used for textile integration are copper (Cu), silver (Ag), aluminium (Al), stainless steel and nickel-chrome (NiCr) (Schwarz and Langenhove, 2013; Cork, 2015; Kumar and Vigneswaran, 2016). ICPs such as polyaniline, polyacetylene, polypyrrole and poly(3,4-ethylenedioxythiophene):polystyrenesulfonate (PEDOT:PSS) are lightweight, flexible and can also be blended with other materials during processing. Ongoing research in this field has been particularly focused on these materials' electrical properties and electronic possibilities, as well as processability, environmental stability and toxicological challenges (Zeng et al., 2014; Qu and Skorobogatiy, 2015). Carbon nanotubes and graphenes are carbon-based conductive materials that have demonstrated great potential for textile applications. At the research stage, their major advantages rely on being lightweight and presenting high mechanical strength (Cork, 2015; Miao, 2015).

2.4.1 Fabrication technologies of conductive textiles

Manufacturing processes of conductive textiles can be conducted at different levels, from fibre or filament to threads, substrates and finishings. Involving conventional and innovative textile processes, fabrication technologies of conductive textiles are based on two major approaches: textiles entirely produced by intrinsically conductive materials and textiles blended or specially treated to gain conductivity (Schwarz and Langenhove, 2013; Cork, 2015).

Conductive fibres include synthetic materials filled with conductive particles, textile fibres coated with conductive materials and fibres or filaments produced entirely by conductive materials, such as metal

monofilaments produced by wire drawing. These fibres and filaments are applied for conductive threads manufacturing, being combined with conventional textile materials, or used directly in substrates processing, for example in the production of conductive nonwovens (Xue et al., 2005; Stoppa and Chiolerio, 2014; Guo et al., 2016).

Metal monofilaments wrapped around a textile-based core thread assume a spring shape, where the twist number defined can vary to tailor the threads' electromechanical properties. Another approach is to spin metal wires with non-conductive filaments, setting one or more conductive strands in the plied thread. In both cases the textile material acts as the load carrier, having higher mechanical strength and flexibility than the metal filaments and accounting for the thread processability and handling. Textile threads can also be plated with a conductive layer. In this case, the overall surface is conductive but it is also more susceptible to cracking. To reduce conductivity issues, this method is commonly applied for the development of multifilament threads (Eichhoff et al., 2013; Locher, 2013; Rakshit and Hira, 2014).

Conductive fibre, filaments or threads are integrated into the textile structure or applied onto the substrates' surface. Through integration processes such as weaving, knitting or braiding, conductive materials are at the same time functional and structural elements of the textile. Their patterning possibilities depend on the textile construction where diverse relations between form and function can be explored. In woven substrates, conductive threads are mostly used in the weft, due to greater flexibility for the circuit design and threads exchange. Conductive threads in the warp are also avoided due to the higher stress that they are exposed during processing and consequent increased possibility to affect or lose conductivity (Eichhoff et al., 2013; Stoppa and Chiolerio, 2014). Veja (2014) researched weaving methods for the integration of conductive materials and electronic devices, highlighting in particular the potential of using double cloth techniques; inlay weft weaving; and manipulation of floats for the development textiles with multiple functions.

Embroidery or sewing processes allow a higher flexibility for the conductive threads pattern definition, as the integration on the surface does not depend on the textile structure. E-broidery (electronic embroidery) technologies have been explored in many applications, taking advantage of precise design control and stitched circuit pattern through CAD (Computer-Aided Design) software (Stoppa and Chiolerio, 2014; Li and Tao, 2015). The Forster Rohner company patented an e-broidery technology that allows the integration of conductive threads and active components during production (Bosowski et al., 2015; Pailles-Friedman, 2016).

Finishing processes also promote the application of conductive materials on the textile surface. Conductive coating techniques include physical and chemical vapour deposition, electroplating, electroless plating, among others. Electrical conductive properties of coated fibres, threads and substrates can be tailored through the coating layer thickness and the conductive materials selected (Shim, 2010; Wang et al., 2010; Zeng et al., 2014). Printing is a versatile method to confer conductivity in textiles, enabling the creation of a desired pattern in localized areas, using conductive materials in paste form. Screen and inkjet printing are the main techniques used, presenting the advantage of low material waste and the possibility of either large-scale or low volume fabrication (Kirstein, 2013; Yang et al., 2013; Torah et al., 2015).

Critical challenges of coated and printed conductive textiles rely on: the textile surface roughness, which interferes in the conductive layer uniformity and thus electrical performance; curing temperature, considering the textile substrates' threshold limits; physical and chemical properties, in particular the change or loss of electrical conductivity as the result of abrasion, bending and washing conditions (Stoppa and Chiolerio, 2014; Li and Tao, 2015; Torah et al., 2015). Research focused on this topic encompasses development of conductive pastes with enhanced properties such as stretchability (Matsuhisa et al., 2015; Jin et al., 2017) and processes to seal the conductive printed layer, involving the production of additional protective layers, commonly applied with polyurethane-based pastes by coating, lamination or screen-printing (Yang et al., 2013; Yokus et al., 2016). The sealing consists of an interface layer applied in the substrate for waterproofing and to create a smooth surface for the conductive paste and an encapsulation layer for electrical insulation and external protection. Although still not optimal, improved results in flexibility and durability to abrasion, washing and dry cleaning have been attained (Kazani, 2012; Gordon et al., 2014; Li and Tao, 2015; Jin et al., 2017).

2.4.2 Conductive textiles

Initial uses of metal-based conductive materials in textiles did not encompass functional applications. Indian metal silk organzas are woven substrates that include silk threads wrapped with thin metal films and provide textiles a brilliant appearance. Regarding aesthetic and social status purposes, embroidery with noble metal-based threads have also been applied in monarchic and ecclesiastical apparel (Schwarz and Langenhove, 2013; Cork, 2015). Contemporary approaches of metal-based textiles have been eminent in the work of Reiko Sudo (Nuno Corporation), namely by exploring technologies not traditionally associated with textiles, in which plating techniques of the automotive industry are an example, inspiring new visions for textile design (Nuno, n.d.).

Within functional aspects, conductive textiles present a wide range of applications. Electrically conductive pathways enable the transfer of energy or data between interconnected electronic devices or other conductive materials, such as thermo-responsive SMAs (Rakshit and Hira, 2014; Qu and Skorobogatiy, 2015). In parallel, conductive materials' properties and structures can be devised to enable electronic functionalities. Textile-based systems may comprise of sensing and actuation behaviour, wireless communication, data processing and energy storage or harvesting (Eichhoff et al., 2013; Langenhove, 2015; Toprakci and Ghosh, 2015; Wang et al., 2015; Wilson and Mather, 2015). Permeated through nanotechnology advances and electronics miniaturization, emerging research aims at the development of textile-based electronics, also including the potential of micro-electronics integration into fibre forms (Dias and Ratnayake, 2015; Varga, 2017).

To create a textile electronic system, the conductive circuit has to be connected to a power source. The technology and interface applied for the elements' link must assure a reliable electrical connection with low electrical resistance (Suganuma, 2014; Mehmman et al., 2017). Joining technologies for conductive textiles encompass permanent or reversible connections. Methods used for fixed connections include soldering (with lead-free solders), crimping, bonding (with conductive adhesives) and also conventional textile processes such as embroidery or sewing. Reversible joining can be produced with the inclusion of conventional or textile-based elements. Some examples include pin headers, metal eyelets, conductive zippers, conductive hook and loop fasteners (Velcro) (Locher, 2013; Mecnika et al., 2015).

According to the conductive textile characteristics and applications, electrical insulation of the connectors and conductive elements may also be required. As previously described, encapsulation layers developed through printing or coating processes with insulator agents can provide this property (Li and Tao, 2015; Jin et al., 2017). Other techniques include embroidery with conventional threads, iron-on patches, adhesive films and ribbons. One major challenge in the development of connections and respective insulation is to achieve stable performance and textile flexibility (Lin, 2015; Kumar and Vigneswaran, 2016).

The application of conductive textiles as sensors and/or actuators involves the transmission and also transformation of energy or data. Textile sensors are able to transform physical stimuli, such as pressure, temperature or humidity, into processable electrical signals. This transformation lies in the change of conductive materials' electrical properties with a specific input. As actuators, conductive textiles convert electrical signal inputs into physical responses, for example light or heat (Langenhove, 2015; Toprakci and Ghosh, 2015). Thermal variation of conductive materials is based on the process by which electrical current passes through a conductive material and, according to their electrical resistance and voltage applied,

power dissipates as heat produces a temperature rise – the Joule effect, also known as Joule or resistive heating. Conductive materials as thermal actuators are also called resistive heaters (Storey, 2009; Mbise et al., 2015; Torah et al., 2015)

Textile heating systems are usually developed to provide safe and comfortable body thermoregulation. An initial example is E-CT from Gorix, a patented fabric that was used in the production of heated boots, gloves, among others (Baurley, 2005). Textile heating in car seats is an established application, where the electrical current that passes through the conductive materials is controlled within the possibility to select different heating levels. Nichrome monofilaments and FabRoc® carbon loaded silicone threads have been reported for this application (Mbise et al., 2015). Performance outdoor, pant liners, vests and scarfs are commercially available examples of heated garments and accessories (Wagner, 2013; Tong and Li, 2015; Kumar and Vigneswaran, 2016). Whereas some applications use heating pads to enable the garments' washing without the conductive textiles, there are already marketed solutions that withstand machine-washing. WarmX® is a brand of self-warming underwear and base-layer garments that use silver-plated polyamide threads in knitted structures. They use a mini power-controller to heat up the textile, being the only element disconnected for washing (WarmX, n.d.; Pailles-Friedman, 2016).

Besides body thermoregulation, resistive heating is also commonly applied for temperature control of TC textiles. As discussed in 2.2.3 section, the heating elements that activate TC colour change have a significant effect on the textile dynamic behaviour and expressions. Thermal variation induced by conductive materials integrated in the textile substrate involves an intrinsic relation between the TC textile and the conductive materials' properties, patterning and fabrication processes. Thus, the physical production of the conductive textile and respective electrical properties are crucial considerations in smart textile design.

The use of conductive materials to activate textile colour change is based on temperature increase, while the textile cooling is not commonly electrically controlled. Hu et al. (2005) researched the development of a cooling fabric with conductive polymer coated fibres, based on the 'Peltier effect' – the effect of heat production or absorption at the junction of two dissimilar metals when electrical current passes through their junction (Gibilisco, 2001; Wang et al., 2010). Although a cooling effect was achieved, the performance was limited also attaining electrical degradation of the polymers. In collaboration with European Space Agency, Grado Zero Espace company developed a textile cooling system adapted from astronaut suits, involving a complex structure of thin tubes for the circulation of a liquid that was cooled by a Peltier element. The cooling system was installed in a F1 pilot racer suit, providing thermo-regulation (Espace, n.d.; Langenhove, 2015).

Future possibilities to integrate cooling effects in thermo-responsive textiles may provide a meaningful tool to design chromic and shape memory textiles behaviour. At the research stage, the challenges involved in the integration of cooling systems in textiles, namely structures' complexity, weight and non-flexibility, still limit potential applications (Langenhove, 2015; Torah et al., 2015). Considering this research aims, the integration of tubing structures and Peltier devices also would compromise textiles' light transmittance. Thus, the use of controlled cooling systems was not considered.

In this research, the integration of conductive materials in textiles substrates aims to provide a means for electrical activation of colour and shape change through resistive heating. For colour change, the conductive pattern will be the thermal actuator. Nitinol alloys are conductive materials and shape change will be produced through their resistive heating properties. The use of conductive materials for shape change activation will establish the electrical connections between Nitinol segments and electronic components. Furthermore, within a great range of materials and properties, conductive materials' electrical properties differ, enabling to explore not just functional performance but also textiles' expressive qualities.

2.5 Light

Natural or artificial light plays an important role in human life. It ensures visibility, it affects our biological rhythms and, among various functional and aesthetic aspects, light also influences how our surroundings are perceived and experienced, for example presenting the ability to visually transform materials' textures and colours as well as space boundaries (Karlen et al., 2012).

It is through interaction with matter that light is perceived, at the same time it also makes objects and environment visible (Cuttle, 2015). Visible light consists of an electromagnetic spectrum with wavelengths between approximately 380 and 740 nm and when it strikes a surface diverse phenomena can occur. (Choudhury, 2014b). Opaque materials reflect light – reflectance – whereas translucent or transparent materials let the light pass through them – transmittance. The amount of light that is reflected or transmitted depends on the proportion absorbed (Yot, 2011). Materials' properties also affect the degree of light diffusion. Matte surfaces scatter the incident light at several angles, while in the case of specular surfaces, light is reflected in a singular direction and there is no diffusion (Innes, 2012).

Furthermore, interaction of light with matter is also crucial to establish colour stimuli. Colour of light is defined by its spectral composition, which respects to the wavelength spectrum and respective radiance. When light strikes a surface, specific light wavelengths are absorbed according to the materials' optical

characteristics, changing the spectral composition of light reflected or transmitted and observed as the materials' colour (Descottes and Ramos, 2011; Lechner, 2015)

Perception of light that is reflected from a surface – brightness – does not depend merely on its physical quantity – luminance. Perceived luminosities can be influenced by context, personal judgement, relation between adjacent areas, among others (Lam, 1992; Maack and Pawlik, 2009). In 1957, S. S. Stevens studied the perception of light change with different magnitude levels, observing that doubling light intensity is not necessarily perceived as twice as bright. When the stimulus doubled was low, the change was perceived as more than twice as bright, whereas its increase resulted in low noticeable changes (Goldstein, 2010). Comprehension of light as a physical and perceptual phenomenon is of great significance when designing lighting scenarios.

2.5.1 Qualitative lighting design

Visual perception is how observed stimuli are apprehended and interpreted, giving rise to our visual experience (Kalat, 2007; Goldstein, 2010). The importance of the observers' active role in this process was not initially considered in lighting design criteria. Previous focus relied on quantitative aspects of light for specific tasks (Descottes and Ramos, 2011). A more comprehensive perspective on lighting has started to evolve, particularly through the work of Richard Kelly and William Lams, giving rise to what is referred to as perception-oriented or qualitative lighting design (Maack and Pawlik, 2009; McAuliffe, 2016).

Kelly declined the definition of light quantity and uniform illuminance as central lighting parameters and in the 1950s he differentiated three fundamental qualities of lighting: ambient light, focal glow and play of brilliance. Lam considered diverse relationships between lighting qualities with human needs for visual information and in the 1970s he established a set of criteria based on activity and biological factors (Ganslandt and Hofmann, 1992; Lechner, 2015).

The activity or activities performed in a space may present different lighting requirements, such as demands of colour rendering and duration or frequency of the task. According to specific activity needs, Lam highlighted the importance of the type of light source, light direction, concentration and colour in order to enable visual acuity and comfort (Lam, 1992).

Biological needs also play a critical role in lighting design, being the major considerations examined by Lam the needs for orientation, physical security and definition of personal territory. For example visual acuity of field boundaries is crucial for space-orientation, whereas the definition of personal territory benefits from local lighting (Lam, 1992). Furthermore, day and night light cycles influence human biological rhythms

(circadian rhythms) and establish lighting associations for time-orientation, such as variations of light intensity, tone and direction (Karlen et al., 2012; Boyce, 2014).

Qualitative lighting criteria also contemplates the importance of personal interpretation of what is observed, including attributive processes, with respect to the attribution of a meaning in response to stimuli; expectations, concerning prior experiences; and affective or emotional responses (Lam, 1992; Goldstein, 2010). A practical example that reflects the role of lighting expectations is the interpretation of a 'bright night' or a 'dark day', although the light levels of such a night are most probably much lower than the day referred.

2.5.2 Lighting in design, arts and architecture

Light inspires researchers and practitioners to shape and transform luminous environments. Drawn upon visual perception and optical interactions, lighting design has been evolving creatively, in scope and resources, such as enabling technologies and light emitting devices (Cuttle, 2015). Although great focus is now placed on applications and control of artificial light sources, lighting effects and atmospheres have been timelessly created through interaction of light with materials, architectural volumes and atmospheric conditions.

In architecture, light is acknowledged with great significance not just in respect to architectural lighting but also in how building structures are conceptualized and developed to interact with light. Louis Kahn's and Tadao Ando's works use light as a central element, in particular through the interplay of light and shadows. Reflecting on his work, Kahn stated "Even a space intended to be dark should have just enough light from some mysterious opening to tell us how dark it really is. Each space must be defined by its structure and the character of its natural light." (Büttikger, 1993).

Relationships between high and low luminosities have been used as a major creative tool to engage visual effects and create atmospheres, a concept associated with lighting sensorial qualities and character (McAuliffe, 2016). James Turrell's light installations involve viewers through transformative perceptions, using static artificial light. In *Afrum Pale Blue* (1968), a light beam is projected into a room corner, which from a distance has a flat rectangle appearance, whereupon moving closer, a 3D cube is perceived. *Two Blues* installation (2008) consists of a dark room with a rectangular opening to a blue light-filled room. The dim lighting does not allow an immediate understanding of the space, just a blue rectangle is perceived. As the eyes' sensibility adapt to the light conditions, space becomes visible (Descottes and Ramos, 2011; Turrell, n.d.). These works reflect on the influence of light qualities and visual perception in the sense of space, considering the viewers location and observation time.

The spatial relationship between observer and light source is an essential aspect in lighting design. Besides luminous effects, the height of the light source is also associated with intimacy concepts, for example, luminaires are commonly placed closer to our bodies in private spaces than in public environments (Descottes and Ramos, 2011). Variation of height hierarchies enable design ambiences that even taking place in a public domain, can still assign an intimate lighting character to a space (Du, 2011).

Furthermore, lighting qualities are also intrinsically related with light diffusion degrees. Olafur Eliasson uses artificial fog to change light expression inside empty rooms, resulting in dense atmospheric effects (Eliasson, n.d.). Light diffusion through fog appears to give it a tangible quality, negating the perception of spacial limits. Eliasson's atmospheric installations create light experiences with limited visibility where "the act of seeing becomes an act of feeling" (Kries and Kugler, 2013).

Through functional and aesthetic perspectives, textiles have a long tradition interacting with light. Able to present varied diffusion properties, textiles are often applied to scatter the harsh light and soften it. In parallel, they also allow the transforming of luminosities and light tones, through different levels and qualities of light reflected and/or transmitted. As a result, textiles and light can be designed to provide visual and thermal comfort, enhance visual qualities for task performance, raise visual interest, create lighting atmospheres, etc. (Chilton and Lau, 2015).

Examples of applications range from clothing and accessories to textiles applied in exterior or interior environments. Ancient roman velarium, was a retractable textile awning featured in coliseums to create shading for the spectators, reducing luminosity and heat (Sear, 2008). Textile curtains and blinds are widely used to vary the light that comes from the exterior to create luminous environments. They are applied either for natural light during day, or blocking exterior light during night. As space dividers, textiles' translucent qualities can confer to spaces a sense of privacy and at the same time allows lighting continuity or cues. Photographic studios often use textile diffusers, changing their positioning and direction in relation to the light sources to adjust and create a particular lighting setup.

Contemporary shading systems have been a growing interdisciplinary subject focused on the design potential to interact with our environment through innovative and expressive materials, processes and performances. For both exterior and interior applications, new structural and interactive possibilities are explored to design lighting ambiences. Gerber Architekten developed a tensile textile facade in King Fahad National Library that is able to reveal and conceal light through a pattern of rhomboid textile awnings, while also aesthetically transforming the building facade (Gerber, n.d.). Interior lighting is defined through the interaction between natural light and the static textile structure.

In addition, increased attention in shading systems includes approaches with dynamic interactions between the environment and the tangible surfaces. In Al Bahar Towers, Aedas architects group created a facade composed by triangular polymeric panels that mechanically change their geometry through computer-system control. The variation between closed and opened areas in the facade is programmed according to weather conditions and enables a reduction of heat gains in the towers, also transforming interior lighting (Cruz, 2016).

Flectofin, developed at the German Institute of Building Structures and Structural Design (ITKE) of the Stuttgart University, researches possibilities to create dynamic shading based on materials performance rather than mechanical assemblies. Inspired by the deformable behaviour of *Strelitzia* flower, flectofin is a hingeless flapping system made of glass fibres and thermoset resin. Through the heat-responsive bending of the system spine, the direction of two flaps is shifted. By changing spatial orientation, the translucent flaps perform a visual organic open and close movement, producing self-adaptable sun-shading (Brownell, 2017).

Within a myriad of applications, the interplay of textiles and light is designed through textile properties and expressions. Emergent possibilities of adaptive and reactive behaviour of smart textiles open up a vast potential to create lighting scenarios that can actively interact with environmental stimuli, resulting in dynamic transformations of the textiles and light. In this research, light transmittance variations are studied through the dynamic behaviour of colour and shape changing textiles. In the design research, textile performances and expressions were studied with artificial light, a medium in which qualities are commonly altered by acting upon the light source.

2.6 Summary

Through an interdisciplinary perspective, a comprehensive discussion of the materials' properties and behaviour principles was presented in this chapter. Enabling technologies, integration processes and applications demonstrated crucial milestones already attained and the direction of ongoing research towards enhanced developments. The examples discussed also highlighted the importance of innovative approaches and methodologies in the design process, to explore future textile performances.

Critical insight was also provided in respect to challenges and opportunities identified to research textiles with dynamic and interactive properties and their interaction with light transmittance.

Empirical processes are applied in the development of screen printing pastes that combine TC and conventional materials. For applications where colour reproduction is required or for the creation of colour palettes that change colour according to a specific ratio, systematic processes of paste recipe formulation are predicted to attain accurate and low time-consuming results.

Focusing on Nitinol alloys to perform shape transfer to the host structure, textiles' shape change behaviour is defined through the geometries memorized in the SMAs. Through the inverse design approach, defining textiles morphologies to guide the Nitinol geometry definition and respective integration in woven substrates, the aim is to enable the creation of dynamic geometric structures.

Conductive materials allow activating thermo-responsive textiles through resistive heating. Within a great range of materials and properties, their electrical performances differ and enable their selection and integration in the textile not just from a functional perspective but also as an integral element of the textile expression.

2.7 References

- AARTS, E. & WICHERT, R. 2009. Ambient intelligence. *In: BULLINGER, H.-J. (ed.) Technology Guide: Principles – Applications – Trends.* Berlin, Heidelberg: Springer Berlin Heidelberg, 244-249.
- ADDINGTON, M. & SCHODEK, D. 2005. *Smart materials and new technologies*, Amsterdam, Architectural Press.
- ADIGUZEL, O. 2015. The Role of Twinned and Detwinned Structures on Memory Behaviour of Shape Memory Alloys. *Advanced Materials Research*, 1105, 78-82.
- AITKEN, D., BURKINSHAW, S. M., GRIFFITHS, J. & TOWNS, A. D. 1996. Textile applications of thermochromic systems. *Review of Progress in Coloration and Related Topics*, 26, 1-8.
- ASPLAND, J. R. 1998. Colorants: Dyes. *In: NASSAU, K. (ed.) Color for science, art and technology.* Amsterdam: Elsevier.
- BAMFIELD, P. & HUTCHINGS, M. G. 2010. *Chromic phenomena: technological applications of colour chemistry*, Cambridge, Royal Society of Chemistry.
- BAURLEY, S. 2005. Interaction design in smart textiles clothing and applications. *In: TAO, X. (ed.) Wearable Electronics and Photonics.* Cambridge: Woodhead Publishing.
- BERZINA, Z. 2004. *Skin Stories: Charting and Mapping the Skin. Research using analogies of human skin tissue in relation to my textile practice.* PhD thesis, University of the Arts London.
- BERZOWSKA, J. 2004. Very slowly animating textiles: shimmering flower. *ACM SIGGRAPH 2004 Sketches.* Los Angeles, California: ACM.
- BERZOWSKA, J. 2005. Electronic Textiles: Wearable Computers, Reactive Fashion, and Soft Computation. *TEXTILE*, 3, 58-75.
- BERZOWSKA, J. & COELHO, M. Kukkia and Vilkas: Kinetic Electronic Garments. 9th IEEE International Symposium on Wearable Computers, 18-21 October 2005 2005 Osaka, Japan.
- BERZOWSKA, J., MAINSTONE, D., BROMLEY, M., COELHO, M., GAUTHIER, D., RAYMOND, F. & BOXER, V. 2007. Skorpions: kinetic electronic garments. *9th International Conference on Ubiquitous Computing.* Innsbruck, Austria.

- BOSOWSKI, P., HOERR, M., MECNIKA, V., T. GRIES, T. & JOCKENHÖVEL, S. 2015. Design and manufacture of textile-based sensors. *In: DIAS, T. (ed.) Electronic Textiles*. Cambridge: Elsevier Science & Technology.
- BOUSSU, F. & PETITNIOT, J. 2006. Development of shape memory alloy fabrics for composite structures. *In: MATTILA, H. R. (ed.) Intelligent textiles and clothing*. Cambridge: Woodhead, 124-142.
- BOYCE, P. R. 2014. *Human Factors in Lighting, Third Edition*, London, Taylor & Francis.
- BROWNELL, B. 2017. *Transmaterial Next: A Catalog of Materials That Will Redefine Our Future*, New York, Princeton Architectural Press.
- BÜTTIKGER, U. 1993. *Light and Space*, Basel, Birkhäuser.
- CABRAL, I. & SOUTO, A. P. 2014. Thermo-chromic Textile Structures: A Dynamic Ambient Light Design. *International Journal of Designed Objects*, 7(3), 23-35.
- CHAN, Y. Y. F., WINCHESTER, R. C. C., WAN, T. R. & STYLIOU, G. K. The Concept of aesthetic intelligence of textile fabrics and their application for interior and apparel. IFFTI International Conference, 7-9 November 2002 Hong Kong. 458-471.
- CHILTON, J. & LAU, B. 2015. Lighting and the visual environment in architectural fabric structures. *In: LLORENS, J. (ed.) Fabric Structures in Architecture*. Cambridge: Woodhead Publishing.
- CHO, C. G. 2010. Shape Memory Material. *In: CHO, G. (ed.) Smart clothing: technology and applications*. Boca Raton, FL: CRC Press, 189 - 227.
- CHOWDHURY, A. K. R. 2014b. *Principles of colour appearance and measurement Volume 1: Object appearance, colour perception and instrumental measurement*, Cambridge, Woodhead Publishing.
- CHOWDHURY, M. A., BUTOLA, B. S. & JOSHI, M. 2013. Application of thermo-chromic colorants on textiles: temperature dependence of colorimetric properties. *Coloration Technology*, 129, 232-237.
- CHOWDHURY, M. A., JOSHI, M. & BUTOLA, B. S. 2014. Photochromic and Thermo-chromic Colorants in Textile Applications. *Journal of Engineered Fabrics & Fibers*, 9(1), 107-123.
- CHRISTIE, R. M. 2013. Chromic materials for technical textile applications. *In: L., G. M. (ed.) Advances in the dyeing and finishing of technical textiles*. Oxford: Woodhead Publishing.
- CHRISTIE, R. M., ROBERTSON, S. & TAYLOR, S. 2007. Design concepts for a temperature-sensitive environment using thermo-chromic colour change. *Colour: Design & Creativity*, 1(1):5, 1-11.
- CIANCHETTI, M. 2013. Fundamentals on the Use of Shape Memory Alloys in Soft Robotics. *Interdisciplinary Mechatronics*. John Wiley & Sons, Inc., 227-254.
- COELHO, M. 2008. *Materials of Interaction: Responsive Materials in the Design of Transformable Interactive Surfaces*. Master Thesis, Massachusetts Institute of Technology.
- COELHO, M. & ZIGELBAUM, J. 2011. Shape-changing interfaces. *Personal Ubiquitous Computing*, 15 (2), 161-173.
- COLLET, C. 2007. The next textile revolution. *In: BONNEMAISON, S. & MACY, C. (eds.) Responsive textile environments*. Halifax, N.S.: TUNS Press.
- CONGALTON, D. 1999. Shape memory alloys for use in thermally activated clothing, protection against flame and heat. *Fire and Materials*, 23, 223-226.
- CORK, C. 2015. Conductive fibres for electronic textiles: an overview. *In: DIAS, T. (ed.) Electronic Textiles*. Cambridge: Elsevier Science & Technology.
- CRUZ, P. 2016. *Structures and Architecture: Beyond their Limits*, London, CRC Press.
- CUTTLE, C. 2015. *Lighting design: a perception-based approach*, London and New York, Routledge.
- DAY, J. H. 1963. Thermo-chromism. *Chemical Reviews*, 63, 65-80.
- DESCOTTES, H. & RAMOS, C. E. 2011. *Architectural lighting: designing with light and space*, New York, Princeton Architectural Press.
- DIAS, T. & RATNAYAKE, A. 2015. Integration of micro-electronics with yarns for smart textiles. *In: DIAS, T. (ed.) Electronic Textiles*. Cambridge: Elsevier Science & Technology.
- DIEFFENBACHER, F. 2013. *Fashion thinking: creative approaches to the design process*, Lausanne, AVA Academia.

- DU, D. 2011. *Interior lighting*, California, Profession Design Press.
- DURASEVIC, V. 2016. Smart dyes for medical textiles *In: LANGENHOVE, L. V. (ed.) Advances in Smart Medical Textiles*. Oxford: Woodhead Publishing, 19-55.
- DYER, P. E. 2010. *Dynamic control of active textiles: the integration of nickel-titanium shape memory alloys and the manipulation of woven structures*. PhD Thesis, University of Brighton.
- DYNALLOY. n.d. *Introduction To FLEXINOL® Actuator Wire* [Online]. <http://www.dynalloy.com/flexinol.php>. [Accessed 20 March 2013].
- EICHHOFF, J., HEHL, A., JOCKENHOEVEL, S. & GRIES, T. 2013. Textile fabrication technologies for embedding electronic functions into fibres, yarns and fabrics. *In: KIRSTEIN, T. (ed.) Multidisciplinary know-how for smart textiles developers*. Oxford: Woodhead Publishing.
- ELAHINIA, M. H. 2016. *Shape memory alloy actuators: design, fabrication, and experimental evaluation*, Chichester, West Sussex, John Wiley and Sons, Inc.
- ELIASSON, O. n.d. *Your atmospheric colour atlas, 2009* [Online]. <http://olafureliasson.net/archive/artwork/WEK100285/your-atmospheric-colour-atlas>. 8 february 2017].
- ESPACE, G. Z. n.d. *Thermo-regulating systems* [Online]. <http://www.gradozero.eu/gzenew/index.php?pg=thermaltech&lang=en>: Grado Zero Espace. [Accessed 2 november 2015 2 november 2015].
- FERRARA, M. & BENGISU, M. 2014. *Materials that change color: smart materials, intelligent design*, Cham, Springer International Publishing.
- FRIŠKOVEC, M., KULČAR, R. & GUNDE, M. K. 2013. Light fastness and high-temperature stability of thermochromic printing inks. *Coloration Technology*, 129, 214-222.
- FRUMKIN, S. & WEISS, M. 2012. Fabrics and new product development. *In: HORNE, L. (ed.) New product development in textiles: innovation and production*. Oxford: Woodhead Pub Ltd.
- GANSLANDT, R. D. & HOFMANN, H. 1992. *Handbook of Lighting Design*, Braunschweig/Wiesbaden, ERCO
- GERBER, A. n.d. *King Fahad National Library* [Online]. <https://http://www.gerberarchitekten.de/en/project/king-fahad-national-library/>. 10 february 2017].
- GIBILISCO, S. 2001. *The illustrated dictionary of electronics*, New York, McGraw-Hill.
- GÖK, M. O., BILIR, M. Z. & GÜRCÜM, B. H. 2015. Shape-Memory Applications in Textile Design. *Procedia - Social and Behavioral Sciences*, 195, 2160-2169.
- GOLDSTEIN, B., E 2010. *Sensation and perception*, Belmont, CA, Wadsworth, Cengage Learning.
- GORDON, P., RUSSEL, T., STEVE, B. & JOHN, T. 2014. An investigation into the durability of screen-printed conductive tracks on textiles. *Measurement Science and Technology*, 25.
- GRADO ZERO ESPACE. n.d. *Oricalco* [Online]. <http://www.gradozero.eu/gzenew/index.php?pg=oricalco&lang=en>. [Accessed 2 September.
- GUO, L., BASHIR, T., BRESKY, E. & PERSSON, N. 2016. Electroconductive textiles and textile-based electromechanical sensors - integration in as an approach for smart textiles. *In: KONCAR, V. (ed.) Smart textiles and their applications*. Amsterdam: Woodhead Publishing.
- HARTL, D. J. & LAGOUDAS, D. C. 2008. Thermomechanical Characterization of Shape Memory Alloy Materials. *In: LAGOUDAS, D. C. (ed.) Shape memory alloys: modeling and engineering applications*. New York: Springer.
- HESSELBACH, J. 2007. Shape Memory Actuators. *In: JANOCHA, H. (ed.) Adaptronics and smart structures: basics, materials, design and applications*. Berlin: Springer, 145 - 163.
- HONKALA, M. 2006. Introduction to shape memory materials. *In: MATTILA, H. R. (ed.) Intelligent textiles and clothing*. Cambridge: Woodhead, 85-103.
- HU, E., KAYNAK, A. & LI, Y. 2005. Development of a cooling fabric from conducting polymer coated fibres: proof of concept

. *Synthetic Metals*, 150(2).

- HU, J. 2007. *Shape memory polymers and textiles*, Cambridge, Woodhead in association with Textile Institute.
- HU, J. & MENG, Q. 2011. Functional shape memory textiles. In: PAN, N. & SUN, G. (eds.) *Functional textiles for improved performance, protection and health*. Oxford: Woodhead Publishing.
- HUANG, W. M., DING, Z., WANG, C. C., WEI, J., ZHAO, Y. & PURNAWALI, H. 2010. Shape memory materials. *Materials Today*, 13(7-8), 54-61.
- HUANG, W. M., YANG, B., AN, L., LI, C. & CHAN, Y. S. 2005. Water-driven programmable polyurethane shape memory polymer: Demonstration and mechanism. *Applied Physics Letters*, 86, 114105.
- HUMBEECK, J. V. 2009. Shape Memory Alloys. In: SCHWARTZ, M. M. (ed.) *Smart Materials*. Boca Raton: CRC Press.
- IBRAHIM, W. 2012. *An Investigation into Textile Applications of Thermochromic Pigments*. PhD thesis, Heriot-Watt University.
- INNES, M. 2012. *Lighting for Interior Design*, London, Laurence King Publishing.
- JANI, J. M., LEARY, M., SUBIC, A. & GIBSON, M. A. 2014. A review of shape memory alloy research, applications and opportunities. *Materials and Design*, 56, 1078-1113.
- JIN, H., MATSUHISA, N., LEE, S., ABBAS, M., YOKOTA, T. & SOMEYA, T. 2017. Enhancing the Performance of Stretchable Conductors for E-Textiles by Controlled Ink Permeation. *Advanced Materials*, 29, 1605848-n/a.
- KALAT, J. W. 2007. *Biological psychology*, Belmont, CA, Thomson/Wadsworth.
- KARLEN, M., BENYA, J. & SPANGLER, C. 2012. *Lighting Design Basics*, Hoboken, NJ, John Wiley.
- KAZANI, I. 2012. *Study of Screen-Printed Electroconductive Textile Materials*. PhD thesis, University of Ghent.
- KETTLEY, S. 2016. *Designing with Smart Textiles*, London, Fairchild Books Bloomsbury
- KIRSTEIN, T. 2013. The future of smart-textiles development: new enabling technologies, commercialization and market trends. In: KIRSTEIN, T. (ed.) *Multidisciplinary know-how for smart textiles developers*. Oxford: Woodhead Publishing.
- KO, F., AUFY, A., LAM, H. & MACDIARMID, A. 2005. Electrostatically generated nanofibres for wearable electronics. In: TAO, X. (ed.) *Wearable Electronics and Photonics*. Cambridge: Woodhead Publishing.
- KONCAR, V. 2016. Introduction to smart textiles and their applications. In: KONCAR, V. (ed.) *Smart textiles and their applications*. Amsterdam: Woodhead Publishing.
- KOOROSHNIJA, M. 2011. *Mask* [Online]. <http://hb.diva-portal.org/smash/record.jsfpid=diva2%3A884770&dsid=-1987-sthash.yMQPONI7.dpbs>: University of Borås. 19 march 2017].
- KRIES, M. & KUGLER, J. 2013. *Lightopia*, Weil am Rhein, Vitra Design Museum.
- KULČAR, R., FRIŠKOVEC, M., GUNDE, M. K. & KNEŠAUREK, N. 2011. Dynamic colorimetric properties of mixed thermochromic printing inks. *Coloration Technology*, 127, 411-417.
- KULČAR, R., FRIŠKOVEC, M., HAUPTMAN, N., VESEL, A. & GUNDE, M. K. 2010. Colorimetric properties of reversible thermochromic printing inks. *Dyes and Pigments*, 86 (3), 271-277.
- KULČAR, R., GUNDE, M. K. & NINA KNEŠAUREK, N. 2012. Dynamic Colour Possibilities and Functional Properties of Thermochromic Printing Inks. *acta graphica*, 23, 25-36.
- KUMAR, L. & VIGNESWARAN, C. 2016. *Electronics in textiles and clothing: design, products and applications*, Boca Raton, FL, CRC Press, Taylor & Francis Group.
- KUMAR, P. K. & LAGOUDAS, D. C. 2008. Introduction to Shape Memory Alloys. In: LAGOUDAS, D. C. (ed.) *Shape memory alloys: modeling and engineering applications*. New York: Springer, 1-51.
- LAH, A. Š., FAJFAR, P., LAVRIČ, Z., BUKOŠEK, V. & RIJAVEC, T. 2016. Preparation of Shape Memory NiTiNOL Filaments for Smart Textiles. *Tekstilec*, 59, 168-174.
- LAM, W. 1992. *Perception and lighting as formgivers for architecture*, New York, Van Nostrand Reinhold.

- LANDIN, H. & WORBIN, L. The fabrication bag - an accessory to a mobile phone. *Ambience* 05, 2005 Tampere, Finland.
- LANGENHOVE, L. V. 2015. Smart Textiles: Past, Present, and Future. *In: TAO, X. (ed.) Handbook of Smart Textiles*. Singapore: Springer.
- LASCHUK, T. 2008. *Application of smart textiles to fashion textile products*. Master Thesis, University of Minho.
- LASCHUK, T. & SOUTO, A. P. Incorporation of SMA technologies in fashion underwear apparel. *Ambience* 08, 2-3 June 2008 2008. 215-218.
- LAWSON, B. C. 2016. *Shape Memory Alloys, Muscle Wires and Robotics*, S.I., CreateSpace.
- LECHNER, N. 2015. *Heating, cooling, lighting: sustainable design methods for architects*, New Jersey, John Wiley & Sons.
- LEDENDAL, M. 2015. *Thermochromic textiles and sunlight activating systems: an alternative means to induce colour change*. PhD thesis, Heriot-Watt University.
- LEE, S. 2005. *Fashioning the Future: Tomorrow's Wardrobe*, London, Thames & Hudson.
- LEENDERS, L. 2000. *Shape Memory Textiles* [Online]. <http://photorepeats.com/en/work/shape-memory-textiles/>. [Accessed 3 September.
- LENDLEIN, A., JIANG, H., JUNGER, O. & LANGER, R. 2005. Light-induced shape-memory polymers. *Nature*, 434, 879-882.
- LEXCELLENT, C. 2013. *Shape-Memory Alloys Handbook*, Hoboken, NJ, ISTE Ltd/John Wiley and Sons Inc.
- LI, Q. & TAO, X. 2015. Fabric Substrates and Interconnectors for Three-Dimensional Surfaces. *In: TAO, X. (ed.) Handbook of Smart Textiles*. Singapore: Springer.
- LIN, S. 2015. Fiber-Based Wearable Electronic Circuits and Systems. *In: TAO, X. (ed.) Handbook of Smart Textiles*. Singapore: Springer.
- LIU, X., WANG, Y., YANG, D. & QI, M. 2008. The effect of ageing treatment on shape-setting and superelasticity of a nitinol stent. *Materials Characterization*, 59, 402-406.
- LIU, Y. 2010. Some factors affecting the transformation hysteresis in shape memory alloys. *In: CHEN, H. R. (ed.) Shape Memory Alloys: Manufacture, Properties and Applications*. New York: Nova Science Publishers.
- LOCHER, I. 2013. Joining technologies for smart textiles. *In: KIRSTEIN, T. (ed.) Multidisciplinary know-how for smart textiles developers*. Oxford: Woodhead Publishing.
- MAACK, T. & PAWLIK, K. 2009. *Light perspectives between culture and technology*, Lüdenscheid, Erco.
- MARCQ, C. 2014. *Dynamic prints* [Online]. <http://etextile-summercamp.org/2015/dynamic-prints/>. [Accessed 27 september 2015.
- MASAYASU, K., OSAMU, S., SHOUZOU, S. & TATSUYA, M. 1992. *Dyeing method and dyed product*.
- MATSUHIRA, N., KALTENBRUNNER, M., YOKOTA, T., JINNO, H., KURIBARA, K., SEKITANI, T. & SOMEYA, T. 2015. Printable elastic conductors with a high conductivity for electronic textile applications. *Nature Communications*, 6, 7461.
- MATSUI n.d. Aqualite Coloring system.
- MATTILA, H. R. 2006. Intelligent textiles and clothing – a part of our intelligent ambience. *In: MATTILA, H. (ed.) Intelligent textiles and clothing*. Cambridge: Woodhead Publishing.
- MBISE, E., DIAS, T. & HURLEY, W. 2015. Design and manufacture of heated textiles. *In: DIAS, T. (ed.) Electronic Textiles*. Cambridge: Elsevier Science & Technology.
- MCAULIFFE, M. 2016. *The perception of light*, London, Oxford Global Press.
- MCQUAID, M. 2005. *Extreme textiles: designing for high performance*, New York, Smithsonian Cooper-Hewitt, National Design Museum.
- MECNIKA, V., SCHEULEN, K., ANDERSON, C., HÖRR, M. & BRECKENFELDER, C. 2015. Joining technologies for electronic textiles. *In: DIAS, T. (ed.) Electronic Textiles*. Cambridge: Elsevier Science & Technology.

- MEHMANN, A., VARGA, M. & TRÖSTER, G. 2017. Reversible Contacting for Smart Textiles. *In: SCHNEEGASS, S. & AMFT, O. (eds.) Smart Textiles: Fundamentals, Design, and Interaction*. Cham: Springer International Publishing, 185-198.
- MEMRY. n.d.-a. *Joining of Nitinol* [Online]. <http://www.memry.com/nitinol-iq/nitinol-fundamentals/joining>. [Accessed 11 January 2014].
- MEMRY. n.d.-b. *Nitinol Wire* [Online]. <http://www.memry.com/products-services/material/wire>. [Accessed 20 March 2013].
- MEMRY. n.d.-c. *Surface Finishing, Coating & Plating of Nitinol* [Online]. <http://www.memry.com/nitinol-iq/nitinol-fundamentals/surface-finishing-coating-plating>. [Accessed 11 January 2014].
- MIAO, M. 2015. Carbon nanotube yarns for electronic textiles. *In: DIAS, T. (ed.) Electronic Textiles*. Cambridge: Elsevier Science & Technology.
- MICHALAK, M., BILSKA, J., KRUCIŃSKA, I., ZIĘBA, J. & GNIOTEK, K. 2013. *Siłownik termiczny (thermal actuator)*.
- MICHALAK, M. & KRUCIŃSKA, I. 2015. A smart fabric with increased insulating properties. *Textile Research Journal*.
- MOSSÉ, A. 2016. Self-actuated textiles, interconnectivity, and the design of the home as a more sustainable timescape. *In: SCHNEIDERMAN, D. & WINTON, A. (eds.) Textile technology and design: from interior space to outer space*. New York: Bloomsbury Academic.
- NDC. n.d. *Nitinol Facts: Surface Finishes* [Online]. <http://www.nitinol.com/nitinol-university/nitinol-facts>. [Accessed 11 January 2014].
- NGO, S. & LAM, N. 2010. *Warning Signs* [Online]. <http://www.itp.nyu.edu/~sn964/SueITPblog/wearables-finalwarning-signs/>. [Accessed 30 April 2013].
- NILSSON, L., SATOMI, M., VALLGÅRDA, A. & WORBIN, L. Understanding the complexity of designing dynamic textile patterns. Proceedings of the Ambience conference, 2011 Borås, Sweden.
- NOVÁK, V., ŠITTNER, P., DAYANANDA, G. N., BRAZ-FERNANDES, F. M. & MAHESH, K. K. 2008. Electric resistance variation of NiTi shape memory alloy wires in thermomechanical tests: Experiments and simulation. *Materials Science and Engineering*, 481-482, 127-133.
- NUNO. n.d. *About Nuno* [Online]. <https://http://www.nuno.com/en/about/>: Nuno Corporation. [Accessed 20 October 2015].
- NURVEREN, K., AKDOĞAN, A. & HUANG, W. M. 2008. Evolution of transformation characteristics with heating/cooling rate in NiTi shape memory alloys. *Journal of Materials Processing Technology*, 196, 129-134.
- OJAVEE, K. & OZSVALD, E. 2012. SymbiosisS. *Leonardo*, 45, 388-389.
- ORTH, M. 2010. *Blip, 2010* [Online]. http://www.maggiearth.com/art_Blip.html. [Accessed 23 January 2013].
- OTSUKA, K. & KAKESHITA, T. 2002. Science and Technology of Shape-Memory Alloys: New Developments. *MRS Bulletin*, 27, pp.01-100.
- OTSUKA, K. & WAYMAN, C. M. 1998. *Shape memory materials*, Cambridge, Cambridge University Press.
- PAILES-FRIEDMAN, R. 2016. *Smart textiles for designers: inventing the future of fabrics*, London, Laurence King Publishing.
- QU, H. & SKOROBOGATIY, M. 2015. Conductive polymer yarns for electronic textiles. *In: DIAS, T. (ed.) Electronic Textiles*. Cambridge: Elsevier Science & Technology.
- QUINN, B. 2010. *Textile futures: fashion, design and technology*, Oxford, Berg.
- RAKSHIT, A. & HIRA, M. 2014. Electrically conductive fibre substrates. *International Journal of Fiber and Textile Research*, 4, 44-48.
- RAO, A., SRINIVASA, A. R. & REDDY, J. N. 2015. *Design of Shape Memory Alloy (SMA) Actuators*, Cham, Springer International Publishing.

- RHODES, E. 1991. *To Dye For Hypercolor Clothes Heating Up Market For Maker Generra* [Online]. <http://community.seattletimes.nwsources.com/archive: The Seattle Times>. [Accessed 3 February 2013].
- RIJAVEC, T. & BRAČKO, S. 2007. Smart dyes for medical and other textiles. *In: LANGENHOVE, L. V. (ed.) Smart Textiles for Medicine and Healthcare: Materials, Systems and Applications*. Cambridge: Woodhead Publishing.
- RITTER, A. 2007. *Smart materials in architecture, interior architecture and design*, Basel, Birkhäuser.
- ROBERTSON, S. 2011. *An Investigation of the Design Potential of Thermochromic Textiles used with Electronic Heat-Profiling Circuitry*. PhD thesis, Heriot-Watt University.
- ROTTIERS, W., VAN DEN BROECK, L., PEETERS, C. & ARRAS, P. Shape memory materials and their applications. Korolev's Readings, 2011 Samara, Russia. Samara State Aerospace University.
- RUBACHA, M. 2007. Thermochromic cellulose fibers. *Polymers for Advanced Technologies*, 18, 323-328.
- SALAÜN, F. 2016. Microencapsulation technology for smart textile coatings. *In: HU, J. (ed.) Active Coatings for Smart Textiles*. Oxford: Woodhead Publishing.
- ŠALEJ, A., BOMBAČ, D., FAJFAR, P. & RIJAVEC, T. 2011. Application of Nickel-Titanium alloys (NiTi-NOL) in textiles and clothes. *Tekstil: Journal of Textile & Clothing Technology*, 60, 123-131.
- SCHNEEGASS, S. & AMFT, O. 2017. Introduction to Smart Textiles. *In: SCHNEEGASS, S. & AMFT, O. (eds.) Smart Textiles: Fundamentals, Design, and Interaction*. Cham: Springer International Publishing, 1-15.
- SCHWARTZ, M. M. 2002. *Encyclopedia of smart materials*, New York, J. Wiley.
- SCHWARZ, A. & LANGENHOVE, L. V. 2013. Types and processing of electro-conductive and semiconducting materials for smart textiles. *In: KIRSTEIN, T. (ed.) Multidisciplinary know-how for smart textiles developers*. Oxford: Woodhead Publishing.
- SEAR, F. 2008. *Roman architecture*, London, Routledge.
- SEEBOTH, A. & LÖTZSCH, D. 2008. *Thermochromic phenomena in polymers*, Shrewsbury, Smithers Rapra.
- SEEBOTH, A. & LÖTZSCH, D. 2013. *Thermochromic and thermotropic materials*, Singapore, Pan Stanford.
- SEYMOUR, S. 2008. *Fashionable technology: the intersection of design, fashion, science, and technology*, Wien, Springer.
- SEYMOUR, S. 2010. *Functional aesthetics: visions in fashionable technology*, Wien, Springer.
- SHABALOVSKAYA, S., ANDEREGG, J. & VAN HUMBEECK, J. 2008. Critical overview of Nitinol surfaces and their modifications for medical applications. *Acta Biomaterialia*, 4, 447-467.
- SHIM, E. 2010. Coating and laminating processes and techniques for textiles. *In: SMITH, W. C. (ed.) Smart Textile Coatings and Laminates*. Cambridge: Woodhead Publishing, 10-41.
- SONG, H., KUBICA, E. & GORBET, R. Resistance modelling of SMA wire actuators. Smart Materials, Structures & NDT in Aerospace, 2011 Quebec, Canada.
- STOPPA, M. & CHIOLERIO, A. 2014. Wearable Electronics and Smart Textiles: A Critical Review. *Sensors*, 14, 11957.
- STOREY, N. 2009. *Electronics: a systems approach*, Harlow, Pearson Education Limited.
- STYLIOS, G. K. 2006. Engineering textile and clothing aesthetics using shape changing materials. *In: MATTILA, H. R. (ed.) Intelligent textiles and clothing*. Cambridge: Woodhead, 165-190.
- SUGANUMA, K. 2014. *Introduction to Printed Electronics*, New York, Springer.
- SUN, L., HUANG, W. M., DING, Z., ZHAO, Y., WANG, C. C., PURNAWALI, H. & TANG, C. 2012. Stimulus-responsive shape memory materials: A review. *Materials and Design*, 33, 577-640.
- TALVENMA, P. 2006. Introduction to chromic materials. *In: MATTILA, H. (ed.) Intelligent Textiles and Clothing*. Cambridge: Woodhead, 193-205.
- TAO, X. 2001. Smart technology for textiles and clothing – introduction and overview. *In: TAO, X. (ed.) Smart fibres, fabrics and clothing: fundamentals and applications*. Cambridge: Woodhead.

- TAO, X. & KONCAR, V. 2016. Textile electronic circuits based on organic fibrous transistors. *In: KONCAR, V. (ed.) Smart textiles and their applications*. Amsterdam: Woodhead Publishing.
- TONG, J. & LI, L. 2015. Thermal Regulation of Electrically Conducting Fabrics. *In: TAO, X. (ed.) Handbook of Smart Textiles*. Singapore: Springer.
- TOPRAKCI, H. & GHOSH, T. 2015. Textile Sensors. *In: TAO, X. (ed.) Handbook of Smart Textiles*. Singapore: Springer.
- TORAH, R., WEI, Y., L, Y., YANG, K., BEEBY, S. & TUDOR, J. 2015. Printed Textile-Based Electronic Devices. *In: TAO, X. (ed.) Handbook of Smart Textiles*. Singapore: Springer.
- TURRELL, J. n.d. *Two Blues (2008)* [Online]. <http://jamesturrell.com/work/two-blues/>. 8 February 2017].
- UGUR, S. 2013. *Wearing Embodied Emotions: A Practice Based Design Research on Wearable Technology*, Springer Publishing Company, Incorporated.
- VALLGÅRDA, A. 2014. Giving form to computational things: developing a practice of interaction design *Personal and Ubiquitous Computing*, 18(3), 577-592.
- VARGA, M. 2017. Electronics Integration. *In: SCHNEEGASS, S. & AMFT, O. (eds.) Smart Textiles: Fundamentals, Design, and Interaction*. Cham: Springer International Publishing, 161-184.
- VASILE, S., GRABOWSKA, K. E., CIESIELSKA, I. L. & GITHAIGA, J. 2010. Analysis of Hybrid Woven Fabrics with Shape Memory Alloys Wires Embedded. *FIBRES & TEXTILES in Eastern Europe*, 18 (1), 64-69.
- VEJA, P. 2014. *An investigation of integrated woven electronic textiles (e - - textiles) via design led processes*. PhD thesis, Brunel University.
- VILI, Y. Y. F. C. 2007. Investigating Smart Textiles Based on Shape Memory Materials. *Textile Research Journal*, 77, 290-300.
- VOKOUN, D., SEDLÁK, P., FROST, M., PILCH, J., MAJTÁS, D. & SITTNER, P. 2011. Velcro-like fasteners based on NiTi microhook-arrays. *Smart Materials and Structures*, 20.
- WAGNER, M. 2013. Automotive applications of smart textiles. *In: KIRSTEIN, T. (ed.) Multidisciplinary know-how for smart textiles developers*. Oxford: Woodhead Publishing.
- WAN, T. & STYLIOS, G. K. 2007. Shape memory training for smart fabrics. *Transactions of the Institute of Measurement and Control*, 29, 321-336.
- WANG, L., WANG, X. & LIN, T. 2010. Conductive coatings for textiles. *In: SMITH, W. C. (ed.) Smart Textile Coatings and Laminates*. Cambridge: Woodhead Publishing.
- WANG, Z., VOLAKIS, J. & KIOURTI, A. 2015. Embroidered antennas for communication systems. *In: DIAS, T. (ed.) Electronic Textiles*. Cambridge: Elsevier Science & Technology.
- WARMX. n.d. *Smart textiles - product development around textile current circuits* [Online]. <http://www.warmx.de/index.php/industry-and-research.html>. [Accessed 25 october 2015].
- WEISER, M. 1991. The computer for the 21st Century. *Scientific American*, 265(3), 66-75.
- WILSON, J. & MATHER, R. 2015. Photovoltaic energy harvesting for intelligent textiles. *In: DIAS, T. (ed.) Electronic Textiles*. Cambridge: Elsevier Science & Technology.
- WINCHESTER, R. C. C. & STYLIOS, G. K. 2003. Designing knitted apparel by engineering the attributes of shape memory alloy. *International Journal of Clothing Science and Technology*, 15, 359-366.
- WORBIN, L. 2010. *Designing dynamic textile patterns*. Doctoral Thesis, University of Borås.
- WU, M. & SCHETKY, L. Industrial applications for shape memory alloys. International Conference on Shape Memory and Superelastic Technologies, 2000 Pacific Grove, California. 171-182.
- WU, X. D., FAN, Y. Z. & WU, J. S. 2000. A study on the variations of the electrical resistance for NiTi shape memory alloy wires during the thermo-mechanical loading. *Materials and Design*, 21, 511-515.
- XUE, P., TAO, X., LEUNG, M.-Y. & ZHANG, H. 2005. Electromechanical properties of conductive fibres, yarns and fabrics. *In: TAO, X. (ed.) Wearable Electronics and Photonics*. Cambridge: Woodhead Publishing.
- YANG, K., TORAH, R., WEI, Y., BEEBY, S. & TUDOR, J. 2013. Waterproof and durable screen printed silver conductive tracks on textiles. *Textile Research Journal*, 83, 2023-2031.

- YEDURU, S. 2013. *Development of Microactuators Based on the Magnetic Shape Memory Effect*, Karlsruhe, Baden, KIT Scientific Publishing.
- YOKUS, M. A., FOOTE, R. & JUR, J. S. 2016. Printed Stretchable Interconnects for Smart Garments: Design, Fabrication, and Characterization. *IEEE Sensors Journal*, 16, 7967-7976.
- YOT, R. 2011. *Light for visual artists: understanding & using light in art & design*, London, Laurence King.
- ZENG, W., SHU, L., LI, Q., CHEN, S., WANG, F. & TAO, X.-M. 2014. Fiber-Based Wearable Electronics: A Review of Materials, Fabrication, Devices, and Applications. *Advanced Materials*, 26, 5310-5336.
- ZHENG, Y., CUI, L. & SCHROOTEN, J. 2004. Temperature memory effect of a nickel–titanium shape memory alloy. *Applied Physics Letters*, 84, 31-33.
- ZYSSET, C., KINKELDEI, T., MÜNZENRIEDER, N., TRÖSTER, G. & CHERENACK, K. 2013. Fabrication technologies for the integration of thin-film electronics into smart textiles. *In: KIRSTEIN, T. (ed.) Multidisciplinary know-how for smart textiles developers*. Oxford: Woodhead Publishing.

MATERIALS AND METHODS

CHAPTER 3

CHAPTER 3. MATERIALS AND METHODS

3.1 Introduction

This chapter describes the materials, equipment and methods applied in the experimental work of the present research. The first section introduces a detailed description of the materials handled. The second section presents the equipment and procedures involved in the samples and research prototypes' manufacturing, their properties evaluation and dynamic behaviour analysis.

3.2 Materials

3.2.1 Textile Materials

The textile substrate applied in the experimental studies with TC leuco dyes and samples screen printed with conductive pigments was a 50% cotton (CO) 50% polyester (PES) plain weave substrate, 115 g/m², 15,0 and 15,5 warp and weft yarns (tex), with a density of 41 ends/cm and 31 picks/cm. This selection was held in order to also conduct a pre-study of folded structures with the same substrate: textile plain weave is a stable structure to develop creases in different directions due to the regular and maximum number of interlacings of the weave fabrics; the selection of a high density yarn substrate and thin enables the creation of sharp creases; and the selection of 50% synthetic fibre (PES) allows the development of permanent creases and resistant to wash.

For the development of a TC study prototype presented in section 4.6, an additional substrate was used: 100% CO 3/1 twill weave, 190g/m², 25 (tex) warp and weft yarns, with a density of 46 ends/cm and 25 picks/cm.

In the experimental studies of Nitinol integration in textile woven substrates, development of electroconductive samples with conductive threads and research prototypes, diverse textile yarns were used in the weaving processes. The warp and weft yarns handled are described in the looms' section (3.3.5), according to each equipment setup.

3.2.2 Pigments

Pigments are defined as insoluble compounds that, when combined with a suitable medium, can be applied to textiles through diverse printing processes. In this work, the pigments handled comprises of three types: conventional, thermochromic (TC) and conductive pigments.

The conventional pigments Atusmic Magnaprint eco used were: yellow HR, orange HD, red HB, pink H5 B, blue HB and black H3B.

The TC pigments handled were the Varioterm AC Base 27 (27°C heat sensitive pigment) in orange (arancio oro), red (vermiglio), magenta, blue (blu nuovo solido) and black (nero solido). The selection of the pigments' variation temperature took into consideration the objective of studying colour change activation through resistive heating and thus, a value below the average ambient temperature in interior spaces was selected.

Two conductive pigments were handled in this research: Dupont PE825 silver-based composite conductor and Bareconductive carbon-based electrical paint.

3.2.3 Binders

Screen printing pastes with TC and conventional pigments were formulated with vinyl acrylic binders, having being used two brands: Atusmic Magnaprint ND extra and Gilaba.

3.2.4 Finishing agents

Diverse finishing agents were handled according to the applications' objectives described in each section. The materials used were: aqueous emulsion vinyl acetate Aktilem 14000; Aqueous emulsions acrylic 13002; aqueous polyurethane dispersion Tanacoat OMP; polyacrylate thickener agent Acraconc 2C-N; polytetrafluoroethylene (PTFE) aqueous dispersion; fluoroalkyl acrylate copolymer Baygard AFF 300% 01 and an insulating agent with an alkyd resin base.

3.2.5 Dyes

Dyes are soluble colourants with different affinity degrees for textile fibres and they are commonly dissolved in a water solution in order to be applied in textiles (Mahapatra, 2016). For a comparative analysis of TC and conventional colourants combination applied to textiles by different processes, two dyes were used: Dianis

orange SG 200% disperse dye, regarding PES fibres of the textile substrate handled; and Levafix orange CA gran reactive dye for CO fibres.

3.2.6 SMAs

The Nitinol wires handled in this research were supplied by Saes Getters, with three diameters: 0,2; 0,3 and 0,5mm. The SMA transformation temperature selected is body-temperature $A_s +30^{\circ}\text{C}$ and $A_f +45^{\circ}\text{C}$. With the objective to anneal the alloys with specific shapes, they were purchased in as drawn state.

3.2.7 Conductive threads

A set of twenty-eight conductive threads were collected and applied in the development of electrical conductive woven samples, to study colour change activation through the threads' resistive heating. After, one conductive thread was selected for the research prototypes development. The conductive threads handled were listed in Table 1 and a brief description of each thread type is presented in Appendix A, according to the suppliers and/or technical data sheet specifications.

Table 1. Conductive threads' list.

1 - Bekinox VN 12/1x275/100Z	15 - Shieldex 110/34 2ply HC+B
2 - Bekinox VN 12/4x275/100S	16 - Elinox SPP 35 300Z
3 - Bekintex BK 50/2	17 - Elinox PES HT 1100 + VN 60 400 t S/Z
4 - Bekintex BK 50/1	18 - LessEmf silver plated nylon
5 - Bekintex VN 14/2X90/175S/HT/PFA	19 - Lamé LifeSaver
6 - Bekiflex CA 63/8X7/80S/0.245/PFA	20 - Linox
7 - High Flex 3981 7X1 Silver	21 - Sparkfun stainless steel 2ply
8 - High Flex 3981 7x1 Kupfer Blank	22 - Sparkfun stainless steel 4ply
9 - Constantan High-Flex 8394 7×1	23 - Copper monofilament 100 μm
10 - Elitex 235/f34 PA/Ag	24 - Insulated copper monofilament 160 μm
11 - Elitex Garn Art I TPU 667_235/f34 PA/Ag	25 - Stainless steel monofilament 50 μm
12 - Elitex 110/f34/2ply PA/Ag	26 - Nichrome monofilament 200 μm
13 - Elitex (Lycra)	27 - Plug and Wear Nm10/3
14 - Shieldex 235/34x4 HC+E	28 - SilverSpun

3.3 Equipment and Methods

3.3.1 Screen printing table

Screen printing consists of pulling over dyestuff through the open areas of a screen mesh to a substrate (Dickinson, 2011). In this research, flat-screen printing processes were conducted on a Zimmer Mini MDF R541 table. This equipment presents several setting options, which were defined to maintain constant in all screen printing samples developed with TC and conventional pigments. The magnetic field level defines the pressure that the metallic rod-squeegee does during paste application on the textile substrate. Level 3 was selected from a range of one to six, low to higher pressure. It is also possible to select the speed of paste application from 0 to 100% of a graded dial and 50% was defined (approximately 7,5 m/min.). Furthermore, the rods used had 12 mm diameter and the table was setup with the high diameter parameter of the two options available.

For each sample developed, a screen was placed above the textile substrate and a screen printing paste previously prepared and mixed with a stirrer, was applied in one layer. After drying, the samples were thermo-fixed in a laboratory oven with time and duration parameters according to the materials applied. The mesh count of the screens used in the studies was described in threads per inch (TPI), in each experimental section.

The studies developed with conductive pigments have tested different options of the screen-printing table and will be described in the respective sections.

3.3.2 Dyeing machine

Dyeing processes were conducted in Ibelus C720 equipment with a programmable controller for the following settings: temperature, time and rotation. The parameters selected depend upon the dyeing programs, which will be described in the experimental sections.

3.3.2 Coating table

Textile coating is a finishing process that imparts the substrate with new or improved functional and/or aesthetic characteristics, through the surface deposition of a material (Sen, 2008; Shim, 2010). In this work, knife coating processes were conducted using a Mathis laboratory coating device type SV with a knife-over-

roll cylinder. Each sample was placed in the pin frame, the micrometre was set at 0,5 mm and each paste was applied with a coating knife shape A.

3.3.4 Furnace

Nitinol annealing processes were developed in a Naber D-2804 furnace. Various experiments were conducted at different temperatures during different time periods, as will be described in the experimental sections.

3.3.5 Looms

In this research, the textile substrates were produced in woven structures. The weaving process comprises of the interlacing of two yarn systems: the warp, oriented along the fabric length of the production direction; and the weft, perpendicular to the warp, in the fabric width. (Humphries, 2008; Behera and Hari, 2010). Woven fabrics can be produced within diverse weave patterns, in this work all samples were woven in a plain weave structure and Nitinol wires were integrated manually in the weft.

The weaving processes were developed in three looms:

- a) Initially a table handloom was used, set up with 3/24 CO yarn (148,7 Tex) warp, 16 ends/cm. In the weft, the same yarn was used and the samples presented 12 picks/cm. The width of the warp was 12 cm;
- b) After initial experiments, the samples were woven in an electronic Jacquard loom with 3456 hooks and a Bonas Series 200 Controller. During this research time frame, the loom warp was changed. The first setup had a 30,8 Tex CO (unbleached) yarn with a density of 38 ends/cm in the warp and in the weft it was used 17,7 Tex PES yarn accomplishing 11 picks/cm. The second setup presented a 17 Tex PES texturized yarn with 3 x 30 cm of black, white and grey yarn colours width and a density of 38 ends/cm. A 25,0 Tex CO (bleached) yarn was used in the weft, with a density of 11 picks/cm. In the experimental section, the respective loom setups will be reported.

In this loom, it was not possible to program the interruption of the weft insertion according to the predefined geometry of the Nitinol integration. The weaving process was conducted in slow mode, in order to ensure the number of textile picks in between the SMAs wires;

- c) Samples woven through a programmed interruption of the weft insertion were developed in the weaving laboratory at The Swedish School of Textiles, University of Borås, Sweden. The equipment

used was a Jacquard Vamatex SD 1701 loom of 5280 hooks, with a Grosse controller and ScotWeave CAD software.

The warp had 41,2 Tex CO (unbleached) yarn with a density of 33 ends/cm and the weft had 14 picks/cm with 14,7 Tex PES yarn. The warp width was 160 cm and the pattern definition contemplates a maximum of 1320 ends within 4 times repetition and a maximum of 2000 picks.

The warp yarn was also substituted during this research path, for a 38,7 Tex bleached CO yarn. The remaining weaving characteristics were equal.

3.3.6 Lux meter

To analyse the light transmittance variation, a light box with a 28 x 18 cm aperture was used to place the textile samples and the light intensity was measured with a DeltaOhm – HD 2302.0 luxmeter. The experiments were conducted with different setups as will be described in the experimental sections.

3.3.7 Spectrophotometer

A spectrophotometer Datacolor International, SF600 Plus – CT with Datacolor Match 3.4 software was used to conduct spectral reflectance measurements, data analysis and paste recipes formulation. This equipment measures the amount of light reflected at each wavelength of visible light spectrum (approximately 380 to 760 nm), according to the average colour on a defined aperture (Xin, 2006).

Previous to the measurements, the spectrophotometer was calibrated with a black trap and white tile. The measurements were developed with the illuminant D65, LAV/Specular Included, standard observer 10° and an aperture measurement of 9 mm. Each sample was measured in three points.

3.3.8 Crockmeter

A crockmeter was used to conduct dry and wet rub fastness test, according to ISO 105-X12 test method (ISO, 2001). Staining of the cotton rubbing fabric was measured in the reflectance spectrophotometer and evaluated from 1 to 5 standard grade scale.

3.3.9 Linitest

Wash fastness test was conducted in Linitest Original-Hanau equipment, according to ISO 105-C06 A1S method (ISO, 2010). Previous to the wash cycle, each test sample was attached to a multifibre fabric

composed of wool, acrylic, polyester, polyamide, cotton and acetate. After washing, the staining in each textile fibre area was evaluated by colour measurements using the reflectance spectrophotometer and evaluated from 1 to 5 standard grade scale.

3.3.10 Accelerated Weathering Tester QUV (AWT)

The equipment Accelerated Weathering Tester QUV was used for a comparative analysis of colour stability to UV light exposure of screen printed samples with TC and/or conventional pigments. The irradiation applied was 0,76W/m².

Taking into consideration the reported reduced light fastness that TC leuco dyes usually present (Talvenma, 2006; Ferrara and Bengisu, 2014), tests were performed for shorter periods of time than standard methods. It was defined to assess the samples after being exposed for 15min., 30 min., 1h, 2h, 4h and 8h. Furthermore, standard light fastness tests are conducted in a Xenotest equipment and apply a blue wool scale with the samples during exposure to light, in order to evaluate the fastness grades from 1 to 8 (Humphries, 2008). Due to the reduced periods of time follow, samples' colours were measured in the reflectance spectrophotometer and data was compared for CIELAB differences.

3.3.11 Power supply

Samples' activation through resistive heating was conducted with DC power supply. Two devices have been used: TENMA 72-8695 power supply and Velleman LABPS3003SM power supply.

3.3.12 Infrared (IR) camera

To study samples' temperature during resistive heating activation, thermal images were recorded with a Testo 876 Infrared camera and analysed with Testo IRSoft software.

3.3.13 Dynamometer

A Hounsfield H10KS dynamometer was used to study the resistance of the Nitinol wire to be removed from the textile host structure. The evaluation was conducted through a Breaking Strength and Elongation test at a loading rate of 5cm/min.

3.3.14 Viscometer

The pastes viscosity was measured in a Brookfield DV-E Viscometer with a LV spindle S4.

3.3.15 Thickness gauge

The measurement of the samples thickness was conducted with a Mitutoyo 7321 Thickness Gauge.

3.4 References

- BEHERA, B. K. & HARI, P. K. 2010. *Woven textile structure: theory and applications*, Boca Raton, CRC Press.
- DICKINSON, K. 2011. The use of colour in textile design. *In: BRIGGS-GOODE, A. & TOWNSEND, K. (eds.) Textile design: principles, advances and applications*. Oxford: Woodhead Publishing and The Textile Institute.
- FERRARA, M. & BENGISU, M. 2014. *Materials that change color: smart materials, intelligent design*, Cham, Springer International Publishing.
- HUMPHRIES, M. 2008. *Fabric reference*, Upper Saddle River, NJ, Prentice Hall.
- ISO 2001. Textile – Tests for colour fastness – Part X12: Colour fastness to rubbing. *ISO 105-X12*.
- ISO 2010. Tests for colour fastness – Part 06: Colour Fastness to domestic and commercial laundering. *ISO 105-C06*.
- MAHAPATRA, N. 2016. *Textile dyes and dyeing*, New Delhi, Woodhead Publishing India.
- SEN, A. K. 2008. *Coated textiles: principles and applications*, Boca Raton, CRC Press.
- SHIM, E. 2010. Coating and laminating processes and techniques for textiles. *In: SMITH, W. C. (ed.) Smart Textile Coatings and Laminates*. Cambridge: Woodhead Publishing, 10-41.
- TALVENMA, P. 2006. Introduction to chromic materials. *In: MATTILA, H. (ed.) Intelligent Textiles and Clothing*. Cambridge: Woodhead, 193-205.
- XIN, J. H. 2006. *Total Colour Management in Textiles*, Cambridge, Woodhead Publishing and The Textile Institute.

THERMOCHROMIC TEXTILES

CHAPTER 4

CHAPTER 4. THERMOCHROMIC TEXTILES

4.1 Colour

Throughout history, mans' great interest and study of colour shares common ground among the arts, design, technology and science. In textiles, colour is one of the main visual qualities and thus, a crucial variable in design and engineering research and practice.

Concerning diverse purposes such as aesthetic, communication, symbolic and functional, colour is imparted to textiles by mean of colourant substances, namely dyes and pigments (Nassau, 1998). Dyes are soluble compounds, able to migrate into textile fibres, while pigments are insoluble, thus requiring to be dispersed in a binder in order to be fixed onto the textile surface (Das, 2009; Mahapatra, 2016).

The use of colour in textiles is intrinsically related with colourant availability and the development of application methods. Early uses of colourants depended on vegetal, animal and mineral resources, defining the possibilities of colour palettes and also denoting value attributes. For example, the colour purple in Greco-Roman times, known as tyrian or imperial purple, was a symbol of status due to the labour process involved, namely the quantity of murex shellfish required to extract reasonable amounts of dye. Also, it did not show a fading effect when exposed to light (Eastaugh et al., 2004; Abel, 2012).

Extending the chromatics obtained directly from nature, ancient Egyptians' techniques are considered at the basis of the first synthetic inorganic pigments of which Egyptian blue pigment is an example. Although, it was only until the discovery of mauveine by William Perkin in 1856, that the synthetic dye industry was established and synthetic organic colourants for textiles underwent increased progress (Aspland, 1998; Abel, 2012).

Furthermore, dyeing and printing processes were developed over the centuries, such as dyeing techniques with mordants, batik, shibori, block and screen printing, which had also undergone accelerated developments during and after the industrial revolution (Clarke, 2011; Briggs-Goode, 2013). Innovation in science and technology domains has enabled the introduction of new colourant classes and development of new technologies to integrate and explore colour in textiles, also accompanied by the establishment of regulations that include environmental considerations and quality control (Hidefi, 2012).

The emergence of colour change materials allowed the introduction of chromatic dynamic qualities to textiles by sensing and reacting reversibly to a stimulus, such as the TC leuco dyes that respond to heat (Schwartz, 2002). The temporal and interactive dimensions of colours with these materials presented a shift in relation to

traditional textiles and opened up the potential to imbue textiles with new expressions, functions and interactions. At the same time, chromic textiles development also creates new demands in respect to different complexity levels of knowledge and competences in diverse domains, entailing new perspectives and challenges for design (Baurley, 2004; Worbin, 2010). Design research in this area highlight the importance of experimental exploration of the materials' behaviour, processes and technologies to integrate them in textiles and design methods to deeper research their potential (Worbin, 2010; Robertson, 2011).

To explore dynamic colour in textile design and research processes to develop TC textiles that change colour according to predefined ratios, it is also crucial to understand the foundations of colour theory and practice, contextualized as a phenomena that involves interaction of light with materials, detected by the eye and interpreted in the brain (Lennie, 2003; Dickinson, 2011).

The human visual system is able to detect and process a portion of the electromagnetic spectrum with wavelengths between approximately 380 and 740 nm, correspondent to visible light (Choudhury, 2014b). Incident light on objects can be reflected (opaque materials) or transmitted (translucent or transparent materials), depending on the selective absorption of light wavelengths (Yot, 2011; Kuehni, 2012). The colour stimulus is thus defined by the radiant energy of the wavelengths range reflected from the materials into the eye, which depends on the spectral composition of the incident light and materials' optical characteristics (Tilley, 2000; Descottes and Ramos, 2011). With TC leuco dyes, temperature variation changes the substances' molecular arrangement affecting their spectral reflectance, thus colour change is perceived (Bamfield and Hutchings, 2010).

When colours are combined, different phenomena occur in regards to the medium involved. Mixing light beams of different colours result in the wavelength addition of each light beam, a process called additive colour mixing. Subtractive colour mixtures respect to the combination of dyes or pigments, where each colour added causes more light wavelengths to be absorbed and consequently less light is reflected into the eye. Therefore, subtractive mixtures are darker than their individual components and the inverse occurs with additive mixtures (Tilley, 2000; Hanson, 2012; Choudhury, 2014b).

According to TC pigments' intrinsic behaviour from coloured to colourless when heated, TC mixtures are darker below the pigments' activation temperature and lighter above. As darker colours absorb a vast intensity of the visible light spectrum than lighter colours, incident light that passes through a TC textile can be transformed in light transmittance tone and intensity parameters, phenomena focused in this research under the concept dynamic light filters.

Although perception of colour concerns the interaction of light and matter, ultimately it depends on how the human visual system perceives it. Physiological processes of colour vision were predicted by two major theories, based on empirical experiments. The trichromatic theory proposed that the human visual system presents three receptor mechanisms, sensitive to different ranges of light wavelengths. The opponent-process theory described colour vision in terms of three pairs of opposed chromatic responses (Kalat, 2007; May, 2007; Goldstein, 2010).

Both theories explain colour vision processes that occur at different stages. When light enters the eye through the pupil, it falls upon the retina at the back of the eye. The retina has two types of photoreceptor cells known as rods and cones. Rods are sensitive to dim light, differentiating shades of black and white, while cones are sensitive to bright light and colours. As proposed by the trichromatic theory, there are three types of cone cells and each type is sensitive to a range of wavelengths: red (long wavelengths), green (middle) or blue (short). The combination of signals from the rods and cones are transmitted to the brain via the optic nerve and, as predicted by the opponent-process theory, the visual system respond to those signals through an increase or decrease of activity to indicate three pairs of opposites – red-green, yellow-blue and white-black. The combination of signals is interpreted in the brain as the colour observed. (Kalat, 2007; Clarkson, 2008; Pérez et al., 2010; Bloj and Hedrich, 2016).

Based on the tristimulus nature of the human eye and light properties, each colour mixture system is commonly assigned with three primary colours, meaning colours that cannot be attained by mixtures but when combined can create the wide range of colours (Hanson, 2012). Additive primary colours red, green and blue are known as RGB system. Subtractive primary colours cyan, magenta and yellow, add black (K) for printing purposes, resulting in the CMYK system. Some colour systems consider blue, red and yellow as subtractive primaries and others define a three dimensional structure based on the opponent-process colours in order to compose the colour space (Bamfield and Hutchings, 2010; Parraman, 2012).

In addition, colour perception also encompasses dynamic processes to transform the signals sensed into the experience of colour (Gregory, 1978; Goldstein, 2010). According to Lam (1992), perception relies on a combination of sensorial data with contextual information and past experience, resulting in colour being recognized or assigned under the effect of diverse factors such as colour surroundings and differences between individuals.

The relationship between the sensorial information and colour experience gave rise to diverse theories and principles focused on how a specific colour phenomenon tends to be perceived, which commonly addresses mechanisms of chromatic adaptation (Hurlbert and Ling, 2012). Colour constancy respects to the ability of an

object colour to be recognized at some extent under different lighting conditions, through a comparison of the surroundings. For example, under a scene with blue light, the constant blue stimulus is compared and reduced to determine the objects' colour (Kalat, 2007; Rizzi and Bonanomi, 2012).

Michel Chevreul's observations on colour effects on each other resulted in the law of simultaneous contrast, which respects to the tendency of one colour to induce the complementary colour or opposite lightness in an adjacent or contained surface (Hurlbert and Ling, 2012). This law reports to opponent processes of colour vision, focusing on contextual influence of colour appearance. Aside from spatial, chromatic contrast can also address temporal processing, as the colour stimulus previous observed affects the visual system. For instance the visual adaptation when one moves from a dark to a light environment and the occurrence of after-images (Krauskopf, 1998; Goldstein, 2010; Rizzi and Bonanomi, 2012).

The perceptual phenomenon of how colours affect each other have been captured special attention of colour researchers and it is a central subject in the design process, as it enables an awareness to analyse and explore colour relationships in chromatic compositions (Sherin, 2012). Johan Wolfgang Von Goethe focused on visual qualities of colour and published his 'Theory of Colours' in 1810. Goethe studies along complementary colour, contrast, shadow and proportion, were influential on further investigations, namely from Johannes Itten's and Josef Albers' works and teaching on colour, which both initiated at Bauhaus Art School (Goethe and Eastlake, 2010; Dickinson, 2011; Tiedman, 2015).

Itten explored subjective colour effects and objective colour principles, particularly through a colour circle that he defined with complementary relations between twelve hues, presenting red, blue and yellow as subtractive primary colours, surrounded by respective secondary and tertiary hues (Feisner, 2006). In his book 'The Art of Color' (1962), colour relationships are also examined and demonstrated through colour schemes, where besides hue, he also considers the importance of "their quantitative proportion and their degree of purity and brilliance" (Itten, 1973). Itten investigated and defined colour harmony and contrast based on equilibrium states, linked particularly to complementary relations, which he defined as the sum of total colours of the pigmentary mixtures that yields grey (Itten and Birren, 1970).

Albers' studies and teaching on colour were based on systematic experimentations, as a means to create awareness of colours' influence on each other. In 'The Interaction of Color' book (1963), Albers presents a comprehensive exploration of colour interactions through practical exercises, colour compositions and discussion on the principles involved, such as how simultaneous contrast can account for compositions where one colour on different backgrounds can be perceived as two different colours (Albers, 2013). His main aim was to provide a method for colour practitioners develop "an eye for color (...) In my color book there is no

new theory of color. But in it there is a way to learn to see" (Albers, 1968). Itten's and Albers' works were seminal and their books are still considered the basis of colour theory programs (Dickinson, 2011).

Moreover, colour perception also unfolds diverse assessments and interpretations depending on individual responses. Colour deficiencies involve a partial loss of the colour vision and interfere in the colours perceived. While aspects such as memory, experience and cultural background influence how colours are assigned to a meaning or emotional response (Feisner, 2006; Goldstein, 2010; Hurlbert and Ling, 2012).

In regards to colour specification and communication, although language is intuitive, it is also subjective and limited, given the different associations that can be undertaken by different individuals and due to the lack of precision that language affords, considering the innumerable chromatic possibilities (Albers, 2013; Westland, 2016).

Throughout colour studies history, visual swatches have been used as a tool to communicate colour more effectively, which are arranged in logical systems to specify and order appearance according to chromatic relationships. Colour wheels or triangles commonly reflect relations along hues, while three-dimensional colour-order systems present relations between hue (colour), lightness (also named value) and chroma (or saturation), of which the Munsell colour system is an example (Brainard, 2003; Feisner, 2006; Setchell, 2012).

Colourimetry is the discipline of quantifying and physically describing human colour perception, taking into account colour specification, colour difference evaluation and prediction of colour appearance (Smith and Pokorny, 2003; Goodman, 2012). Numerical data is applied for a systematic colour notation, also providing accurate communication (Choudhury, 2010; Westland, 2016).

The International Commission on Illumination (CIE – Commission Internationale de l'Éclairage) is the main standardization entity for colour measurement and specified the CIE 1931 XYZ colour space based on tristimulus values, which are expressed by two coordinates in a chromaticity diagram (Marcus, 1998; Goodman, 2012; Westland, 2016). CIE $L^*a^*b^*$ system (CIELAB) was specified in 1976 and is a colour-opponent space with three coordinates: L^* , a^* and b^* . Dimension L^* corresponds to perceived lightness, representing a perfect black with $L^* = 0$ and a perfect white at $L = 100$. The coordinates a^* and b^* are the colour-opponent dimensions with a^* for red ($+a^*$) and green ($-a^*$) while b^* for yellow ($+b^*$) and blue ($-b^*$). Furthermore, Chroma (C^*) and hue angle (h) are defined according to L^* , a^* and b^* values, as represented in Figure 6 (Marcus, 1998; Gupte, 2010; Choudhury, 2014b).

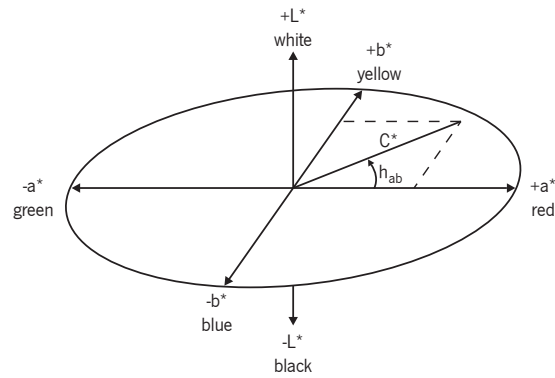


Figure 6. CIE L*a*b* colour space.

Colour measurements are conducted under specific standards, namely illuminant and observer, where the radiant energy at each wavelength of the visible spectrum reflected from a coloured surface is converted into the CIELAB colour coordinates' values. The characteristics of light source are crucial parameters for colour perception as well as for colour measurements. CIE defined standard illuminants, in order to reproduce specific lighting conditions. D65 illuminant has a colour temperature of 6500 K and represents average daylight, referring to diffuse skylight without direct sunlight (Marcus, 1998; Gupte, 2010). In regards to the eye physiology, standard observers based on a 10° viewing field have been considered a good correlation to reproduce colour vision (Marcus, 1998; Choudhury, 2014b).

Additionally to colour specification, it is also possible to quantify differences between two colours. CIELAB colour difference respects to the distance between colours' location in the CIELAB space and is calculated through each colour coordinate distance – dL^* , da^* and db^* . The total colour difference is expressed as dE^* (Brainard, 2003; Pérez et al., 2010). How different two colours can be, before it is perceptible to the human eye, can depend on diverse factors such as hue and the direction of colour differences. For example, a small difference in hue between two dark colour samples can be more perceptible than a higher difference in lightness between two bright colour samples (Marcus, 1998). Thus, tolerance limits of colours difference can guide colour matching performance, but a visual assessment is also required to be considered acceptable. In the textile industry, 1,0 dE^* is a common reference value (Field, 1998; Gangakhedar, 2010; Choudhury, 2014a).

Furthermore, two colours can be perceived equal under a specific illuminant, but present differences when the illuminant changes, which is called illuminant metamerism. For a colour match independent of lighting conditions, colours should have identical spectral reflectance curves (Hunt, 2004; Setchell, 2012).

Colour reproduction involves the quantification of colorant proportions required to match a predefined colour. Previously, the colourants' concentration prediction was confined to a trial and error method with visual

evaluation of the results, being a time-consuming and skilled process. With colourimetric systems, it is possible to formulate colourant recipes by applying instrumental methods (Gangakhedar, 2010; Choudhury, 2014a).

Colour formulation involves the use of a spectrophotometer, a computer and appropriate software. Calibration data of the colourants used is required, consisting on a database with the colourimetric properties measured in samples at different concentrations of each colourant. Samples' substrate and colourant application process should be equal among the concentration samples. Colour formulation is calculated based on the spectral data of a pattern colour and the database created with the colourant concentration samples. A recipe to reproduce the pattern colour is formulated, and after the development of the respective samples, an evaluation of the results is conducted between pattern colour and sample by comparison of spectral reflectance data and visual perception (Ingamells, 1993; Kuehni, 2012; Choudhury, 2014a).

Within the complexity and subjective nature of colour perception, colour theory permeates perspectives to work with colour systematically without excluding creative and intuitive approaches. In this research, colourimetry and colour principles also delineate possibilities to work with colour change in interaction with light and contribute to an understanding of instrumental processes involved to formulate paste recipes, for colour reproduction.

4.2 Introduction to the Experimental Work

In this chapter, TC pigments were researched towards the development of TC textiles, which dynamic behaviour presents predefined colour ratios through temperature variation. The design concept inherent to the materials' research hinges on the interaction of the textile chromic behaviour and light, aiming to transform similar light intensities and tones to heterogeneous, as well as the inverse.

Dark colours absorb a vaster intensity of the visible light spectrum than lighter colours. Thus, TC textiles change the light that passes through them differently, when they are below or above their activation temperature. A preliminary analysis was conducted in order to study light transmittance variation created by the chromic behaviour of textiles screen printed with different TC pigments' colours, concentrations and combination processes with conventional colourants.

The experimental work concerned with the development of TC textiles that change colour according to predefined ratios has involved two main studies, focused on processes of paste recipe elaboration with TC and conventional pigment and respective application in textile substrates. First, the objective was to study the

combination of pigments' colours and concentrations towards screen printed textiles that change from different to similar colours with temperature increase. After, the colourimetric properties of the pigments handled were measured and the results applied in the development of a database for paste recipes formulations, which colours change from similar to different upon the thermal stimulus. Besides screen printing processes, this study also included the development of a study prototype through rotary printing (section 4.5.2).

Additionally, the colourfastness properties of the TC and conventional pigments handled were examined, in regards to their stability to rubbing, washing and lighting.

The TC pigments handled were the Varioterm AC Base 27 (27°C TC heat sensitive pigment), orange (arancio oro), red (vermiglio) magenta, blue (blu nuovo solido) and black (nero solido) and the conventional pigments applied were ATUSMIC Magnaprint eco yellow HR, orange HD, red HB, pink H5B, blue HB and black H3B. All procedures were conducted in an ambient temperature below the activation temperature of the TC pigments used, except when the inverse is mentioned.

4.3 Experimental 1 – Thermochromic Textiles and Light Transmittance

For a preliminary analysis of the light transmittance variation that colour change textiles may produce, two studies were conducted. First, the relation of light and colour change was studied through screen printed samples with different TC pigment colours and concentrations in the paste. After, the phenomena was analysed through samples, which application of TC and conventional colourants in the textile substrate was developed by different processes.

4.3.1 *Materials and Methods*

To study how colour change may transform the incident light that passes through TC textiles, a set of samples was developed comprising of five samples of each TC pigment colour: orange, red, magenta, blue and black, at 10% concentration (samples A to E, respectively); three samples with TC pigment black at different concentrations in the paste: 10, 5 and 1% (samples E to G, respectively); and three samples, which combination of TC and conventional colourants was applied to the textile substrate by different processes: screen printing of TC and conventional pigments combined in the same paste (H), overprinting of conventional and TC pigments in different pastes (I) and screen printing of TC pigment in a pre-dyed substrate with conventional colourants (J). Table 2 presents the samples' description.

Table 2. Description of samples A to J.

Sample	Description
A	Screen printed with 10% TC orange
B	Screen printed with 10% TC red
C	Screen printed with 10% TC magenta
D	Screen printed with 10% TC blue
E	Screen printed with 10% TC black
F	Screen printed with 5% TC black
G	Screen printed with 1% TC black
H	Screen printed with a mixture of 10% TC black and 1% conventional pigment orange
I	Screen printed with 1% conventional pigment orange, dried and screen printed with 10% TC black
J	Dyed with 1% orange disperse dye and 1% orange reactive dye, dried and screen printed with 10% TC black

All samples were developed with the 50% CO and 50% PES textile substrate. Screen printing processes were conducted in a Zimmer Mini MDF R541 with the settings defined in section 3.3.1, using an open screen of 101,6 TPI and Gilaba vinyl acrylic paste binder. Dyeing processes were conducted in an Ibelus C720 equipment. For the PES fibres of the textile substrate, a Dianix orange SG 200% disperse dye was used at 1% concentration in a bath ratio of 1/10 with 35g/L of salt and 10g/L of sodium carbonate. CO fibres were dyed with Levafix orange CA gran reactive dye at 1% concentration, in a bath ratio of 1/10 and with pH 4,5. Dyeing programs applied for disperse and reactive dyes are presented in Figure 7 left and right, respectively. After being dyed and/or screen printed, each sample completed a process of drying and thermo fixing in an oven at 150°C during 3 minutes.

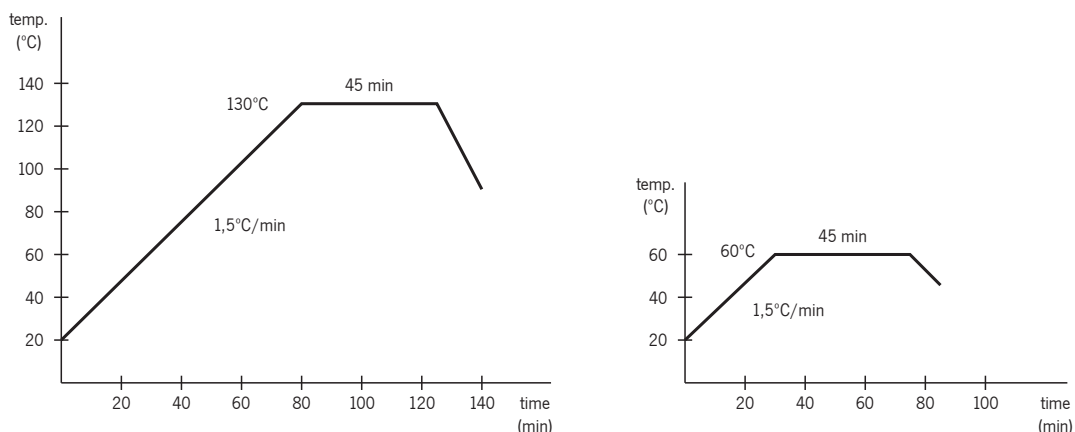


Figure 7. Dyeing programs applied for disperse and reactive dyes (left and right, respectively).

Chromic behaviour effect on light transmittance was analysed by direct observation, photographic record and light intensity measurement. The study was conducted in a dark room, where each sample was placed on the

open face of a light box. In the photo record, the light box was set with the open face perpendicular to a white wall and a camera set on a tripod. Camera settings were equal for all photos recorded, for a comparison between luminosities. In the light intensity measurement, the open face of the light box was set in vertical position, 1m from the luxmeter in the first measurement cycle and 0,5m in the second. After the lamp was turned on, luxmeter values were recorded on three points of each sample. A dryer was used to heat up the TC samples above 27°C.

Additionally, for a comparative analysis of the TC samples in decolourized state, a spectral reflectance measurement was conducted in the spectrophotometer and data was set in colour coordinates and CIELAB differences. To maintain the samples heated during colour measurement, a hot water rubber deposit was placed in the samples' backside.

4.3.2 Results and Discussion

Figure 8 presents the photos of samples screen printed with different TC colours, placed on the open face of the light box. Differences of light transmittance between samples, below and above their activation temperature, were observed and compared through the blur size and tone of light reflected on the wall.

Below 27°C, light transmittance tones were perceived accordingly to each sample colour and light reflected areas were higher with A and B samples, whereas with D and E, they were slightly perceived. Above 27°C, similar luminosities were expected, as the TC pigments were in the decolourized state and all samples were developed with the same textile substrate. However, small differences were observed: while A and B samples presented similar areas of light reflected on the wall and light tone, C appeared to be slightly larger and more red, D was slightly smaller and less red and E presented the highest light intensity and was more yellow than the other samples. Comparing light transmittance variation with temperature increase, it was observed that A and B samples presented the lower differences and the highest was attained with E sample.

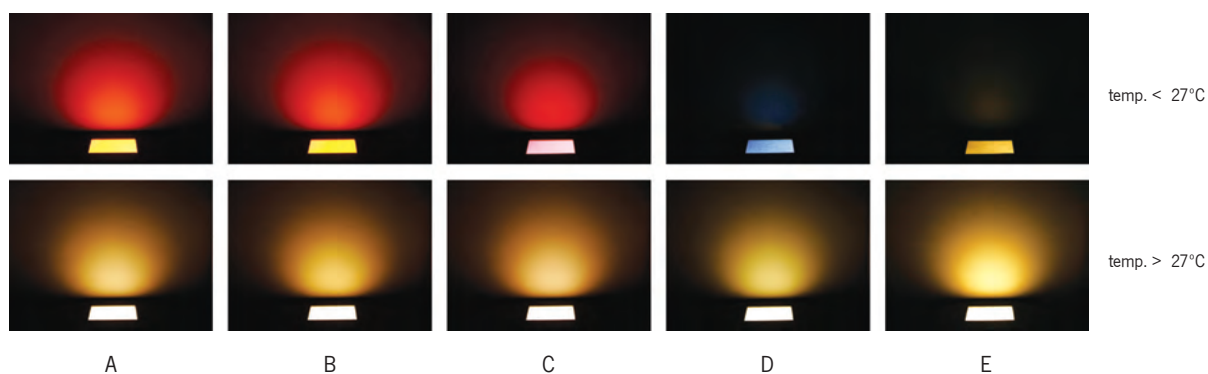


Figure 8. Light transmittance variation with samples A, B, C, D and E.

Figure 9 presents the photos of screen printed samples with different concentrations of the TC pigment black: 10, 5 and 1% from E to G, respectively. Along the decrease of the pigment concentration below 27°C, light transmittance increases and thus, light variations decreases with colour change. Above 27°C, sample G appeared to have a slightly higher light projection area in relation to E and F samples.

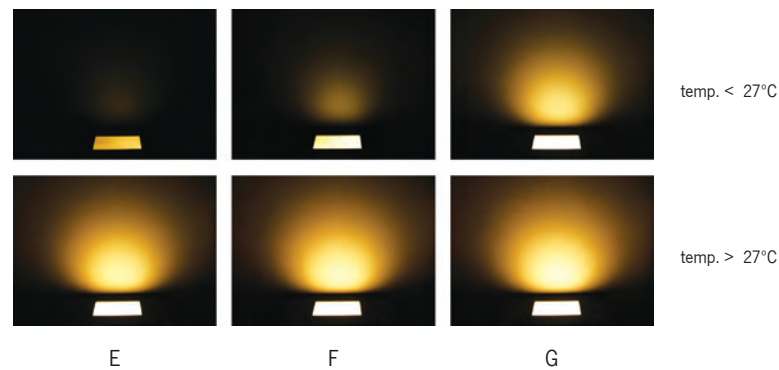


Figure 9. Light transmittance variation with samples E, F and G.

Table 3 presents the mean values of light intensities attained with samples A to G and respective percentual luminosity differences with temperature variation. At the cold state, light intensity values presented great differences between samples. A and B samples (TC orange and TC red) attained the higher light intensities of samples screen printed with 10% TC, with values approximately 400% higher than D and E (TC blue and TC black). With the concentration decrease of TC pigment black, light intensity increased approximately 100% from E to F (10 to 5%) and 500% from E to G (10 to 1%). At the heated state, sample D (TC blue) attained the lowest light intensity value and C (TC magenta) had the highest, with a difference of approximately 11%. With TC black samples, light transmittance of E was approximately 16% lower than G.

The percentual luminosity difference with temperature variation is higher for samples D and E. The pigment's concentration decrease from E to F samples represented a luminosity variation reduction of 12% and from F to G it was 38%. Moreover, while sample B (10% TC red) and G (1% TC black) attained different light intensities at each temperature state, the percentual luminosity difference was similar.

The results attained demonstrate the dependency of the TC pigments' colours and concentrations applied, for the magnitude and ratio of light transmittance variation, in regards to light intensity and tone parameters. Furthermore, percentual luminosity differences in each sample for measurements conducted at 1 m and 0,5 m confirmed similarities. Further tests were carried at 1 m distance between textile sample and luxmeter.

Table 3. Mean values of light intensities with samples A to G.

Sample	Light intensity (lx)		Luminosity difference (%)	Light intensity (lx)		Luminosity difference (%)
	temp.<27°C	temp.>27°C		temp.<27°C	temp.>27°C	
A	2,13	3,84	45	5,32	9,54	44
B	2,23	3,72	40	5,43	9,43	42
C	1,42	4,07	65	3,52	10,24	66
D	0,47	3,61	87	1,22	9,40	87
E	0,45	4,00	89	1,19	10,57	89
F	0,95	4,20	77	2,72	11,53	76
G	2,82	4,63	39	7,45	12,30	39

distance sample/luxmeter = 1 m
distance sample/luxmeter = 0,5 m

In the photo record and light intensity measurement, TC samples presented differences in the colourless state, when similarities were expected, as previously mentioned. To analyse further these results, a colour measurement was conducted with samples heated above 27°C. Table 4 presents the results attained for each sample and the textile substrate applied. Data was set in colour coordinates and CIELAB differences, where the substrate was set as the pattern colour.

All screen printed samples are darker than the substrate and E presented the lower lightness value. TC samples were also more green and yellow than the substrate, except A and C which presented higher a* values and B had similar results. CIELAB differences varied between samples' colours, with sample C attaining the lower value (8,0) and E highest (13,2). According to the reduction of TC pigment concentration in the pastes, there was also a decrease of colour difference: G is approximately 2,8 times lower than E. The results attained suggest an incomplete decolourization of the TC pigments handled, which varies differently in regards to the pigments' colour and concentration in the paste.

Table 4. Colour coordinates and CIELAB differences of samples A to G, above 27°C.

Sample	L*	a*	b*	C*	h	dE*
substrate	93,93	2,77	-7,26	7,77	290,92	-
A	89,59	8,57	2,56	8,94	16,62	12,2
B	92,06	2,66	4,30	5,05	58,29	11,7
C	87,24	6,15	-4,35	7,54	324,74	8,0
D	90,43	-3,40	1,76	3,83	152,69	11,5
E	85,94	-2,21	2,04	3,01	137,27	13,2
F	88,24	-1,10	0,13	1,11	173,49	10,1
G	91,48	0,88	-3,59	3,70	283,81	4,8

In regards to samples developed by different application processes of TC and conventional colourants, Figure 10 presents the photos of light transmittance variation recorded. Below the TC pigments' activation temperature, sample I attained a larger light projection on the wall than H and J. When heated, sample I also appeared to have a slightly higher blur size and the smallest was J, which was also more red. It was not clearly perceived which sample performed greater light transmittance variation.

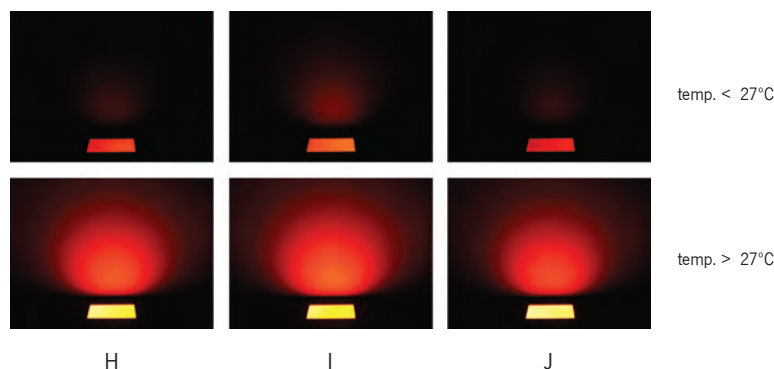


Figure 10. Light transmittance variation with samples H, I and J.

Mean values of light intensities presented in Table 5, confirmed the observations previously described and showed that the percentual luminosity difference is equal for H and J samples while I was 5% lower. Although below 27°C, light transmittance with sample I was lower than with H, by direct observation of samples before placement in the light box, I sample appeared darker. The overlapping layers with the TC black at the surface, created an apparent darker colour in relation to sample H, where TC and conventional pigments were mixed in the same paste, but the light transmittance results indicated that less TC pigment was absorbed.

Table 5. Mean values of light intensities with samples H, I and J.

Sample	Light intensity (lx)		Luminosity difference (%)
	temp.<27°C	temp.>27°C	
H	0,27	1,89	86
I	0,38	2,03	81
J	0,23	1,61	86

Table 6 presents the colour measurement results obtained with samples H, I and J, below and above 27°C. Colour coordinates of orange screen printed and orange dyed substrates were also included for a comparison of the results with the samples heated. CIELAB differences respect to orange print as pattern colour for H and I samples and orange dyed for J.

Below 27°C, H and I attained the greater differences of the three samples, being H lighter, more red and yellow than I. According to the previous observations, the results demonstrate the effect of pigments'

application processes in colour appearance of the textiles, with emphasis in the lightness axis: L* value distance between H and I samples was approximately 9.

Above 27°C, H was also lighter and more yellow than sample I, while red values were similar. Comparing the samples' colours above 27°C with the respective pattern sample, the highest colour difference was attained with sample I (14,5) and the lowest with J (4,5). Hence, the application processes of TC and conventional colourants also interfere in the TC pigment residual colour.

Table 6. Samples' colour coordinates below and above 27°C and CIELAB differences between heated samples and respective conventional colourant substrate.

	Sample	L*	a*	b*	C*	h	dE*
	orange print	61,14	51,88	54,17	75,01	46,24	-
	orange dyed	61,14	42,31	43,49	60,68	45,79	-
temp. <27°C	H	39,53	13,65	14,24	19,73	46,20	-
	I	30,46	10,43	7,94	13,11	37,26	-
	J	32,79	11,03	11,52	15,96	46,25	-
temp >27°C	H	60,34	44,16	45,66	63,52	45,96	11,5
	I	58,41	43,87	42,43	61,03	44,04	14,5
	J	58,34	38,81	43,93	58,62	48,54	4,5

In this section, the values attained with the experiments conducted relate to the specific characteristics of the textile substrate and colourants applied. However, they set up a preliminary understanding of the TC pigments handled and light transmittance variation produced by textile colour change regarding TC pigment colours, concentrations and application processes, also delineating the potential to further research TC textiles with predefined chromic ratios, towards the development of dynamic lighting scenarios. Screen printing with TC and conventional pigments combined in the same paste was the process selected to apply in the following experimental sections, with the objective to develop systematic processes of paste recipe elaboration.

4.4 Experimental 2 – Colour ratio: from different colours to similar ones

In this section, the combination of TC and conventional pigments in screen printing pastes was researched towards the development of textiles that change from different to similar colours with temperature increase. The study conducted focused on colours and concentration ratio between TC and conventional pigments in respect to the colour selection to maintain constant in samples' colourless state and colours palette in the cold state, as well as on the variation of TC pigment and binder concentrations in the colour change effect.

4.4.1 Materials and Methods

In this study, TC and conventional pigments were combined with Atusmic Magnaprint ND extra binder. All samples were developed with the 50% CO and 50% PES textile substrate, screen printed in a Zimmer Mini MDF R541 table, using an open screen with 101,6 TPI and completed a process of drying and thermo fixing in an oven at 150°C for 3 minutes.

Initially, a base framework of screen printed samples was developed, with the objective to build a visual tool of colours combination with the pigments handled, at defined concentrations. The screen printing pastes combine 5% concentration of one colour of each pigment type, totalizing 10% pigments and 90% binder in each sample. Due to the colour change objective, TC and conventional pigments with the same colour were not screen printed.

After, a second framework was produced to analyse how the variation of the pigments' concentration affects samples' colours, below and above 27°C. This study was conducted with mixtures of conventional pigment yellow and TC pigment orange, magenta, blue or black. All screen printing pastes have 90% binder, the conventional pigment percentage varies from 5; 4; 3; 2; 1 to 0.5% and the TC pigments complete the remaining percentages: 5; 6; 7; 8; 9 and 9,5%, respectively. Samples of both frameworks were analysed and compared by direct observation, below and above 27°C.

Additionally, the effect of TC pigment and binder percentage variations was studied with four samples, which screen printing pastes present the same concentration and colour of conventional pigment (1% yellow) combined with TC blue 14, 11, 7 and 4%, samples K, L, M and N, respectively. Samples' spectral reflectance above 27°C was measured in the spectrophotometer and a comparative analysis was conducted with colour coordinates and CIELAB differences data, considering K as the pattern colour. Furthermore, a similar analysis was conducted with samples which screen printing paste combines 1% conventional pigment yellow with equal concentration of TC pigments but different colours: 14% TC blue (K sample), 14% TC magenta (O) and a mixture of 5% TC blue and 9% TC magenta (P).

Light transmittance variation produced with the chromic behaviour of K, O and P samples was analysed through a photographic record and light transmittance measurement, with the setup described in 4.3.1 section for 1 m distance between sample and luxmeter.

4.4.2 Results and Discussion

Figure 11 presents the base framework of samples screen printed with 5% concentration of each pigment type, below and above 27°C (left and right, respectively). The first row presents the textile substrate on the left, followed by the samples screen printed with 5% TC pigment aligned by orange, red, magenta, blue and black colours. First column follows the same logic for samples with 5% conventional pigment, yellow, orange, red, magenta and blue, from top to bottom. Samples screen printed with mixtures of TC and conventional pigments were aligned in the matrix, according to the respective pigment vs. colour combination.

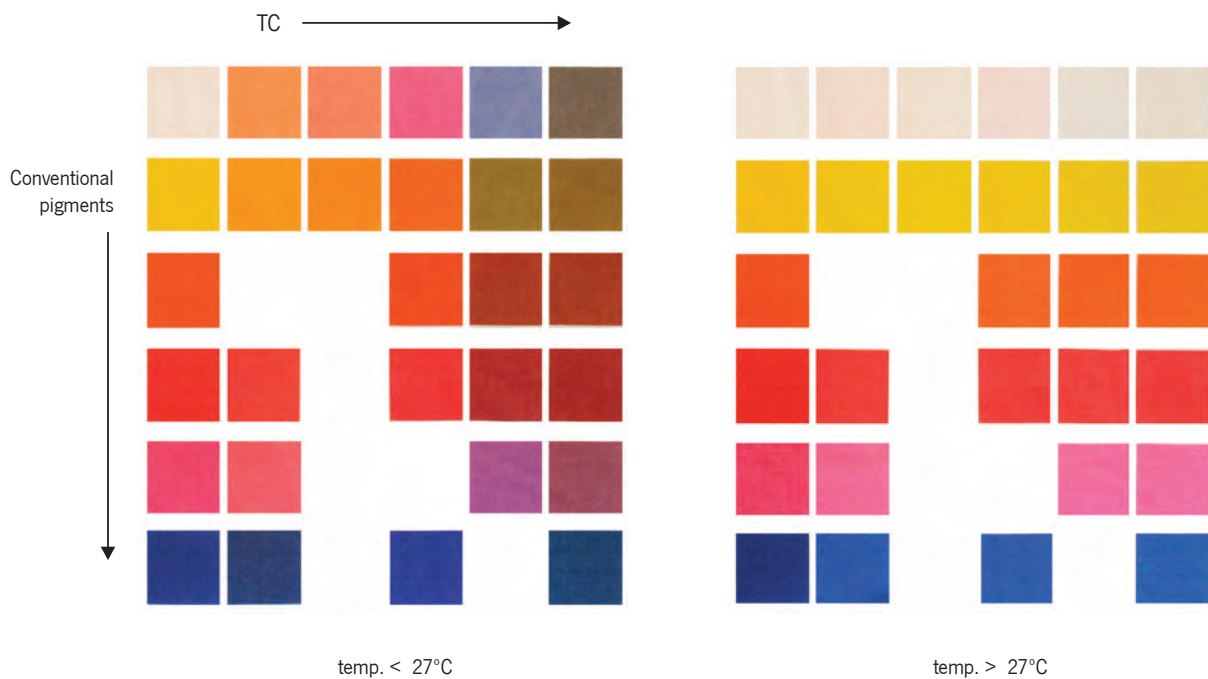


Figure 11. Base framework of screen printed samples, below and above 27°C.

Through the framework analysis it was observed that by using the same concentration of both pigment types, samples screen printed with lighter conventional pigment colours attained a vast chromatic palette below 27°C than samples with darker colours. For example, samples developed with conventional pigment blue attained shades in the blue spectrum, whereas samples with conventional pigment yellow presented different colours. As the colour strength of the conventional pigment demonstrated to be higher than the TC pigments, in order to achieve a vast combination of colour change effects, the TC pigment concentration should be higher than the conventional, also considering the colour(s) selected.

Above 27°C, the TC pigments' residual colour was observed in the first row samples through subtle colour nuances, while the effect was barely perceived in samples with both pigments' types combined. However, as analysed in section 4.3, the incomplete decolourization of TC pigments also depends on their concentration,

which is an important parameter to take into consideration, particularly when colour change ratio from different to similar is to be designed, as will be further analysed.

Figure 12 presents the framework of samples screen printed with a decreased ratio of conventional pigment yellow in relation to TC pigment increase, totalizing 10% pigments' concentration in each paste. Samples with TC orange, magenta, blue or black were organized in the framework from left to right columns. The framework picture on the left is below 27°C and on the right is above.

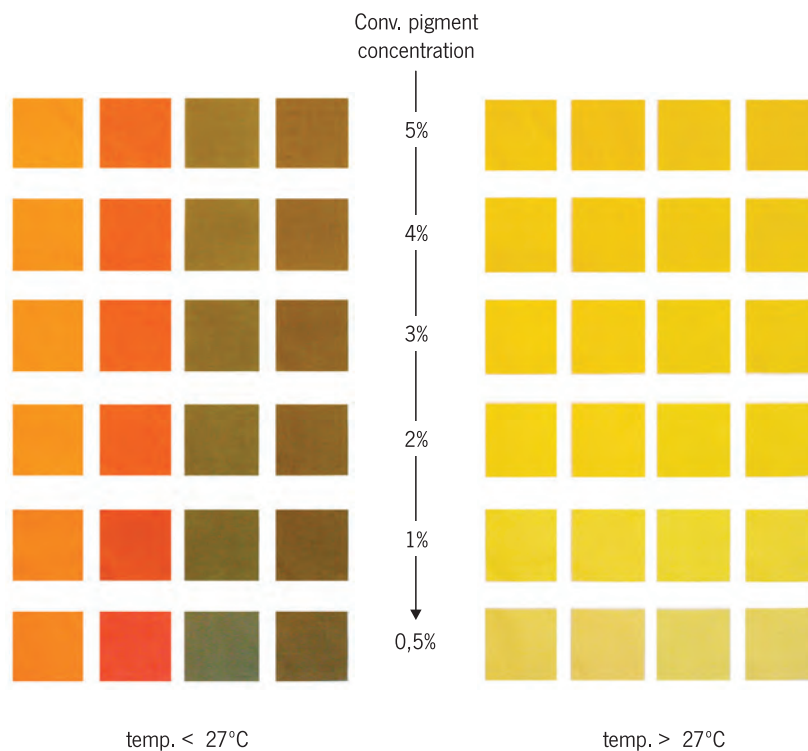


Figure 12. Framework of samples with different TC and conventional pigments' concentrations, below and above 27°C.

With the decrease of conventional pigment concentration, from top to bottom in the framework arrangement, samples change from lighter to darker colours below 27°C and the inverse occurs when heated. Although the changes rely mostly on colour lightness, a transition between orange and red colours was observed in samples at the cold state, where TC magenta was combined (second column) and conventional pigment yellow varies from 2% to 1%. In samples with 0,5% conventional pigment and 9,5% TC pigment, the incomplete colourless state of the TC pigments was perceived.

The development of study samples with variation of pigments' concentration provided an important tool to understand colour effects with the colourants handled and to aid an informed definition of colour and concentration of the conventional pigment to maintain constant in all samples, according to a colour palette. For the following experiments, 1% of conventional pigment yellow was defined to apply in all pastes.

Within the colour ratio focused in this study, TC and binder concentrations can also vary as well as more than one TC pigment colour can be combined, to explore a vaster colour set below samples activation temperature. However, these mixtures can also highlight colour differences in samples' heated state, in terms of TC pigment residual colour and binder concentration. To analyse how the variation of TC pigment and binder concentrations affect samples' colours, a study was conducted with K, L, M and N samples (screen printed with 1% conventional pigment yellow and TC blue at 14, 11, 7 and 4%, respectively). Samples' photos below and above 27°C are presented in Figure 13 and Table 7 presents the spectral reflectance data attained for measurements conducted with samples above 27°C.

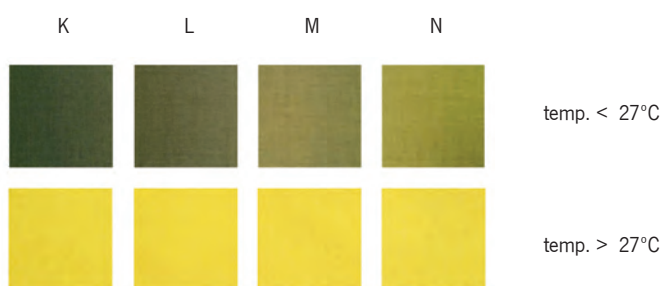


Figure 13. K, L, M and N samples, below and above 27°C.

Table 7. Colour coordinates and CIELAB differences of K, L, M and N samples, above 27°C.

Sample	L*	a*	b*	C*	h	dE*
K	79.22	11.40	72.87	73.75	81.11	-
L	79.43	12.48	75.15	76.17	80.57	2,5
M	79.90	12.76	74.69	75.77	80.31	2,4
N	80.53	13.25	77.23	78.36	80.27	4,9

Below 27°C, samples' colours vary from dark to light green with the concentration range from 14 to 4% of TC pigment blue. Above 27°C, samples K, L and M appeared similar, while with N a lighter yellow colour was perceived. Colour measurement results with samples heated show that K is darker, less red and less yellow than the other samples, with the highest values distance of 1,31 (L*), 1,85 (a*) and 4,36 (b*) in relation N. Considering sample K as the pattern colour, CIELAB difference with N is approximately twice than in samples L and M. Moreover, while sample L is slightly lighter than M and thus more similar to K, its dE* is slightly higher. The opposite relation would be expected, with the higher difference of TC pigment concentration in relation to the pattern sample presenting a higher colour difference due to the TC residual colour effect. This result suggests that the incomplete colourless of the TC leuco dyes handled is not homogeneous along pigments concentration.

Furthermore, in regard to the samples developed and the colour compared above 27°C (yellow), the values attained between 14 and 7% TC samples were considered reasonable, considering that by direct observation the differences were not evident. The possibility to vary the TC pigment and binder concentration in pastes that change from different to similar colours extends the colour palette range to be defined, below the TC pigment activation temperature.

To study how the combination of different TC pigment colours affects samples colours above 27°C, a similar analysis was conducted with samples K (14% TC blue), O (14% TC magenta) and P (5% TC blue with 9% TC magenta). Samples' photos and spectral reflectance data are presented in Figure 14 and Table 8, respectively.

By direct observation of samples' colours above 27°C, K appeared darker and greener than the other samples with more relevant differences in relation to sample O. Colour coordinates confirmed that K is darker, more green and less yellow than O and P samples, also showing that the high values distance take place in a* coordinate, attaining a difference of 5,44 with sample O and 3,82 with P. Sample P attained a lower CIELAB difference in relation to K than O, as expected because it presents 5% concentration of the same TC pigment colour of the pattern sample, but it was still higher than samples developed with 11 and 7% TC pigment blue (L and M).

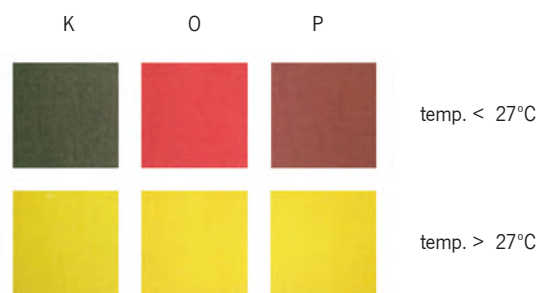


Figure 14. K, O and P samples, below and above 27°C.

Table 8. Colour coordinates and CIELAB differences of samples K, O and P, above 27°C.

Sample	L*	a*	b*	C*	h	dE*
K	79,22	11,40	72,87	73,75	81,11	-
O	80,06	16,80	76,07	77,91	77,55	6,3
P	79,79	15,22	74,37	75,91	78,44	4,1

Samples K, O and P were also analysed in regards to the light transmittance variation produced with the chromic effect. Figure 15, presents the photos attained at different temperatures. Below 27°C, sample O presented the highest light intensity and the lowest was observed with K. Above 27°C the light areas reflected

on the wall appeared similar in size, however light tones were different, reflecting the influence of the TC residual colour in the light transmitted, differentiated particularly by the warmer light tone with sample O.

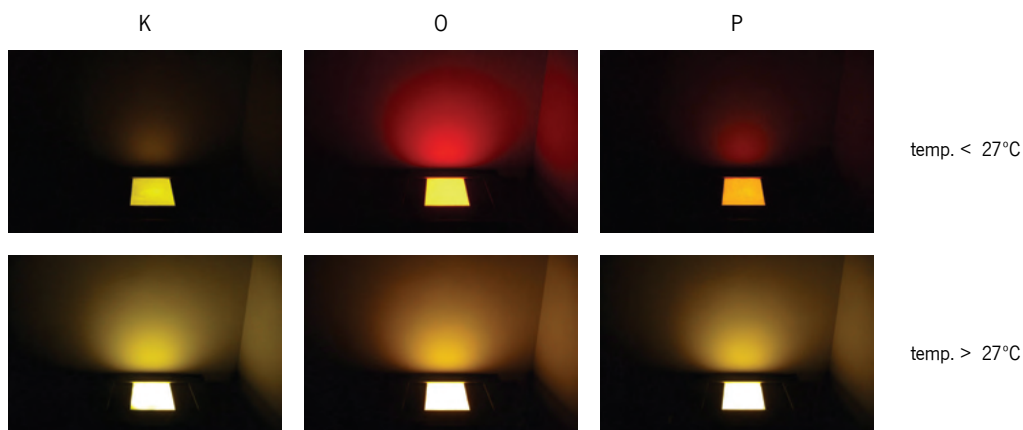


Figure 15. Light transmittance variation with samples K, O and P.

Results of light intensity measurement (Table 9) demonstrate that below 27°C, the highest light intensity difference is 0,46 lux representing 135,3% increase from K to O sample. Above 27°C light intensity between samples is similar, being the highest difference of only 2% between K and P samples. Colour change of sample K attained the higher luminosity difference.

Table 9. Mean values of light intensities with samples K, O and P.

Samples	Light intensity (lx)		Luminosity difference (%)
	temp.<27°C	temp.>27°C	
K	0.34	3.01	89
O	0.80	3.04	74
P	0.42	3.07	86

The studies conducted in this section propose a process to develop TC textiles that change from similar to different colours. To achieve this colour ratio, the colour and concentration of the conventional pigment are independent variables in all screen printing pastes, whereas the TC pigment colours and concentration in relation to the binder are variable parameters. This study also allowed the creation of light transmittance variations from multiple light intensities to similar ones.

Moreover, it was found that the incomplete colourlessness of the TC pigments handled affected the colours' similarities with more relevance when using TC pigments of different colours than by applying the same pigment colour (blue) at a concentration range from 4 to 14%. This effect, which was also perceived during light transmittance experiments, may be reduced with the addition of small percentages of conventional pigments of different colours, in order to homogenize the TC residual colours between samples, in the

decolourized state. The possibility to match colours can be studied through paste recipe formulation processes, a method researched and presented in the follow section.

Furthermore, a sample with a geometric pattern was designed and screen printed with mixtures of TC and conventional pigments (K, O and P screen-printing pastes), to demonstrate the defined colour change ratio, Figure 16. With the pattern sample developed, the differences between screen-printed pastes colours above 27°C appeared less obvious than comparing K, O and P samples, printed in solid colours.



Figure 16. Sample: from different to similar colours ratio.

4.5 Experimental 3 – Colour ratio: from similar colours to different ones

In this section, the combination of TC and conventional pigments was researched towards the development of screen printed textiles that change from similar to different colours with temperature increase. The study conducted has researched optimization processes of screen printing pastes definition for TC textiles, by means of the colourimetric properties of the pigments handled, instrumental recipes' formulation and colour assessment.

4.5.1 Materials and Methods

Two textile substrates were used in this study: 50% CO and 50% PES plain weave and 100% CO 3/1 twill weave (item 3.2.1). TC and conventional pigments were combined with Gilaba binder and the screen printing processes were conducted in a Zimmer Mini MDF R541 table, using an open screen with 101,6 TPI and completed a process of drying and thermo fixing in an oven at 150°C during 3 minutes. This study has also involved the development of a study prototype by rotary printing, which was conducted in an industrial context and used four cylinders of 150 cm width and 91,4 cm diameter, with a 125 mesh (openings per linear inch).

In the first phase of this study, a set of screen printing samples was developed comprising of a defined concentration range for each pigment type and colour. TC pigments were screen printed with 5 to 10%,

concentration at 1% interval, totalizing six samples per each TC colour handled: magenta, blue, black, red and orange. Conventional pigments were screen printed with 0,5 ; 1; 2; 3; 4 and 5% concentration, also summing six samples for each colour: magenta, blue, black, red, orange and yellow. The textile substrate applied was the 50% CO and 50% PES plain weave.

After being screen printed and thermo fixed, the samples were measured in the spectrophotometer, at a temperature below 27°C, following the procedures described in section 3.3.7. The spectral reflectance results were used to create a database in Datacolor MATCH software, corresponding the samples' colourimetric properties according to colours and respective concentrations of each pigment type, defined as distinct colourant groups. This definition, allowed the formulation of paste recipes with different combinations of pigments' types and colours, given a pattern colour and according to the colour change effect aimed. The database created also included the textile substrate colourimetric data in samples' description.

To study the differences between colours of each pigment type, samples with 10% concentration of each TC pigment colour were screen printed using the 50% PES and 50% CO substrate, measured and defined as pattern colours in order to formulate paste recipes with the database created, just selecting the conventional pigments type. Each sample was screen printed with the respective formulated recipe, thermo fixed and measured. The spectral reflectance results were compared with the correspondent pattern colour through colour coordinates and CIELAB differences data.

A study was conducted, which defined a mixture of two TC pigments as pattern colour, to formulate paste recipes with mixtures of TC and conventional pigments that can change from similar to different colours. To systematize the specification of pigment vs. colour combinations, capital letters were used to define the pigment' type, TC for thermochromic leuco dyes and C for conventional pigments, while lower case letters represent the colours' first letter (has used in RGB or CMYK systems with capital letters). Black is described with letter k.

The samples developed in this study relied on the follow combinations: TCm + TCb; TCm + Cb and Cm + TCb. Sample Q combined 5,5% TCm with 5,5% TCb and after being developed and measured in the spectrophotometer, it was setup as the pattern colour for instrumental recipe formulation, which defined the pigments' concentration for Q1 (TCm + Cb) and Q2 (Cm + TCb). According to the recipes obtained, each paste was elaborated and samples were screen printed with the same substrate as the concentration samples, dried and thermo fixed.

A comparative analysis of Q, Q1 and Q2 was conducted by direct observation of samples' colours and respective spectral reflectance measurement. Focused on colour's similarities in the TC pigments' colourized state, the quantitative data presented respects to the colours measured with samples below 27°C. Results were set in colour coordinates and an overlap of spectral curves, which provides a visual profile of the colour wavelength characteristics, showing the radiant power reflected at each wavelength of the visible light spectrum (Xin, 2006). To analyse light transmittance variation through samples' colour change, a photographic record and a light meter measurement were conducted with the setup described in 4.3.1 section, for 1 m distance between sample and luxmeter.

With the objective to study the possibility of improving similarities between samples' colours of formulated paste recipes in relation to the pattern colour defined, an additional study was conducted. The process described for the development of samples Q, Q1 and Q2, was implemented for a new pattern sample R (TC_m + TC_b + TC_k + Cy) and three formulated paste recipes: R1 (C_m + TC_b + TC_k + Cy), R2 (TC_m + C_b + TC_k + Cy) and R3 (C_m + C_b + C_k + Cy).

After samples' screen printing, thermo-fixing and measurement, colours below 27°C were analysed by direct observation and by comparison of colour coordinates in relation to the pattern colour. The most distant values of L*, a* and b* coordinates were taken into consideration to perform adjustments in the previous recipes, by maintaining, adding or subtracting of small percentages of pigments. This study has included a paste recipe composed just with conventional pigments, to analyse the colour matching effect in a combination that was expected to be more challenging, due to the use of only conventional pigments to reproduce a pattern colour developed only with TC pigments.

Furthermore, this study has also encompassed a change of the textile substrate. The database previously created includes the data of the substrate used in the concentration samples. When defining the parameters for paste recipe formulation, substrate definition can be altered, allowing the formulation of recipes in regards to a new textile substrate colour. In this study the textile substrate applied was the 100% CO, 3/1 twill weave.

After the development of the optimized paste recipes, samples that attained greater similarity with the pattern sample were analysed and selected for the development of a study prototype through rotary printing. This process, involves the continuous rotation of pre-engraved cylindrical screens above the textile substrate and each printing paste is fed inside a cylinder, where a squeegee presses the paste out into the fabric (Miles, 2003; Briggs-Goode, 2013).

Previously to the textile printing, which applied the same substrate used in samples R, pastes' viscosity were adjusted and printing parameters tested – rod squeegee size and magnetic field applied. With this study prototype, the effect of process change in colour similarities was analysed.

4.5.2 Results and Discussion

Figure 17 presents the photos of the concentration samples screen printed with conventional pigments (first row) and TC pigments (second row), decreasing concentration from the bottom upwards in each colour set. Concentrations range selected for each pigment type, took in consideration colour strength differences previously identified. However, with 0,5 to 5% concentrations for conventional pigments and 5 to 10% for TC pigments, relevant differences were still observed. Samples' spectral reflectance was measured and applied for the creation of a database with the colourimetric properties of the pigments handled. Samples' colour coordinates are presented in Appendix B.



Figure 17. Samples with different concentrations of conventional pigments (1st row) and TC pigments (2nd row).

The first experiment aimed to reproduce the colours of each TC pigment, in samples screen printed with conventional pigments, by formulating paste recipes through the developed database. By defining a TC sample as pattern colour and selecting the software commands to reproduce it with the conventional pigment of the corresponding colour, it was observed that the recipe options have attained high predicted dE^* values for magenta and blue and no recipe was formulated for red and orange colours, due to the software limit of CIELAB difference 10 to formulate a recipe. Thus, each paste recipe was formulated with all conventional pigments' colours selected in the software commands, which resulted in recipe possibilities with lower

predicted differences than previous recipes. For each TC pattern colour, the three recipes with the lowest predicted dE* were selected to develop the samples. With TC orange as pattern colour, there were just two options. Table 10 presents the samples' description with the respective paste recipes.

Table 10. Samples' description and respective paste recipes.

Pattern colour (10% TC pigm.)	Study sample	Paste recipe with conventional pigments (%)					predicted dE*	
		magenta	blue	black	red	orange		yellow
magenta	magenta a	1,617	0,009				0,3	
	magenta b	1,619	0,010				1,7	
	magenta c	1,561		0,003			1,9	
blue	blue a		0,343	0,004	0,030		0,0	
	blue b	0,056	0,264	0,008			0,0	
	blue c		0,319	0,010			4,5	
black	black a		0,130	0,262			0,043	0,0
	black b		0,057	0,290				1,6
	black c			0,309				2,1
red	red a				0,152	0,084		2,7
	red b				0,224		0,075	4,3
	red c	0,469				0,138		6,1
orange	orange a				0,116	0,452		5,8
	orange b	0,279				0,539		8,1

Screen printed samples are presented in Figure 18. For each colour group, TC pattern sample was placed on the left (vertical) and samples developed with conventional pigments on the right (horizontal). Table 11 presents the colour coordinates and CIELAB differences attained between each study sample and respective pattern sample.



Figure 18. TC pattern samples and conventional pigment samples.

Table 11. Samples' colour coordinates and CIELAB differences.

Sample	L*	a*	b*	C*	h	dE*
10% TC magenta	53,60	45,29	-18,50	48,92	337,78	-
magenta A	53,66	45,47	-19,47	49,46	336,82	2,4
magenta B	48,62	49,16	-22,09	53,89	335,8	7,3
magenta C	54,77	44,54	-17,54	47,87	338,51	1,0
10% TC blue	59,38	-5,84	-28,39	28,99	258,38	-
blue A	56,88	-7,61	-32,14	33,03	256,68	3,9
blue B	55,19	-7,15	-35,30	36,20	258,56	8,2
blue C	57,73	-12,10	-40,07	41,85	253,19	13,3
10% TC black	36,66	-0,76	0,50	0,91	146,53	-
black A	43,92	-2,31	-0,83	2,46	199,68	7,6
black B	47,53	-0,21	-2,19	2,20	264,62	11,2
black C	49,10	1,60	0,15	1,61	5,39	12,7
10% TC red	64,88	47,36	18,37	50,80	21,20	-
red A	65,56	40,35	15,06	43,07	20,46	7,8
red B	65,24	37,45	14,85	40,29	21,62	10,5
red C	61,58	42,05	14,26	44,40	18,73	7,5
10% TC orange	63,20	56,60	42,08	70,53	36,63	-
orange A	62,23	46,91	36,58	59,48	37,95	11,2
orange B	59,91	47,47	37,50	60,49	38,31	10,7

By a comparative analysis of the samples' colours and measurements results, it was possible to observe: a) Sample magenta C presented great similarity with the TC pattern colour and attained a dE* lower than the predicted, 1,0 instead of 1,9; b) For blue, the lower colour difference value was 3,9, with sample A. By direct

observation it was possible to perceive that all samples were more blue than the pattern colour, confirmed by colour coordinates which also attained lower values for lightness and higher for green; c) Black study samples showed low similarity with TC black, being all relevantly more lighter. The sample developed only with black conventional pigment – black C – attained the higher dE^* (12,7); d) All red samples were less red and yellow than the pattern colour, lightness was similar for A and B while C was darker. Although the results of the measurements conducted present relevant differences, colours appeared to have similarities in particular sample C; e) High colour differences were found in both orange samples, with a dE^* of approximately 11. Comparing colour coordinates the most relevant value distance respects to a^* axis, where samples formulated are less red than the pattern sample. Visually, they didn't appear as different as the highlighted results.

Furthermore, all samples attained a higher CIELAB difference than predicted, except sample magenta C. In black samples the differences were visually notable and dE^* was high, whereas similarities in samples red and orange were observed despite of the dE^* values attained.

The study conducted allowed the development and an initial analysis of samples whose colour was defined by paste recipe formulations, given a pattern colour. Although the results obtained have shown a low colour similarity between the pigments handled, they have demonstrated the possibility to setup an initial paste recipe, which by experimental mixing would be more challenging to attain. It is also important to highlight that by direct observation and comparison of pastes composed by TC and conventional pigments (individually or combined), the colour obtained after samples screen printing, drying and thermo fixing, is different. Thus, a direct matching of the pastes' colours is not reliable.

Moreover, while the preliminary analysis focused on paste recipe formulation only with conventional pigments, the objective of this study is to implement the database created for the development of textile colour change behaviour. Therefore the pattern colour does not have to be reproduced entirely by conventional pigments.

The second experimental study of paste recipes formulation through the database created, focused on the reproduction of a pattern colour defined by a combination of two TC pigments, with samples that combine TC and conventional pigments. Pattern (Q) and samples with formulated pastes recipes (Q1 and Q2) are described in Table 12. Figure 19 presents the screen printed samples with the lower half heated above 27°C.

By direct observation, samples appeared to have a resembling appearance below 27°C, in particular comparing Q and Q1 samples, while Q2 appeared to be slightly more blue. When samples are heated, the TC pigment fades away and it is detected the lack of colour on sample Q, the conventional pigment magenta on Q1 and blue on Q2, attaining the colour ratio with similarities below 27°C to different colours above it.

Table 12. Paste recipes of samples Q, Q1 and Q2.

Sample	Paste recipe (%)			
	TC magenta	TC blue	C magenta	C blue
Q	5,500	5,500		
Q1		6,128	0,616	
Q2	5,047			0,131



Figure 19. Samples Q, Q1 and Q2, respectively.

Comparing the samples' colour coordinates (Table 13), pattern sample Q is lighter than Q1 and darker than Q2. Q is also more red and less blue than both samples, with a higher difference of values with Q1 for red and with Q2 for blue. Although visually the samples' colour match appeared reasonable, CIELAB differences were higher than expected.

Table 13. Colour coordinates of samples Q, Q1 and Q2, below 27°C.

Sample	L*	a*	b*	C*	h	dE*
Q	55,34	19,03	-27,74	33,64	304,45	-
Q1	54,92	15,54	-28,77	32,69	298,38	5,8
Q2	56,76	18,23	-30,28	35,34	301,06	4,2

For a better understanding of colour differences along the visible spectrum, samples' spectral curves were analysed. The overlapping of spectral curves in Figure 20, depicts the relation between the spectral reflectance at each wavelength of the three samples. At a temperature below 27°C, Q2 had the blue higher reflectance (approximately 450-490 nm) and the lower reflectance on red wavelength (approximately 620-740 nm) while Q and Q1 curves are more alike. Although total colour difference (dE*) of Q2 in relation to Q was lower than Q1, the spectral curves emphasized Q2 differences in specific wavelength ranges, being also visually more evident.

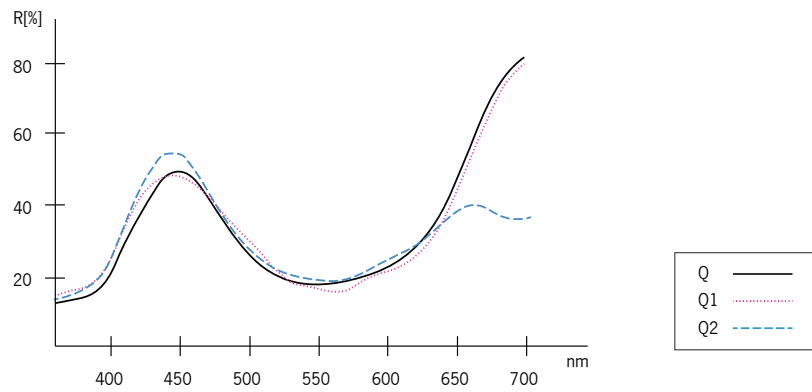


Figure 20. Spectral curves of samples Q, Q1 and Q2, below 27°C.

Light intensity that passes through the textile samples was analysed in regards to the colour change ratio from similar to different, with temperature increase. Photos of samples' colours in light transmittance (Figure 21) provide a visual confirmation of reasonable similarity between Q and Q1 below 27°C, whereas Q2 is perceived as darker. Above 27°C, samples' colours are distinct. Comparing the images of light transmittance variation with the light box perpendicular to the wall (Figure 22), it was observed that below 27°C, sample Q attained a slightly smaller area of light reflection on the wall than Q1 and Q2, while the tone of light was similar. When heated, the lighting areas between samples decrease from Q to Q1 and Q2, also presenting different colours.

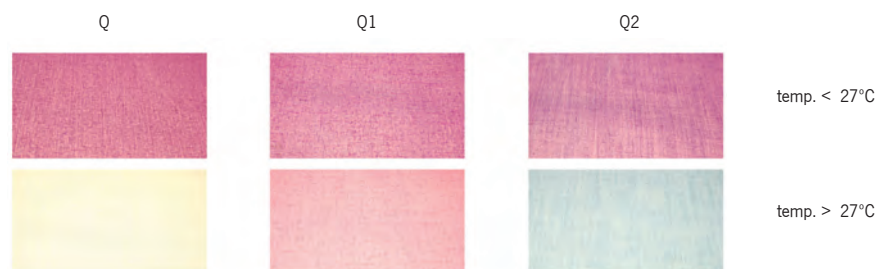


Figure 21. Colour of samples Q, Q1 and Q2 in light transmittance, below and above 27°C.

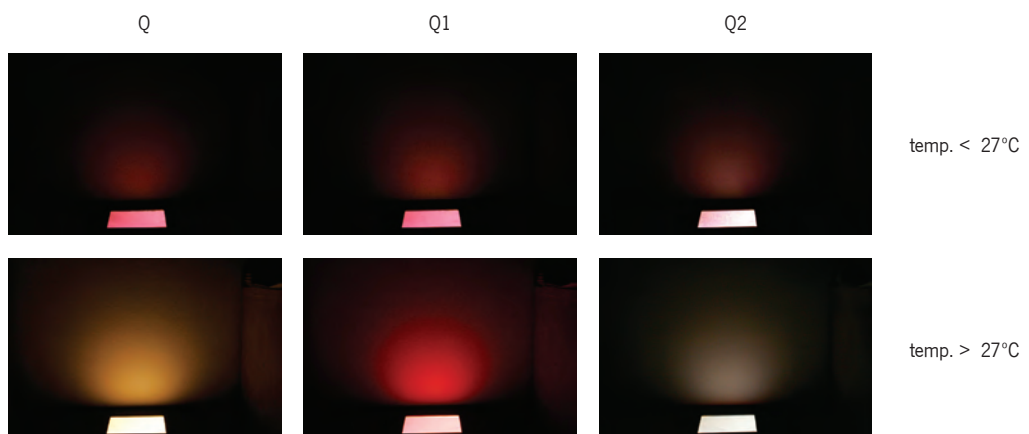


Figure 22. Light transmittance variation with samples Q, Q1 and Q2.

Mean values of light intensity measurements also confirmed that whereas samples' colours appeared similar below 27°C, light intensity varied. Sample Q attained the lower value with a difference of 0,78 lux from Q1, which is similar to Q2. When samples are heated, the higher difference observed was 3,32 lux between Q and Q2, representing 48% of light intensity difference. Upon temperature variation, the percentual luminosity difference increased from Q2, Q1 and Q.

Table 14. Mean values of light intensities with samples Q, Q1 and Q2.

Samples	Light intensity (lx)		Luminosity difference (%)
	temp.<27°C	temp.>27°C	
Q	1,23	6,86	82
Q1	2,01	4,24	53
Q2	1,96	3,54	45

The paste recipes defined for Q, Q1 and Q2 samples were applied for the development of a sample with a geometric pattern, in order to demonstrate the colours resemblance level below 27°C by comparison of the colour change in intercalated triangle areas, as well as to depict the colour change ratio defined: from similar to different with temperature increase. Figure 23 presents the sample heated in the area on the right.



Figure 23. Sample: from similar to different colour ratio.

In despite of the reasonable comparison between the samples' colours below 27°C, high resemblances were aimed. With the objective to study the possibility to improve colour similarities, a third experiment was conducted where, after an analysis of the samples screen printed with the formulated paste recipes, colour-matching adjustments were conducted based on the samples' spectral reflectance characteristics in the colourized state. Colour coordinates' analysis provides a comprehensive understanding of the differences between formulated samples and pattern colour. Along L*, a* and b* results, a relation between the pigments' concentration combined in paste can be approximately deduced.

This study was conducted with the 100% CO substrate, which was measured in the spectrophotometer and the results were applied for the textile substrate definition in the software, during paste recipe formulations.

Pattern sample R was defined with the follow setup TCm + TCb + TCk + Cy and samples with paste recipes formulated encompassed three combinations of pigments vs. colours parameters. Table 15 presents the samples' description with respective paste recipes.

Table 15. Description of R, R1, R2 and R3 samples and respective paste recipes.

Sample	Pigments vs. colours combination	Paste recipe (%)			
		magenta	blue	black	yellow
R	TCm + TCb + TCk + Cy	0,85	12,76	1,28	0,12
R1.0	Cm + TCb + TCk + Cy	0,14	13,00	0,05	0,12
R2.0	TCm + Cb + TCk + Cy	2,50	0,40	0,27	0,12
R3.0	Cm + Cb + Ck + Cy	0,20	0,35	0,01	0,13

After samples development, a comparative analysis was conducted. Figure 24 presents the screen printed samples and the results of samples' colour measurement were set in colour coordinates and CIELAB differences, in Table 16. Through visual comparison, sample R1.0 showed chromatic resemblances with R, while R2.0 was perceived as more blue and R3.0 more green. Comparing colour coordinates of samples with formulated paste recipes in relation to the pattern sample R, it was observed that: a) R1.0 is lighter, more green and more blue, with the higher values distance between coordinates on b* (2,37 difference) and L* (1,56); b) R2.0 is also lighter, more green and more blue, with the higher difference on b* (4,94) and a* (2,54); R3.0 is lighter, more green and less blue with high values distance on a* (7,36) and L* (5,48). The greater differences were found on the sample that combines four conventional pigments (R3.0), attaining 9,2 dE*. R1.0 was the sample which colour was more alike to the pattern sample.

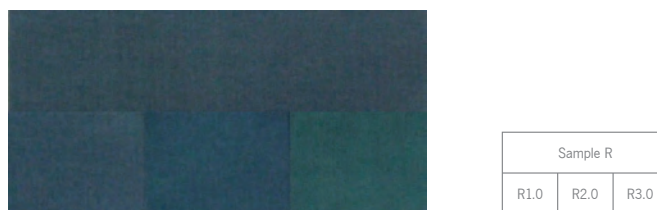


Figure 24. Samples R, R1.0, R2.0 and R3.0, below 27°C.

Table 16. Samples R, R1, R2 and R3 colour coordinates and CIELAB differences, below 27°C.

Sample	L*	a*	b*	C*	h	dE*
R	38,54	-7,27	-8,07	10,86	228,01	-
R1.0	40,10	-8,37	-10,44	13,38	231,26	3,0
R2.0	39,93	-9,81	-13,01	16,30	232,99	5,7
R3.0	44,02	-14,63	-7,15	16,28	206,03	9,2

After analyse the differences between samples' colour coordinates, addition, subtraction or maintenance of the pigments' concentrations was defined. The quantities to vary took in consideration the samples' value distance for each colour coordinate in relation to R, the previous percentage applied for each pigment and the pigment type, as the conventional pigments present higher colour strength than the TC pigments handled.

The first adjustments conducted in relation to the initial paste recipes are presented in Table 17, defined as follows: for sample R1.1 it was applied a concentration increase in Cm (0,02%) and TCk (0,03%); in R2.1, Cb was reduced (0,02%) and TCk increased (0,73%); in R3.1 there was a percentage increase for Cm and Ck (0,1 and 0,07%, respectively), while Cy was reduced (0,01%).

Table 17. Samples' paste recipes adjustments.

Sample	Pigments vs.colours combination	Paste recipe (%)			
		magenta	blue	black	yellow
R1.0	Cm + TCb + TCk + Cy	0,14	13,00	0,05	0,12
R1.1		0,16	13,00	0,08	0,12
R2.0	TCm + Cb + TCk + Cy	2,50	0,40	0,27	0,12
R2.1		2,50	0,38	1,00	0,12
R3.0	Cm + Cb + Ck + Cy	0,20	0,35	0,01	0,13
R3.1		0,30	0,35	0,08	0,12

Figure 25 presents the new screen-printed samples and respective pattern sample R. Table 18 presents the colour measurement results of the new samples, in comparison to previous ones with the same pigments' combination setup. Samples screen printed with optimized paste recipes were more similar to the pattern sample than previous samples and attained a relevant decrease of CIELAB difference, new values range between 2,0 and 2,5. However, colour differences were still perceived visually, particularly with R2.1 and R3.1 samples. Comparing the values for each colour coordinate, all samples presented results more similar to the pattern sample except colour opponent b* in sample R1.1 that was slightly more blue and R3.1 that was less blue than the previous sample.

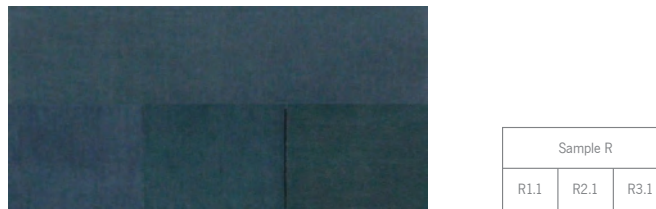


Figure 25. Samples R, R1.1, R2.1 and R3.1, below 27°C.

Table 18. Samples' colour coordinates and CIELAB differences, below 27°C.

Sample	L*	a*	b*	C*	h	dE*
R	38,54	-7,27	-8,07	10,86	228,01	-
R1.0	40,10	-8,37	-10,44	13,38	231,26	3,0
R1.1	38,53	-7,00	-10,58	12,69	236,51	2,5
R2.0	39,93	-9,81	-13,01	16,30	232,99	5,7
R2.1	38,11	-8,75	-9,40	12,84	227,04	2,0
R3.0	44,02	-14,63	-7,15	16,28	206,03	9,2
R3.1	37,29	-8,41	-6,32	10,52	216,92	2,4

Taking into consideration the improvement of colours similarity, additional cycles of paste recipes adjustments were performed. For each pigment combination, screen printed samples with the greater colour similarity with R are presented in Figure 26 and Table 19 presents the respective colour measurement results.

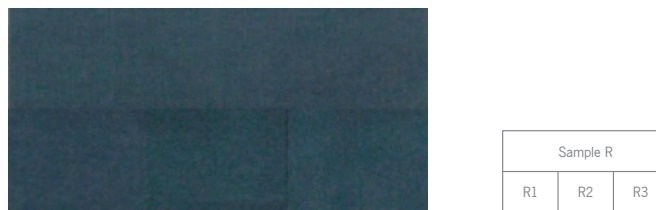


Figure 26. Samples R, R1, R2 and R3, below 27°C.

Table 19. R, R1, R2 and R3 colour coordinates and CIELAB differences, below 27°C.

Sample	L*	a*	b*	C*	h	dE*
R	38,54	-7,27	-8,07	10,86	228,01	-
R1	38,35	-7,17	-9,17	11,64	231,96	1,1
R2	38,44	-8,77	-8,45	12,18	223,94	1,6
R3	38,23	-7,90	-8,77	11,80	227,98	1,0

By direct observation, samples' colours appeared similar to the pattern sample, although it was still possible to detect a slightly greener nuance in R2. Colour coordinates confirmed the perceived resemblances and the highest value distance was 1,5 in a* coordinate of R2 sample. CIELAB differences with R1 and R3 were 1,1 and 1,0, respectively, and with R2 it was 1,6.

The overlapping of samples' spectral curves is presented in Figure 27. R1 spectral curve was similar to R, while R2 and R3 presented relevant differences, both with higher reflectance in the violet band (below approximately 450 nm) and lower red reflectance (above approximately 620 nm). The high divergence within the red band, was also identified in sample Q2 in relation to Q and Q1 samples, highlighting differences between pigments' types in respect to the colour blue: samples which pastes were elaborated with conventional pigment blue presented a lower reflectance within the red band, in comparison to samples' pastes developed with TC pigment blue.

Furthermore, while R2 and R3 curves were similar, by direct observation in natural light and comparison of colour coordinates conducted for measurements with illuminant D65/10, R3 was more similar to R than R2. Regarding this divergence, by observing samples under different light sources, similarities in relation to R slightly vary with R2 and R3 samples. The illuminant metamerism is particularly perceived with a subtle violet nuance in samples R and R1. In despite of this variation, samples' colours were still perceived to be similar.

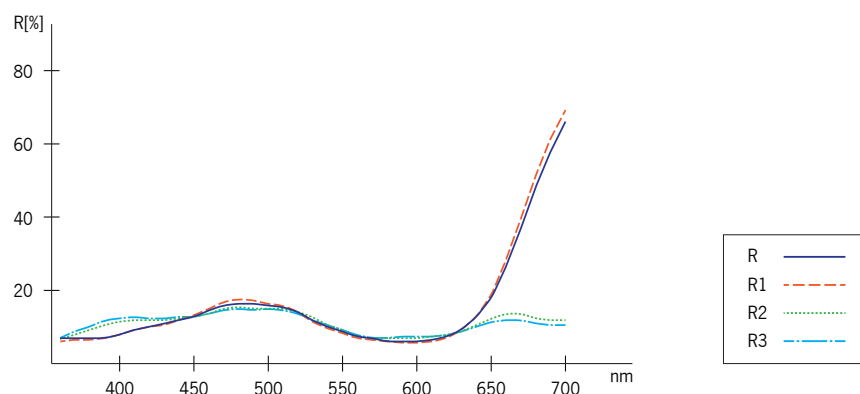


Figure 27. Spectral curves of samples R, R1, R2 and R3, below 27°C.

A study prototype was developed in an industrial context through rotary printing process, with the same substrate and paste recipes defined for samples R, R1, R2 and R3. Pastes' viscosity varied between 23, 27, 45 and 50 dPa from R to R3, respectively and a thickness agent was applied to present 90dPa in each paste. Rotary printed study samples were developed with different rod-squeegee numbers (differing in diameter and weight) and magnetic field applied, to analyse colours and select the parameters to apply in the study

prototype printing. The study prototype accomplished 22,0 x 1,5 m, developed with a geometric pattern composed by four cylinders with 91,4 cm rapport.

Figure 28 presents a photo of a section of the study prototype, below 27°C (image on the left) and with an area heated above 27°C (image on the right). Below 27°C, the study prototype colours have shown a decrease in similarity in relation to R samples' colours. Also being more obviously perceived is the colours metamerism as illustrated in Figure 29, which presents a part of the study prototype illuminated with two different artificial light sources.



Figure 28. Study prototype section, below and above 27°C.

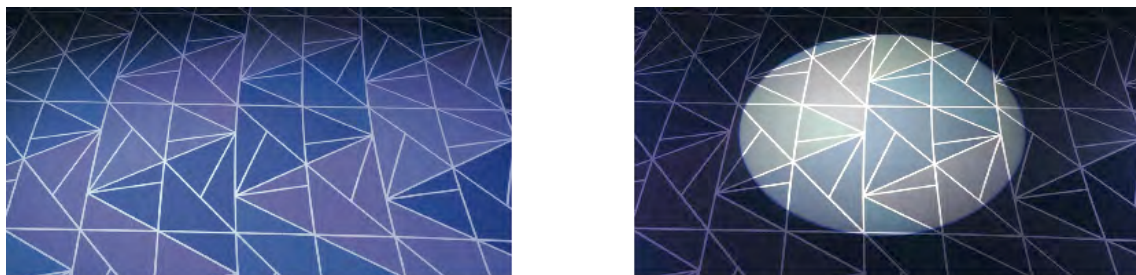


Figure 29. Study prototype section, under two different artificial light sources.

Reflecting the effect of the pigments' application process on colours, the results attained highlight the importance of creating the software database with concentration samples developed with the same process and respective parameters to apply in final products.

4.6 Experimental 4 – Rub, wash and light fastness

TC leuco dyes behaviour relies on a reversible colour change upon a thermal stimulus. A permanent variation of initial colour or a lost chromic behaviour, is not commonly desirable. In this section, the colourfastness

properties of the TC and conventional pigments handled were assessed, in regards to their resistance to rubbing, washing and lighting.

4.6.1 Materials and Methods

For a comparative analysis of the rub, wash and light fastness qualities of the pigments handled, a set of samples was screen printed comprising of paste recipes with mixtures of both pigment types: samples Q, Q1 and Q2 (Table 12); pastes with one TC pigment: sample S (3,6% magenta) and sample T (10,2% blue); and pastes with one conventional pigment: sample U (0,5% magenta) and sample V (0,5% blue).

Dry and wet rub fastness tests were conducted in the crockmeter equipment (item 3.3.8), according to ISO 105-X12: 2001 test method (ISO, 2001). After placement of the screen printed samples in the crockmeter sample holder (one at the time) and a white cotton cloth in the upper holder, 10 rubbing cycles were conducted for each test. For wet rubbing test, the white cotton cloth was soaked in distilled water before placement in the crockmeter. Staining in the white cloth was measured in the spectrophotometer and assessed within a standard grade scale from 1 to 5, where 1 stands for severe staining or colour change, thus poor fastness, and 5 for excellent fastness (Humphries, 2008).

Linitest equipment (item 3.3.9) was used to study samples' wash fastness, according to ISO 105-C06 A1S method (ISO, 2010). Previous to the wash cycle, each test sample was attached to a multifibre fabric composed of wool, acrylic, polyester, polyamide, cotton and acetate. Each sample was washed in a solution of 150mL with 4g/L of ECE soup, with 10 metallic balls and the test was conducted for 30 minutes at 40°C. Staining in the multifibre fabric was measured in the spectrophotometer and evaluated from 1 to 5 standard grade scale.

Stability under UV light exposure was studied using the equipment Accelerated Weathering Tester QUV (item 3.3.10). Samples were exposed to light for the follow time cycles: 15min., 30 min., 1h, 2h, 4h and 8h. Samples' colour change below 27°C was measured in the spectrophotometer and data was compared for CIELAB differences.

4.6.2 Results and Discussion

The results of dry and wet rub fastness tests are presented in Table 20. All samples attained similar staining grades from the sample to the white rubbing cloth. In the dry tests, there was only staining in sample V (conventional pigment blue), with the value 4-5. In the wet fastness test, the value 4-5 was common to all

samples except in sample S (TC pigment magenta), which did not present staining. The TC pigments handled presented a rub fastness quality similar or better than the conventional pigments.

Table 20. Staining grade in dry and wet rub fastness tests.

Sample	Dry	Wet
Q	5	4 - 5
Q1	5	4 - 5
Q2	5	4 - 5
S	5	5
T	5	4 - 5
U	5	4 - 5
V	4 - 5	4 - 5

Table 21 presents the results attained in the wash fastness tests. Grade 5 was obtained in all samples for the following fibres: acrylic, polyester, polyamide, bleached cotton and diacetate. Only in wool fibres, samples Q and Q1 presented the value 4-5. The results demonstrate a high wash fastness of the pigments handled.

Table 21. Staining grade in wash fastness tests.

Sample	wool	acrylic	polyester	polyamide	cotton	diacetate
Q	4 - 5	5	5	5	5	5
Q1	4 - 5	5	5	5	5	5
Q2	5	5	5	5	5	5
S	5	5	5	5	5	5
T	5	5	5	5	5	5
U	5	5	5	5	5	5
V	5	5	5	5	5	5

Colour differences attained in the light fastness tests are presented in Table 22. Until 30 minutes of light exposure, CIELAB differences vary from approximately 1 and 2 in all samples. With the increase of time exposure until 8 hours, the colour degradation of samples whose screen printing pastes just include TC pigments is very relevant (Q, S and T samples), having obtained dE^* values near or above 12. Samples where TC was combined conventional pigment (Q1 and Q2), presented lower colour differences, although the light effect on colour was still high. The results attained with the pigments handled are consistent with the reported poor stability of TC leuco dyes to light exposure.

Table 22. CIELAB colour differences in light fastness tests.

Sample	15 min.	30 min.	1 h	2 h	4 h	8 h
Q	1,0	1,0	1,2	2,2	5,3	11,6
Q1	0,7	1,5	2,0	3,9	4,4	7,2
Q2	1,3	1,3	1,4	2,5	4,2	9,9
S	1,0	1,9	2,9	3,8	7,0	12,6
T	1,0	1,1	1,4	2,5	5,7	11,9
U	0,8	1,0	1,9	3,2	3,3	4,0
V	0,6	1,1	1,4	1,6	2,1	2,6

4.7 Conclusions

Throughout the research conducted in this section, textile chromic effect on light transmittance was analysed, TC pigments behaviour and properties were studied and two process proposals were researched. Paste recipes were elaborated with TC and conventional pigments to screen print textiles that change colour according to predefined ratios.

TC textile behaviour as dynamic light filter entails a set of dependent variables for the designer to explore. The preliminary analysis allowed an initial understanding on the relation of light transmittance and TC pigments' colour, concentration and application processes. According to pigments absorption of specific ranges of light wavelengths to reflect or transmit their colours, samples screen-printed with different TC pigment colours at the same concentration attained different luminosity differences through the chromic behaviour. By changing the TC pigments concentration in the paste, the results demonstrated the possibility to create ratios of light transmittance variation. For example, 10% TC red (sample B) attained similar percentual luminosity difference than 1% TC black (sample E). Besides the quantitative data, perception of the light change in a dark room was evident, regarding intensity levels but also with great emphasis on light tone transition.

Application processes of the colourant in the substrate also affected the light transmitted and samples' appearance. By using the same pigments' colours and concentrations, the sample developed with TC and conventional pigments mixed in paste (H) attained higher luminosity difference than the sample where individual pastes for each pigment were screen printed through a layer overlapping (I). On the other hand, the two pigments' layers sample with TC on top (I) attained a darker expression, which for applications not focused on light transmittance purposes, present the possibility to use less TC pigment or explore darker

colour change effects with similar pigments' quantities than by mixtures in the same paste. The combination of dyeing and screen printing processes have also shown great potential to explore colour change effects.

Regarding the combination of TC and conventional pigments in the screen printed paste, the process outlined for the development of TC textiles that change from different to similar colours with temperature increase, demonstrated that colour and concentration of the conventional pigment (or combination of conventional pigments) fixed parameters, whereas the TC pigment colours and concentrations are variable parameters. Samples with the chromic ratio defined varied light transmittance from heterogeneous to similar luminosities.

To screen print TC textiles that change from similar to different colours, the process developed applied instrumental methods of paste recipe formulation. The database created with the colourimetric properties of the conventional and TC pigments colours, below their activation temperature, provided the possibility to formulate paste recipes where colours of each pigment type are selected as distinct colourant groups. This individual selection enabled the definition of pigments' colours in respect to their dynamic or static behaviour, depending on the colour change effect aimed. Samples with similar colours in relation to a defined pattern sample were developed, through one paste recipe attempt for each pigments' combination. Colour resemblance below the TC pigments activation changed to different colours with temperature increase, extending similar light transmittance to heterogeneous luminosities.

However, the colour match of a pattern sample with samples which pastes have the opposite pigment type was found to be challenging to attain, an issue also affected by the pigment colours' number in the paste and the combination with specific colours. Thus, an additional process of paste recipe adjustment was proposed to be conducted after the development of paste recipe formulation, based on a comparison of samples' colour coordinates. Samples developed attained CIELAB differences of approximately 1.

The optimization of paste recipes formulation and screen printing processes developed, provide a tool to explore colour change ratios across a wide range of colour palettes and textile applications. These processes apply some base procedures that are well known by the industry, which can enhance a path between TC textile design and manufacturing, through the systematization of procedures working with TC pigments and the colour match within textile collections. Nevertheless, the designer must fully understand the TC chromic behaviour in order to define colours and select the appropriate commands in the software to attain the desired colour change effect.

In the experimental works conducted, it was observed that the TC pigments handled presented considerably low colour strength in comparison to the conventional pigments as well as low colour similarity between

pigment types. Moreover, the TC pigments' transition from coloured to colourless with temperature increase was incomplete. A residual colour was perceived in the pigments' decolourized state, depending on colours and concentrations applied. With samples screen printed with different colours of 14% TC pigment, more obvious differences between residual colours were perceived than in samples with the same pigment colour at different concentrations for a 10% interval (4 to 14%).

Furthermore, the TC pigments used have presented similar or greater stability to rub and wash in relation to the conventional pigments, but light fastness was low: after 8 hours of UV light exposure, TC samples obtained CIELAB differences from 7,2 to 12,6, in relation to samples' colours before light exposure. Regarding this research objective to work with artificial light in interior spaces, poor light stability would not directly affect TC behaviour lifespan. However, this is a major issue for a broad range of applications and, although research have been conducted on this topic, there are still great limitations.

The research conducted in this section and the results attained through the samples developed and respective behaviour analysis, provides an understanding to design TC textiles and set up base procedures to implement in future developments in dynamic light filters research (chapter 7).

4.8 References

- ABEL, A. 2012. The history of dyes and pigments: from natural dyes to high performance pigments. *In: BEST, J. (ed.) Colour design: theories and applications*. Oxford: Woodhead Publishing and Textile Institute.
- ALBERS, J. 1968. *Oral history interview with Josef Albers, 1968 June 22-July 5* [Online]. <https://http://www.aaa.si.edu/collections/interviews/oral-history-interview-josef-albers-11847>: Archives of American Art, Smithsonian Institution. [Accessed 13 march 2012].
- ALBERS, J. 2013. *Interaction of Color*, New Haven, Yale University Press.
- ASPLAND, J. R. 1998. Colorants: Dyes. *In: NASSAU, K. (ed.) Color for science, art and technology*. Amsterdam: Elsevier.
- BAMFIELD, P. & HUTCHINGS, M. G. 2010. *Chromic phenomena: technological applications of colour chemistry*, Cambridge, Royal Society of Chemistry.
- BAURLEY, S. 2004. Interactive and experiential design in smart textile products and applications. *Personal and Ubiquitous Computing*, 8, 274-281.
- BLOJ, M. & HEDRICH, M. 2016. Color perception. *In: CHEN, J., CRANTON, W. & FIHN, M. (eds.) Handbook of visual display technology*. 2nd Ed. ed. Berlin: Springer.
- BRAINARD, D. 2003. Color appearance and color difference specification. *In: SHEVELL, S. K. (ed.) The science of color*. Amsterdam: Elsevier.
- BRIGGS-GOODE, A. 2013. *Printed textile design*, London, Laurence King Publishing.
- CHOUDHURY, A. 2010. Scales for communicating colours. *In: L., G. M. (ed.) Colour measurement: principles, advances and industrial applications*. Cambridge: Woodhead Pub.
- CHOUDHURY, A. K. R. 2014a. *Principles of colour and appearance measurement: Volume 2: Visual measurement of colour, colour comparison and management*, Cambridge, Woodhead Publishing.
- CHOUDHURY, A. K. R. 2014b. *Principles of colour appearance and measurement Volume 1: Object appearance, colour perception and instrumental measurement*, Cambridge, Woodhead Publishing.

- CLARKE, S. 2011. *Textile design*, London, Laurence King.
- CLARKSON, J. 2008. Human capability and product design. *In: SCHIFFERSTEIN, H. & HEKKERT, P. (eds.) Product Experience*. San Diego, CA: Elsevier.
- DAS, T. 2009. Surface design of fabrics for interior textiles. *In: ROWE, T. (ed.) Interior textiles: design and developments*. Boca Raton: CRC Press.
- DESCOTTES, H. & RAMOS, C. E. 2011. *Architectural lighting: designing with light and space*, New York, Princeton Architectural Press.
- DICKINSON, K. 2011. The use of colour in textile design. *In: BRIGGS-GOOD, A. & TOWNSEND, K. (eds.) Textile design: principles, advances and applications*. Oxford: Woodhead Publishing and The Textile Institute.
- EASTAUGH, N., WALSH, V., CHAPLIN, T. & SIDDALL, R. 2004. *The pigment compendium: a dictionary of historical pigments*, Oxford, Elsevier Butterworth-Heinemann.
- FEISNER, E. A. 2006. *Color Studies*, New York, Fairchild Publications.
- FIELD, G. G. 1998. Color imaging: printing and photography. *In: NASSAU, K. (ed.) Color for science, art and technology* Amsterdam: Elsevier.
- GANGAKHEDAR, N. 2010. Colour measurement methods for textiles. *In: L., G. M. (ed.) Colour measurement: principles, advances and industrial applications*. Cambridge: Woodhead Pub.
- GOETHE, J. & EASTLAKE, C. 2010. *Goethe's theory of colours*, LaVergne, TN, Kessinger Pub.
- GOLDSTEIN, B., E. 2010. *Sensation and perception*, Belmont, CA, Wadsworth, Cengage Learning.
- GOODMAN, T. M. 2012. International standards for colour. *In: BEST, J. (ed.) Colour design: theories and applications*. Oxford: Woodhead Publishing and Textile Institute.
- GREGORY, R. L. 1978. *Eye and brain: the psychology of seeing*, New York, McGraw-Hill.
- GUPTA, V. 2010. Expressing colours numerically. *In: L., G. M. (ed.) Colour measurement: principles, advances and industrial applications*. Cambridge: Woodhead Pub.
- HANSON, A. R. 2012. What is colour? *In: BEST, J. (ed.) Colour design: theories and applications*. Oxford: Woodhead Publishing and Textile Institute.
- HIDEFI, M. 2012. Understanding and forecasting colour trends in design. *In: BEST, J. (ed.) Colour design: theories and applications*. Oxford: Woodhead Publishing and Textile Institute.
- HUMPHRIES, M. 2008. *Fabric reference*, Upper Saddle River, NJ, Prentice Hall.
- HUNT, R. W. G. 2004. *The reproduction of colour*, Chichester, John Wiley & Sons.
- HURLBERT, A. & LING, Y. 2012. Understanding colour perception and preference. *In: BEST, J. (ed.) Colour design: theories and applications*. Oxford: Woodhead Publishing and Textile Institute.
- INGAMELLS, W. 1993. *Colour for textiles: a user's handbook*, Bradford, Society of Dyers and Colourists.
- ISO 2001. Textile – Tests for colour fastness – Part X12: Colour fastness to rubbing. *ISO 105-X12*.
- ISO 2010. Tests for colour fastness – Part 06: Colour Fastness to domestic and commercial laundering. *ISO 105-C06*.
- ITTEN, J. 1973. *The art of color: the subjective and objective rationale of color*, New York, Van Nostrand Reinhold.
- ITTEN, J. & BIRREN, F. 1970. *ITTEN The Elements of color*, New York, Van Nostrand Reinhold Co.
- KALAT, J. W. 2007. *Biological psychology*, Belmont, CA, Thomson/Wadsworth.
- KRAUSKOPF, J. 1998. Color vision. *In: NASSAU, K. (ed.) Color for science, art and technology* Amsterdam: Elsevier.
- KUEHNI, R. G. 2012. *Color: an introduction to practice and principles*, Hoboken, J. Wiley & Sons.
- LAM, W. 1992. *Perception and lighting as formgivers for architecture*, New York, Van Nostrand Reinhold.
- LENNIE, P. 2003. The physiology of color vision. *In: SHEVELL, S. K. (ed.) The science of color*. Amsterdam: Elsevier.
- MAHAPATRA, N. 2016. *Textile dyes and dyeing*, New Delhi, Woodhead Publishing India.
- MARCUS, R. T. 1998. The measurement of colour. *In: NASSAU, K. (ed.) Color for science, art and technology* Amsterdam: Elsevier.
- MAY, M. 2007. *Sensation and perception*, New York, Chelsea House Publishers.

- MILES, L. W. C. 2003. *Textile printing*, Watford, Merrow Pub. Co. Ltd.
- NASSAU, K. 1998. Fundamentals of colour science. *In: NASSAU, K. (ed.) Color for science, art and technology*. Amsterdam: Elsevier.
- PARRAMAN, C. 2012. Colour printing techniques. *In: BEST, J. (ed.) Colour design: theories and applications*. Oxford: Woodhead Publishing and Textile Institute.
- PÉREZ, V., SAIZ, D. & VERDÚ, F. 2010. Colour vision: theories and principles. *In: GULRAJANI, M. L. (ed.) Colour measurement: principles, advances and industrial applications*. Cambridge: Woodhead Pub.
- RIZZI, A. & BONANOMI, C. 2012. Colour illusions and the human visual system. *In: BEST, J. (ed.) Colour design: theories and applications*. Oxford: Woodhead Publishing and Textile Institute.
- ROBERTSON, S. 2011. *An Investigation of the Design Potential of Thermochromic Textiles used with Electronic Heat-Profiling Circuitry*. PhD thesis, Heriot-Watt University.
- SCHWARTZ, M. M. 2002. *Encyclopedia of smart materials*, New York, J. Wiley.
- SETCHELL, J. S. 2012. Colour description and communication. *In: BEST, J. (ed.) Colour design: theories and applications*. Oxford: Woodhead Publishing and Textile Institute.
- SHERIN, A. 2012. *Design elements color fundamentals*, Beverly, MA, Rockport Publishers.
- SMITH, V. & POKORNY, J. 2003. Color matching and color discrimination. *In: SHEVELL, S. K. (ed.) The science of color*. Amsterdam: Elsevier.
- TILLEY, R. J. D. 2000. *Colour and optical properties of materials: an exploration of the relationship between light, the optical properties of materials and colour*, Chichester, John Wiley & Sons.
- TRIEDMAN, K. 2015. *Colour: The professionals' guide: Understanding, appreciating and mastering colour in art and design*, Lewes, Ilex.
- WESTLAND, S. 2016. Color communication. *In: CHEN, J., CRANTON, W. & FIHN, M. (eds.) Handbook of visual display technology*. 2nd Ed. ed. Berlin: Springer.
- WORBIN, L. 2010. *Designing dynamic textile patterns*. Doctoral Thesis, University of Borås.
- XIN, J. H. 2006. *Total Colour Management in Textiles*, Cambridge, Woodhead Publishing and The Textile Institute.
- YOT, R. 2011. *Light for visual artists: understanding & using light in art & design*, London, Laurence King.

SHAPE MEMORY TEXTILES

CHAPTER 5

CHAPTER 5. SHAPE MEMORY TEXTILES

5.1 Shape

Shape memory textiles behaviour comprehends a material system that performs physical transformations. Regarding temporal and spatial relationships, shape change can be visually perceived as movement (Gordon, 2004). Along speed and direction parameters, motion perception also includes the ability to recognize a shape in different positions or seen from different viewpoints, called viewpoint invariance (Goldstein, 2010). Thus, during shape change, two configurations are perceived as different positions or orientations of the same shape.

In nineteenth century, the German mathematician Felix Klein defined a group of shape transformations perception, according to invariant geometric properties (Nefs, 2008). Figure 30 illustrates the four groups: isometry, similarity, affinity and projectivity. The original images are depicted with a thicker line than the transformed images and they are represented in 2D but can also be reported for three-dimensional shapes.

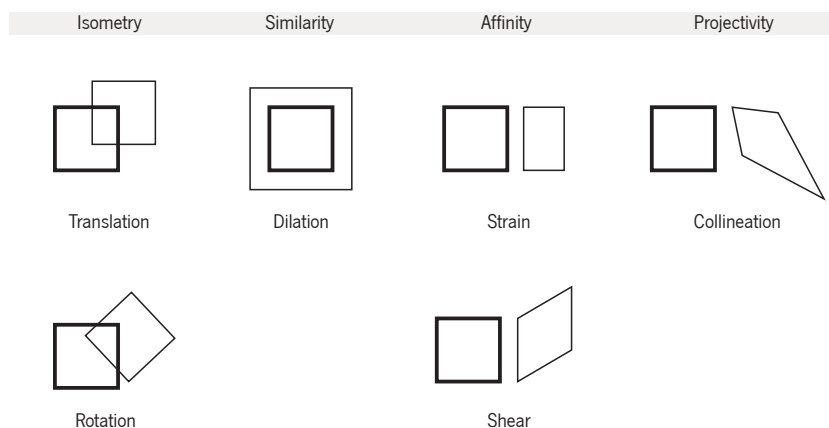


Figure 30. Klein transformations (Nefs, 2008).

Isometry is the change in position of equal shapes, they maintain the angles and distance of their geometry and vary position in space according to translation and/or rotation processes. In similarity transformation the points of an object maintain their angles and distance ratio with a point in the field, as can be observed in dilation. All isometries are also similarities and shape perception within this transformation allows us to recognize an object, for example, independently of its size or depth in the visual field. Affinity is the transformation that preserves parallel relations while position and distance ratios can vary. This transformation includes strain effect, where one dimension of the object can be increased or decreased and shear effect where parallelism is maintained within displacement in one dimension as a function of a second dimension,

for example when a shape is distorted to an angle perspective. Finally, projectivity is the transformation where all collinear points (points that lie in a single straight line), maintain collinearity in the transformed object (Nefs, 2008; Sibley, 2015).

Furthermore, the visual system also attempts to organise what is perceived in order to make sense of the world (Nefs, 2008). Based on the principle that the whole is different from the sum of the parts, Gestalt psychologists have proposed laws of perceptual organization (May, 2007). The law of *pragnanz* defends that stimulus patterns of grouped elements are perceived and interpreted as simple as possible, meaning that in the presence of complex shapes, the visual system tries to organize them in the simpler way (Goldstein, 2010). This law is central in the Gestalt psychology and based on it, several principles have been outlined, which can be relevant to be familiar with, when working with shape memory textiles, such as: similarity, proximity, good continuation, closure, common fate and synchrony. Figure 31 presents an example for each of the aforementioned principles, also called laws.

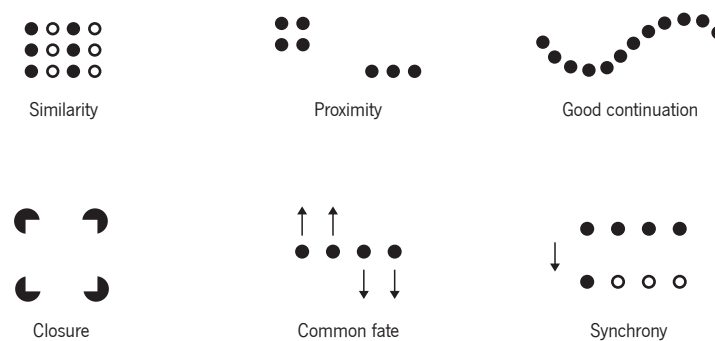


Figure 31. Gestalt laws: similarity, proximity, good continuation, closure, common fate and synchrony.

Similarity law refers to the tendency of elements with similar characteristics appear to be grouped. In the illustrated example, dots of the same colour can be perceived as vertical columns. Diverse characteristics can fulfil this effect such as shape and texture. The law of proximity refers to objects that are closer also appearing to be grouped, independent of their shapes. Good continuation refers to the tendency of perceiving elements that show smooth connections as a unit. Thus, shapes rearranged in lines or curves are more likely to be grouped. Closure means that it is possible to perceive complete figures, despite some parts are incomplete. The visual system is able to fill the gap of the missing information. Common fate law refers to objects that move in the same direction appearing to be grouped. Events that occur at the same time also can be perceived as belonging together and that is the law of synchronism (Gordon, 2004; May, 2007; Nefs, 2008).

Gestalt principles are considered important in the visual perception field, for an understanding of how the visual system tends to organize what is observed. Nevertheless, the observation time can also play a crucial

parameter of how images are perceived and usually longer time falls in a more complex and detailed analysis. Additionally, several visual illusions are also related with Gestalt laws (Nefs, 2008).

In context of shape change textiles, the described principles highlight the possibilities of shapes being perceived as a unit or pattern according to their similarities, proximity and rearrangement; the perception of a complete shape being attained within incomplete images; and the activation of shape change across equal direction and/or time of event, being able to group individual elements.

The change in shape of physical interfaces can also be characterized according to different variables. Rasmussen et al. (2012) suggest eight types of changes that can occur individually or grouped: orientation, form, volume, texture, viscosity, spatiality, adding or subtracting and permeability. Regarding changes from one form to another without dividing or joining elements, they are defined in mathematics as homeomorphic or topological equivalents (Coelho and Zigelbaum, 2011; Rasmussen et al., 2012). In this research, the development of shape memory textiles address material system with homeomorphic behaviour, which trained and programmed mutable shape is triggered through changes in materials properties.

With the objective of understanding characteristics and qualities of movement, several authors examined movement-based concepts through an interdisciplinary approach. Vaughan (1997) analysed movement in theatre and psychology, namely through the theory of affordances coined by J. J. Gibson, which refers to the action possibilities perceived through the materials or objects' properties, what they afford. Young et al. (2005) explored choreography based-concepts through Laban theory, a method developed for movement notation. Young used the metaphor of language considering the element of movement as the alphabet, which he defines as path, volume, velocity and direction to discuss sequence and qualities of movements as the grammar and syntax.

Rasmussen et al. (2012) discussed movement through a critical review of shape-changing interfaces, distinguishing kinetic parameters as the physical specifications of movement, based on Youngs' alphabet, and defined association and adjectives as the expressive parameters of how movement is perceived. He described expressive association is respect to the changes being perceived either mechanical or organic and the expressive adjectives as the traits and qualities assigned to the changes.

The interrelation between shape, materials and dynamic behaviour is transversal to diverse domains focused in shape-changing structures. Hensel and Menges (2006) reflect upon self-organization examples in the natural world to study how form emerges and continually differentiates, transforms and performs. Through digital fabrication and performance analysis methods, they design new approaches on complex adaptive

systems for architecture (Hensel et al., 2006). Concerning soft mechanic systems, Coelho and Zigelbaum (2011) focus on topological, textural and permeable transformations with SMAs, to analyse emergent possibilities for shape-changing applications.

Developing shape memory textiles with the ability to perform predefined geometric configurations also demands a study of the textile physical form or shape – morphology (Hensel and Menges, 2006). Textile substrates can be manipulated or shaped to exhibit different textures or structures, where diverse techniques can be applied such as folding, smocking, 3D shibori and finishing processes (Richards, 2012; Wada, 2012; Singer, 2013). In this study, the solution for the requirement of geometric rigor and generation of morphologies with different number of layers was developed through origami techniques.

Origami is an ancient Japanese art of folding paper that in the last decades have been inspiring an emergent field of sciences and engineering (Hartl et al., 2014). Across diverse materials, this technique presents new possibilities to fabricate, assemble, store and morph structures (Peraza-Hernandez et al., 2014), within applications at different scales: from DNA approaches at nano-scale (Edwards and Yan, 2014) to structures for space (Miura, 1994; Lang, 2009).

Surface effects, haptic qualities, sculptural and functional aims have been approached within origami textiles, where besides traditional methods to create origami models by manual experiments, there are also software applications which can generate crease patterns such as Origamizer, TreeMaker and Oripa (Tachi, 2010; Lang, 2011; Mitani, 2011). Issey Miyake and his Reality Lab team developed – 132 5. Issey Miyake – a label of “a piece of cloth”, based on origami concepts and software development which explores how textile structures can extend from a flat foldable piece to a three dimensional garment or accessory (Ugur, 2013; Shimizu, 2016).

Regarding the combination of active materials and origami, Peraza-Hernandez et al. (2014) highlight as critical design parameters the actuation strain, actuation stress and the necessity to balance the actuators characteristics within the structures' scale. Some examples of self-folding structures include: Programmable Matter, where a triangular tiled sheet was combined with SMA foil actuators and flexible electronics to create a material that performed a self-folding boat and airplane (Hawkes et al., 2010; Paik et al., 2011); a laminated composite with two outer layers of SMA film, able to form three-dimensional structures (Hartl et al., 2012); and paper transformations where SMAs wires were taped, sewed or attached with snaps (Koizumi et al., 2010; Saul et al., 2010; Qi and Buechley, 2012).

In this research, the behaviour of the SMAs wires integrated in woven structures, aims to perform transformations between predefined geometric shapes, to attain layer variation and affect light transmittance. Thus, textile morphology seeks for structural and expressive possibilities, taking into consideration shape, material system and defined behaviour as dissociated elements.

To illustrate the origami folds, a crease pattern or origami diagram is implemented. Crease patterns consist of drawing mountain and valley folded lines necessary to depict the origami creases (Jackson, 2011). They can be represented in different ways. In this study a black continuous line for mountain fold and red dashed line for valley fold were applied.

There are origami base folds that can be combined to develop more complex models (DiLeonardo-Parker, 2016). Origami tessellation is based on repetition of common base patterns of folded pleats and twists, creating intricate patterns (Gjerde, 2009). These origamis can display a property of flat foldability, which means the origami model is flat after being folded. Surfaces folded through tessellation techniques create areas with different amount of layers. Additionally, origami models which display movements in their folded state are named action origamis.

In *shadowfolds*, Rutzky and Palmer (2011) combined the concept of pleat and translucency for origami tessellations developed in textiles. They highlighted the expressive quality that these models may exhibit such as the light shining through and the revelation of the folds' depth. In this research, the translucency of textile origamis is studied in a dynamic perspective, in which the interaction of the shape memory textile with light will design dynamic light for expressive and functional purposes.

5.2 Introduction to the Experimental Work

The aim of this research section is to develop shape memory woven textiles in which dynamic behaviour achieves predefined geometric morphologies. The design concept inherent to the material research focuses on the interaction of the textile SME and light.

The requirement of geometric morphology was addressed through origami techniques. Combining foldability properties with shape change, it is possible to design textile structures with a variable number of layers. Initially, it was conducted a preliminary analysis of differences in light transmittance according to layer variation.

The experimental work concerned with the shape memory textile development and performance analysis has involved several studies. First, the objective was to analyse and optimize the accuracy of the shape's angles memorized in the Nitinol alloys, in relation to the predefined geometry. Having achieved an understanding of the associated parameters, the question raised was how to integrate SMA wires in textile substrates that can perform predefined morphologies. The experimental setup have involved the development of physical models comprised of a) paper samples to define morphology, shape change and Nitinol wires' geometry according to the crease pattern; b) textile samples to research manufacturing processes, morphology coherency as well as shape change behaviour and characteristics.

Study samples of origami base folds and an intricate origami pattern were developed, in order to research a workflow setup for the development of shape memory textiles that change from one temporary to a memorized morphology. Textile activation through resistive heating was also studied and the results have highlighted the requirement to increase adhesion of the Nitinol within the host structure as well as electrical insulation of the alloys. Several finishing processes were studied along to the influence of a selected one in the shape change behaviour.

After, the experimental work focused on the development of shape memory textiles able to perform two shapes behaviour. A different Nitinol integration approach was proposed in order to improve the textile behaviour and the effect of changes in the Nitinol geometries was studied across samples dimensions and positioning during shape change activation.

The experiments conducted have attained an understanding of the manufacturing processes and performative variables to develop and assess the shape change textiles behaviour within predefined geometric shapes. The results attained will be implemented in a design research, where interaction of textile SME with light transmittance will be further studied and presented in dynamic light filters chapter.

5.3 Experimental 1: Textile Morphology and Light Transmittance

For a preliminary analysis of the transmittance variation that the dynamic textile morphology may produce and for a proof-of-concept in an initial stage of the work, two experiments were conducted. First, the relation was studied using simple pile-up of textile layers. After, two origami-based textiles were developed to analyse the phenomena upon layer variation in specific areas, attained by the folding and unfolding behaviour.

5.3.1 Materials and Methods

To understand how the amount of layers can transform the fraction of incident light that goes through them, a photographic record and a light meter measurement were conducted using pile-up layers of the 50% CO 50% PES textile substrate.

The tests were conducted in a dark room and different amounts of textile layers were placed on the open face of a light box. For the photo record, the light box was set with the open face perpendicular to a wall and a camera set on a tripod. In the light intensity measurement, the open face of the light box was set in vertical position, 1 m from the luxmeter. The lamp was turned on and the luxmeter values recorded on three points.

For the study of layer variation upon the folding and unfolding, two textile origamis were developed, with the aforementioned substrate. The origami models comprise of intricate patterns based on the waterbomb and squaretwist crease patterns (Figure 32). They are origami base folds and were chosen for this experiment and for the study of the SMA integration in textiles, due the different level of complexity that they might present for shape memory textile development and performance. Waterbomb is based on pleats while squaretwist displays pleats and twist. The origami patterns that can be designed with these base folds are limitless.

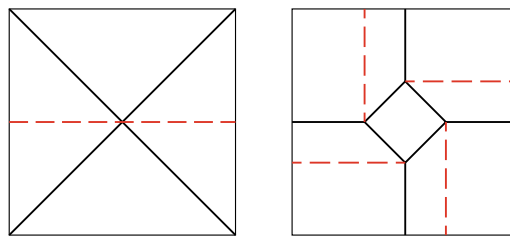


Figure 32. Waterbomb and Squaretwist crease pattern (left and right, respectively).

The unfolding of the samples was carried out manually and focused on the creation of spaces between the folds, instead of achieving the complete unfolding of the textile surface. To evaluate light transmittance, the luxmeter was placed 5 cm above the light box top, pointing to a white surface placed 1,0 m in front of the light box, in a first measurement cycle, and 0,5 m in the second measurement. Light intensity values were recorded on three points.

5.3.2 Results and Discussion

The images of the pile-up layers from one to six are presented in Figure 33. Light projection on the wall allows visualization of the relation between the blur size of the projected light and light intensities. The decrease of light transmittance among layer number is perceived and, comparing one textile layer (image on the left) with six pile-up layers (image on the right), the light projection area appears to be less than 50%.



Figure 33. Pile-up of textiles from one to six layers (left to right, respectively).

Table 23 shows the mean values of measured light intensities attained with the pile-up layers. According to the results, it is possible to conclude that the variation of the number of textile layers achieves a considerable change of light transmittance. From one to two layers, the reduction was about 43%, additional layers produced a transmittance decrease of approximately 10% per layer, until five layers. From five to six layers the difference was only 4%. The values attained until five layers were considered significant to design dynamic light filters and present a base framework for the following experimental sections within origami samples.

Table 23. Mean values of light intensities.

N° of layers	Light intensity (lx)	Difference (%) 1 layer to x layers
1	13,38	-
2	7,62	43
3	5,17	61
4	3,83	71
5	2,64	80
6	2,09	84

The resulting origami model presented in Figure 34 consists of pleated squares created by waterbomb folds in each square vertex. The unfolding was carried out by pulling up the centre square, causing a volume increase with a partial unfolding of the waterbomb folds. In Figure 35, the model is composed of squaretwist folds, regularly aligned. This origami presents vertical and horizontal tabs created by the twist of the squares. The shape change was produced by folding the horizontal tabs orthogonally to the origami surface.

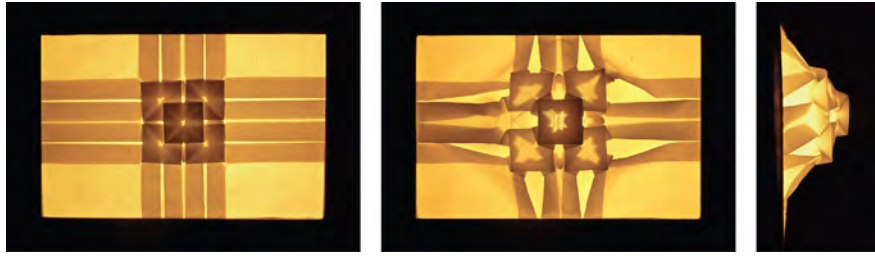


Figure 34. Study model waterbomb fold based: folded (left) and unfolded (centre and right).

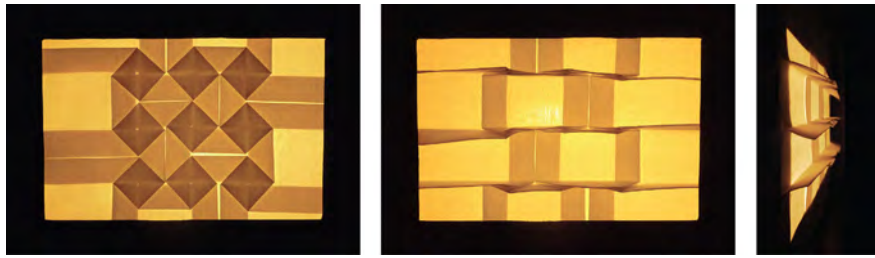


Figure 35. Study model squaretwist fold based: folded (left) and unfolded (centre and right).

Table 24 presents the measured light intensities of the folded and unfolded models. The results show a difference of light transmittance between 61% and 57% with the waterbomb based sample and between 74% and 71% in the squaretwist based sample. By direct observation, it was also perceived the change of the ambient light intensity.

Table 24. Mean values of light intensities.

Sample	Distance (m)	Light intensity (lx)		Luminosity difference (%)
		Folded	Unfolded	
Waterbomb based	1,00	2,54	6,55	61,00
	0,50	5,05	11,73	57,00
Squaretwist based	1,00	1,42	5,38	74,00
	0,50	2,18	7,44	71,00

The values of the experiments conducted relate to the specific characteristics of the textile substrate applied and the origami crease patterns. However, they set an initial understanding of the transmittance variation that might be achieved with different number of textile layers, presenting the possibility to create dynamic light with textiles structures whose morphology displays shape change.

5.4 Experimental 2: Nitinol Shape Set

To train the SME of the Nitinol wire, it is necessary to fix it in the desired shape and condition it to high temperatures (Hesselbach, 2007). This study aimed to optimize the heat treatment parameters for the selected SMAs, considering the geometries defined.

5.4.1 Materials and Methods

The Nitinol wires handled in this experiment have three diameters: 0,2; 0,3 and 0,5 mm. To study the accuracy of Nitinol performance in reacquiring the programmed shape, a 90° angle was defined. The experiments conducted to shape set the Nitinol, took into consideration the annealing parameters indicated by the supplier – temperature and duration of the heat treatment. It was advised to apply a temperature between 450°C and 550°C. Duration was suggested to be tested, highlighting that long periods of time could interfere with the wire's fatigue and the ability to perform repeatable accurate predefined shape changes throughout several cycles.

A stainless steel sheet with 1mm thickness was used to produce a die to create the desired shape. The exact location of the wire crease was set with an orifice through which the wire is led, and the wires were fixed with screws and nuts Figure 36. The distance between the screws and the crease orifice is 5,5 cm and after the treatment the alloys were cut at 5 cm distance of the crease point to avoid the curly ends.

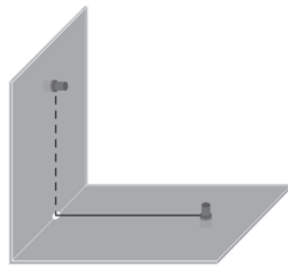


Figure 36. Nitinol die setup.

First experiments were carried out for 5 minutes, at temperatures of 500°C and 550°C. New experiments were developed at a temperature of 550°C and varying the period of time for each sample set – 20, 15 and 10 minutes – a sample set being composed by five Nitinol samples of each of the three wire diameters, totalling fifteen.

The prepared samples were then analysed by submitting the wires to five cycles of deformation and heat stimulus. For this purpose, they were placed one at a time in a heat chamber, after being deformed at the

cooling phase – martensite (M). In the chamber, temperature was increased from 20°C to 45°C (Af temperature) and, for each cycle, the sample was removed, placed on a surface with a guideline and photographed. The angles attained on the captured images were measured in Adobe Illustrator software.

5.4.2 Results and Discussion

At an ambient temperature, the angles measured above 95° in the samples that were heat treated during 5 and 10 minutes. At 20 minutes, the wires presented a significant variation of angles between the different cycles. In the wires treated during 15 minutes, angles between 90° and 92° for Nitinol of 0,2mm thickness (1st row of Figure 37); 90° to 91° for Nitinol of 0,3mm (2nd row of Figure 37) and of 0,5mm (3rd row of Figure 37) were obtained.

Considering that the results attained with the heat treatment of 550°C during 15 minutes present small, acceptable variations from the pre-programmed 90° angle, this condition was selected for further experimentation.

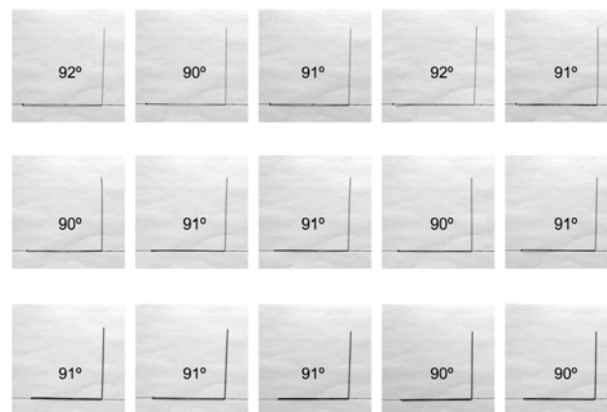


Figure 37. Angle values attained throughout 5 cycle tests for each Nitinol wire, with heat treatment during 15 minutes. Upper row to lower row: 0,2; 0,3 and 0,5mm diameter.

5.5 Experimental 3: Study Samples of Origami Base Folds

The objective of this experiment was to study the integration process of Nitinol wires in woven substrates and their ability to recover the defined morphology when activated. The predefined geometry of the shape memory textiles dictates the Nitinol wires' shapes, according to the crease pattern and the specific location where each alloy will be integrated. This condition highlights the drawing and manufacturing of different wire geometries to be embedded in the same textile structure, as it will be illustrated.

5.5.1 Materials and Methods

In order to study the shape change behaviour within predefined geometric configurations, the origami base folds – waterbomb and squaretwist – were implemented on basis of woven samples, by integrating Nitinol wires of the three selected diameters.

The integration of Nitinol wires was done in a plain weave structure. This selection was due to the regularity and maximum number of interlacings of this woven structure and their improved control of Nitinol for the shape change (Dyer, 2010). It was defined that the final samples dimensions would be 12x12cm with Nitinol wires inserted in the weft at every 1,5 cm.

To achieve the final folding effect, the shapes to be memorized on each of the Nitinol wires depend on the origami morphology while folded. To define these wire geometries, a paper model with horizontal lines spaced by 1,5 cm was folded with the shape of the selected origami. The resulting wire geometries were then taken from the model. Each model includes seven Nitinol wires and some of the wire configurations are equal. The waterbomb model contains four different wire shapes (Figure 38), whilst the squaretwist model has three (Figure 39).



Figure 38. Waterbomb model open and close (left and centre); SMA shapes (right).

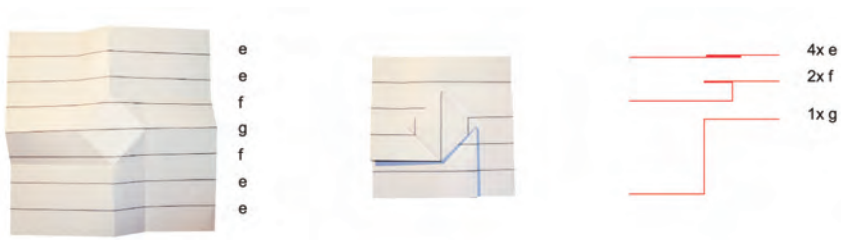


Figure 39. Squaretwist model open and close (left and centre); SMA shapes (right).

After defining the Nitinol wire shapes, the die for each geometry was designed and produced (Figure 40). The wires' extremities were fixed with screws and the wire shape followed the die geometry by passing orifices placed at the exact crease locations.



Figure 40. Waterbomb dies (left); Squaretwist dies (right).

Finally, samples of the base structures were produced, which involves the following steps: training the Nitinol wires with the predefined shapes; setting up the loom and weaving the samples. A total of six samples were developed – for each origami model (waterbomb and squaretwist) three samples were produced with the different SMA wire thickness (0,2; 0,3 and 0,5 mm).

Nitinol training consisted of fixing the wire, one at the time, in each die and placing it in the furnace for 15 minutes, which was pre-heated at 550°C. When removed from the furnace, samples were water quenched, being exposed to a temperature of approximately 10°C and were then deformed to a straight shape.

The samples were woven in a table handloom. The same CO yarn was used for the warp and the weft and one specific pre-trained Nitinol wire was inserted every 1,5 cm, according to its position in the origami crease pattern, into a plain weave structure.

To analyse the behaviour of the developed study samples, it was conducted a video and photographic record. The samples were deformed at M phase, placed on a horizontal surface and thermal activation was induced with a heater, attaining approximately 45°C.

5.5.2 Results and Discussion

Figure 41 illustrates the waterbomb samples' performance in five different phases, with the first row displaying the images of the sample produced with 0,2 mm Nitinol wire; the second row with 0,3 mm and the third row with 0,5 mm. Figure 42 follows the same sequence for squaretwist samples.



Figure 41. Waterbomb samples during thermal activation (1st row 0,2 mm wire sample, 2nd 0,3 mm and 3rd 0,5 mm).



Figure 42. Squaretwist samples during thermal activation (1st row 0,2 mm wire sample; 2nd 0,3 mm and 3rd 0,5 mm).

The samples developed achieved different performances depending on the wire thickness and origami diagrams. The shape change transfer follows the predefined configurations, however, final geometries did not reach the exact angles defined and trained in the Nitinol wires.

In the waterbomb configuration, the sample with 0,5 mm Nitinol exhibits better shape recovery than the ones of 0,3 mm and 0,2 mm. Conversely, in the squaretwist origami, the 0,5 mm sample achieved the lowest performance. Due to the existence of more creases in the squaretwist diagram than in the waterbomb one, the woven structure appears to have a higher constraining effect on thicker wires. Better performance on squaretwist samples was achieved with 0,3 mm and 0,2 mm Nitinol.

The shape change process was recorded in three videos for each sample. In both origamis, the samples with 0,2 mm Nitinol wires needed more time to recover their shape when compared with other samples, of approximately 50 seconds. In the waterbomb diagram, the average duration for samples developed with 0,3

mm and 0,5 mm was of 18 seconds, whilst in the squaretwist diagram, the values were slightly higher: 22 seconds for 0,3 mm and 25 seconds for 0,5 mm samples.

Difficulties were found in deforming the samples on flat surfaces. It was not possible to deform the Nitinol creases to assume a straight shape by hand deformation. In some of the creases, wire protruding the woven structure was observed. This was more evident in samples with 0,5 mm thick wire.

Nitinol 0,3 mm thickness wire was selected for the following developments, given that its overall behaviour was found more stable in regards to the aforementioned variables. Furthermore, weave density is to be increased to improve shape transfer of the Nitinol integrated in the textile.

5.6 Experimental 4: Squaretwists Pattern Sample

This study applies the process setup proposed in the preliminary experiments, to the design of a shape memory textile based on an intricate origami. The sample development encompasses an increase of the weave density with the aim to improve shape transfer of the Nitinol integrated in the textile. The shape was defined with basis on the geometry of squaretwist tabs fold up, as described in 5.4 section and the sample activation was triggered through resistive heating. Finally, light transmittance variation generated through the sample performance was analysed.

5.6.1 Materials and Methods

To define the textile morphology, the base fold selected was the squaretwist. In the folded state, this origami presents a square area with five layers, four tabs with three layers (in the area exterior to the square) and a remaining area with one. The tabs are two by two, parallel to the correspondent square diagonals (vertical and horizontal). When tabs with the same direction are pulled up to an orthogonal plane, in relation to the folded origami, it is possible to obtain a valley fold in a square diagonal attaining a variation in the amount of layers. When the square and two tabs are folded up, what remains in the origami surface are two tabs with three layers and one layer in the overall structure, as illustrated in Figure 43.



Figure 43. Layer number variation per areas: sqauretwest (left), vertical tabs fold up (centre) and colour subtitles (right).

The shape change described was implemented in the sample development. The origami crease pattern designed combines eight sqauretwests with asymmetrical distribution in a quadrangular frame. Dash-dot green lines in the crease pattern presented in Figure 44, depict Nitinol wires placement. Seventeen Nitinol segments were defined.

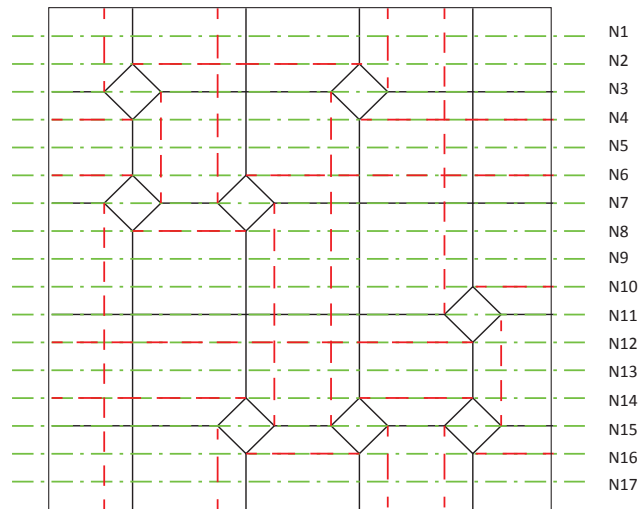


Figure 44. Sample crease pattern.

As previously explained for the base folds study, once again the origami creases define the geometry that the wires should be trained with. After folding the model with the configuration that should be assumed, when heated, each wire shape was drawn (Figure 45 left) and subsequently, the die for each shape was drawn and produced (Figure 45 right). This model displays five different wire shapes. Numbered from top to bottom, *A* corresponds to wire number 1, 2, 4, 5, 6, 8, 9, 10, 12, 13, 14, 16, 17; *B* is 3; *C* is 7; *D* is 11 and *E* is 15.

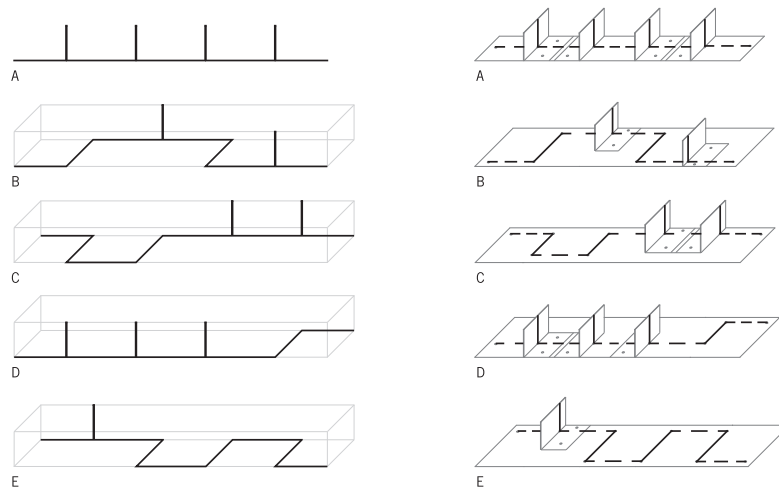


Figure 45. Nitinol wires' shape (left); Nitinol dies' shape (right).

Nitinol heat treatment was conducted with the same equipment applied in the preliminary study. Nitinol size and the mass of the die can influence the optimization of the temperature and time parameters of the annealing process (Liu et al., 2008; Rao et al., 2015), they were retested and the values set were 550°C for 10 minutes.

The weaving process was developed in the Jacquard loom with the first set up. Nitinol segments have been integrated manually in order to assure accuracy within the crease pattern. The alloys were deformed to a straight shape at M temperature and inserted in each section of 21 textile picks, totalizing 2 cm distance between each Nitinol wire. To maintain a straight shape in the correct location, the wire ends were held during the next weft textile yarn insertion.

5.6.2 Electrical Activation

The thermal activation of the shape memory textile was produced through resistive heating – a method commonly applied to heat shape memory textiles (Lee, 2005; Berzowska and Coelho, 2005; Seymour, 2008; Seymour, 2010; Coelho and Zigelbaum, 2011).

The electrical current required to attain the Nitinol activation temperature depends on the Nitinol characteristics, ambient temperature and duration of power supply. A study to specify the current value was conducted, to ensure that the A_f temperature would be attained (45°C) without overheating the wire.

The experiment took place at an ambient temperature of 23,8°C. For each Nitinol segment integrated in the woven structure, a specific voltage was applied using a TENMA 72-8695 power supply. The resulting electrical current was measured and a thermal image was recorded with a TESTO 876 Infrared camera, after 5 seconds

of power supplied. For thermal isolation from the table surface, a polyethylene (PE) board was placed below the sample.

Nitinol has a tough oxide layer that does not allow an accurate resistance measurement and presents difficulties in joining processes, such as soldering (Rao et al., 2015). A mechanical abrasion of the Nitinol ends was done prior to the described measurement.

Voltage variation from 0,5 to 3,0 V was supplied in intervals of 0,5 V increases. The electrical current values attained for each segment were similar, as well as their temperature. Mean values are presented in Table 25 and thermal images of Nitinol wire number 3 are presented in Figure 46.

Table 25. Mean values of electrical current and maximum temperatures attained.

V (V)	I (A)	temp. (°C)
0,50	0,12	26,20
1,00	0,23	27,80
1,50	0,37	32,20
2,00	0,51	37,80
2,50	0,63	46,80
3,00	0,75	54,10

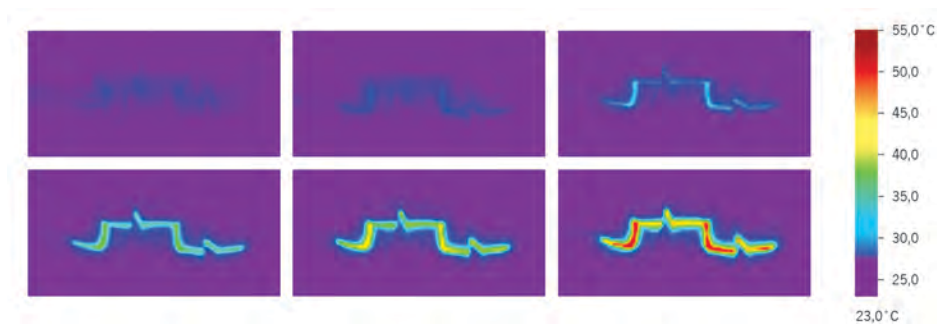


Figure 46. Thermal images of Nitinol wire number 3 during voltage variation.

An analogous experiment was conducted linking the Nitinol segments two by two, in a series circuit. Relation between electrical current and temperature was similar to the results within one segment, as expected. As will be explained later, the series connection will allow simplifying the electrical circuit used to control the SME.

Despite a mean maximum temperature of 46,8°C attained with 0,63 A, thermal images demonstrate that wire temperature is not homogeneous. Also, ambient temperature during the tests can be considered slightly

higher than the common definition of room temperature. A current of 0,7 A was found to be an adequate value to drive the Nitinol wires.

In order to achieve a controlled heating of the Nitinol wires, and considering that the simultaneous activation of all 17 wires would require a considerable amount of current, a sequential activation was implemented. For this purpose, an Arduino microcontroller board was used to control the process. The power stage was implemented using ULN2003A Darlington-transistor arrays, which feature 7 channels with a maximum current of 0,5 A each. To drive the wires with 0,7 A, it was necessary to use two channels in parallel for each wire, reducing the number of controllable wires to 3 per each transistor. To simplify the circuit, wire segments on the textile were paired and connected in series, which allows reducing the number of wires to control to 8+1 (8 pairs and one single), using three ULN2003A chips instead of 6. Figure 47 shows the circuit diagram of the power stage. The Nitinol wires are connected in series with pull-up resistor R_p , which has been dimensioned to allow a current of 0,7 A. All of the resistors are of equal value except the one which drives the single wire. Figure 48 shows the very simple code used to activate the wires sequentially, with a heating time of 6 seconds and a delay of 1 second between channels.

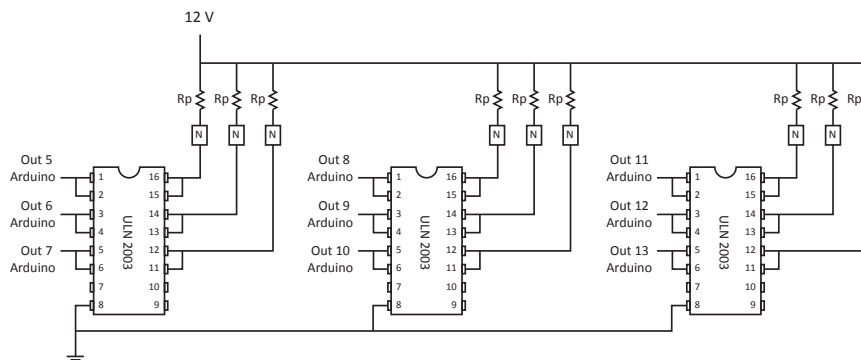


Figure 47. Circuit diagram with "N" representing the Nitinol wires.

```
const int digitalOutPins[9] = {13,12,11,10,9,8,7,6,5};

void setup() {
  // initialize serial communications at 9600 bps:
  for (int i=0; i <= 8; i++)
    pinMode(digitalOutPins[i], OUTPUT);
  delay(3000);
  for (int i=0; i <= 8; i++){
    digitalWrite(digitalOutPins[i], HIGH);
    delay(6000);
    digitalWrite(digitalOutPins[i], LOW);
    delay(1000);
  }
}

void loop() {
  delay(100);
}
```

Figure 48. Arduino code.

Having completed the prototype development, an analysis focused on shape change performance, thermal measurement and transmittance variation was conducted. The shape change performance was recorded on

video and the frame of the final textile morphology attained was compared with the predefined geometry. A thermal imaging record was made to analyse temperature in each Nitinol wire during current flow. Light transmittance variation was measured before and after activation (temperature $< A_s$ and temperature $> A_s$, respectively), with a similar setup described for the results presented previously in Table 2.

5.6.3 Results and Discussion

The photographic record of the prototype, before and after activation, is presented in Figure 49. For a visual comparison of the morphology achieved and defined, an image of the paper model depicting the defined activated morphology was also included.

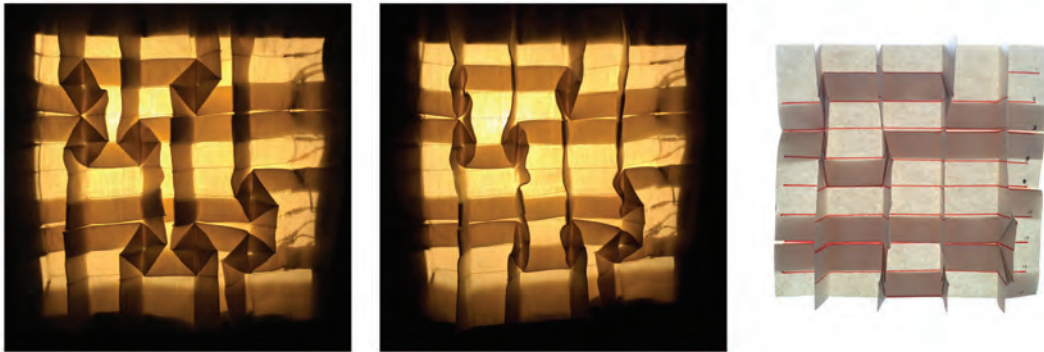


Figure 49. Prototype before activation (left); activated (middle) and paper model (right).

It is possible to conclude that some areas achieved equal or similar configurations to the predefined ones. There is a main incongruity in the bottom right square area, as the tabs are not perpendicular to the prototype surface, resulting in a non-folded square.

The prototype was also analysed regarding textile and Nitinol materials' interaction. There are some areas with Nitinol wire protrusion; however, they are less prominent than in the study samples. Also perceived is the ability of the Nitinol to slide out of the textile structure and rotate around its axis.

Thermographic images have presented some issues on the electrical activation. Due to the origami structure characteristics and the wire protrusion in specific crease areas, some Nitinol segments are close or in contact with other segments. This compromises the planned electrical current flow and the temperature that needs to be attained. Figure 50 illustrates the activation of Nitinol wires number 9 and 10. It is possible to detect a short circuit area, in which there is an overheating, as defined by the dark red area, being the remaining wire below the activation temperature. This explains the described anomaly in the bottom right area of the textile.

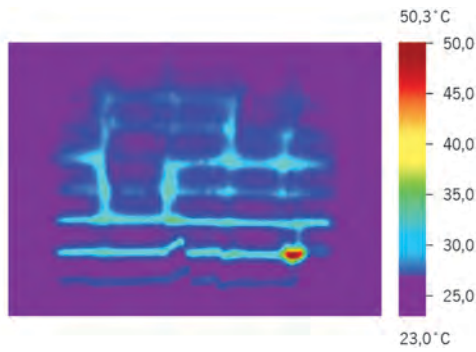


Figure 50. Thermal images of Nitinol number 9 and 10, being activated.

The aforementioned issues are due to the smoothness of the Nitinol wire and the fact that they are not electrically isolated. This finding has delineated the development of a future study with the purpose of implementing a finishing process in order to increase adhesion and thus avoiding slip, rotation and protrusion of the Nitinol from the textile substrate; to isolate the wire to avoid issues with undesired electrical contact between wires.

The origami scale defined also appears to be relatively small in comparison to the textile's thickness. In some areas, the overlapped layers constrain the SME, reducing the ability to perform with greater accuracy within the predefined geometry.

During the observation and recording of the shape change, transmittance variation was perceptible. The light intensity measurement provided a quantification of the variation. The luxmeter was pointed to a white surface placed 1m from the light box and the values were recorded on three points. Mean values reached a percentage difference of 42% (Table 26).

Table 26. Mean values of light intensity.

Light intensity (lx)		Luminosity difference (%)
temp.<As	temp.>Af	
0,56	0,97	42,27

5.7 Experimental 5: Finishing Processes

Nitinol surface can be modified in order to customize their qualities to the applications requirements (Shabalovskaya et al., 2008). In this study, finishing processes were applied in woven textiles that integrate Nitinol alloys, aiming to improve adhesion of the Nitinol with the host structure and electrical insulation of the alloys in one process. Using different agents, an experimental study of textile finishing processes was

developed and a comparative analysis is reported, regarding mechanical performance, electrical insulation, weight and thickness of the developed samples.

5.7.1 Materials and Methods

The study of the finishing processes was conducted with samples woven in the Jacquard loom Bonas. Samples A to E were produced with the first setup of the loom, samples F to I were developed with the second set up. The samples' size is 11 x 5 cm with one Nitinol wire previous annealed with a 90° angle, integrated in 10cm of the weft. Figure 51 depicts the samples' geometry and dimensions (cm).

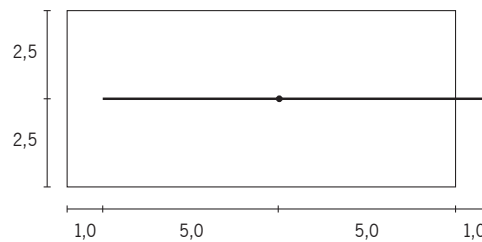


Figure 51. Schematic of the samples' geometry.

The materials selected to conduct this study were:

- 1 – A paste that combines Aktilem 14000 and Aktilem 13002 with a vinyl acrylic binder. Concentrations applied were 15%; 15%; 70%, respectively and viscosity, measured in the viscometer was 3700cP;
- 2 – A paste that combines used Tanacoat OMP and Acraconc 2C-N. Concentrations applied: 99,9%; 0,1%, respectively and viscosity measured of 2300cP;
- 3 – PTFE;
- 4 - Baygard AFF 300% 01;
- 5 – Insulating agent with an alkyd resin base.

The finishing processes applied were screen printing using an open screen with 101,6 TPI and magnetic field $n^{\circ}3$, knife coating, impregnation and pulverization (spraying).

Table 27 presents a description of the samples developed. For a comparative analysis, a sample without treatment of each loom set up was developed (samples A and F).

Table 27. Description of samples' materials and finishing processes.

Samples	Material n°	Finishing process
A	-	-
B	1	screen printing
C	2	screen printing
D	1	coating
E	2	coating
F	-	-
G	3	impregnation
H	4	impregnation
I	5	spraying

Samples B, C, D and E were thermo fixed in a laboratory oven at 150°C during 5 minutes. Sample H was thermo fixed at 160°C during 1 minute and sample G and I were dried at ambient temperature.

The samples evaluation comprises of a shear strength measurement and an electrical insulation analysis. The effect of the finishing processes in the Nitinol ability to slide of the textile substrate was measured in a dynamometer with a breaking strength and elongation test. The sample was placed in the dynamometer with the Nitinol end attached to the superior grip and the opposite sample side was hold in the textile area with the lower grip. To analyse if the electrical insulation was attained, a multimeter continuity test was conducted with one test lead connected to the Nitinol end and the other touching the Nitinol crease point.

Additionally, has the textile thickness and weight also can influence the shape memory textile behaviour, these samples' properties were also measured and compared.

For a greater understanding of the colour and shape change possibilities, after the selection of one of the material and finishing process, a screen printed sample was developed with a 10% TC red paste, before the finishing application and evaluated within the aforementioned parameters.

5.7.2 Results and Discussion

Table 28 presents the result of the breaking strength and elongation tests. Comparing A and E samples, it is possible to verify that the textile substrate characteristics of A present higher interfacial adhesion of Nitinol alloys with the host structure than E. In relation to the processes and materials applied, screen printed samples attained a greater increase of the force necessary to initiate the removal of the alloy from the woven structure and the value is higher for sample B. Samples developed with impregnation also attained relevant

increase of adhesion while pulverization attained low and samples with knife-coating process presented values approximating zero and D testing was inconclusive.

Table 28. Breaking strength and elongation values.

Sample	A	B	C	D	E	F	G	H	I
Breaking Strength (N)	0,65	31,65	27,65	-	0,35	0,35	6,15	9,50	0,85
Extension (%)	0,50	7,73	5,00	-	0,60	0,50	0,85	1,60	0,15

Regarding the multimeter continuity test, just sample I have presented electrical insulation of the Nitinol alloy. The remaining samples have maintained conductivity behaviour.

Samples thickness and weight values are presented in Table 29. Sample A, developed in first loom setup, presents thicker and heavier characteristics than sample F, woven with the second setup. Impregnation process in samples G and H, attained the higher increase of the measured characteristics and the pulverization (sample I) presents the lowest increase.

Table 29. Samples thickness and weight.

Sample	A	B	C	D	E	F	G	H	I
Thickness (mm)	0,47	0,49	0,49	0,51	0,51	0,41	0,47	0,63	0,45
Weight (g)	0,86	1,13	1,4	1,02	1,15	0,63	2,72	1,76	0,69

Sample I has a low adhesion increase value in comparison with screen printed and impregnated samples. However, it was the solution that had provided electrical insulation and presents the lowest increase of thickness and weight values. Thus, it was the option selected to apply in the following samples development.

The colour and shape change sample developed attain 2,85 N with 0,15 % extension on the breaking strength and elongation test, it is electrically insulated in the Nitinol integration area and the thickness and weight values are 0,52 mm and 0,848 g, respectively.

5.8 Experimental 6: Effect of finishing processes in shape change

Textile structure characteristics play a significant role in Nitinol ability to perform the shape change transfer to the host structure (Dyer, 2010; Vasile et al., 2010). This experimental section studies the effect of the finishing process selected in the shape change behaviour of treated samples.

5.8.1 Materials and Methods

A comparative analysis was conducted to observe the shape change of samples with and without the finishing processes. With the perspective to develop dynamic light filters that perform colour and shape change behaviour, the samples handled in this study were also screen printed with TC pigments.

The first test was conducted with 4 samples, two were woven in the electronic Jacquard loom with PES warp and the other two in Jacquard Vamatex loom with the coarser warp setup. They have followed the same geometry depicted in Figure 27. One sample of each loom type was screen printed with a 10% TC red paste, thermo-fixed and later the finishing agent was applied. The remaining samples were not treated.

To study the shape change behaviour, the samples were hanged with the Nitinol wire deformed in straight shape and placed in a vertical position. A power supply plug was directly linked to the upper end of the alloy, the lower end was connected to a conductive thread with a crimp bead and linked to the power supply. For each sample it was driven an electrical current of 0,7 A. The samples' behaviour was recorded on video and the frames corresponding to the shape before and after activation stage were compared, between each group of samples.

With the objective to study the finishing effect in a more complex structure, a sample with squaretwists pattern was also analysed. The crease pattern and the shape change definition of the sample corresponds to the lower area of the model developed in 5.6 section, from Nitinol number 9 to number 17 (Figure 20). This sample was woven in the Jacquard Vamatex loom with the coarser CO warp and each Nitinol wire was integrated after 27 textile picks.

For the analysis, the Nitinol alloys were linked in 2 series circuits, the sample was folded, placed in horizontal position and their behaviour was video recorded. After, the sample was unfolded, screen printed with a 8% TC red and 2% TC black paste, thermo fixed, the finishing agent was applied and the aforementioned analysis process was repeated.

The activation temperature of the Nitinol handled (Af 45°C) was higher than the TC pigments selected (27°C), thus, the shape change behaviour will occur simultaneously to the colour change, revealing the Nitinol integration pattern in the textile colour. The research focused on the design possibilities working with two thermo-responsive materials will be address in chapter 6.

5.8.2 Results and Discussion

The images captured on the first test are presented in Figure 52. By a visual analysis it is possible to identify that after activation, samples not treated attained an angle more similar to Nitinol 90° geometry than samples treated. Comparing the samples woven equipment, Bonas loom (loom A) has a lower number of interlacings and samples are lighter than in Vamatex loom (loom B) and have performed a higher angle of shape change.

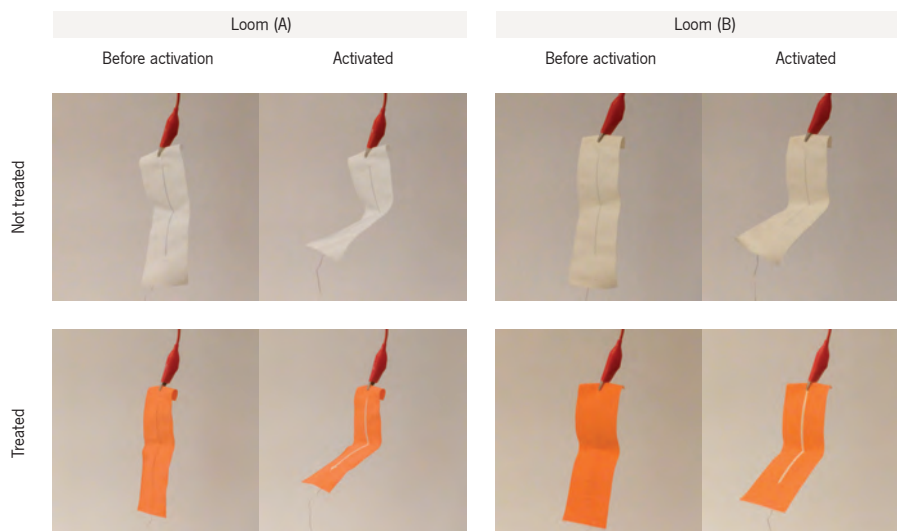


Figure 52. Samples before activation and activated.

The origami sample was activated in two sequences, starting in the lower area and after in the upper area. The frames selected to conduct this analysis refer to the sample deformed at M temperature, activated in sequence 1 and 2. First and second raw of Figure 53 illustrates the sample behaviour before and after treatment, respectively.

Before the finishing processes, the sample attained the fold up squares more near to the orthogonal position than after treatment. The tabs show similar shape in the areas with Nitinol wires integration. However, the sample tops don't integrate the alloys and before treatment the textile is softer and don't follow the shape change movement as well as in the sample treated.

In both activation tests, it was observed that the shape change is not similar in the overall sample. The squares located in the right side were able to perform a higher fold up angle than the other squares. This heterogeneous behaviour appear to be related to textile contraction after screen printing, wire protrusion in some points and layer composition along the substrate thickness, affecting the accuracy of the Nitinol wires geometry in regards to the folded host structure and resulting in areas with different SME constrains.

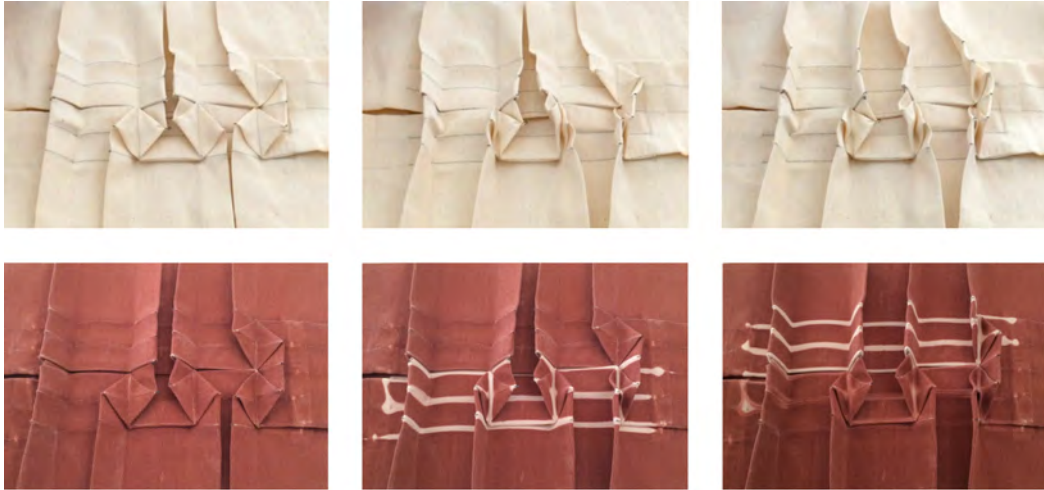


Figure 53. Sample before and after treatment during sequential activation.

This study attained a visual understanding of the effect of selected finishing process in the shape memory behaviour and the possibility to combine shape change and colour change in the same textile. The results also highlight the need to study alternative approaches of how to integrate Nitinol wires in woven structures, towards higher similarities of shape change attained in comparison to the predefined one. This requirement will be further researched in the Experimental 8 and 9.

5.9 Experimental 7: Two Shapes Behaviour

Previous experiments focused on the shape change from one temporary to a memorized morphology. The objective of this study is to develop shape memory textiles able to perform two shapes behaviour. In the literature review, the possibility to anneal Nitinol alloys with two-ways shape memory effect was reported. However, this method was not considered to be addressed in this research due to their limitations, in particular the decrease of the transformation forces and the possibility of memory lost with a slight overheating (Wan and Stylios, 2007; Rottiers et al., 2011; Cianchetti, 2013).

The shape change behaviour between two memorized morphologies was explored with a bias mechanism, the integration of two groups of Nitinol alloys whose geometry and alternate activation, triggers two different configurations. For a preliminary analysis, the two shapes behaviour was researched in a flat study sample.

5.9.1 Materials and Methods

A sample was woven in the electronic Jacquard loom with PES warp, integrating six Nitinol wires: three with a 90° angle and the other three annealed with a straight shape (Figure 54 light and dark green lines, respectively). The Nitinol wires defined to perform each shape were called actuator groups and the alloys were integrated in intercalated arrangement at every 2 cm in 10 cm of the weft.

For the sample behaviour analysis, the alloys of each actuator group were connected in a series circuit and activated in different moments. First, the sample was deformed to a flat shape at M temperature and the 90° angle alloys group was driven with 0,7A during 10 seconds followed by a pause of 5 second. After, straight shape actuators were activated. The sample behaviour was recorded on video and the frames corresponding to the described activation stages were analysed.

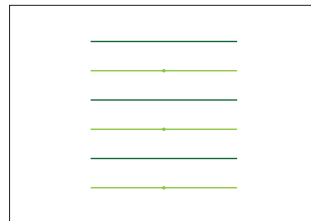


Figure 54. Diagram of Nitinol alloys configuration

5.9.2 Results and Discussion

The sample behaviour is illustrated in Figure 55, presenting the sample deformed into a flat shape (left image), first actuator group activated (centre) and second actuator group activated (right).



Figure 55. Sample deformed (left); 1st Actuator group activated (centre) and 2nd Actuator group activated (right).

The image on the left presents an overall flat shape however, as the Nitinol creases are not able to be completely deformed, they create a small undulation on the surface. The activation of the 90° actuator group have performed the shape change of the textile while also deforming the second actuator group. The non-activated alloys present forces contrary to the movement of the activated group influencing the predefined angle attained, which did not reach the 90° shape. The same effect happens during activation of the straight shape group. Comparing the sample manually deformed in flat shape and the sample with the second actuator group activated, they should present similar shapes but the activated result was not as flat as the predefined shape.

Despite the morphology accuracy was lower than the pre-defined, the shape change was evident and the sample attained two different morphologies. The proposed bias mechanism was found valid to be implemented and further researched in self-folding textiles.

5.10 Experimental 8: Nitinol integration based on the crease axis

In order to further research the two shapes behaviour in origami structures and address the shape accuracy improvement aim, a different Nitinol integration approach was proposed. Nitinol wire integration across the full width of the host structure enhances the influence of the textile substrate constrains in the SME, across the Nitinol wire protrusion and geometry accuracy in regards to the folded structure, as discussed in 5.8.2 section. Furthermore, some sections of the alloys do not convey shape change, their purpose is to connect the actuator parts along the samples' width. This connection can be developed with conductive threads, allowing greater flexibility to define the Nitinol diagrams maintaining the required conductivity between the alloys. A method approached in the following sections.

In this study, Nitinol integration in the woven substrate will be defined by segments, in specific areas of the origami crease pattern, taking into consideration the crease axis sections. Previous to the sample development, the textile contraction attained after screen printing and thermo-fixing processes was also analysed, to scale up the weft density of the woven substrate in order to increase the morphology accuracy.

5.10.1 Materials and Methods

To fold up and fold down the vertical tabs and square area of the squar twist origami, the main crease axis correspond to the vertical valley folds and the horizontal diagonal of the square (that when is folded, it twists and becomes vertical).

The grey shadows in Figure 56 (left) highlights these creases axis in the unfolded origami and when the diagram is folded, they overlap in one central axis (vertical red line).

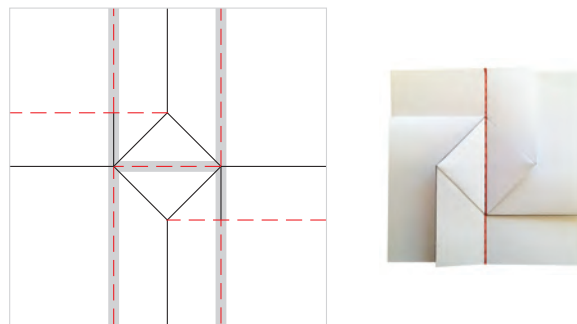


Figure 56. Squaretwist crease pattern (left) and model folded (right).

The models' layers and overlapped creases were studied in order to define the main axis for Nitinol integration areas. Crease pattern of samples with two Nitinol actuation groups will be depicted with black continuous line for mountain fold and black dashed line for valley fold. The actuator group performing fold up behaviour is illustrated with light green lines and the fold down in dark green. The points added in the Nitinol lines identify the alloy's crease points.

The samples' shape defined for this study consists of squaretwist fold with 6 cm square diagonal. In sample S6 A (Squaretwist 6 cm), the Nitinol creases are aligned in the vertical valley fold corresponding to the lower layers of the folded model. The alloys of the two actuator groups, present four different geometries (Figure 57).

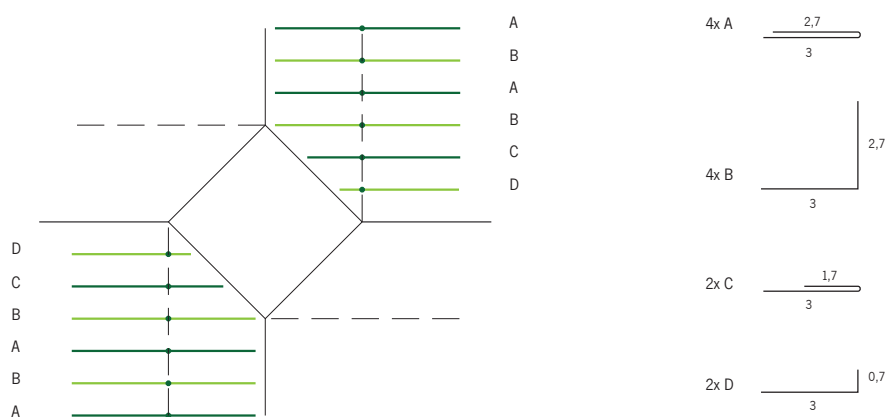


Figure 57. Sample S6 A crease pattern (left) and Nitinol wire geometries (right).

Sample S6 B integrates the alloys in the crease axis of the origami upper layer and also present four geometries. In this case, the fold down actuator group (dark green lines E and G of Figure 58), instead of performing the decrease of a 90° angle as in S6 A, they have to increase it until 180°.

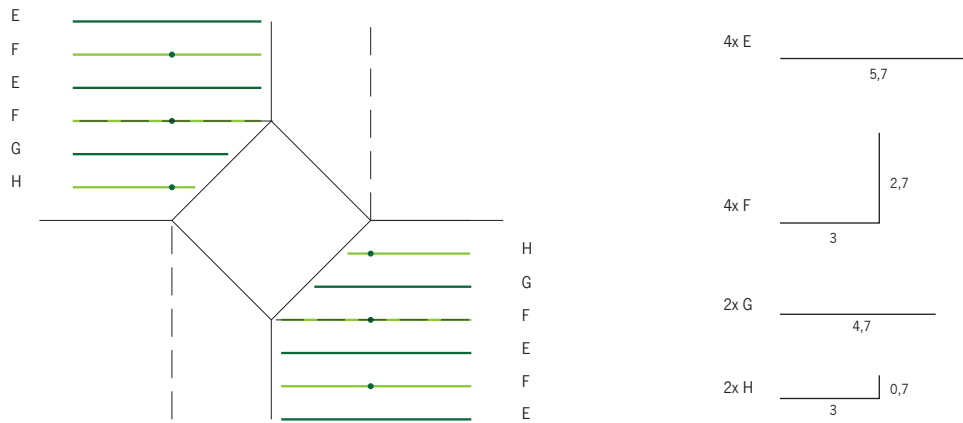


Figure 58. Sample S6 B crease pattern (left) and Nitinol geometries (right).

A 3rd sample (S6 C) was developed combining the previous samples' actuators geometries. In the areas exterior to the square, the Nitinol alloys are integrated in the full width of the sample (Figure 59).

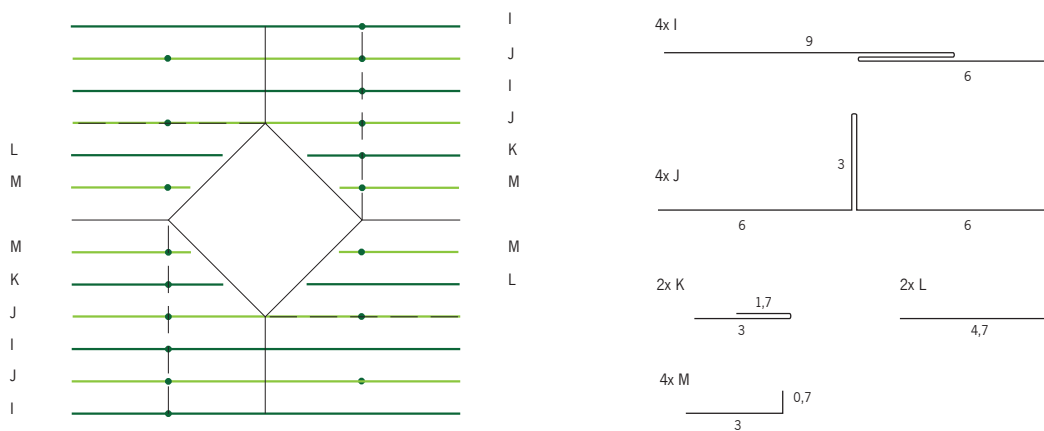


Figure 59. Sample S6 C crease pattern (left) and Nitinol geometries (right).

The samples were woven in the electronic Jacquard loom with PES warp and 1 cm of Nitinol spacing. Previous to their development, a test sample was produced in the same equipment with Nitinol wires integrated at every 1 cm, in order to analyse textile contraction after being screen printed and thermo-fixed. The contraction value was approximately 10%, establishing an increase of 1 pick/cm in relation to previous samples, thus 12 textile picks plus 1 Nitinol wire per cm.

The shape memory textiles development followed the process previously defined in section 5.6. Additionally, they were screen printed with 10% TC red, thermo-fixed and finished with the insulation agent. The alloys of

each actuator group were connected in a series circuit and, after the origami being folded, their performance was recorded on video and the frames of each activation stage were compared. Each Nitinol group was driven 0,7 A by a Velleman power supply.

5.10.2 Results and Discussion

Figure 60 presents the samples' images before activation and at fold up and fold down stages. During the manual folding process, it was observed that samples A and B presented a less constrained ability than C, the decrease of Nitinol length improved the textile handling and appearance. However, the fold up behaviour was not compromised with the actuator material reduction, sample A attained a similar fold up square than C, but sample B had a lower angle behaviour. The fold down was similar among all the samples. Sample A and B also present less Nitinol wire protrusion than C and, as the Nitinol creases happen in the considered back side of the samples A and B, they are not visually perceived.

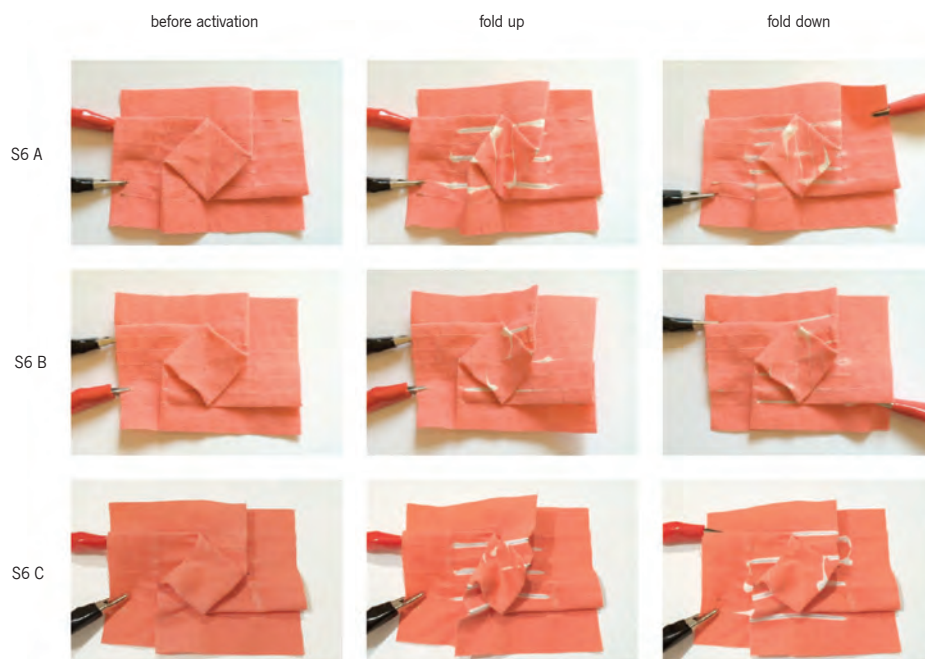


Figure 60. Samples behaviour comparison: S6A, S6B and S6C.

The development of two shapes behaviour in origami textiles with the proposed approach of Nitinol integration based in the main creases presents important advantages in comparison to the Nitinol integration in the full samples' width, particularly within sample S6 A setup. The sample presents greater folding accuracy within less Nitinol material and thus less expensive. The decrease of Nitinol crease points reduces the protrusion number and they are less prominent. Furthermore, it is also easier and faster to develop, the dies are simpler and they have a lower number of segments to insert in the woven structure.

The similarities between the shapes defined and attained still demands experimentation. The proposed approach of Nitinol segments in specific areas of the textile, allows the possibility to increase the memorized Nitinol angle to compensate the contrary forces to the movement. It was selected the sample A main crease axis definition for the Nitinol integration, to be implemented in further experimental work.

5.11 Experimental 9: Nitinol angles and Textile angles

Previous samples attained shape change behaviour with lower angles than the geometries annealed in the Nitinol wires. In order to compensate the SME constraints in the alloys shape transfer, this study proposes to increase the Nitinol angles definition in relation to the intended textile performance.

5.11.1 Materials and Methods

Plain and squaretwist samples were developed to study the effect of the Nitinol memorized angle in the textiles shape change. All samples were woven in the electronic Jacquard loom with PES warp.

Plain samples are composed by two Nitinol wires with 10 cm integrated in the weft – one alloy performs the fold up and the other, the fold down. With the objective to attain a fold up behaviour of 90° , the alloys' angles defined for this behaviour were 100° , 110° and 120° , comprising two different spacing between the fold down alloys – 1 and 2 cm – totalling 6 samples. Nitinol fold down angle it is equal to the S6 A samples, 0° .

The increase of the fold up wire's angle was expected to affect the fold down. With the squaretwist model, two samples were developed with 110° fold up actuators with different integration setups: S6 D sample presents a regular Nitinol spacing intercalating one fold up with one fold down actuator (Figure 61 left), S6 E has two fold down alloys at 0,5 cm distance, per each fold up at 0,75 cm (Figure 61 right). After their development and performance analysis, they were produced two additional samples following the S6 E setup, with a higher angle definition: S6 F present 120° angle of the fold up alloys and S6 G have 130° . The samples development and analysis followed the process described in the previous section 4.10.



Figure 61. Crease pattern samples S6 D, F and G (left), S6 E (right).

5.11.2 Results and Discussion

Figure 62 shows the results attained with the plain samples. Comparing the fold up shape in samples with different Nitinol spacing, alloys at 1 cm distance attained angles more similar to 90° than samples with actuators at 2 cm distance, highlighting that the distance between the 2 Nitinol wires with different shapes and activated in different moments, affects the ability to the activated actuator deforms the alloy at M phase. The comparison among the angles defined, samples with Nitinol at 1 cm distance show similar shapes for 110° and 120° samples. In all samples, the fold down behaviour presents low accuracy in relation to the Nitinol geometry.

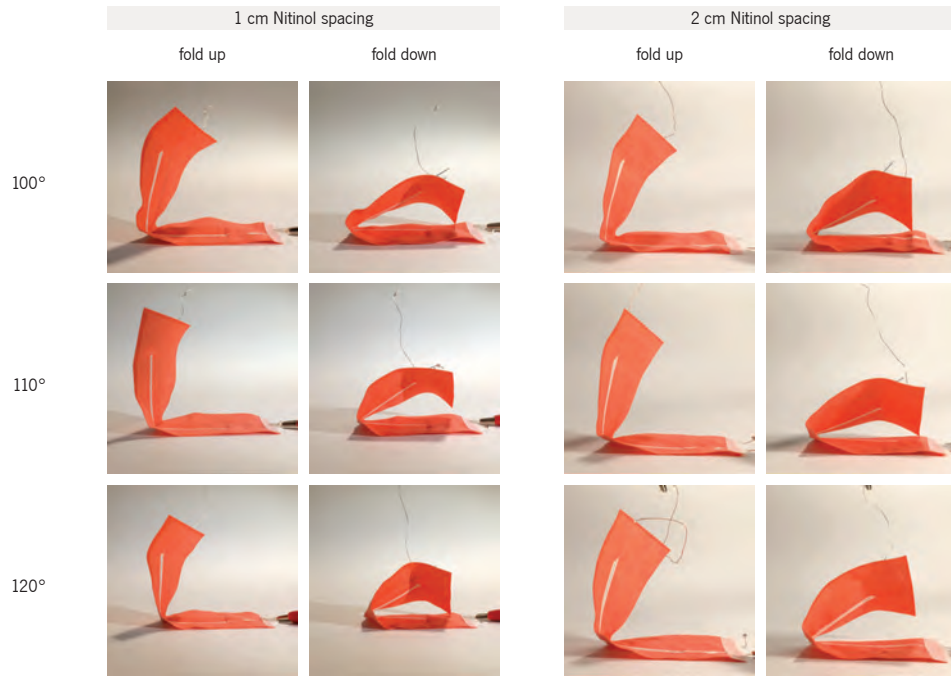


Figure 62. Study samples with different memorized angles and alloys' spacing.

Figure 63 presents the shape change results of samples S6 D and E, as well as the images of the previous developed S6 A sample, for a comparison between the activated shapes with and without fold up angle increase. Sample D have improved the angle behaviour during fold up in relation to the sample S6 A, but the fold down activation was slightly inferior. Sample E, which presents two fold down actuators per each fold up, had similar performance in the fold down and lower in the fold up in comparison to S6 D.

The behaviour of origami samples with equal setup for fold up wires with 110°, 120° and 130° angle, is illustrated in Figure 64. Sample G attained a fold up shape more similar to the predefined, it is possible to observe a slightly more closed effect of the tabs and square area, comparing to samples D and F. The fold down was relatively similar in all samples, although the morphology is not as flat as the predefined.



Figure 63. Samples behaviour comparison: S6A, D and E.

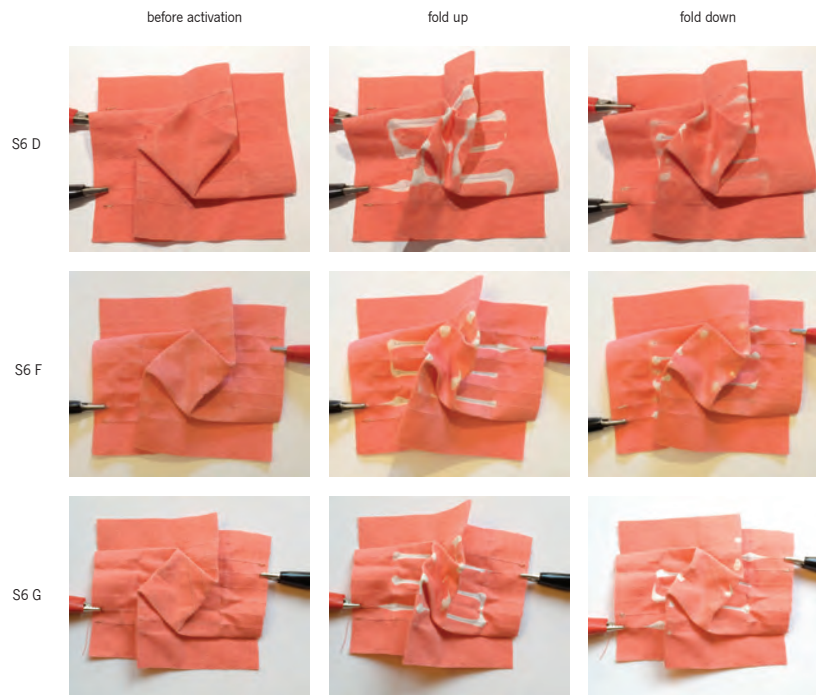


Figure 64. Samples behaviour comparison: S6 D, F e G.

In this study, the improvement between the fold up shape defined and the textile behaviour, was attained within the increase of Nitinol wires' angle. However, the fold down was compromised and the actuators performed slightly inferior shape accuracy. The sample with two fold down actuators for each fold up Nitinol did not promote a better performance. Taking into consideration that in this model setup, a decrease of the

alloys' angle creates a cross point which would affect the Nitinol integration in the weft direction, the change of the fold down actuator angle was not addressed.

In conclusion, the change of Nitinol angles in relation to the textile morphology, affects the behaviour of each actuator group and can be selected in regards to the final objectives. In the present research, the compromise between a greater accuracy of the fold up in relation to the fold down behaviour also took into consideration the aim to create textile layers variation. When the tabs are orthogonal to the textile sample, a large area with 1 textile layer is attained. If the textile is able to perform the fold down behaviour, the decrease of accuracy interfere in the layers distance but the final morphology layers' number is attained, thus higher light transmittance variation is possible if the fold up is more accurate than the fold down.

5.12 Experimental 10: Shape change and samples scale

The origami samples developed in the previous section, researched the textiles shape accuracy within crease patterns of equal dimensions – 6 cm square diagonal. This section studies the shape change development and performance with larger scales shape memory textiles.

5.12.1 Materials and Methods

Two squaretwist samples were produced following the S6 G process development and Nitinol fold up angle definition – 130° . The dimensions selected include a 12 cm square diagonal sample (S12) and a second sample with 18 cm (S18), thus double and triple the previous square diagonal size. Their crease pattern and Nitinol integration setup are illustrated in Figure 65 and the spacing between Nitinol alloys is 1 cm for S12 and 1,5 cm for S18.

The samples activation was conducted with a Velleman power supply and 0,7 A was applied to each actuator group. The performances were recorded on video and the frames of each activation stage were compared across the 6, 12 an 18 cm square diagonal samples.

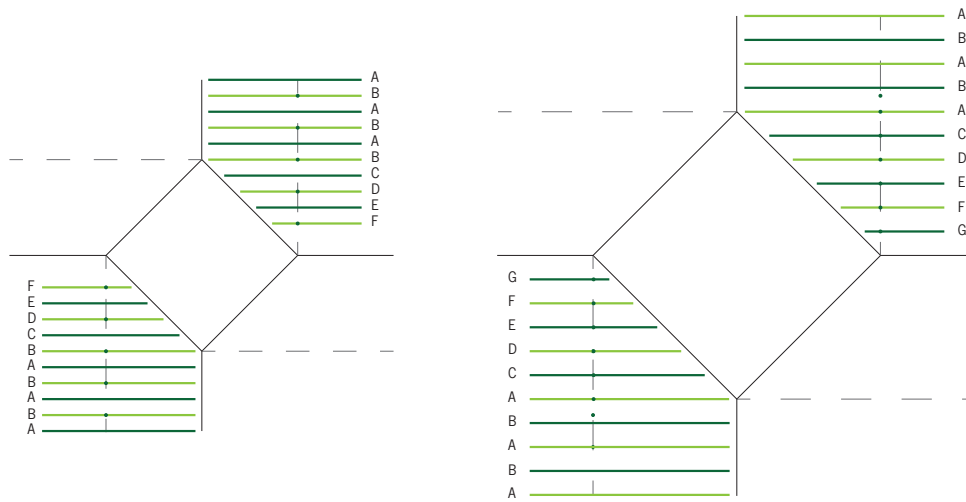


Figure 65. Crease pattern of S12 sample (left) and S18 sample (right).

5.12.2 Results and Discussion

In Figure 66 it is possible to observe the samples' scale in comparison to the dimensions of the previous S6 samples. S18 presents a dark colour in the laterals due to the loom warp setup with colour yarns.



Figure 66. Samples scale S6G, S12 and S18.

Figure 67 presents the samples' images before activation and at fold up and fold down stages. It is possible to observe that the fold up activation shape was more closed in the square area, from smaller to larger samples, while the fold down was more open in S18. Although S12 and S18 present twenty Nitinol alloys each and S6 G has twelve, the wires number increase was not sufficient enough to attain a similar fold up behaviour. The size of the samples with the same woven cloth set, are directly related to their weight, thus interfering in the forces required for the SMAs to perform the shape transfer. Besides, as the samples were placed in horizontal position, the fold down behaviour is enhanced with heavier textiles. Nitinol angle and integration setup should be optimized, regarding the samples characteristics.

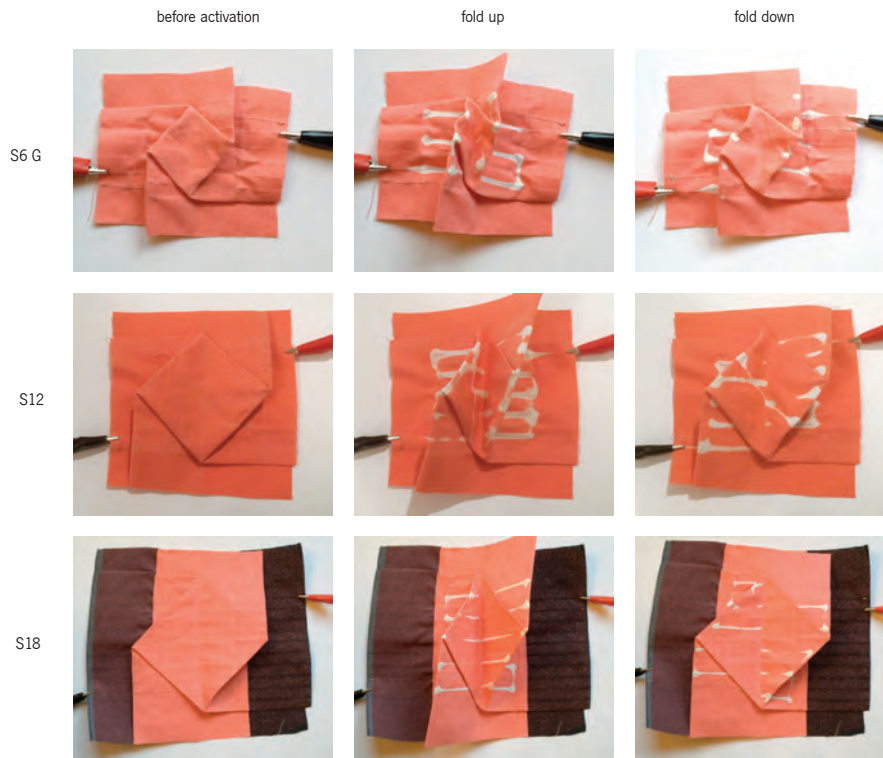


Figure 67. Samples behaviour comparison: S6G, S12 and S18.

Across the morphologies attained with fold up and fold down activation, it was also possible to observe shape change when the actuator group which was heated up, cools until M temperature and the other group is not immediately activated. This effect was discreet in S6 samples, but in S12 and S18 was evident.

Figure 68 presents the shape stages of activation and pause after it, for S18 sample placed in horizontal position (1st row) and vertical position (2nd row). The fold up was activated during 10 seconds, followed by a pause of 10 seconds and the fold down and pause after it, with the same time durations.

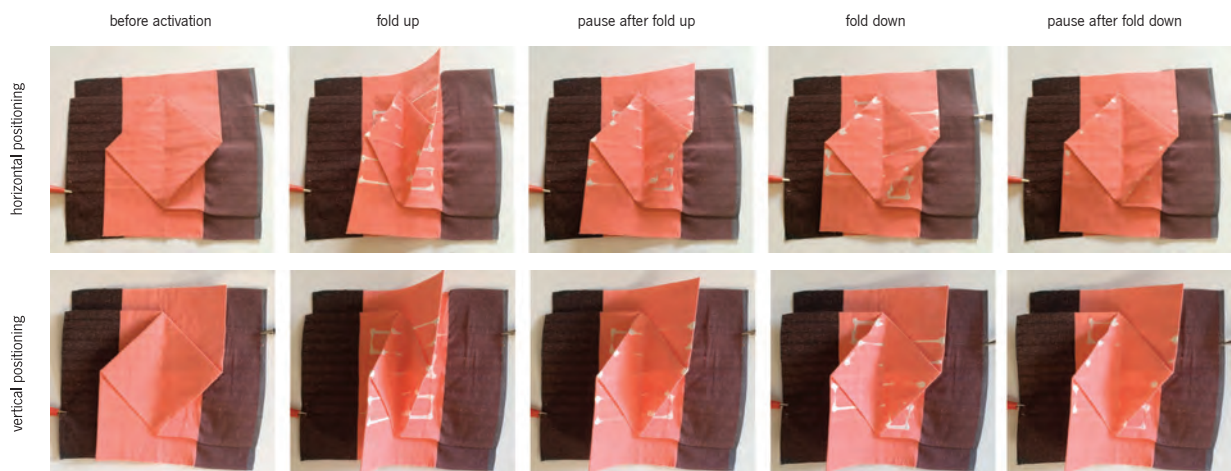


Figure 68. S18 sample behaviour in horizontal and vertical positioning.

In horizontal position, the shape attained during the pause after fold up is more closed than the pause after the fold down, meaning that the previous activation shape influences it. Comparing the horizontal and vertical position, the fold up is slightly more closed when the sample is placed in vertical position and less open during the fold down, highlighting the influence of the gravity force in the sample behaviour.

Samples scale and placement affects the overall shape change behaviour at the activation stages as well as after activation. During the SMAs activation pauses, the textile structure assumes a shape in relation to the previous activation stage, the two actuator groups' forces at M phase, their positioning and host structure characteristics. This study attained an understanding of the shape change performance in the selected morphology and scales and highlighted the optimization requirement of the Nitinol geometry and textile integration towards shape memory textiles design.

5.13 Conclusions

In this study, a novel approach was conducted in regards to: Nitinol wire shapes being defined accordingly to a textile geometric morphology; integration of Nitinol segments with different shapes in the same woven textile structure; and interaction of the textile SME with light transmittance.

Design and development of shape memory textiles encompass a systematic process. The material research conducted outlines a process to develop shape memory textiles with the ability to perform two shapes change behaviour similar to predefined morphologies.

The workflow setup consists of: defining the origami morphology and shape change; selecting the Nitinol wire and defining geometries, depending on their integration in the woven structure; drawing and production of the dies; optimizing the annealing parameters following the Nitinol heat treatment and finishing processes; and integrating Nitinol wires in the weaving process.

The proposed bias mechanism demonstrates potential to perform shape change for two different morphologies without application of external forms, considering a resistive heating activation method. However, the relation of SME constrains between actuator groups and textile substrate is more complex than in textiles that just perform shape change behaviour from one temporary to a memorized shape. Within the origami samples developed, the results attained suggest that a compromise on the definition of one of the memorized shapes appear to be necessary.

Additionally, the results have demonstrated the influence of the samples dimensions, weight and positioning in the overall shape change behaviour. According to the design requirements and textile characteristics, the Nitinol wires' angle and integration in the woven structure based on the main crease axis areas, should be optimized towards greater similarities between predefined and resulting morphologies, as well as to specific application goals.

Textile morphology definition, based on origami techniques to define Nitinol geometries, was found to be successful in the design of shape memory textiles with dynamic light filter behaviour. The methodological processes conducted and the results attained through the samples developed and their behaviour analysis afford an informed understanding to design shape memory textiles and set a framework aimed to be implemented at future developments in dynamic light filters research.

5.14 References

- BERZOWSKA, J. & COELHO, M. Kukkia and Vilkas: Kinetic Electronic Garments. 9th IEEE International Symposium on Wearable Computers, 18-21 October 2005 2005 Osaka, Japan.
- CIANCHETTI, M. 2013. Fundamentals on the Use of Shape Memory Alloys in Soft Robotics. *Interdisciplinary Mechatronics*. John Wiley & Sons, Inc., 227-254.
- COELHO, M. & ZIGELBAUM, J. 2011. Shape-changing interfaces. *Personal Ubiquitous Computing*, 15 (2), 161-173.
- DILEONARDO-PARKER, B. 2016. *Six simple twists: the pleat pattern approach to origami tessellation design*, Boca Raton, CRC Press/Taylor & Francis Group.
- DYER, P. E. 2010. *Dynamic control of active textiles: the integration of nickel-titanium shape memory alloys and the manipulation of woven structures*. PhD Thesis, University of Brighton.
- EDWARDS, A. & YAN, H. 2014. DNA origami. In: KJEMS, J., FERAPONTOVA, E. & K., G. (eds.) *Nucleic Acid Nanotechnology*. Berlin: Springer, 93-133.
- GJERDE, E. 2009. *Origami tessellations: awe-inspiring geometric designs*, Massachusetts, A K Peters.
- GOLDSTEIN, B., E 2010. *Sensation and perception*, Belmont, CA, Wadsworth, Cengage Learning.
- GORDON, I. E. 2004. *Theories of Visual Perception*, Hove and New York, Psychology Press, Taylor and Francis Group.
- HARTL, D. J., LAGOUDAS, D. C., MALAK, R., FRECKER, M. & OUNAIES, Z. 2014. Active materials and structures for origami engineering. *Smart Materials and Structures*, 23, 090201.
- HARTL, D. J., LANE, K. & MALAK, R. Computational design of a reconfigurable origami space structure incorporating shape memory alloy thin films. Conference on Smart Materials Adaptive Structures, and Intelligent Systems, 2012 Georgia, USA.
- HAWKES, E., AN, B., BENBERNOU, N. M., TANAKA, H., KIM, S., DEMAINE, E. D., RUS, D. & WOOD, R. J. 2010. Programmable matter by folding. *Proceedings of the National Academy of Sciences*, 107, 12441-12445.
- HENSEL, M. & MENGES, A. 2006. *Morpho-ecologies*, London, Architectural Association.
- HENSEL, M., MENGES, A. & WEINSTOCK, M. 2006. *Techniques and technologies in morphogenetic design*, London, Wiley-Academy.
- HESELBACH, J. 2007. Shape Memory Actuators. In: JANOSCHA, H. (ed.) *Adaptronics and smart structures: basics, materials, design and applications*. Berlin: Springer, 145 - 163.
- JACKSON, P. 2011. *Folding techniques for designers: from sheet to form*, London, Laurence King Publishing.

- KOIZUMI, N., YASU, K., LIU, A., SUGIMOTO, M. & INAMI, M. 2010. Animated paper: A toolkit for building moving toys. *Comput. Entertain.*, 8, 1-16.
- LANG, R. J. Computational origami: from flapping birds to space telescopes. Proc. of the XXV Annual Symposium on Computational Geometry, 2009 New York. ACM, 159-162.
- LANG, R. J. 2011. *Origami design secrets: mathematical methods for an ancient art*, Natick, MA, A K Peters.
- LEE, S. 2005. *Fashioning the Future: Tomorrow's Wardrobe*, London, Thames & Hudson.
- LIU, X., WANG, Y., YANG, D. & QI, M. 2008. The effect of ageing treatment on shape-setting and superelasticity of a nitinol stent. *Materials Characterization*, 59, 402-406.
- MAY, M. 2007. *Sensation and perception*, New York, Chelsea House Publishers.
- MITANI, J. 2011. A Method for Designing Crease Patterns for Flat-Foldable Origami with Numerical Optimization. *Journal for Geometry and Graphics*, 15 (2), 195-201.
- MIURA, K. 1994. Map Fold a La Miura Style, Its Physical Characteristics and Application to the Space Science. In: TAKATI, R. (ed.) *Research of Pattern Formation*. Tokyo: KTK Scientific Publisher, 77-90.
- NEFS, H. T. 2008. On the visual appearance of objects. In: SCHIFFERSTEIN, H. & HEKKERT, P. (eds.) *Product Experience*. San Diego, CA: Elsevier, 11-39.
- PAIK, J. K., AN, B., RUS, D. & WOOD, R. J. Robotic origamis: self-morphing modular robots. II Int. Conf. on Morphological Computation, 2011 Venice, Italy.
- PERAZA-HERNANDEZ, E. A., HARTL, D. J., MALAK JR., R. J. & LAGOUDAS, D. C. 2014. Origami-inspired active structures: a synthesis and review. *Smart Materials and Structures*, 23, 094001.
- QI, J. & BUECHLEY, L. Animating paper using shape memory alloys. Proceedings of the SIGCHI Conference on Human Factors in Computing Systems, 2012 Austin, Texas, USA. ACM, 749-752.
- RAO, A., SRINIVASA, A. R. & REDDY, J. N. 2015. *Design of Shape Memory Alloy (SMA) Actuators*, Cham, Springer International Publishing.
- RASMUSSEN, M. K., PEDERSEN, E. W., PETERSEN, M. G. & HORNB, K. 2012. Shape-changing interfaces: a review of the design space and open research questions. *Proceedings of the SIGCHI Conference on Human Factors in Computing Systems*. Austin, Texas, USA: ACM.
- RICHARDS, A. 2012. *Weaving textiles that shape themselves*, Ramsbury, Crowood.
- ROTTIERS, W., VAN DEN BROECK, L., PEETERS, C. & ARRAS, P. Shape memory materials and their applications. Korolev's Readings, 2011 Samara, Russia. Samara State Aerospace University.
- RUTZKY, J. & PALMER, C. K. 2011. *Shadowfolds: surprisingly easy-to-make geometric designs in fabric*, New York, Kodansha International.
- SAUL, G., XU, C. & GROSS, M. D. End-user Design and Fabrication of Interactive Paper Devices. TEI'10 fourth international conference on tangible, embedded, and embodied interaction, 2010 Cambridge, Massachusetts, USA. 205-212.
- SEYMOUR, S. 2008. *Fashionable technology: the intersection of design, fashion, science, and technology*, Wien, Springer.
- SEYMOUR, S. 2010. *Functional aesthetics: visions in fashionable technology*, Wien, Springer.
- SHABALOVSKAYA, S., ANDEREGG, J. & VAN HUMBEECK, J. 2008. Critical overview of Nitinol surfaces and their modifications for medical applications. *Acta Biomaterialia*, 4, 447-467.
- SHIMIZU, S. 2016. *Creativity is Born: Issey Miyake and Reality Lab*, s.l., PIE International.
- SIBLEY, T. Q. 2015. *Thinking geometrically: a survey of geometries*, Washington, D.C., Mathematical Association of America.
- SINGER, R. 2013. *Fabric manipulation: 150 creative sewing techniques*, Newton Abbot, David & Charles Publishers.
- TACHI, T. 2010. Origamizing polyhedral surfaces. *IEEE Trans. Vis. Comput. Graphics*, 16, 298-311.
- UGUR, S. 2013. *Wearing Embodied Emotions: A Practice Based Design Research on Wearable Technology*, Springer Publishing Company, Incorporated.
- VASILE, S., GRABOWSKA, K. E., CIESIELSKA, I. L. & GITHAIGA, J. 2010. Analysis of Hybrid Woven Fabrics with Shape Memory Alloys Wires Embedded. *FIBRES & TEXTILES in Eastern Europe*, 18 (1), 64-69.
- VAUGHAN, L. C. 1997. Understanding movement. *CHI'97*, 548-549.

- WADA, Y. I. 2012. *Memory on Cloth: Shibori Now*, New York, Kodansha International.
- WAN, T. & STYLIOS, G. K. 2007. Shape memory training for smart fabrics. *Transactions of the Institute of Measurement and Control*, 29, 321-336.
- YOUNG, R., PEZZUTTI, D., PILL, S. & SHARP, R. 2005. The language of motion in industrial design. *Design and semantics of form and movement*, 6-12.

ELECTROCONDUCTIVE TEXTILES

CHAPTER 6

CHAPTER 6. ELECTROCONDUCTIVE TEXTILES

6.1 Conductive Materials Catalogue

For the development of this research section, a *Conductive Materials Catalogue* was built comprising of materials that conduct electrical current and can be integrated in textile substrates. Swatches of the materials collected were organized by type: fibres, threads, yarns, ribbons, tapes, fabrics and pigments. In each section type, swatches of the same brand were grouped and brief description was included.

The initial purpose of this catalogue was to assemble a list of the conductive materials gathered, providing a visual and tactile analysis, also allowing the inclusion of additional samples. The concept of collection was addressed. Collection as a set of items of a specific class and collection as an act of gathering together, a work in process that can continuously grow and expand (Collection, n.d.). Within this perspective, the catalogue scope has evolved to a collection of data attained in the experiments with the conductive materials, focused on resistive heating activation of thermo-responsive textiles.

In each experiment, the body of results involved quantitative and qualitative data with a range of interdependencies. Conventional methods of data assembling by type or category were not found to be comprehensive for an analysis of the materials' properties and behaviour, thus data documentation alternatives were explored.

Regarding abstract data, Stamatellos (2007) defined the concept of collection in computer science as “a grouping of some variable number of data items that have shared significance to the problem being solved and need to be operated upon together in some controlled fashion.”. The main idea of data relations and influence in a specific phenomena or problem, lead to the logic behind the data organization conducted in this research documentation. The focus was not data types, rather the relations between dependent variables, according to the objective of each experiment.

6.2. Introduction to the Experimental Work

Given the research aim to activate colour and shape change textiles through resistive heating, this chapter studies the integration of conductive materials in textile substrates and presents an initial analysis on their resistive heating behaviour.

The first section of the experimental work concerned with conductive threads integration in plain weave structures and studied their electrical resistance properties for textile colour change activation. In the second experimental section, a similar study was conducted with conductive pigments, focusing on the screen printing parameters influence in the printed traces electrical resistance and consequently resistive heating effect. In addition, electrical resistance of each integrated material type was also analysed with the textile samples folded.

Nitinol alloys are conductive materials and shape change activation aimed to be performed through their resistive heating properties, whereas the Nitinol segments connection will be developed with additional conductive materials, which will be further researched in chapter 7.

6.3 Experimental 1: Conductive Threads

This experimental section is aimed to integrate conductive threads in plain weave structures, to study their resistive heating behaviour and respective activation of TC textiles colour change.

6.3.1 Materials and Methods

Two electro-conductive samples were woven in the Jacquard loom with Bonas controller, PES warp and CO weft, integrating a selection of conductive threads in the plain weave structure. Sample A integrated 28 conductive threads, each accomplishing two weft insertions of 15 cm, at a distance of 1 cm (10 picks CO plus 1 pick conductive thread), totalizing 31 cm length plus the floating ends for connection with a power supply. The distance between each conductive thread type was also 1 cm. Figure 69 presents the weaving schematics with dimensions in cm and Table 30 lists the conductive threads used, in respective order of weaving integration.

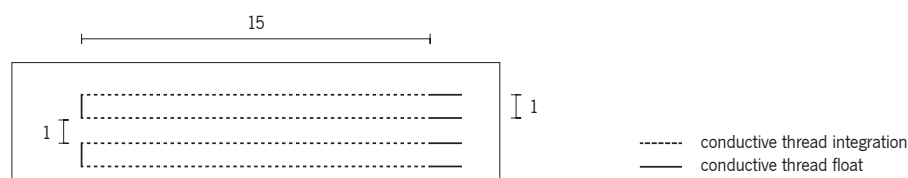


Figure 69. Schematic of the conductive threads integration in sample A woven structure.

Table 30. List of the conductive threads (CT) integrated in the woven substrate.

CT1 - Bekinox VN 12/1x275/100Z	CT11 - Elitex Garn Art I TPU 667_235/f34 PA/Ag	CT21 - Sparkfun stainless steel 2ply
CT2 - Bekinox VN 12/4x275/100S	CT12 - Elitex 110/f34/2ply PA/Ag	CT22 - Sparkfun stainless steel 4ply
CT3 - Bekintex BK 50/2	CT13 - Elitex (Lycra)	CT23 - Copper monofilament 100 μm
CT4 - Bekintex BK 50/1	CT14 - Shieldex 235/34x4 HC+E	CT24 - Insulated copper monofilament 160 μm
CT5 - Bekintex VN 14/2X90/175S/HT/PFA	CT15 - Shieldex 110/34 2ply HC+B	CT25 - Stainless steel monofilament 50 μm
CT6 - Bekiflex CA 63/8X7/80S/0.245/PFA	CT16 - Elinox SPP 35 300Z	CT26 - Nichrome monofilament 200 μm
CT7 - High Flex 3981 7X1 Silver	CT17 - Elinox PES HT 1100 + VN 60 400 t S/Z	CT27 - Plug and Wear Nm10/3
CT8 - High Flex 3981 7x1 Kupfer Blank	CT18 - LessEmf silver plated nylon	CT28 - SilverSpun
CT9 - Constantan High-Flex 8394 7x1	CT19 - Lamé LifeSaver	
CT10 - Elitex 235/f34 PA/Ag	CT20 - Linox	

Additionally, a list of the conductive threads and respective images is presented in [page X](#) tab, which can be unfolded to follow the analysis and discussion of this experimental section. A description of each thread type is presented in Appendix A.

Sample B integrates four conductive threads, each accomplishing twelve weft insertions of 11 cm each, also at a distance of 1 cm, totalizing approximately 143 cm length. Figure 70 presents the schematic of the conductive threads weaving pattern and type.

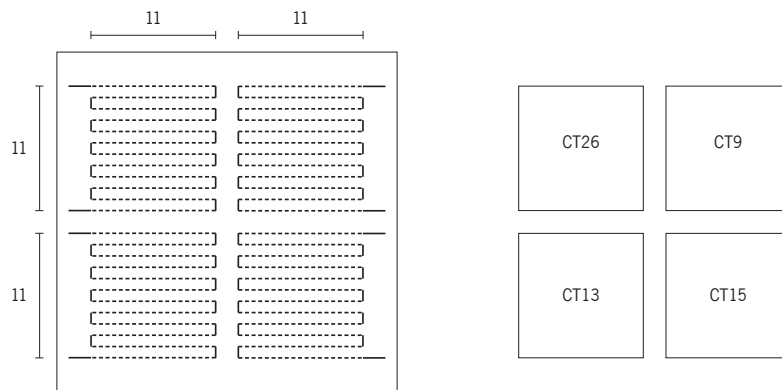


Figure 70. Schematic of the conductive threads integration in sample B woven structure.

After being woven, samples were screen printed (sample A was screen printed with 10% TC orange and sample B with 9% TC black with 6% TC red) and thermo fixed at 150°C during 3 minutes. Conductive threads number 5, 6 and 11 have a plastic insulated layer and they were tested in the thermo fixing conditions, previously to the definition of their integration in the substrate. The threads demonstrated stability to the conditions submitted.

Sample A experiments were conducted at an ambient temperature of approximately 22°C, where the minimum voltage required for each conductive thread to heat up above 27°C and thus start to change the textile colour was tested and supplied for approximately 15 seconds. Electrical current attained was registered and a thermal image and photo were recorded with a TESTO 876 IR camera. This process was repeated for voltage value increase, which was performed in a sequence of steps during 15 seconds each, until a maximum temperature of approximately 45°C was detected through the IR camera. In sample B, a similar test was conducted at an ambient temperature of approximately 20°C and each stage of power supply last 30 seconds. All samples were tested in horizontal positioning and placed above a PE board.

With the objective to work with folded structures and shape change, electrical resistance of the conductive threads was measured with a multimeter, during handling of the sample from flat state to folded with a crease perpendicular to the conductive threads integration.

6.3.2 Results and Discussion

The set of conductive threads integrated in sample A have different visual and tactile characteristics, which was possible to perceive through the textile surface appearance and handling. Figure 71 presents sample A below 27°C, with detail images of the area from CT5 to CT11 (left) and a perspective of the sample top (top right) and backside (bottom right). Complete images of sample A are presented in Appendix C.

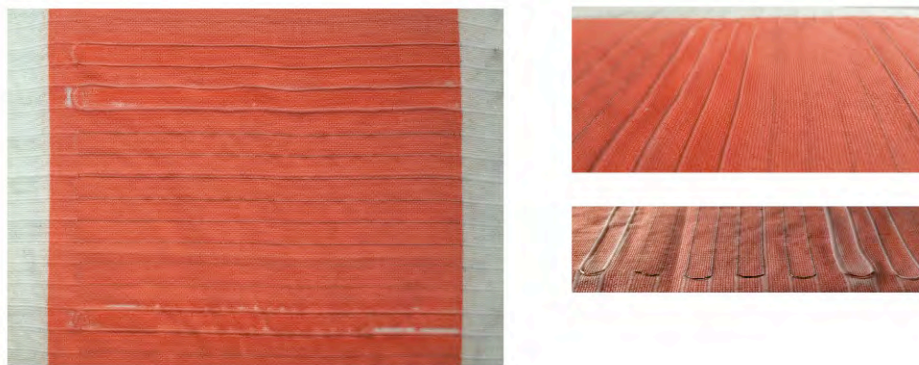


Figure 71. Sample A: front view from CT5 to CT11 (left); perspective top side (right, top) and perspective back side (right, bottom).

The plastic insulated layer of CT5, 6 and 11 have affected the screen-printed result with the lack of pigment in some areas. Other non-insulated threads that are as thick or more than the plastic insulated threads, have not presented issues during the printing process as they are more malleable. Conductive materials' thicknesses and colours also attained varying integration levels in the textile substrate appearance, being observable through the light colour of the TC pigment selected as discrete or evident. Furthermore, some

threads have also created a wrinkle effect in the textile, which was found to be more obvious after the thermo fixing process in particular with CT13, 16, 17 and 27.

The tests conducted with sample A involved a set of relations between variables as identified:

- All conductive threads were integrated with the same pattern and length in the textile structure, as well as screen-printed and thermo fixed parameters. Thus, besides the conductive threads' type, all the variables of the sample production were maintained constant.
- During the tests, ambient temperature, test setup, sample positioning and time between each power supply stage were also equal.
- The dependent variables were: conductive threads characteristics (materials, production process, electrical resistance, thickness, stiffness and colour); power supplied at each stage (defined according to the start of colour change until attaining approximately 45°C) and electrical current in respect to the conductive thread electrical resistance; interaction of the conductive thread temperature(s) with the textile substrate and printed TC layer.

Considering the relations between variables, a framework was defined for the results documentation. The test conducted with each conductive thread was considered as a 'system', where the independent variable was voltage, affecting electrical current, temperature in the thread and colour change effect (dependent variables). Data was organized in respect to each conductive thread with the dependent results grouped in relation to each voltage stage. The analysis presented in this section includes specific data results according to the discussed findings, whereas the complete documentation was compiled in Appendix C.

The results attained with CT1 are presented in Figure 72, also displaying the conductive threads' electrical resistance calculated and the IR colour scale defined. With 1,6 V power supply CT1 attained 0,16 A, electrical current found required in the test setup to start to observe colour change, as depicted in the first image of the photo column, recorded after 15 seconds of supplied power. The first IR image shows that at this stage, temperature in the conductive thread and nearby areas ranges in between approximately 30 and 34°C. With this thread, each voltage variation stage was defined with a 0,2 V increase and the results show how electrical current and temperature in the thread varied and affected the textile heat transfer performing a pattern of colour change from thin to thick stripes.

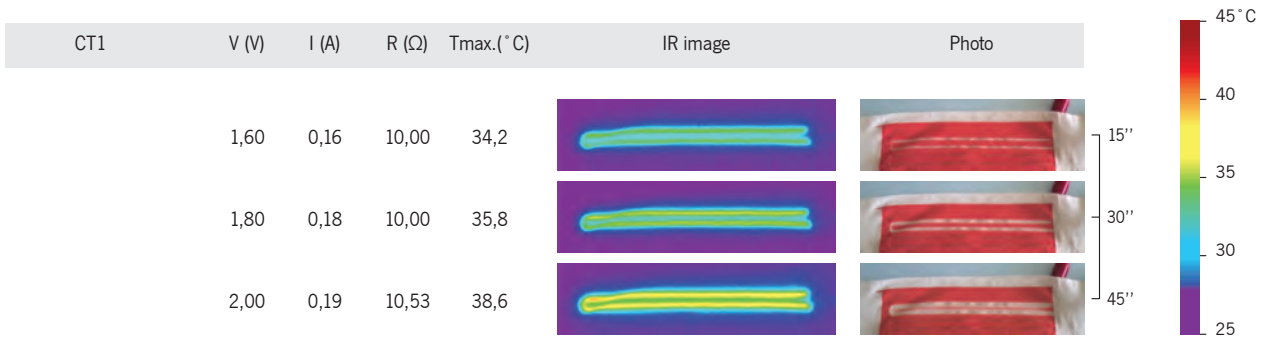


Figure 72. Results of test conducted with conductive thread number 1 (CT1).

During the experiments conducted it was observed that aside each conductive thread required a specific electrical current value to attain a temperature above 27°C , heat along the conductive threads' length presented different behaviours. In CT1 length, temperature appears to be similar, attaining colour change stripes with similar thicknesses during power supply, whereas other threads attained distinct temperatures along their length. To analyse and discuss resistive heating behaviour of each conductive thread, they were distinguished as homogeneous or heterogeneous, where in the last group, two main expressions were observed – irregular lines and traces. Figure 73 presents one example of each of these classes, with data results of each thread in the third voltage stage corresponding to 45 seconds of power supply.

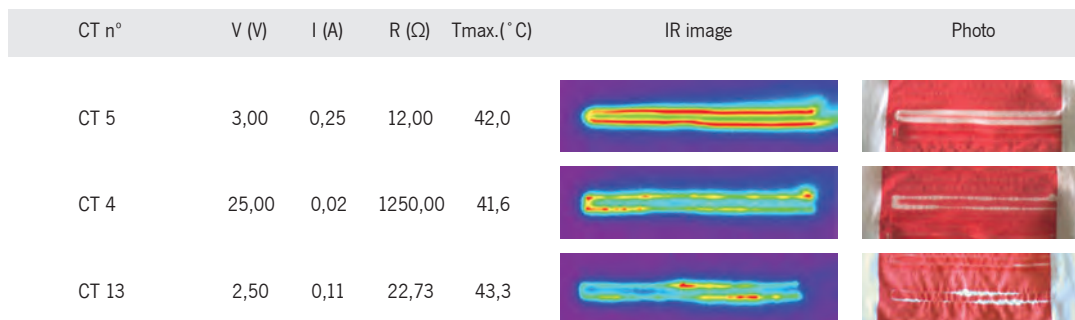


Figure 73. Results attained with CT5, CT4 and CT13, in the 3rd stage of power supply defined (45'').

As CT1, CT5 also exemplifies the homogeneous resistive heating in the thread length resulting in similar thicknesses along the colour change lines. In CT4 and CT13, temperature along their lengths is heterogeneous, observed with the colours variation in IR images and colour change effects in the photos. The results also demonstrate the two main sub-categories of the expressions observed with heterogeneous temperatures. In irregular lines (CT4), heat variation along the thread appears to maintain a small temperature variation along the thread length presenting some areas with increased temperature and attaining a linear expression of colour change with different thicknesses. In traces (CT13), the heat

differences along the conductive thread have a larger interval and colour change is only observed in some sections of the thread.

The irregular heat distribution in the threads can be interpreted as an incorrect behaviour for resistive heating purposes. Indeed, in few cases increased attention was required to not overheat the textile, interrupting the power supply before the stipulated 15 seconds per stage. Alternatively and through a design perspective, the graphic effects analysed demonstrate the possibility to create different colour change expressions with conductive threads, which appear challenging to be produced by other means. Adding new languages to the chromic patterns, heterogeneous resistive heating of conductive threads can be explored in TC textile design, considering the possibility of controlling maximum temperatures in the thread or in applications where high temperature in the substrate is not an issue.

Furthermore, temperature variation along each thread length is not related to the absolute values of the conductive threads' electrical resistance and electrical current flow, rather it is also associated with the threads' materials and structure characteristics. Figure 74 presents the results of three conductive threads with different relations. CT15 and CT27 have the same electrical resistance and distinct heat behaviour in the threads, as observed in the IR images and photos recorded during similar electrical current flow, attaining distinct expressions: traces and homogeneous, respectively. CT15 is an example where the temperature increased quickly at a specific point, exceeding 45°C. Comparing CT26 and CT27, the inverse relation was observed, both presenting homogeneous colour change lines but different electrical resistances.



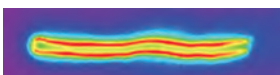

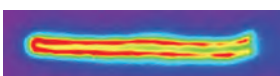

CT n°	V (V)	I (A)	R (Ω)	Tmax.(° C)	IR image	Photo
CT 15	6,00	0,04	150,00	49,2		
CT 26	1,50	0,30	5,00	41,0		
CT 27	9,00	0,06	150,00	44,2		

Figure 74. Results attained with CT15, 26 and 27, in the 3rd stage of power supply defined (45'').

In addition, small irregularities in the edge of colour change stripes can also be observed with some conductive threads that present homogeneous temperature in their length. This effect occurred in threads that created a physical wrinkle in the textile substrate, affecting the heat transfer on the printed surface, as observed in CT16 (Figure 75).

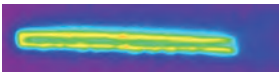

CT n°	V (V)	I (A)	R (Ω)	Tmax.(° C)	IR image	Photo
CT 16	10,00	0,04	250,00	38,9		

Figure 75. CT16 results in the 3rd stage of power supply defined (45'').

Thermal expansion in the textile areas between the threads' lines also differed. Comparing examples with homogeneous temperature in each conductive thread, some were able to perform a heat transfer above 27°C in the textile areas between them with the time frame defined, while others didn't. Figure 76 shows CT9 and CT20 results, where is possible to observe similar temperatures in each thread but different heating results in the textile. CT20 attained a complete colour change in the area between their lines while CT9 still presented an area with the TC pigment in colourized state.

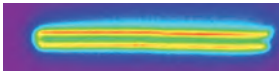

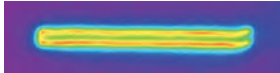

CT n°	V (V)	I (A)	R (Ω)	Tmax.(° C)	IR image	Photo
CT 9	3,00	0,16	18,75	39,5		
CT 20	8,00	0,06	133,33	39,5		

Figure 76. Results attained with CT9 and CT20, in the 3rd stage of power supply defined (45'').

Electrical resistance measurement during the sample folding attained different levels of values variation in each thread. The conductive threads integrated in the woven and printed sample that presented more stable results were CT1, 2, 7, 8, 9, 19, 21, 23, 24, 25 and 26.

To further explore the linear woven pattern of conductive threads and colour change in larger areas of the textile, sample B was developed with four conductive threads, one for each category defined: homogeneous with higher and less thermal expansion (CT26 and CT 9, respectively), heterogeneous with irregular lines and traces (CT15 and CT13, respectively). The sample was screen-printed with a darker TC colour, to observe the changes through increased colour luminosity difference between temperature variation. Data documentation followed the previous setup, presenting the results of each conductive thread at the second voltage stage defined, corresponding to one minute of power supply (Figure 77).

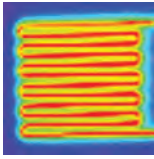
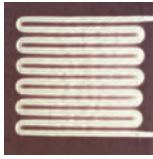
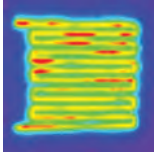

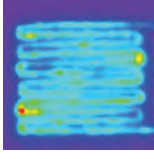
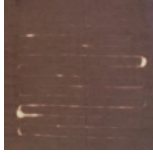
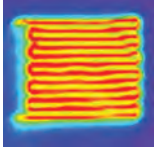

CT n°	V (V)	I (A)	R (Ω)	Tmax.(° C)	IR image	Photo
CT9	20,00	0,23	86,96	42,9		
CT13	11,00	0,29	37,93	42,0		
CT15	30,00	0,06	500,00	39,8		
CT26	10,00	0,42	23,81	44,2		

Figure 77. Sample B results with CT9, 13, 15 and 26 in the 2nd stage of power supply defined (1').

CT26 and CT9 were selected to observe homogeneous heating with different thermal expansions, in each square area of their integration. The results attained have shown differences between the threads behaviour than in sample A, where CT26 heated completely the textile area in between their lines with a lower electrical current (0,3A) while CT9 presented a similar effect. The heterogeneous heating along CT13 length displayed variations of colour change stripes thickness, but also required higher electrical current to heat up above 27°C in comparison with sample A. In CT15, the last stage of power supply was 30V (the limit of the equipment used) attaining a maximum temperature of 39,8°C and colour change effect with colourless traces of varied thicknesses.

This test was conducted at a slightly lower ambient temperature than sample A tests, while the time of power supply was increased. The results attained highlighted that these variables strongly affect textile temperature and colour change effect, having delineated further studies to systematically analyse their influence in textile thermo-responsive behaviour, which will be presented in chapter 7.

6.4 Experimental 2: Conductive Pigments

This experimental section is aimed to screen-print conductive pigments in textiles, to study their resistive heating behaviour and respective activation of TC textiles colour change.

6.4.1 Materials and Methods

A silver-based conductive pigment was used to analyse the effect of screen printing parameters in the electrical resistance of a printed traces' set. The pigment studied (Dupont PE825) was suggested by the supplier for application in flexible textile structures, but without indication of folding possibilities.

The screen printing processes were conducted in a Zimmer screen printing table with a screen of 163 TPI and the textile substrate used was 50% CO and 50% PES. Conductive traces of 10,0 x 0,2 cm were screen printed with variation of the follow parameters: magnetic field applied by the screen printing table; number of screen printed layers and textile substrate without and with treatment of a finishing layer. Table 31 describes the samples developed.

Table 31. Description of conductive pigment samples C and F.

	Magnetic field 3			Magnetic field 6		
	1 layer	2 layers	3 layers	1 layer	2 layers	3 layers
Substrate	C1	C2	C3	C4	C5	C6
Treated substrate	D1	D2	D3	D4	D5	D6

The textile substrate finishing layer was screen printed with a paste compose of 15% Aktilem 14000, 15% Aktilem 13002 and 70% Gilaba binder and thermo fixed at 150°C during 3 minutes. After, the conductive pigment was screen printed according to the parameters defined for each sample and the thermo fixed at 140°C during 10 minutes.

For a comparative analysis of samples electrical resistance and resistive heating behaviour, a test was conducted with a similar setup as described in 6.3.1 for sample A, at an ambient temperature of approximately 20°C. For each conductive trace of silver-based pigment, 1,5 V was supplied for 15 seconds, the current attained was registered and a thermal image recorded.

To study the possibility to develop a conductive printed circuitry to activate colour change in folded structures and shape changing textiles, each conductive trace was folded manually with one crease in the middle. For an analysis of the folding effect in the printed pigment, the tests previously conducted were repeated and images of the crease point were recorded with a magnifying glass Leica EZ4, 30x magnification.

Previous to this study a carbon-based conductive pigment was also tested (Bareconductive). However, the results were not satisfactory for TC colour change activation as the pigment screen printed in textiles

presented high resistance: with 20 V of power supplied, printed traces of 10,0 x 0,2 cm attained a maximum of 0,01 A, resulting in 2K Ω or more and registering maximum temperatures below 30°C. Therefore, this pigment was not considered for the present research.

6.4.2 Results and Discussion

For a comparative analysis of the results, Figure 78 presents the data arranged in a framework, according to samples' relation between textile substrate and treated substrate, table magnetic field (mf) and screen printing layers number. It is possible to observe that the conductive traces screen printed in the treated substrate attained slightly lower electrical resistance values than the correspondent traces developed in the untreated textile. The increase number of printed layers also resulted in samples' electrical resistance decrease, with larger value variation in substrates without finishing layer. Conductive traces printed with the magnetic field 6 (mf 6) presented higher resistance than with mf3, also with larger differences in samples with the untreated substrate.

Resistive heating behaviour depicted by thermal images shows that heat in each conductive trace is not homogeneous, higher temperatures were attained in the edges of each trace length, observed in most of the samples with two red lines and yellow in the middle. The effect of the printing parameters in the temperatures attained appeared subtle. The more representative relation was observed in regards to conductive traces screen-printed with mf 6 presenting a slight increase of temperatures attained in comparison to mf 3.

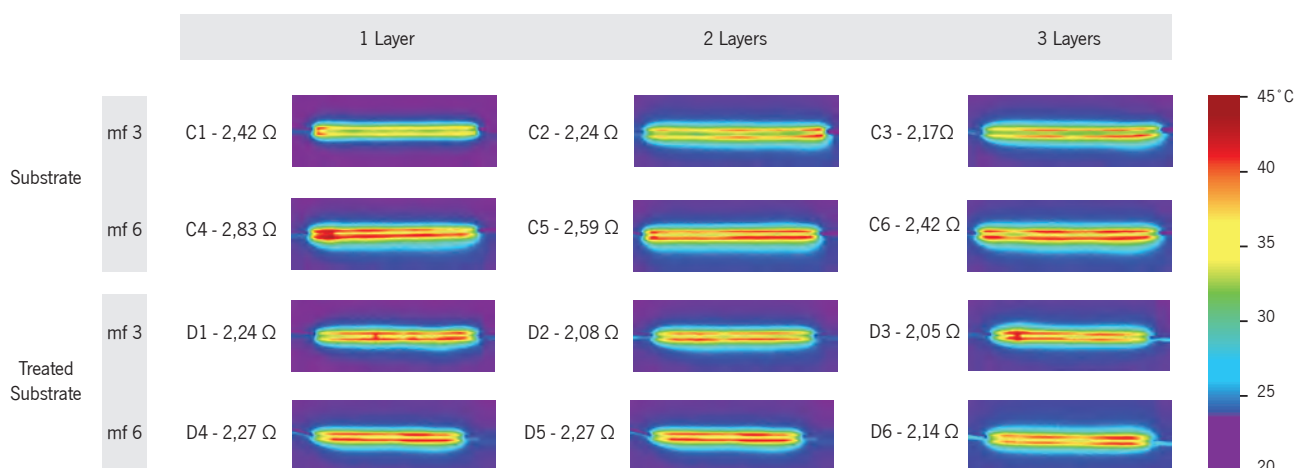


Figure 78. Electrical resistance and IR images of samples C and D, with 1,5 V power supply.

After the presented analysis, the folding effect on conductive traces was studied. The magnifying glass record has shown that all conductive traces crackled in the crease line, being more visible for samples with treated

substrate. Resistive heating tests demonstrated an overheating effect in the folded areas, with a more concentrated heat spot in samples with untreated substrate. Figure 79 presents C1 and D1 results.

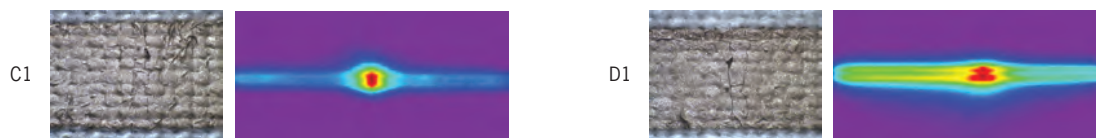


Figure 79. Magnifying glass photo and IR image of C1 and D1, after being folded.

To illustrate colour change with the studied conductive pigment, Figure 80 presents a sample developed with the same printing parameters of the conductive trace C6, with the 50% CO 50% PES substrate and 10% TC orange. Printed on the samples' back, the conductive pattern is visually perceived through the TC pigment layer before activation (front view image). With power supplied, the sample changed colour in the area of the conductive pigment pattern, whereas thermal expansion in the textile was reduced considering a maximum temperature of 45°C during activation.

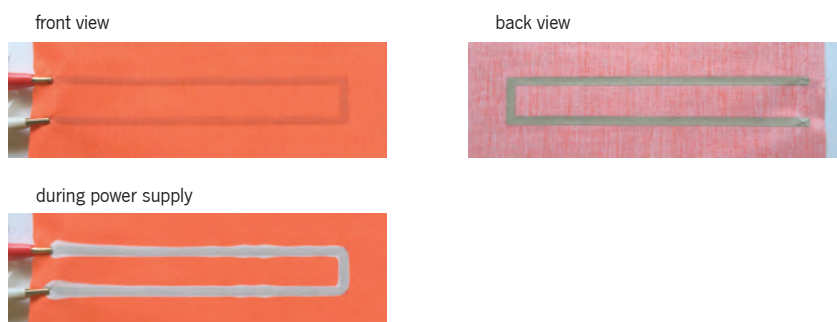


Figure 80. Conductive pigment sample front and back view before power supply (top left and top right, respectively) and during power supply (bottom).

6.5 Conductive material selection

Towards the development of study samples and prototypes to further research textile dynamic behaviour (Chapter 7), a conductive material was selected. Considering the results attained in 6.3 and 6.4 sections, conductive threads presented greater properties to be integrated in colour and shape change textiles due to electrical resistance stability during textile folding states with a threads set: CT1, 2, 7, 8, 9, 19, 21, 23, 24, 25 and 26. Additionally, their integration in a plain weave structure also allows the folding of textile piled up layers, without requiring electrical insulation.

The conductive thread selection also took into consideration the electrical resistance level, heating behaviour, possibility of programmed integration in the weaving process (not manually), tactile and visual characteristics.

Compared to the substrate textile threads used, CT2 is very thick and affected the textile sample tactility and folded morphology, reason why CT24 and 26 were also not selected, given their stiffness. CT23 and 25 can be broken manually and thus it was considered that their low tensile strength could present issues to support the tensions exposed during the programmed weaving process.

Furthermore, electrical resistance and resistive heating behaviour determined the conductive thread selection in respect to the objectives of the research prototypes scale, morphologies and activation. With the aim to activate complete areas of colour change, homogeneous heat along the threads' length was selected, as it enables similar heat transfer in the textile areas in between the conductive threads. CT21 presented heterogeneous heating and thus it was not considered.

The textile activation was also defined to be performed through different conductive series circuits, each being integrated in larger areas than, for example, sample B (11 x 11 cm integration area of each conductive thread). This scale estimation has considered the size decrease within folded origami tessellations and the objective to integrate conductive threads in the overall textile area. Besides each material type, each circuit electrical resistance depends on the conductive thread length used and as larger the circuit as higher the voltage required to attain a specific electrical current ($V = I \times R$). It was then defined to choose a low resistance thread and the selection fallen into CT7 (High Flex Silver), also due to their lighter colour, compared to CT8, presenting a more discrete appearance in the textile printed surface. A woven test was conducted in the loom Jacquard Vamatex with 41,2 Tex CO warp and 14,7 Tex PES weft, and the programmed integration of the CT7 in the woven substrate was successfully verified.

6.6. Conclusions

The integration of conductive materials in textile substrates enables the creation of soft structures with electrical properties. In this research section, electroconductive textiles were developed to study integration processes of conductive threads and pigments in textiles and their resistive heating properties towards TC pigments colour change activation.

Conductive materials electrical resistance and electrical current required to heat up above the TC pigment activation temperature are important parameters. However, resistive heating behaviour and colour change also encompass other variables' relations.

Integration pattern of conductive threads in the woven structure defines the possible areas of textile heat transfer. The results attained have demonstrated that resistive heating is not necessarily homogeneous along the threads length, affecting temperature variation in the textile and respective areas where the TC pigment transits from colourized to decolourized state. Thus, colour change expressions also depend on conductive threads expressive qualities. The outcomes observed were defined as homogeneous or heterogeneous with the last distinguished between irregular lines and traces.

Furthermore, thermal expansion in the textile also varied. Different conductive threads with homogeneous resistive heating and at similar temperatures have attained different colour change areas between the threads, observed through TC complete or incomplete decolourization. A consideration for this effect respects to the differences between the conductive threads fabrication, for example a textile metal spun thread or a textile metal plated, resulting in different contact areas between the conductive materials and the textile hold structure consequently affecting textile heat transfer.

The study conducted with silver-based pigment observed that printing parameters affect the electrical properties of the conductive printed pattern. However, the differences attained were not significant in the resistive heating outcomes. Taking into consideration the results attained with textile substrate handled and processes developed, the conductive pigment studied have presented great potential to explore colour change patterns with textiles developed by printing processes, but did not showed satisfactory resistive heating behaviour for the development of textile folded structures.

Towards the integration of one conductive thread in the development of study samples and research prototypes (Chapter 7), the selection fallen in CT7 – Karl Grimm High Flex 3981 7x1 Silver – regarding their resistive heating properties, soft tactility and light colour.

Regarding data documentation, the intrinsic properties of the conductive material studied comprise technical and expressive qualities, which were analysed as interconnected relations with the textile chromic behaviour. The way the results were framed aimed to depict technical and design findings as well as their relations, exploring a vocabulary that connects abstract with visual languages towards a comprehensive documentation within a technical and design approach of materials resistive heating and colour change behaviour.

This method associated with the frameworks organization in the conductive materials catalogue built a meaningful tool for this research, to analyse, compare and communicate conductive materials and textile behaviour. This documentation process was implemented in further experimental studies, conducted during the dynamic light filters design research.

6.7 References

- COLLECTION. n.d. *in Merriam-Webster's online dictionary* [Online].
<https://en.oxforddictionaries.com/definition/collection>. [Accessed 18 February 2017].
- STAMATELLOS, G. 2007. *Computer ethics: a global perspective*, USA, Jones and Bartlett Publishers.














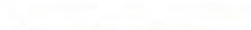






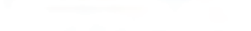



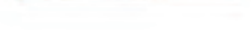



	CT1 - Bekinox VN 12/1x275/100Z
	CT2 - Bekinox VN 12/4x275/100S
	CT3 - Bekintex BK 50/2
	CT4 - Bekintex BK 50/1
	CT5 - Bekintex VN 14/2X90/175S/HT/PFA
	CT6 - Bekiflex CA 63/8X7/80S/0.245/PFA
	CT7 - High Flex 3981 7X1 Silver
	CT8 - High Flex 3981 7x1 Kupfer Blank
	CT9 - Constantan High-Flex 8394 7x1
	CT10 - Elitex 235/f34 PA/Ag
	CT11 - Elitex Garn Art TPU 667_235/f34 PA/Ag
	CT12 - Elitex 110/f34/2ply PA/Ag
	CT13 - Elitex (Lycra)
	CT14 - Shieldex 235/34x4 HC+E
	CT15 - Shieldex 110/34 2ply HC+B
	CT16 - Elinox SPP 35 300Z
	CT17 - Elinox PES HT 1100 + VN 60 400 t S/Z
	CT18 - LessEmf silver plated nylon
	CT19 - Lamé LifeSaver
	CT20 - Linox
	CT21 - Sparkfun stainless steel 2ply
	CT22 - Sparkfun stainless steel 4ply
	CT23 - Copper monofilament 100 µm
	CT24 - Insulated copper monofilament 160 µm
	CT25 - Stainless steel monofilament 50 µm
	CT26 - Nichrome monofilament 200 µm
	CT27 - Plug and Wear Nm10/3
	CT28 - SilverSpun

Figure 81. List of conductive threads integrated in this chapter woven samples.

DYNAMIC LIGHT FILTERS

CHAPTER 7

CHAPTER 7. DESIGN RESEARCH: DYNAMIC LIGHT FILTERS

7.1 Introduction

Smart textiles are able to interact with the environment and perform dynamic changes over time. Introducing new reactive and adaptive qualities to conventional textiles' functions and expressions, smart textiles open up innovative potential for the design of responsive environments, as they are able of sensing and responding to stimuli and they are an active element in shaping the environment.

The phenomenon approached in this research focuses on the design possibilities of smart textiles to filter light that passes through them, creating responsive lighting scenarios according to their physical and dynamic qualities. This interaction was explored through colour and shape thermo-responsive textiles, towards changing light transmittance without acting upon the light source: Dynamic Light Filters.

Through a materials research perspective, TC and SMAs behaviour was studied and integration processes in textile substrates were developed. Interaction of textile colour with light has demonstrated the ability to transform light transmittance from similar to different luminosities and tones as well as the inverse, in respect to the textiles chromic behaviour developed with defined colour ratios (chapter 4). Textile shape change behaviour based on origami tessellation morphologies displayed light changes through the variation of the textile layers number, also attaining a change of the light transmittance pattern in the textile surface with geometric areas of different luminous intensities (chapter 5).

Conductive threads and pigments integrated in textiles were studied for electrical activation of colour change (chapter 6). The experimental results have demonstrated that the electrical current value and the materials' electrical and expressive properties affect heat transfer and textile thermal expansion, highlighting the importance of these variables in how the textile changes colour. Conductive materials can present different visual properties when observed in light transmittance and through folding processes their performance can be compromised. The design criteria that in parallel to the electrical and expressive properties, guided the conductive thread selection for this research. Nitinol alloys are electrically conductive and shape change aimed of being studied through their resistive heating properties.

The results and the findings obtained in the previous chapters created a base framework for the development of smart textiles, which was implemented in the present research with the objective to explore colour and shape behaviour and their interaction with light, through a design perspective.

A central subject in smart textiles design involves the changes between states and how the textile performs over time. Designing with temporal forms extrapolates the physical medium definition to embrace the dynamic qualities of the textile behaviour, as they play crucial roles in the expressions and functionality of the design outcomes (Worbin, 2010; Vallgård, 2014).

Being an emergent dimension in textile design, the introduction of time and movement as inherent dynamic variables presents opportunities and challenges for materiality and methodology, entailing new perspectives in respect to how the textile changes and what it expresses, as well as how they are designed. Therefore, smart textiles require a new understanding of the variables and methods that the designer can work with and develop to explore textile dynamic and expressive possibilities (Redström, 2010; Mossé, 2016). For example, dynamic qualities are found more comprehensively in disciplines and natural phenomena where temporal dimensions are inherent. Some researchers evolved their methods by seeking and drawing relationships to dynamic phenomena such as in dance (Loke et al., 2015) and music (Jansen, 2013), as a way of thinking and exploring time and movement-based concepts in smart and interactive surfaces.

To study textile dynamic and expressive qualities, design possibilities are investigated through the variables that have an active role in the temporal forms and how they are articulated. In this research, the focus lied on temperature as a dynamic design variable to explore qualities and expressions of change in colour, shape and light performances.

How temperature varies is a critical consideration with the materials selected. They present gradual transformations during a temperature interval both on heating and on cooling. When researching thermo-responsive textiles electrically activated, temperature involves three perspectives: temperature of the conductive materials, temperature of the textile and ambient temperature. For each of these perspectives or dimensions, diverse variables can account for thermal variation, composing a set of relationships that can influence textile behaviour qualities and thus how light is transformed.

In working with two thermo-responsive materials in the same textile structure, the designer has to consider thermal variation for both behaviours, according to the materials' activation temperature selected. Possibilities to create simultaneous or independent changes can be explored to extend textile and lighting dynamic qualities.

The practice-based design research presented in this chapter proposes to study colour and shape behaviour of thermo-responsive textiles, with the objective to discuss and demonstrate dynamic qualities of change, based on: the relationship between design variables that the designer can consider and act upon to

influence how textile temperature varies; the interaction with light that passes through the textile and how it can transform and be transformed through light luminosities and tones; how textile and light behaviour can unveil expressions with different intensity levels.

The research program included two experimental studies and the development of two research prototypes. The initial experimental work has explored the influence of selected design variables in the dynamic qualities of textile behaviour and their interaction with light. The first study focused on textile colour and shape and the second study included interaction of textile and light. The research prototypes were developed with the objective to explore the relationship between the variables as a system in the expressions of colour, shape and light change and to discuss new possibilities and challenges when designing dynamic behaviour of thermo-responsive textiles.

7.2 Exploring textile dynamic behaviour

Temperature as a dynamic design variable encompasses several relationships between the electrical activation definition, physical context and textile characteristics. This section discusses the experimental studies conducted, aiming at analysing how a set of selected variables influences temperature variation and their relationship with dynamic qualities of textile colour and shape behaviour.

Considering the diverse interdependencies that can influence temperature variation, each experiment focused on one independent variable at a time and defined other variables to maintain a constant. Design criteria for variables selection was framed through initial questions raised on textile behaviour. The definition of each test parameters is presented in a graphic setup and ambient temperature was approximately 20°C in all tests, except when specified otherwise.

Colour change studies comprise of six experiments and were developed with two electroconductive samples screen printed with TC pigments with equal substrate characteristics, only varying dimension and morphology (sample X and Y). Shape change is studied with one sample (Z) and comprises of four experiments. Sample X and Y development is described in appendix D and sample Z in chapter 5 (sample S12). Activation temperature of the TC pigment used is 27°C and Nitinol alloys is As 30°C and Af 45°C.

To document and analyse temperature variation and textile behaviour, each experiment was recorded via thermal images and video. For a visual communication of the changes over time, thermal images and video frames were organized in a framework, according to a defined timeline.

7.2.1 Colour Change

Experiment A aimed to study how textile chromic behaviour can be influenced by the definition of an electrical current value for thermal activation. Two tests were conducted. A1 analysed colour change transitions on heating and on cooling for a defined time period. A2 investigated how slow and how fast the textile can change from colourized state to complete colourless areas and the inverse, from total colourless to full colour return.

For test A1 setup (Figure 82), the duration of power supply was 1 minute, after which colour return was also analysed during the same time period. The electrical current values tested ranged between 1,0 and 1,5 A with 0,1 A interval each.

Textile changes over time are illustrated in Figure 83 framework, displaying the visual record of thermal variation (IR images) and chromic behaviour (video record frames) at each 15 seconds of the timeline, for each electrical current level.

When the power supply is switched on, the conductive threads' pattern is revealed through the transition from textile solid colour to parallel colourless lines. This initial colour change stage is perceived in the first 15'' of activation with all electrical current values tested. However, the stripes' thicknesses are already distinct in this phase. With 1,0 A, a thin striped pattern is observed, while with 1,5 A the stripes appear to be as thick as the textile areas still in colourized state.

During 1' of activation, thermal expansion in the textile areas in between the conductive threads increased in a noticeable faster pace with higher currents. Activated with 1,3 A or more, the sample attained an overall colourless effect, whereas with inferior power, the stripped pattern was still perceived.

When power was interrupted, textile temperatures were different for each test, influencing how the textile changed to colourized state. Besides affecting the time required to cool down, it was also observed that colour return exhibited a sharper edge in the linear pattern in tests with lower current values and with higher values the colourization trajectory showed less relevance of the conductive lines. The stripes were still perceived, although they displayed a blurred effect with the overall shades of colour return.

Considering the direct observations of the overall performances, perception of the first stage of change from solid colour to stripe pattern is evident. During thermal expansion the gradual changes of colour through the colourless lines thickness increase are slower and not as obvious.

Test A1 Independent variable: Electrical current value (during a defined activation time)

- X 1 = 1,0A
- X 2 = 1,1A
- X 3 = 1,2A
- X 4 = 1,3A
- X 5 = 1,4A
- X 6 = 1,5A

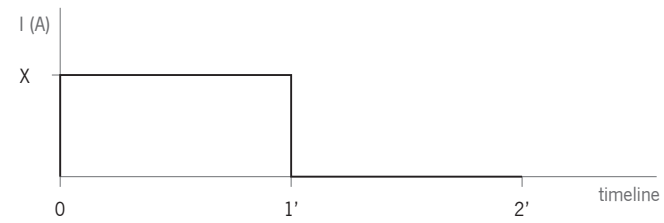


Figure 82. Test A1 setup.

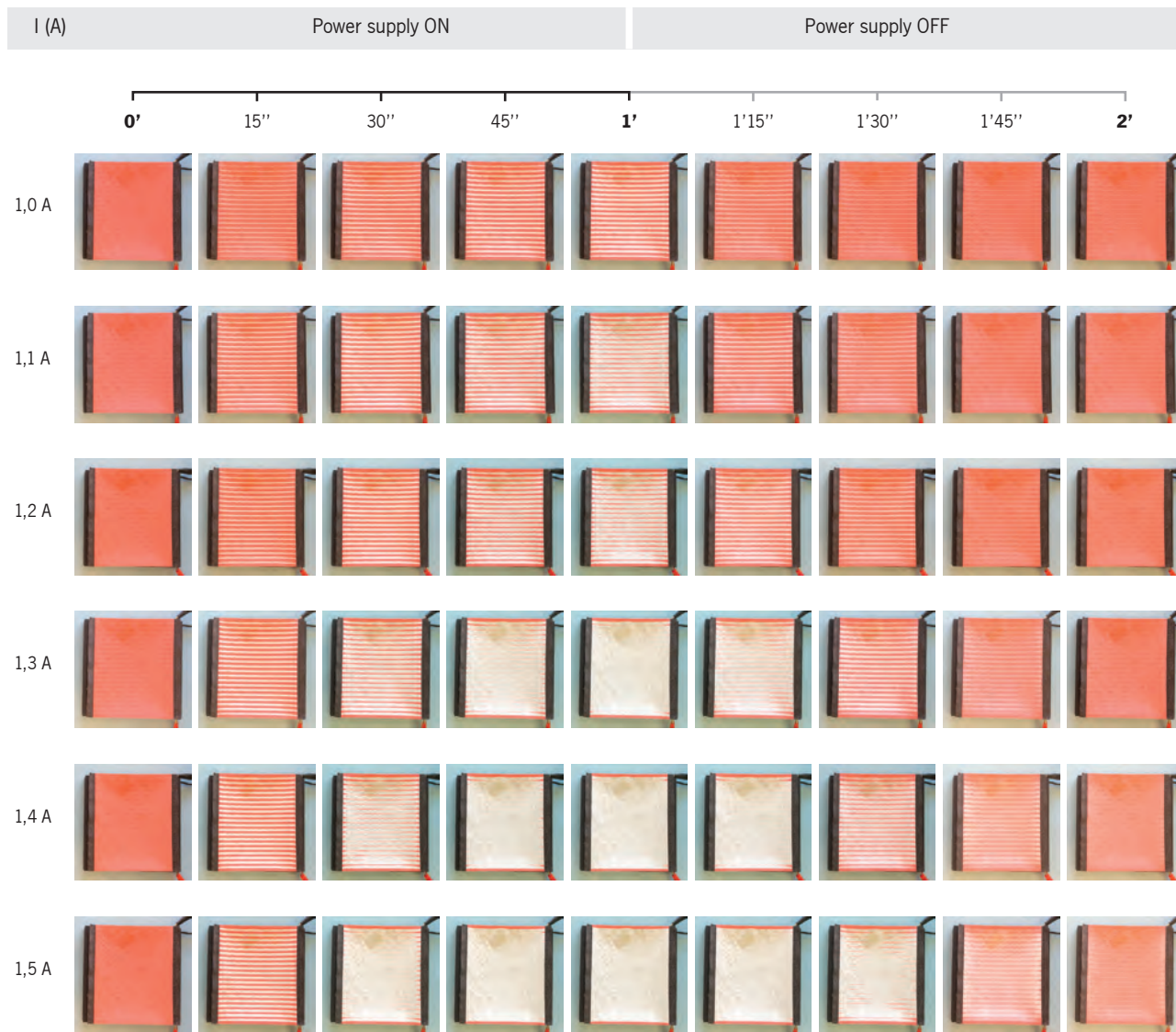
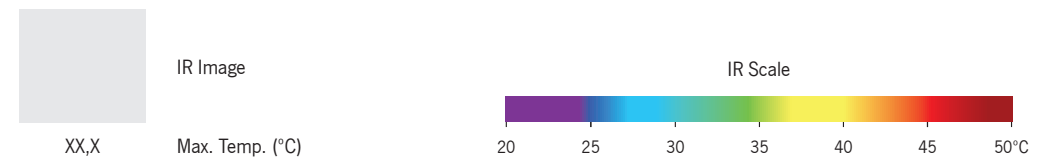
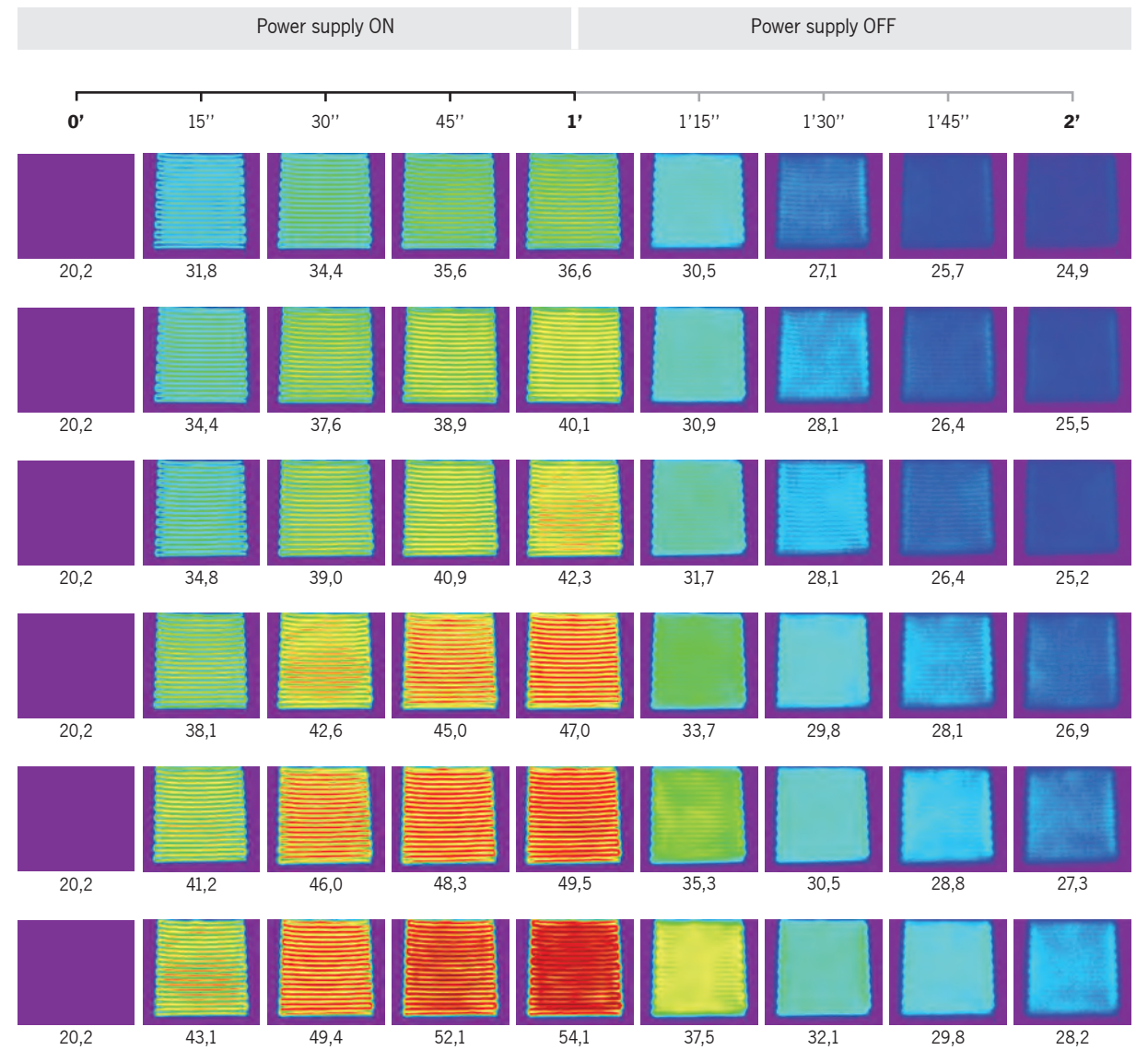


Figure 83. Test A1 results.



Electrical current levels play a significant effect in textile temperature variation, influencing duration of changes, the possibility to attain specific expressions, such as complete colourless, as well as affecting the chromic behaviour during transitions. As a result, the selection of electrical current values comprises of diverse possibilities to explore and design textile colour change qualities.

Furthermore, through this experimental data it was also observed that textile thermal expansion is not necessarily larger when the conductive threads present higher temperatures. Thermal images of 1,3 A at 1'; 1,4 A at 45''; and 1,5 A at 30'' appear similar. Although, for the stages mentioned, a complete colourless effect is just observed with 1,3 A, presenting a lower maximum temperature than with 1,4 and 1,5 A, where colourless is not as complete. This observation underlines the importance of time for colour change qualities, a variable focused in the following experiment.

With the objective to explore textile paces between two defined expressions, experiment A2 studied how the activation with constant electrical current values influences the time required to heat up the textile until a full colour change and to cool down until complete colour return. Test A2 setup is presented in Figure 84.

Textile activation was performed until maximum temperatures of approximately 50°C were detected with the thermal camera. On cooling it was difficult to identify when colour return was completed by direct observation. Subtle differences of colour nuances can be observed during several minutes, which can differ between activation tests in the same sample. For a comparative analysis, the colour return trajectory was considered since the interruption of power until the textile maximum temperature was below 27°C, the TC trigger temperature.

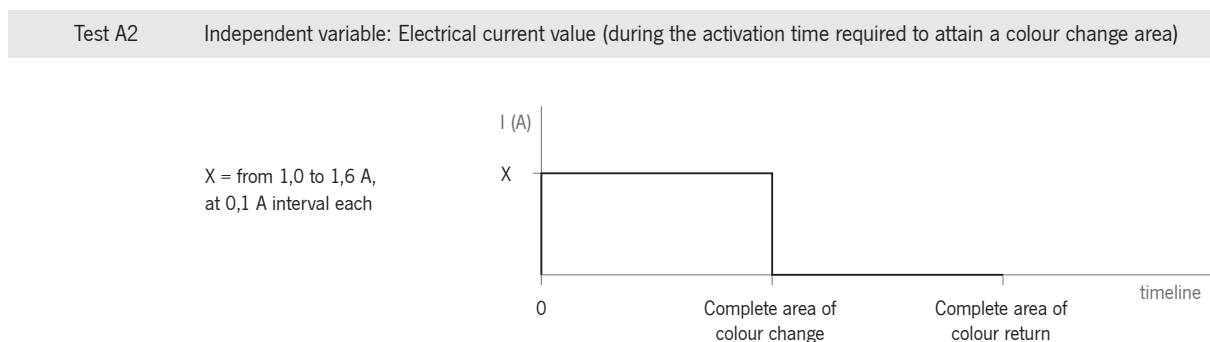


Figure 84. Test A2 setup.

Time and maximum temperatures attained in the predefined stages of colour transitions are presented in Figure 85. The temperature increase during power presents different rates, according to electrical current levels. Although, after an activation period, the conductive threads temperature as well as thermal

expansion started to stabilize, maintaining the colour change effect. This behaviour was analysed in the tests with 1,0 and 1,1 A, where full colour change was not attained. With 1,0 A, a maximum temperature of 39,3°C was measured after 5' of power and in the subsequent 5', both temperature and textile expression were similar over time. With 1,1 A, the maximum temperature increased only 1°C from 5' to 10'.

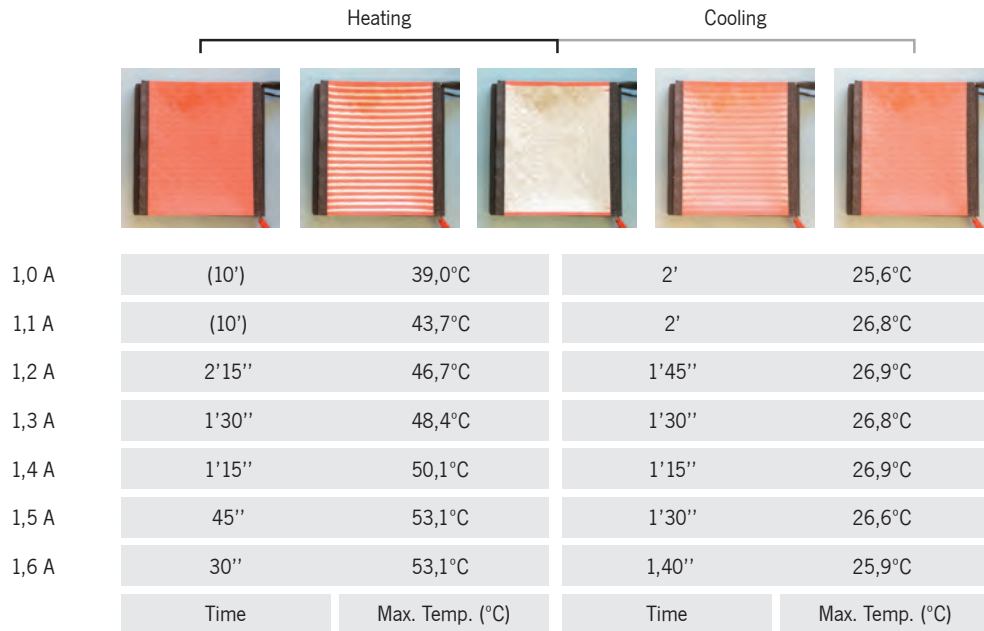


Figure 85. Test A2 results.

This analysis highlights the possibility to design colour change behaviour, where colourless expression can be maintained during long periods without overheating the textiles. For this performance, a relation between optimum current level and temperature in the conductive threads that attains constant colour change areas requires experimentation.

Observing the results attained with 1,2 A, the textile became decolourized at 2'15'', with only 3°C maximum temperature higher than with 1,1 A. Whereas maximum temperatures were similar, an analysis of the thermal images of the stages mentioned showed that with 1,1 A few areas attained the maximum temperature, observed through orange and red colour of the IR chromatic scale, while the thermal image with 1,2 A presented a more homogeneous distribution of the high temperatures in the textile. Nevertheless, mean temperatures in the textile areas between the conductive threads were not very distinct, reflecting the impact that small temperature differences can have on colour change expressions and the importance of understanding these relationships to design thermo-responsive behaviour.

Colour return after switching off power supply at the complete colourless state is also influenced by the relation between electrical current level and time of activation. Comparing the tests from 1,2 to 1,6 A, time

on heating until full colourless decreases and maximum temperatures increases, whereas the time of colour return transition decreases from 1,2 to 1,4 A tests and increases from 1,4 to 1,6 A. The cooling effect is not only associated with the maximum temperatures attained but with the overall textile temperatures that affect how the textile returns to colorized state.

Higher electrical current values allow for designing faster colour change behaviour, while colour return pace is also affected by the previous period of power supplied. Considering the setup defined for this study, 2'15'' with 1,2 A was the slower colour change on heating and 30'' with 1,6 A was the faster. Whereas the graphic shows data until 1,6 A, higher values were also tested, attaining temperatures above 50°C in the conductive threads before complete colourless area was observed, which set the limit for this test analysis.

Colour change activation may comprise of different sequences of textile heating and cooling down. Test B aimed to compare textile temperature variation and resulted in colour change effects of two consequent cycles of full colour change and full colour return. The electrical current value defined for experimental B setup was 1,4 A (Figure 86).

The images framework presented in Figure 87 enable a visual comparison of the results attained in the two consecutive cycles of activation. The sample was in colorized state in the beginning of each cycle, but their temperature differences influenced the textile behaviour. The textile was warmer at the starting of the 2nd cycle than in the 1st cycle and attained a decrease of colour change duration until colourless of approximately 15'' and an increase in the time of colour return also approximately 15''.

Visually, the colour behaviour in the 2nd cycle was particularly affected in the beginning, where the stripe pattern rapidly showed the increase of the line thickness, while the last stage to complete a colourless area appeared as slow as in the 1st cycle. During the performance observations on cooling, the gradual and slow colour return was also perceived as similar in both cycles, the differences in the last phase of this transition were observed through the IR images.

To explore and design colour change expressions, the focus relies on how the visual changes are perceived. However, the thermal analysis provides information that can be used as an additional tool when taking design decisions. For example if a 3rd consecutive cycle is conducted, the designer can select to start the activation at 5' or later, so the paces of colour change could be more similar to the 2nd cycle, or to the 1st cycle if the time without activation is enough for the sample to cool down until ambient temperature. If activation is programmed to start at 4'45'', where visually the textile appears to be at complete colourless

Test B Independent variable: Activation cycle

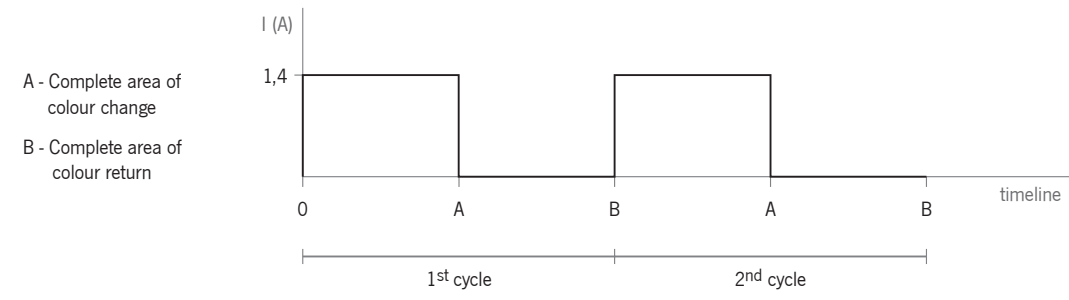


Figure 86. Test B setup.

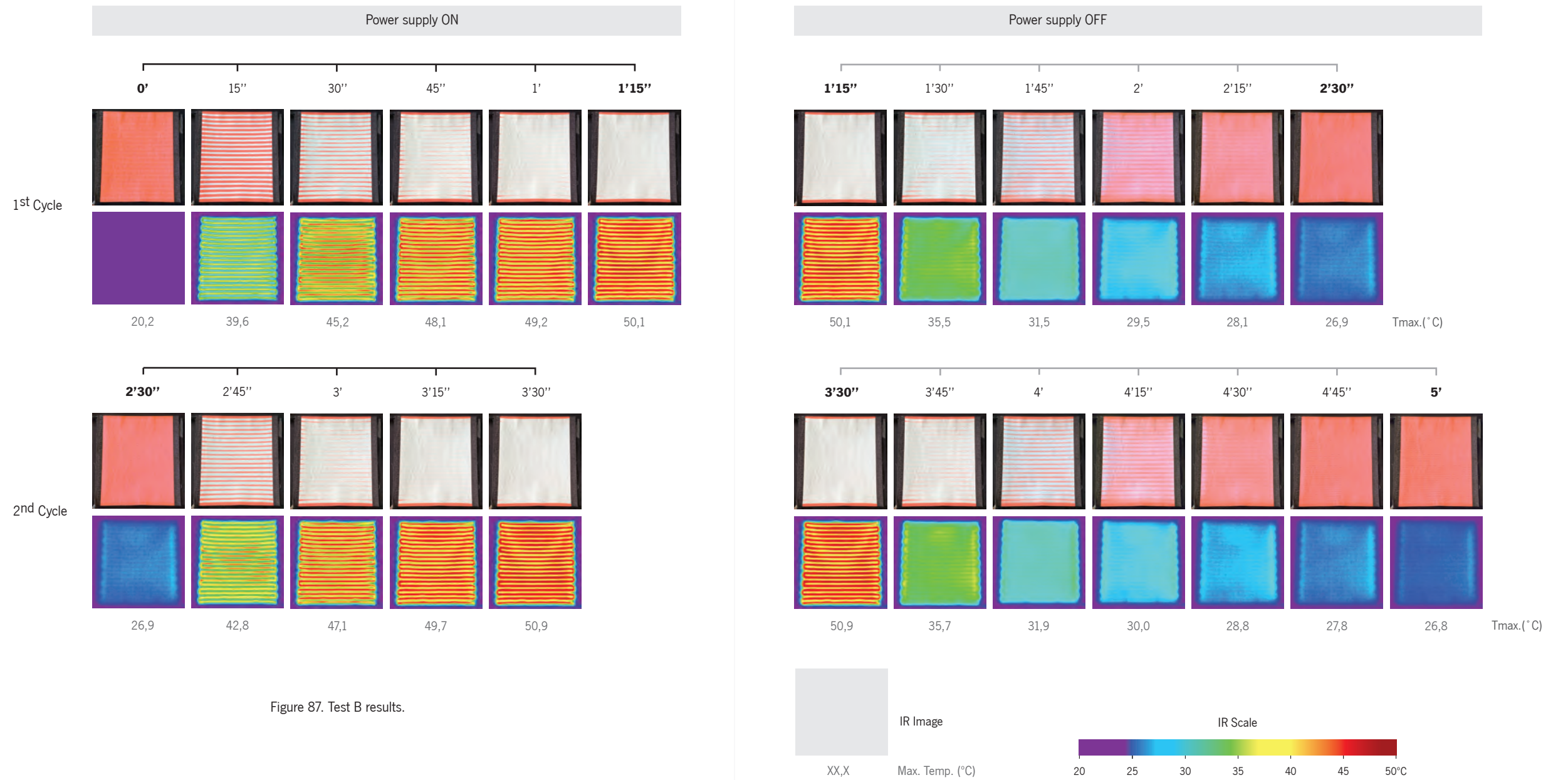


Figure 87. Test B results.

state but the temperature is slightly higher than in the beginning of the 2nd cycle, a decrease in colour change duration might be expected.

Colour change activation may also comprise of a variation of the electrical current levels supplied. With the objective to study design possibilities transform the paces of colour change, experiment C analysed the effect of supplying a higher electrical current value in the first stage of textile activation, followed by a decrease until textile thermal expansion in the areas between the conductive threads is complete.

The test definition and analysis took into consideration the A2 test results. Activation with 1,6 A attained the colourless state at 30'' and maximum temperature of 53,1°C; the activation with 1,4 A lasted 1'15'' and maximum temperature 50,1°C. Test C setup (Figure 88) was defined with 1,6 A in the first 20'' of activation, followed by a decrease to 1,4 A until complete colourless after which the power supply was interrupted and textile colour return was also analysed. The aim was to decrease the colour change time of the previous test with 1,4 A, maintaining the colour return time.

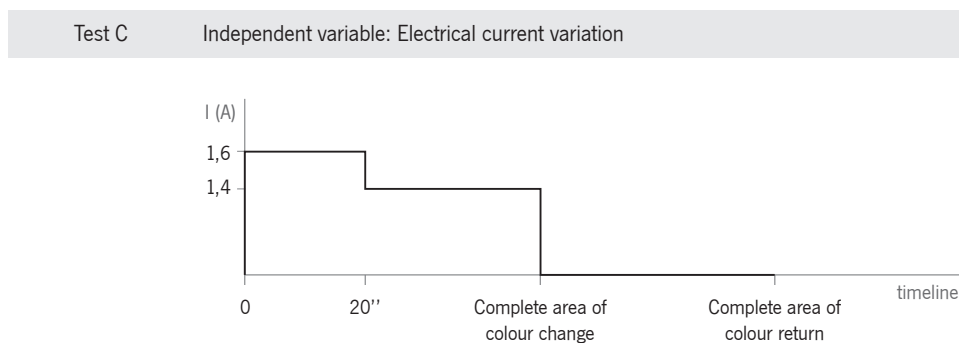


Figure 88. Test C setup.

Results presented in Figure 89 show the colour change transition until colourless attained in 1' and colour return until 2'30''. Comparing the results attained with A2 test 1,4 A, there was a decrease of 15'' on heating with a slight increase of the maximum temperature and a 15'' increase on cooling. The results can also be compared with the images of A1 test where with 1,4 A in 1', small colour change differences can be observed in some areas of the textile margins that are still coloured.

If the design parameters focus on the overall colour change duration, activation just with 1,6 A can be selected, as it was significantly faster on heating and presented approximate duration on cooling as well as maximum temperatures.

The potential highlighted by using electrical current variation relied on the possibility of having faster transitions in particular moments of the activation, thus enabling to design different rhythms of colour

change behaviour from on state to another. In this test, expressions of change had a faster pace within the stripe pattern, emphasizing the beginning of the colour change transition. If the activation is defined with low electrical current levels in the first phase and higher levels after, slower changes will be created when the performance begins, increasing the rhythm of change that completes the textile colourless effect.

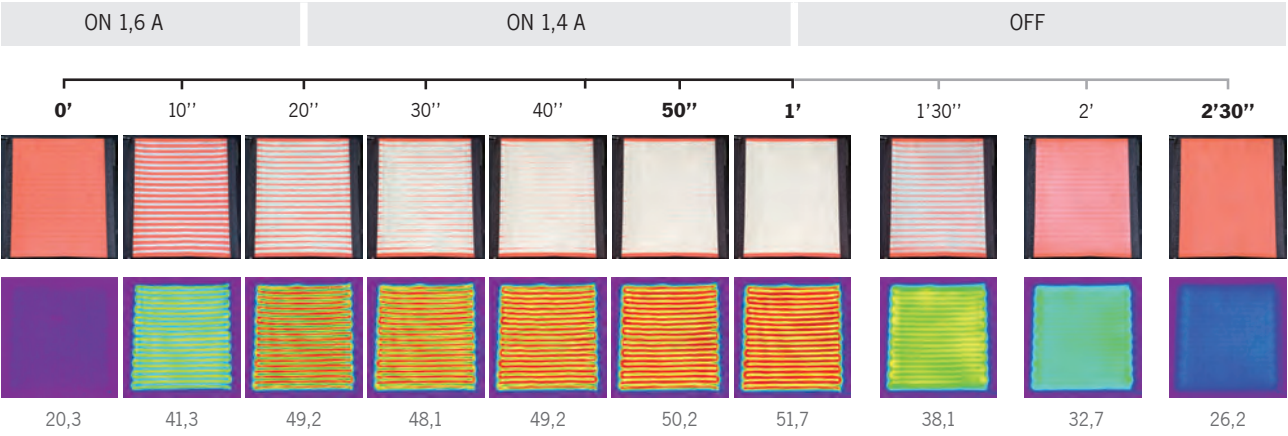


Figure 89. Test C results.

Ambient temperature is a variable of the physical context where colour change occurs. Experiment D studied the effect of two different ambient temperatures in the textile chromic behaviour, with the same current supplied. D setup was defined with 1,4 A activation, to be tested at 16 and 20°C ambient temperatures (Figure 90).

As analysed in the Figure 91 framework, ambient temperature significantly affects changes of textile colour. At 20°C ambient temperature, the striped pattern of colour change starts to blur into colourless areas at 45'' and at 16°C ambient temperature, a similar expression is observed at 1'45''. The decrease of 4°C in the physical context has changed the time required for the textile attains full colour change to be twice as much.

The effect on the textile cooling down to temperatures below 27°C was not as distinct in duration. As previously discussed, the duration of power supplied during activation plays an important role in the colour return changes. However, other qualities of colour return behaviour were affected. At the lower ambient temperature, colour return in the textile areas in between the conductive threads was perceived very fast after the power supply was switched off and the lines' edges appeared more sharp, while at the higher ambient temperature the colourization changes had a blurred expression.

These results highlight that even in interior environments, where ambient temperature might present small variations, it can exhibit a perceived effect in the dynamic qualities of the textile behaviour. Considerations should be taken when defining and programming the activation sequences, in respect to the textile physical context.

Test D Independent variable: Ambient temperature

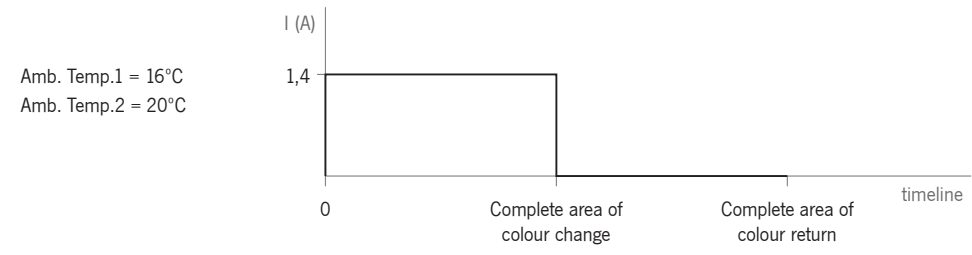


Figure 90. Test D setup.

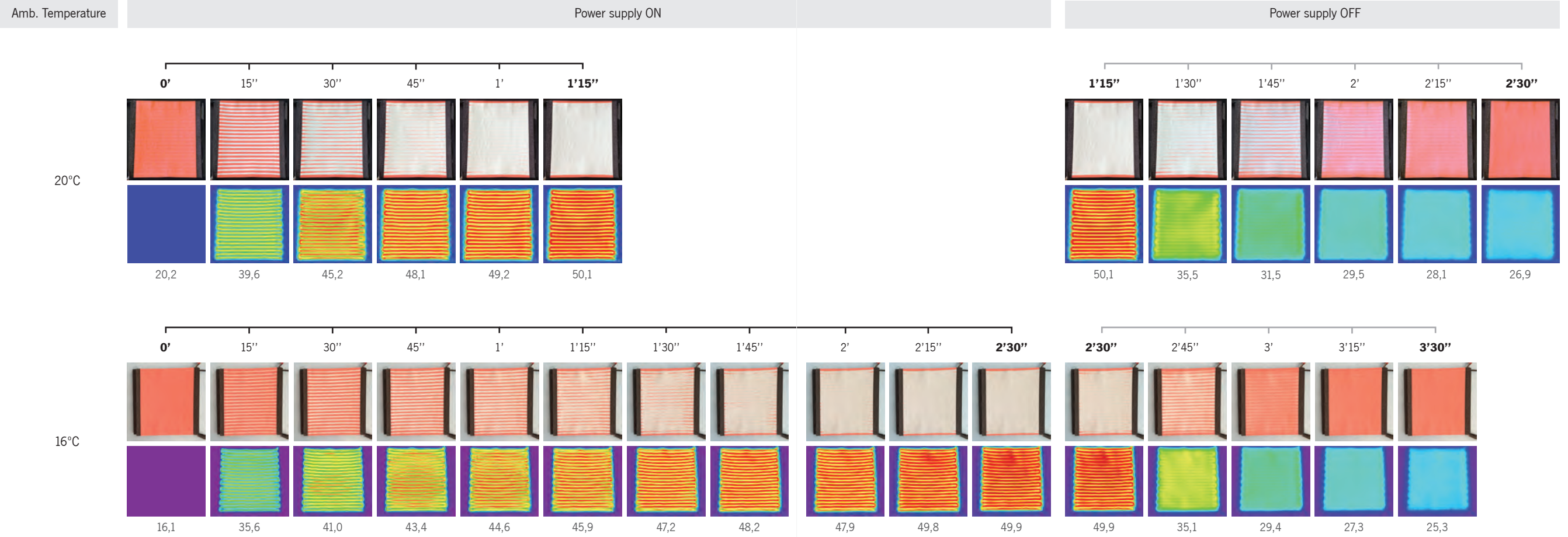
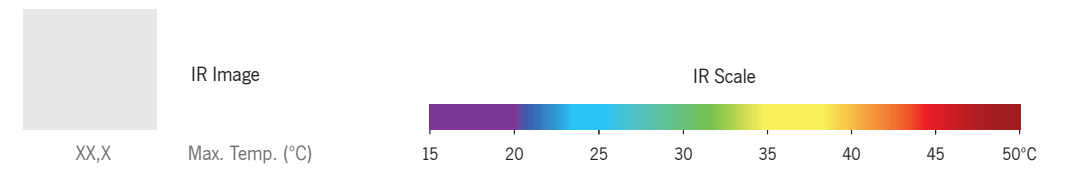


Figure 91. Test D results.



In experiment E the objective was to explore design possibilities of dynamic colour behaviour by acting upon the textile morphology through origami techniques. The sample used in this study (sample Y) is similar to the sample used in the previous tests, but it was folded into a squaretwist origami pattern. Colour change was activated with 1,2 A and the textile dynamic expression were analysed on heating and on cooling, according to the timeline defined in test E setup (Figure 92).

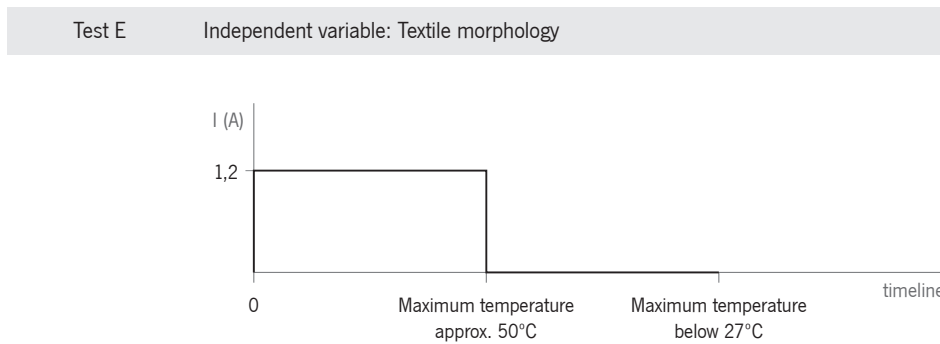


Figure 92. Test E setup.

The conductive threads integrated in the sample substrate are parallel. However, the squaretwist folding of the textile has created areas with different pile-up layers and a square area that was twisted, changing the direction of the conductive threads in the textile upper layer, which become perpendicular to the threads in the lower layers. As a result, textile morphology has influenced thermal variation and colour change expressions (Figure 93).

In the first stage of the activation, thin lines of colour change are revealed vertically in the twisted square area and horizontally in the remaining areas. Through thermal expansion in each layer and across pile-up layers, the colourless lines created a spotty expression in the sample central square. The perceived dots correspond to the textile areas still in colourized state and as thermal expansion increases in the dots' background, they become smaller until exhibiting a complete colourless effect. Thermal variation in the horizontal lines also showed a heterogeneous change with areas where the colourless spread at different paces, according to the pile-up layers differences of the folded substrate.

After interrupting the activation, the textile returned to colourized state very slowly, particularly in the twisted square, corresponding to the area with more pile-up layers. During the 3' required to cool down the sample until temperatures below 27°C, changes between colourless and shades of colour appearing presenting a blurred effect and discreet dots in a small phase of the colour transition.

This study demonstrates the potential of exploring dynamic qualities of colour change through textile origami morphologies. Diverse origami base folds, folded pattern compositions, techniques, scales, etc. can be applied to transform the substrate, changing the geometry of the integrated heating elements, thus enabling the creation of colour change patterns with different dynamic expressions.

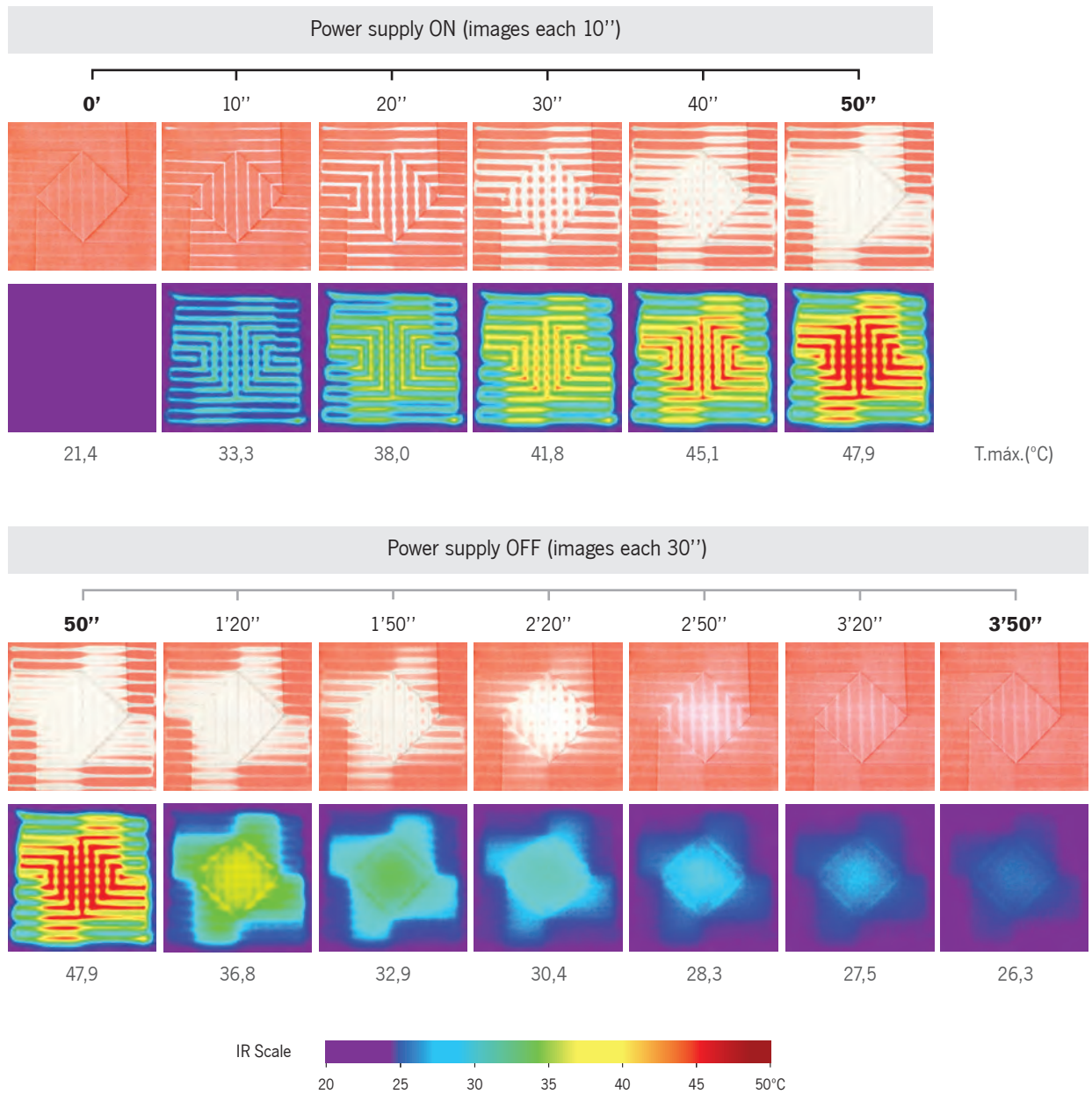


Figure 93. Test E results.

7.2.2 Shape Change

Similarly to the tests conducted in experiment A for colour change, experiment F studied how shape change behaviour is influenced by the electrical current levels. Sample Z activation from deformed flat shape to fold up was conducted until a maximum temperature of approximately 45°C (Nitinol Af). After power supply was cessed, textile cool down was analysed until the textile maximum temperature was below 30°C (Nitinol Mf), (Figure 94). The electrical current values tested ranged between 0,6 and 0,9 A with 0,1 A interval each.

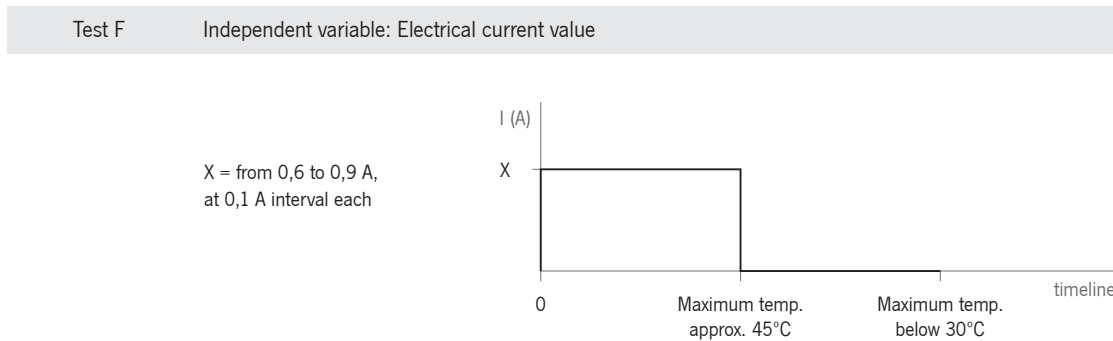


Figure 94. Test F setup.

The sample used to study shape change behaviour was screen-printed with a TC pigment that has a lower activation temperature than the Nitinol alloys used. As a result, the activation of shape change also changed the textile colour, revealing the SMAs integration pattern. At the angle that the tests were recorded, the colourless lines were mostly perceived when the textile folds up, adding a new variable in the perception of the shape change behaviour.

The shape change between two states can be designed with different paces according to the electrical current values defined for activation. The study on this relationship is depicted in Figure 95. Through a direct or video record analysis, the slow movement observed with 0,6A appeared discreet and after a first activation phase, it was not clear if the textile shape was still or slowly changing. The images framework showed that from 15'' to 50'' the shape has changed slightly.

The increase of electrical current levels attained faster shape change, whereas the movements had an organic expression independently of the paces. Thermal variation was faster with 0,7 A than with 0,6 A, but the main perceived behaviour appeared to be similar, as can be visualized in the images until 15''. This analysis points out that decreasing the power supplied does not necessarily slow down the pace of the perceived change. With the increase of the electrical current values from 0,7 to 0,9 A, faster shape change was more obvious.

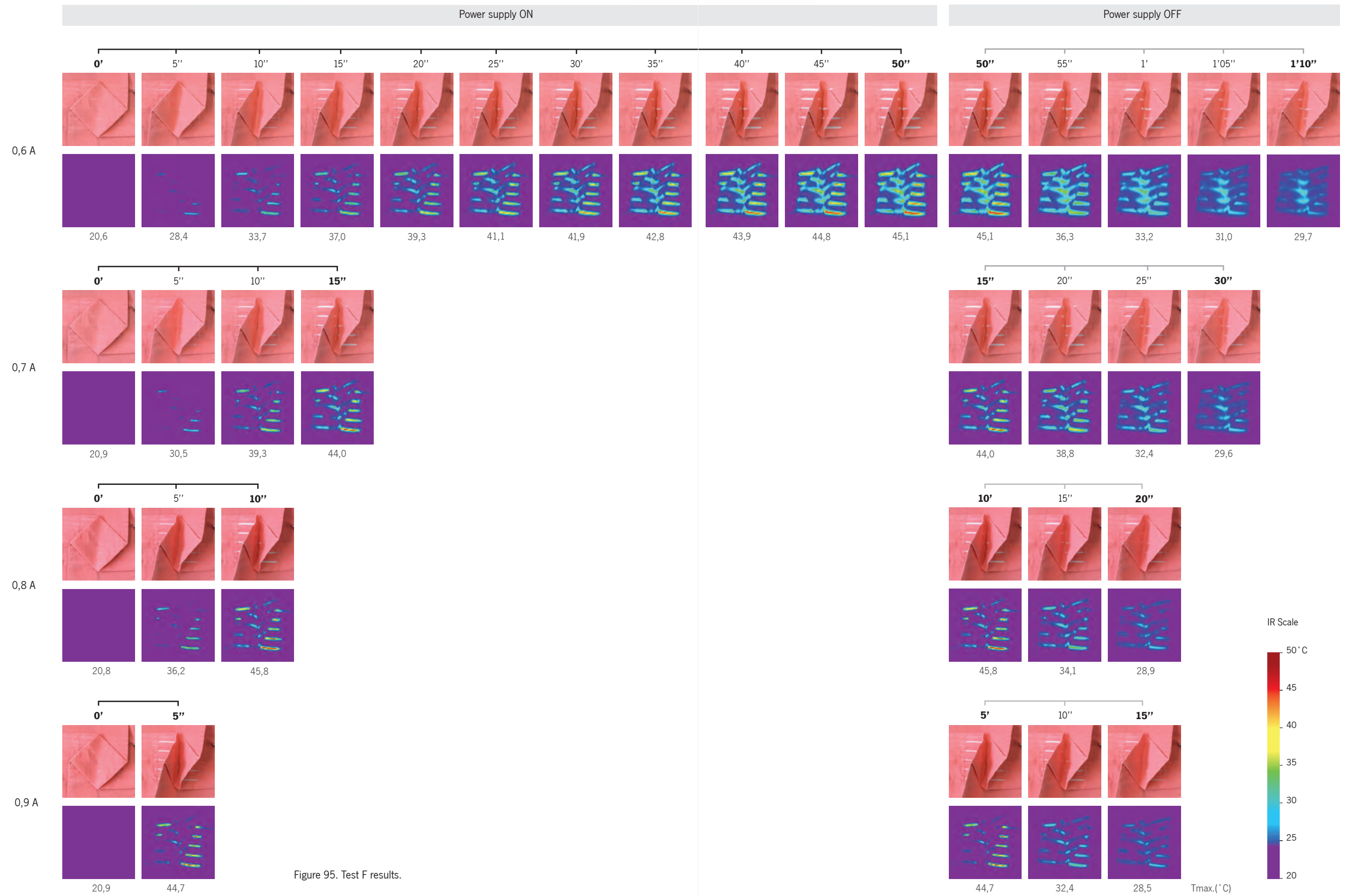


Figure 95. Test F results.

In all tests, power was switched off when the sample attained approximately 45°C. As observed in colour change studies, textile thermal expansion according to time of power supplied has influenced the Nitinol cool down. Furthermore, small changes of shape were observed during the temperature decrease, as previously analysed in chapter 5.12. This effect highlights the possibility to design textile behaviour that even just comprising of activation for one memorized shape, the changes on cooling can be explored in respect to the textile morphology, scale of the folded motif, sample weight, previous activation parameters, positioning, etc. In the tests conducted, this movement was perceived as slower when the textile was activated during a longer period (0,6 A) while in the other tests the changes appeared similar.

In test G, textile changes between deformed flat morphology and fold up were analysed at 17 and 20°C ambient temperatures, following the setup presented in Figure 96.

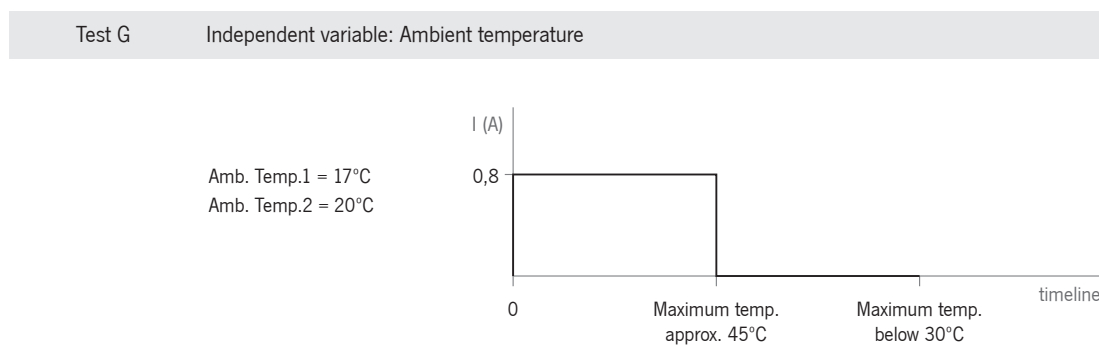


Figure 96. Test G setup.

With the same activation parameters, textile shape change at the two ambient temperatures tested attained similar qualities (Figure 97). Temperature increase was slower at 17°C than 20°C but did not have a noticeable effect on the textile temporal forms during activation neither during the SMAs return to deformable state. The studies on ambient temperature influence on textile behaviour showed that this parameter is more critical in the qualities of colour changes than shape, considering one activation cycle.

Focusing on textile shape behaviour to perform variation between fold up and fold down morphologies, the activation of two Nitinol groups, one for each shape, can be defined according to electrical current values, time of power supply, as well as pause time in between the activation of each memorized shape.

If fold down is activated immediately after the fold up, or the inverse, Nitinol alloys are in the process of recovering the pre-memorized shape when the other Nitinol group is still above the temperature that can be deformed. There is a time duration increase to attain the complete shape change, in regards to the time required for the actuator group previously heated up to cool below 30°C.

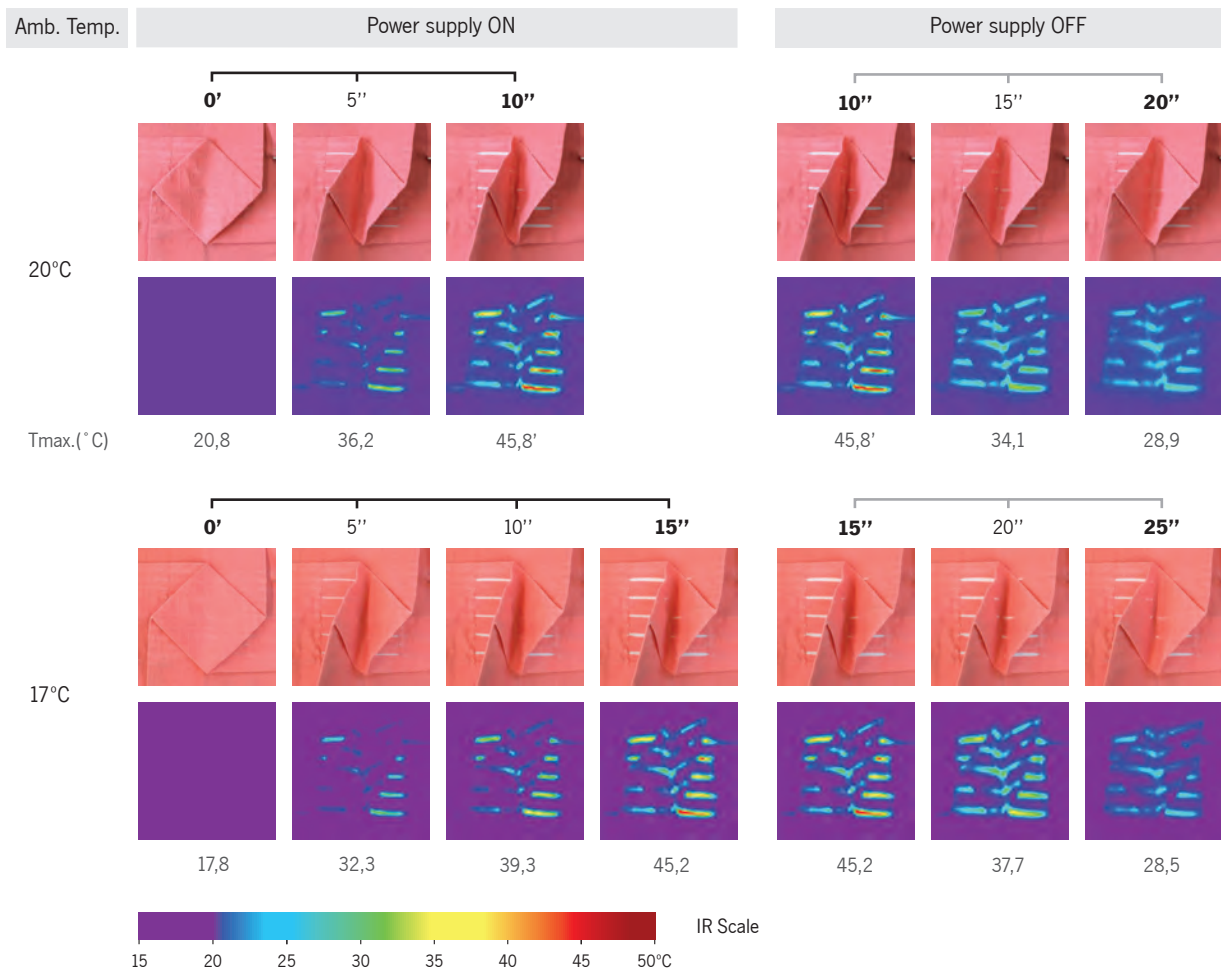


Figure 97. Test G results.

Test H studied the influence of non-activation times between the textile fold up and fold down activation in the qualities of change. The setup of the two tests conducted are depicted in Figure 98, where 0,8 A is supplied for 10 seconds for fold up and fold down in both tests and the pause time after each activation is 20 seconds in H1 and 10 seconds in H2.

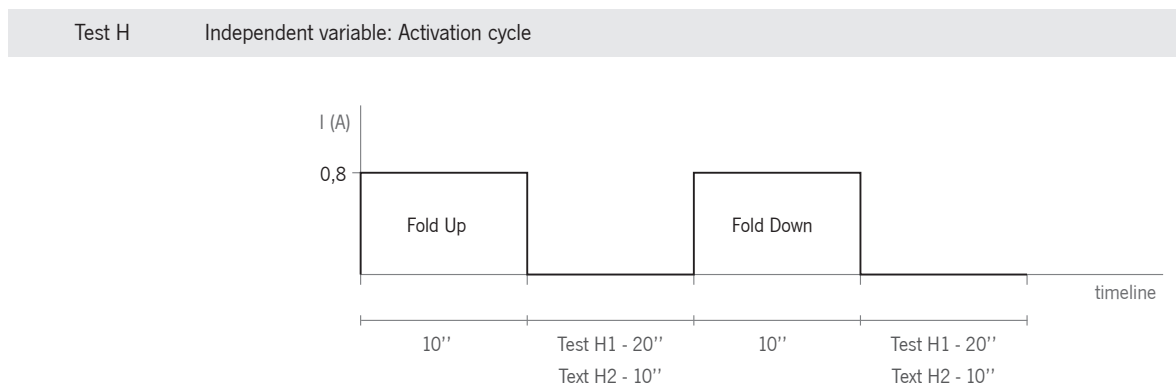


Figure 98. Test H setup.

Different cooling times create the frame for the changes duration, influencing temperature variation and how the textile changes shape (Figure 99). When fold down was activated, textile maximum temperatures in H1 and H2 tests were below the Mf, meaning that the Nitinol fold up group previously activated was in the deformable state and after 10'' of fold down activation the textile presented similar shapes.

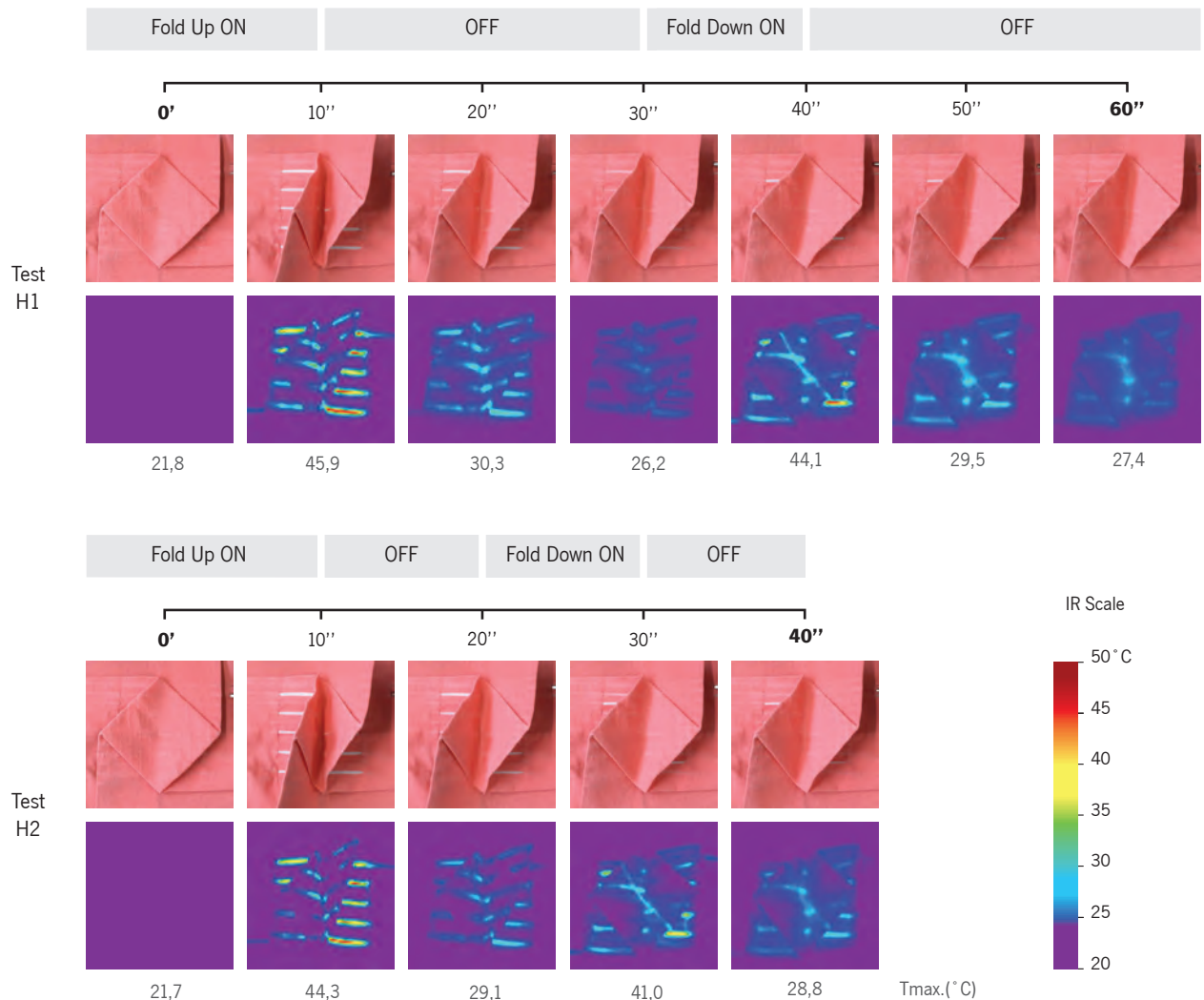


Figure 99. Test H results.

The shape change performed during the pause after the fold up activation time, displays movement in the direction of the fold down. Depending on the pause duration, this transition can present different qualities. With a 10'' pause, the change after fold up activation was perceived as the beginning of the fold down, which when activated, continued the previous movement. With 20'' pause, the shape change was perceived in 'steps': it started to fold down, maintained the shape for some seconds and then continued to fold down.

Displaying great potential to explore rhythms of textile movement, these expressions that also apply for the inverse transition (fold up to fold down), depend on diverse parameters. For example in chapter 5.12, the

comparative study of shape change in vertical and horizontal positioning, observed subtle differences between the textiles morphologies after the activation pause. Therefore, the relation between activation and non-activation times requires experimentation with the intended textile structure and placement, whose dynamic qualities aim to be designed.

The sequential activation between two Nitinol groups creates movement that can continuously evolve from one state to another. The objective of experiment I was to study how shape change activation through consecutive cycles may influence textile temperatures and morphologic behaviour. Test I setup (Figure 100) was defined with two fold up and fold down cycles, supplying 0,8 A for 10 seconds in each activation stage and 5 seconds for each pause in between activations.

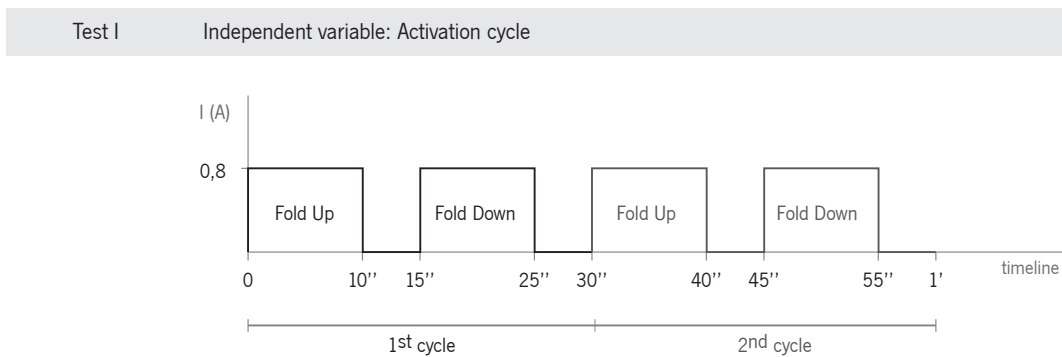


Figure 100. Test I setup.

Activation of two consecutive activation cycles affected thermal variation of the Nitinol alloys and also the textile areas in between them (Figure 101). Temperature differences were mostly emphasized in colour change, whereas in shape change the performances appeared almost similar but displaying a slightly more closed effect on the 2nd cycle fold down and a slight shape change on cooling in the 1st cycle fold up, that did not occur in the other paused states.

The framework shows that the 5'' pause after fold up and fold down activation was not sufficient to cool down the SMAs until the deformable state, reflected in the subtle or lack of shape change on cooling, which in previous tests were obviously perceived.

Additional exercises have analysed the textile performance with increasing cycles. It was observed that the activated shape changes started to be affected, presenting lower abilities to fold up and fold down until the movements were near imperceptible, as both Nitinol groups simultaneously achieved in high temperatures.

Continuous activation sequences significantly affect the qualities of the textile movements and its ability to perform over time. According to design criteria, cooling times can be considered in respect to pauses in between two shapes activations and after a programmed cycle or sequences.

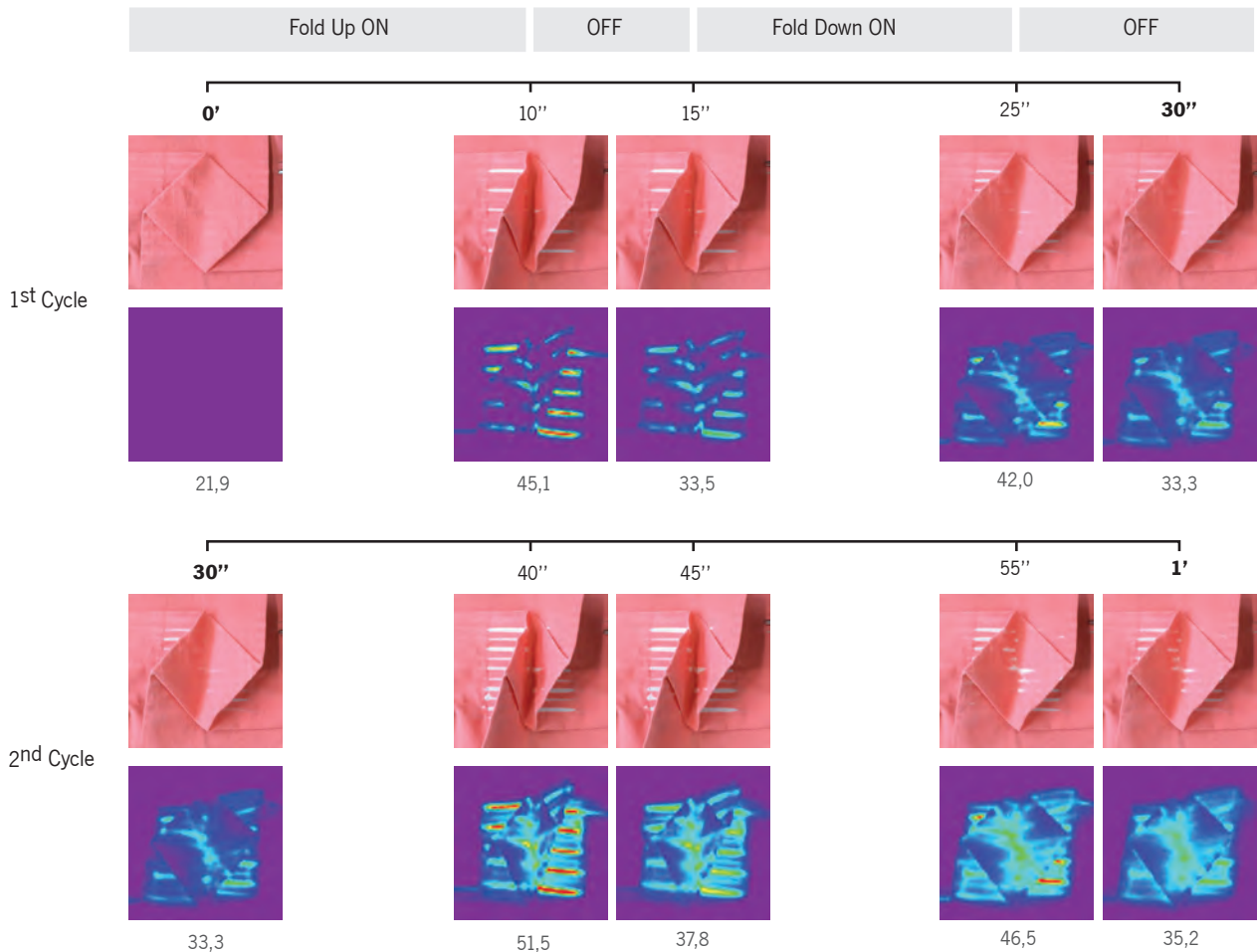


Figure 101. Test I results.

7.2.3 Discussion

The relationship between thermal variation and the independent variables studied have demonstrated to be crucial when designing textile thermo-responsive behaviour, since it has played a relevant role in the dynamic qualities of change. The experimental work presented has comprehended selected parameters of temperature as a dynamic design variable, distinguished in three dimensions: activation, physical context and textile.

Experiments on activation parameters have analysed how textile temperature and expressions of change can be influenced by electrical current value, constant or variable; activation time and non-activation time;

and cycles. Giving insight into design possibilities of paces of change, rhythms and expressions of temporal forms, the studies have illustrated the complex interdependences that evolve in heating and on cooling.

One critical parameter to explore dynamic qualities of change lies in the distinction between activation time and duration of change, inversely to other actuators. For example a LED emits light when the required power is supplied and turns off when power is interrupted. With thermo-responsive textiles changes can occur independently of the activation time through a nuance of transitions comprehending heat and the inherent properties of the colour and shape change textiles. This quality presents challenges but also opportunities to design smart textile behaviour.

Whereas the selection of activation parameters may initially appear to be attributed to a technical decision, their influence in the textile dynamic qualities suggest they are expressive variables of colour and shape change. For example, how paces and expressions of colour change can vary, when the textile is activated during the same time with different electrical current values.

Thermo-responsive behaviour with materials which activation temperature is higher than average ambient temperature is commonly focused on temperature increase. To explore and design dynamic qualities of change, cooling has shown to be as important as heating, considering the dynamic qualities when temperature decreases and also its effect during activation cycles.

Besides duration of activation pause, ambient temperature is also a critical variable in the changes on cooling, particularly in thermal variation of the textile substrate. On heating, ambient temperature is also more relevant in changes that occur or are influenced by textile thermal expansion, thus affecting with greater impact textile colour change considering colourless and colour return areas beyond the conductive pattern. Ambient temperature may or may not be controllable in the context of placement or use of the textile and due to their effect on the textile performances, it is an important consideration in the design process.

The relationship between the textile properties, thermal variation and temporal forms is inherent to all the experiments conducted. The test that has individually approached textile as an independent parameter suggested textile origami morphologies as a design variable to explore dynamic qualities of colour change. Furthermore, this study has also highlighted that the first phase of colour transition is not merely defined by the integration pattern of conductive materials in the substrates, design possibility also demonstrated in chapter 6 experiments with the expressive behaviour of conductive threads heterogeneous heating.

Dynamic and expressive possibilities analysed in the experimental studies have built up an understanding on textile behaviour, in respect to selected design variables and heat, defining a base framework to further research textiles' temporal colour and shape as a physical and immaterial system in interaction with light. Moreover, the studies have also raised new questions for the design research.

Reflection has evolved considering diverse aspects of textile dynamic qualities. Dynamic colour and shape changes are not familiar behaviours in textiles and relationships, for example, pace of changes being perceived as slow or fast does not involve previous expectations, such as tree leaves colour change during autumn and day and night light cycles. Furthermore, during the experiments analysis it was found crucial to discuss dynamic qualities considering different intensity levels of change, meaning if the textile changes were perceived as obvious or if they were subtle. The understanding of the importance of these expressions of change in how textile behaviour is perceived, has raised diverse questions:

What textile qualities may define a subtle or evident change? What pace of change the textiles should perform at to be perceived as subtle? Intensity levels of change are just associated with the speed or duration of change? How is the scale of textile behaviour interferes if the change is perceived as evident or almost camouflaged? How can the movement of different textile morphologies address different perception, even performing at the same pace? How can the relationship between textile and dynamic qualities amplify or reduce the intensity levels of change?

With the objective to further research textile behaviour and address the research questions, two research prototypes were developed. The objective was to explore and discuss design possibilities of textile colour and shape dynamic qualities with different intensity levels of change and to study textile and light interaction. Previous to the prototypes development, an experimental study focused on textiles and light was conducted.

7.3 Exploring textiles and light

A series of exercises on textiles and light were developed as a sketching process, an early ideation phase of the research prototypes that explored both fixed and dynamic relationships through physical samples. The main objective was to give insight into *Dynamic Light Filters* qualities.

7.3.1 Textile and light transmittance

Textile morphologies based on origami tessellation techniques involve design decisions that independently of the dynamic behaviour, draw different expressive and structural possibilities. Despite the limitless folding techniques and patterns, considerations must be taken into account on how they are materialized. In this research, decisions on textile substrate construction were particularly articulated with the parameters of smart materials integration. However, other folding aspects were explored in respect to the surface stiffness and creasing characteristics.

Textile stiffness can be varied to redefine origami textile expressive and structural qualities. Figure 102 shows a selection of samples screen-printed with different stiffness agents, folded into a waterbomb pattern and hung in a vertical plane. The first image on the left shows the textile without treatment and the remaining images demonstrate possibilities of how textile stiffness can affect their structural characteristics. In the second sample, there was an evident textile weight increase and low stiffness improvement. The textile held up better the folding structure than the sample without treatment, while presenting a rubber touch. In the third and fourth samples, greater stiffness was conferred to the textile, maintaining the more folded morphology, with a more stable structure in the fourth sample, although the touch was rough.

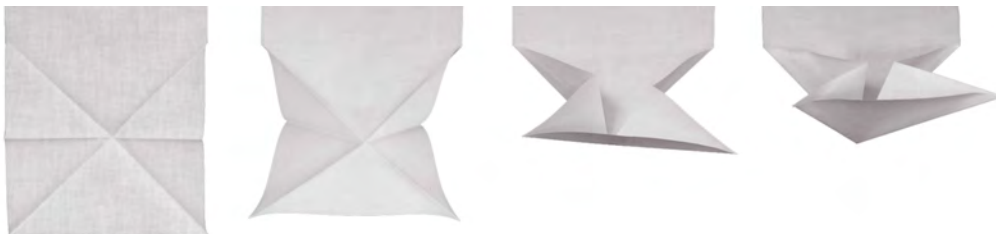


Figure 102. Textile stiffness variation in textile origami.

Varying the applied agents' concentration, a scale between soft and stiff characteristics can be explored to impart textiles' different qualities. In textile origamis with high dimensions, stiffness is a critical variable as the substrate weight significantly affects the morphologies, thus benefiting of increased structural properties.

Folding processes with textiles can be developed through different techniques such as manual folding with iron creasing; oven pleating with the textile in between two paper sheets previously folded; machine-based pleating processes and sew folding, a technique developed by Rutzky and Palmer (2011) for origami tessellations where similarly to smocking processes, a pattern of dots is sewed and knots are tied to define

common points of the textile folded morphology. With these techniques and according to the heat and pressure applied, crease characteristics can vary.

In combination with the textile stiffness properties, decisions concerning the more or less sharp creases influence the textiles and light transmittance expressions. Figure 103 presents two squaretwist samples placed above a light box. The textile on the left was ironed, attaining a flat effect and a sharp definition of the geometric light transmittance areas with different layers number. The origami on the right was developed by sew folding without creasing, showing volume in the pile-up layers' areas and rounded edges. In this sample, the layers' distance enables light diffusion in between them, changing how the play of light and shades reveal the textile morphology.

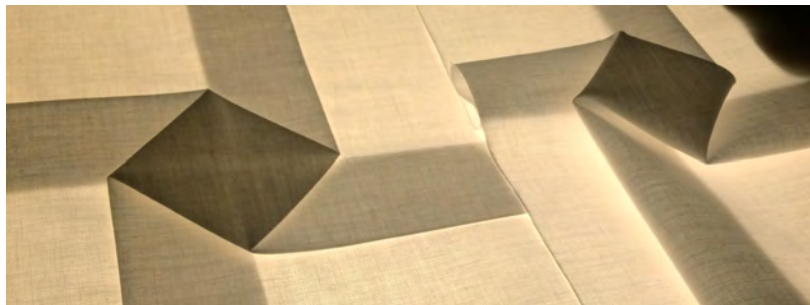


Figure 103. Textile origami with and without creases.

Origami textiles were also explored in respect to changes in light source placement and direction. A squaretwist flat sample was used with the backside turned to the viewer, omitting the central twisted square in the absence of light behind it. Figure 104 shows how the textile morphology is revealed without light transmittance and when light behind it is switched on. In the centre image, diffused light was used and textile geometric areas with the same layer number attained homogeneous shades. In the right image, the sample was illuminated with side light, placed in the sample top right and pointing to its centre. The textile layers present slight thicknesses differences, which were emphasized in side light by the edges luminance. Lighting decisions have composed a pattern of geometric figures and lines, also showing a great variation within darker and brighter nuances. Light placement and direction are design variables that can transform the expressions of textile light transmittance patterns.



Figure 104. Light transmittance patterns.

Artificial light source and placement were defined to be fixed parameters in the research prototypes. A set of samples was developed with the objective to create thin structures that could be placed behind the smart textile and be devised in any shape. Figure 105 shows three lighting alternatives produced, recorded with a red squarewrist textile above them. One structure used LED modules set on a rigid base with a diffusion foil in between the LEDs and the textile (left image). Given the textile proximity with the LEDs (2cm) and their light intensity, a spotty lighting effect was still perceived. LED stripes were set in the laterals of a rigid frame attaining a homogeneous lighting, with a good rendering of the textile morphology (centre image). A woven sample integrating side emitting plastic optical fibres (POFs) was also developed and tested (right image), demonstrating very low light intensity, only visible in the textile area of the light-emitting sources. LED stripes option was selected.

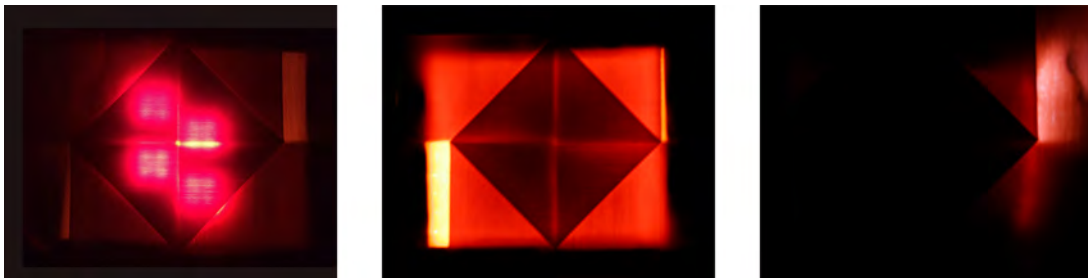


Figure 105. Squarewrist textile above three light structures: LEDs module (left), LEDs stripe (centre) and woven POFs (right).

7.3.2 Colour, shape and light

Exercises on colour, shape and light were developed with the objective to analyse textile behaviour in light transmittance and the dynamic effect on light luminosities and tones. In parallel, textile chromic and movement sequences were explored, considering dynamic possibilities with different intensity levels of change, varying the electrical activation parameters.

As an inherent condition of visual perception, light influences how we perceive and experience our surroundings, materials' textures, shapes, colours, etc. Textiles dynamic behaviour can transform light that passes through them and light can also transforms how textile and textile behaviour are perceived. Photos of the textile squaretwist screen-printed with TC red (sample Y) illustrate how light reveals the sample colours and morphology, with and without light transmittance (Figure 106).

In the two lighting conditions, the textile coral nuance observed on the left image is transformed in light transmittance, depending on the layer number of the textile structure. Textile brightest areas have just one textile layer, increasing colour saturation and decreasing colour lightness along areas in higher number layers. In result, pile-up textile layers enabled to create strong and dark red expressions, using relatively low pigments' concentration, suggesting the use of light and tessellation origami techniques as additional design tools to explore and create textile colours and patterns.

Furthermore, the way light transmittance reveals textile morphology is not just perceived according to layer variation. The bright horizontal and vertical lines in the central twisted square also reveal how the textile structure overlaps in the samples' backside.

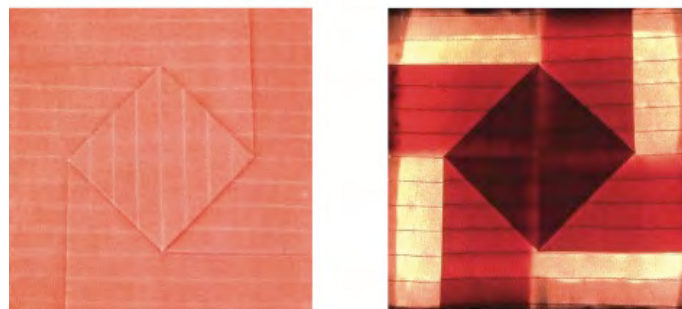


Figure 106. Sample Y without and with light transmittance.

This analysis has pointed out considerations for the prototype development process. When formulating TC pigments pastes for textiles that change colour according to predefined colour ratios, colour comparison and definition should encompass an analysis phase with samples in light transmittance. Moreover, as light transmittance parameters interfere in how colours are perceived, it was important to previously define them. Besides light source and placement, colour temperature to apply was defined at this research stage, 2700K warm white light.

Colour change behaviour in interaction with light is illustrated in Figure 107. The change from solid colour to the colour change pattern, gradually allows more light passing through, but the stronger effect is observed with complete areas becoming colourless, creating an enhanced change of light luminosities and

tones. The spotty colour change effect occurs in the darkest textile area and the layer shades reduce contrast between the colourless lines and the colourized areas. This dynamic expression is not as evident as when observed without light transmittance, where the colourized dots are more clearly defined by crisp white lines (test E).

Despite the central square being the darkest textile area, it also warms up and becomes colourless faster than the other areas, resulting in slower cool down and colour return transitions. However, the principle that lighter colours absorb less light cannot be directly applied in this event, since the number of textile layers also affects light absorption, as the 4th image in Figure 107 illustrates. The relationships between colour, shape and light are paramount in this research where textile colour and shape change are not explored as just two independent behaviours but also how one affects another and enables to extend textile and lighting dynamic qualities and expressive possibilities.



Figure 107. Colour change (1st to 3rd image) and colour return (3rd to 5th image) in light transmittance.

Exercises in colour and shape change with samples in light transmittance explored lighting variations and also activation sequences. The experiments conducted took into account the observations and findings attained in 7.2 section and projected to gain further understanding of dynamic possibilities through patterns of change.

The concept of pattern in textile design comprises of structural organization of imagery or motifs through repetition, which can be regular, such as straight, half drop and mirror, or irregular (Clarke, 2011). Whereas this description is associated to static visual representations, pattern and sense of rhythm evolved through repetitions are also familiar concepts in dynamic events, for example patterns of sounds, movements and cadence of spoken words (Bradley, 2012). Exploring patterns of change in textile behaviour, the experiments were developed through the repetition of activation and pause cycles with varied durations and electrical current values, to create activation sequences.

In these exercises, the patterns of change defined the patterns of activation considering that activation and pause durations were not previously established, rather they depended on the objectives of each

experiment. For example, a colour change exercise has studied the possibility to create subtle variations within the dots' diameter. After defining the electrical current value, based on the previous results (7.2 section), power was switched on and off according to the textile chromic behaviour. In addition, some exercises involved the variation of the electrical current value, with the objective to study different rhythms of change during the same transition – between one state to another – a possibility previously discussed in test C. With a focus on real-time observation of textile behaviour, a video record was kept, but a thermal record was not.

The experimental phase encompassed a comprehensive number of tests, since each exercise included several trial and error attempts. The systematic practice was crucial to develop a better understanding of the possibilities and limitations of thermo-responsive behaviour and to explore the relationship between activation parameters through patterns and sequences towards specific dynamic qualities.

The frames presented in Figure 108 illustrate selected activation phases with colour change. The first and second frames' rows respect to sections of the exercises on varying the dots' diameter. The discreet changes of colour and light required particular attention and tests to select the phase of the dots appearance to switch the power supply off, as in this area the colourless transitions carry on after the activation is stopped. In the first row, 36'' details the moment that power was switched off and until 42'' the colourless area expanded in the central square and colour return occurred in the remaining areas, being faster where the textile structure has just one layer. These changes garnered attention for how one activation decision can unfold two opposite colour transitions, enabled though the textile morphology.

The second row depicts the changes through repeated activation patterns that are observed particularly when low electrical current values are selected. Differences in textile temperature do not occur merely according to the layer number area, as the centre of the twisted square reveals temperature differences, exhibiting small dots that start to blur into colourless areas and the dots near the square perimeter are larger. These two examples demonstrate that exploring subtle textile dynamic expressions can embody intricate performances, which are expressed in a subtle way.

The third row of Figure 108 presents a section of an exercise focused on creating more intense dynamic expression. Sequential changes between colourless and colour return around the twisted square attained the effect intended; as more light passes through less textile layers, colour change in these areas captured greater light variation. Furthermore, these transitions also displayed a pace pattern through sequential activation, fast on heating and slow on cooling, creating a sense of rhythm in the changes. The paces'

differences are illustrated through the textile behaviour frames with 10'' interval each, showing greater changes on heating (from the 1st to the 3rd image) and lower changes on cooling (from the 3rd to the 5th image).

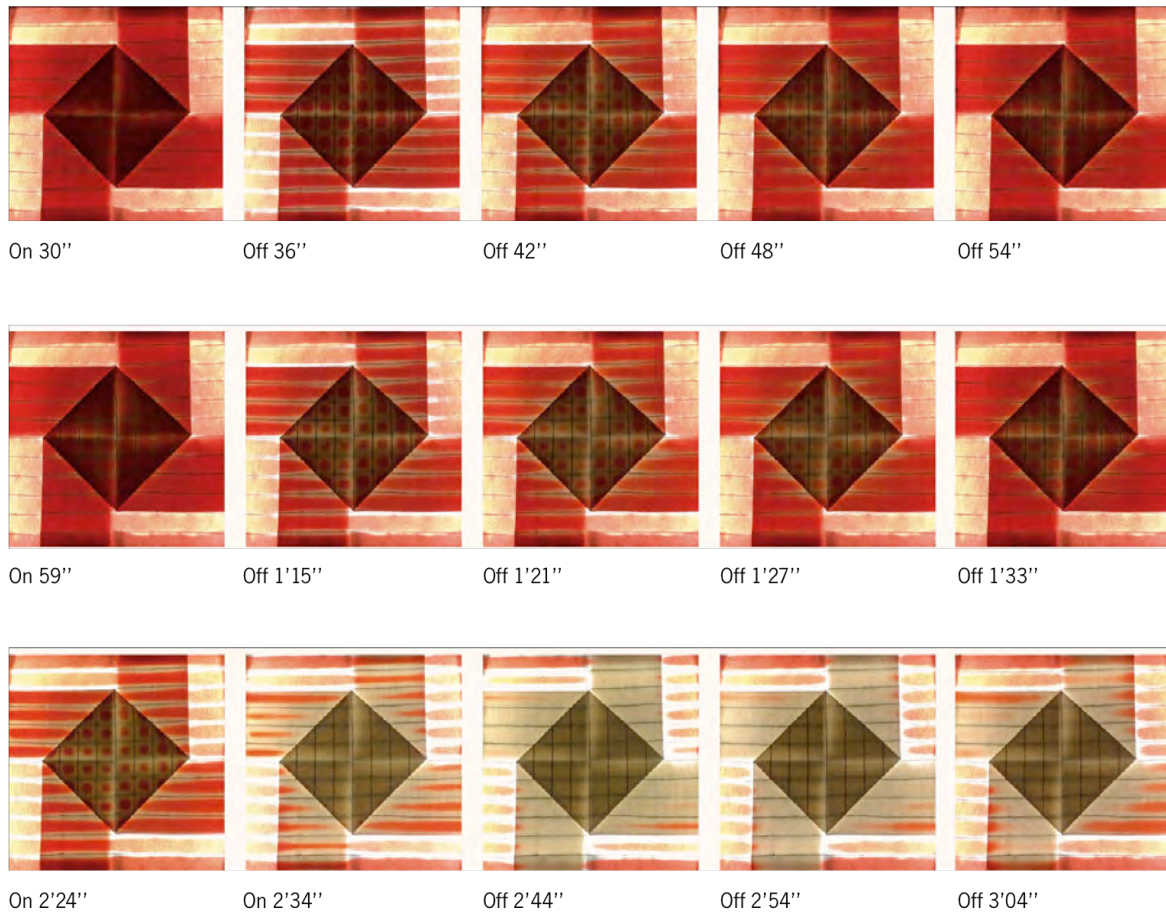


Figure 108. Frames of colour change sequences.

Selected sections of shape change sequences are presented in Figure 109. Images in the first row respect to experiments of movement continuity with textile changes displayed after power being switched off. The frames present the textile folding up at 4'', the cooling down with a slow opening movement at 5'', and the activation of the fold down also at 5''. Variations between the activation patterns repeated allowed the changing of paces between fold up and fold down, being: faster/slower; slower/faster; slower/slower; faster/faster. Second row images show a section of the faster/ faster experiment.

Faster transitions of the two movements did not encompass activation pauses, either fold up or fold down were in activation stages. High electrical current was selected and through continuous activation patterns of 2'' or 1'', the textile started to display decreasing ability to change shape, given the high temperatures in both Nitinol groups. Whereas this experiment reflects textile behaviour limitations, it also adds an expressive possibility to design shape changes that vary from higher amplitudes to lower. To invert these movement

transformations, from lower amplitudes to higher, activation pauses were required for the textile cool down, thus increasing the paces of change.

All shape change experiments illustrated in Figure 109 were conducted with the textile sample in the vertical position, but the squaretwist angles are different. The third row experiment was conducted with the textile dynamic tabs diagonal to the horizontal plane. Besides analysing how this placement parameter interferes in shape change, the possibility to reverse one movement before attaining the final state was explored. Lower row images show the textile folding up (32'' to 35''), starting the fold down movement (35'' to 43'') and reversing again to fold up (43'' to 45''), finally performing the complete fold down (45'' to 58'').

This experiment describes a different method to create a movement transformation similar to the one presented in the second row, but with different paces and greater control to define if the textile performs larger or lower movements, once textile temperatures are lower. Textile morphology displayed a small effect of the squaretwist direction in shape change with the lower textile tab folding up slightly less than the upper tab and reversely for fold down. The influence of the textile direction in this sample was discreet, but with larger and heavier samples, an increased effect is expected.

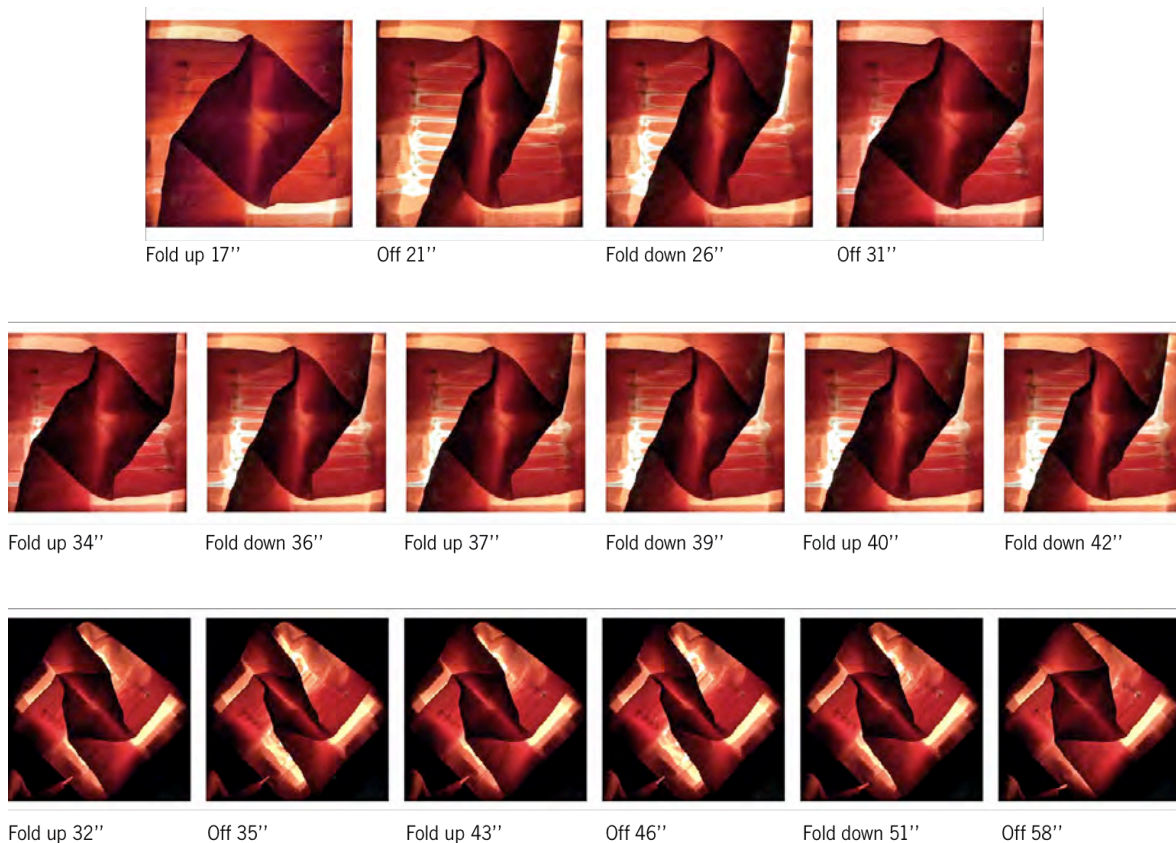


Figure 109. Frames of shape change sequences.

Interaction of textile shape change and light is not as distinct as with colour change. Subtle lighting transformations are perceived in the sequences illustration mostly by the chromic effect resultant from the Nitinol activation. To research textiles behaviour with colour and shape change in the same structure, selection of activation temperatures of each material and their thermal variation has to consider not just one behaviour, but also the influence that the activation of one behaviour can have on the other.

The activation temperatures of the materials selected in this research were 27°C for TC pigments and 30°C As – 45°C Af for Nitinol alloys. Shape change cannot be triggered without colour change, unless the TC screen-printed pattern avoids the Nitinol integration areas, using just conventional pigments. In this case, pattern definition should also consider textile thermal expansion that occurs during shape change activation.

TC trigger temperature is slightly lower than the SMAs selected. Tests conducted with a base sample that integrates Nitinol alloys and conductive threads in the substrate at 5 mm distance each, showed that when power is supplied to the conductive threads, textile temperature increase is able to trigger shape changes. Defining the conductive threads' maximum temperature as 50°C, through textile thermal expansion the SMAs temperature did not attained the 45°C required to perform complete shape change and therefore, displayed a small movement and incomplete shape change. The time to heat up the Nitinol alloys depended on the electrical current values and time of activation.

The development of colour and shape change study samples involved a phase of exploring colour ratios and diverse textile morphologies. Experiments included textile samples that did not integrate Nitinol alloys, movement was tested manually enabling to develop less time-consuming exercises on dynamic light filters possibilities. Figure 110 presents a study sample developed to explore dynamic light expressions and shape change paces through manual transformations. As a method to experiment and generate alternatives, manual shape change was crucial to test and define morphologies and scale of the smart textiles to develop.

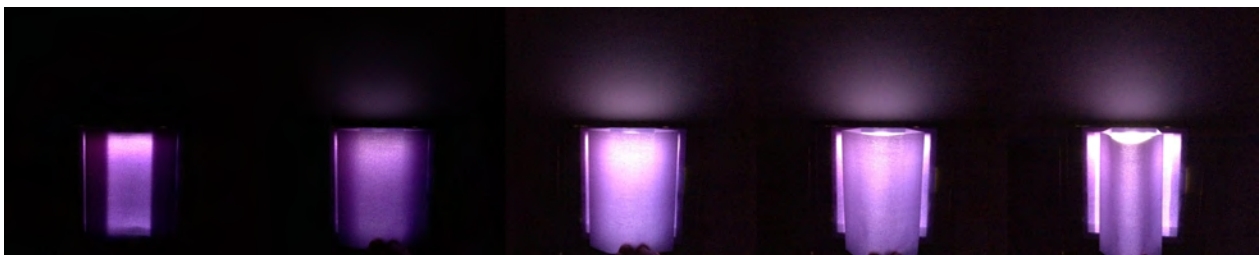


Figure 110. Exploring dynamic light and movement through manual shape change.

7.3.3 Discussion

The exercises displayed and discussed in this section represent a preliminary phase of the prototype development research. Presented in the following sections, the prototypes were not conceived as finished products, they were physical tools to research textile chromic and morphologic behaviour as a physical and dynamic system in interaction with light.

The experimental studies developed have presented challenges during photo and video recording. To document dynamic light, camera settings should be constant. In the tests photo recorded, light intensity and tone differences intended to capture have required several attempts to find the parameters that could document the luminous interval. In video, manual settings are not a common parameter in regular cameras, which automatically adjusts the lighting settings. This challenge highlighted the importance of a professional video camera for a more accurate documentation of the research prototypes.

7.4 Research prototype I: Narratives of Winter Daylight

Narratives of Winter Daylight is a research prototype inspired by the dynamic qualities of natural light. Day and night commonly present different rates and changing patterns of light intensities, colours tones and direction, depending on the geographic location, season and weather conditions. For this research, one winter day was observed and photos were recorded each hour from 6 a.m. to 6 p.m. Figure 111 presents the photo record conducted on 31.12.2015 at latitude: 41.178084, longitude: -8.66061, with equal camera settings for a comparison between luminosities.

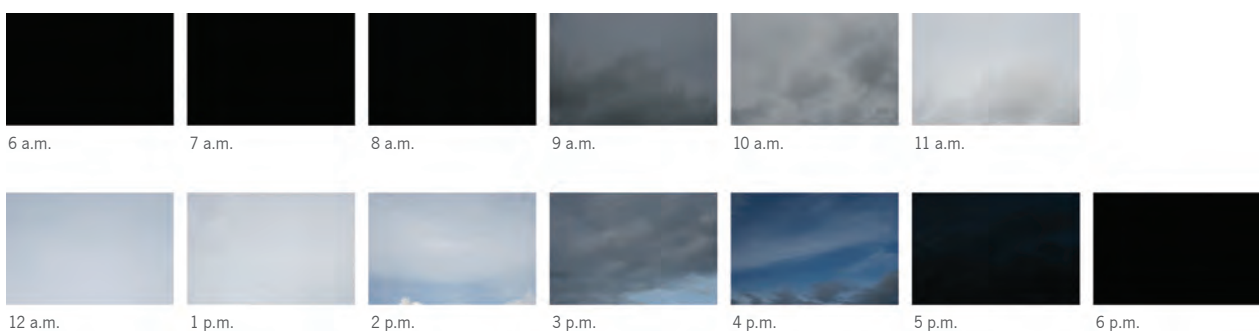


Figure 111. Photos record from 6 a.m. to 6 p.m.

Perception of natural light variations involves a relation between the luminosities observed with established expectations and rates of change (Cuttle, 2015). Commonly, subtle light changes are expected during the day, while more obvious changes are prevalent in early morning and late afternoon. Rhythms of light

variation can allow an experience of the passing of time, perceived not only by the changes of the light parameters but also in respect to the duration of the events in time (Le Poidevin, 2015).

During the day observed, higher luminosity levels were perceived from 11 a.m. to 2 p.m. with predominant light greys and light blues. From 9 to 10 a.m. the sky tones varied between cold greys and from 3 to 4 p.m. it changed between blues. Before and after the time periods described, light intensities were reduced regarding the camera fixed parameters, resulting in dark images. Camera settings were tested in the previous days to the record presented, but a higher range of light intensities was not attained without blurring the photos in the brighter day periods. By direct observation, a cold greyish dark blue was observed in early morning and in late afternoon a subtle violet nuance in a dark blue.

Along the paces of light variations illustrated through the photos, faster from 8 to 9 a.m. and from 4 to 5 p.m., clouds also created changes during the brighter periods. Although the luminosity changes were low, compared to the overall day and night cycle, obvious changes were created, occurring in shorter time periods. The relationship between patterns and expressions of light change with perceived luminosities and tones, set up a basis to define the prototype colour change palette and shape changing morphologies, having also delineated dynamic qualities to explore in the prototype behaviour. Initially, the photos were set in one row and related luminosities and colours were interpreted and grouped according to similarities between time intervals (Figure 112). Symbols '-' and '+' were used to establish a hierarchy of luminosities.



Figure 112. Conceptual bar of luminosities and colours.

With the objective to explore intensity levels of change according to colour differences, textile colour change defined comprises of variations between similar colours, different blue tones and different colours. The colour change ratio defined for the prototype was from similar to different upon heating, with a dark blue colour in the cold state changing to the range of colours presented in the bar, when above the activation temperature of the TC pigments handled. Furthermore, it was intended that shape change activation would not change the textile colour and a screen-printing paste that combined just conventional pigments was defined for the Nitinol integration areas.

To study how different scales of shape change interfere in the dynamic expressions, textile transformation aimed to create volume variations in individual textile areas with different dimensions. Dynamic morphologies were explored through folding techniques in particular through origami pleats, consisting of parallel fold lines, alternating valley and mountain creases, or the inverse (Jackson, 2011).

The prototype morphology presents two piled up textile layers. The front layer combines six pleat units aligned horizontally in the textile substrate and the geometry defined for each unit consists of a mirrored sequence of two vertical pleat folds (Figure 113 left). Attached to a plain textile layer (back layer), the folded geometry creates areas with a variation of textile layer number and distance, through the fold up and fold down movements of the pleats (Figure 113 right). Width proportion of each pleat was defined according to the luminosity and colour similarities set framework.

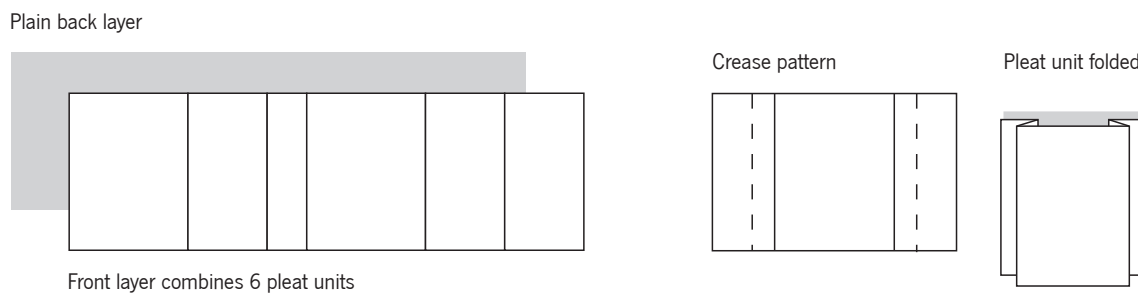


Figure 113. Prototype layout folded (left), pleat fold crease pattern and pleat unit folded (right).

Textile morphology and colours were tested in light transmittance with study samples. Shape change with textile pleat units in light transmittance included analysis through manual transformations, as depicted in Figure 110 of the previous section. The prototype intended to explore calm and smooth transitions of textile colour and shape states, to transform light transmittance through vary dynamic expressions. It was defined that each pleat unit could be individually activated for fold up and fold down and display colour change in the front and back layers. Thus, the six pleats' prototype totalizes 24 activation channels.

In addition, the dynamic light filter behaviour focused on changes in local lighting, proposing a closer spatial relationship with the textile. The prototype scale was defined according to the possibility to observe the changes in proximity and dimensions when folded were approximately 70 x 24 cm.

The integration processes of smart and conductive materials in textile substrates previously researched and discussed in chapters 4, 5 and 6 were implemented in the prototype development. A description of the processes conducted is summarized as follows:

- a) Definition of textile shapes and respective weaving plan for Nitinol wires integration; definition of Nitinol geometries encompassing two sets of Nitinol wires (one group to perform fold up and another for fold down); drawing and production of dies; optimization of the annealing parameters followed by Nitinol heat treatment; and sandblasting of Nitinol wires' ends.
- b) Weaving of the textile substrate in a plain weave structure with cotton yarns in the warp and polyester yarns in the weft, where conductive threads were woven at every 1,0 cm and the Nitinol alloys were integrated at every 2,0 cm, with 0,5 cm distance of the conductive threads.
- c) Formulation of screen-printing paste recipes given a pattern colour, through a database created with colourimetric properties of the TC and conventional pigments handled; elaboration of the pastes; screen-printing of the textile substrate with TC pastes and after with a stiffness agent (according to methods described in 6.4.1) in front areas of each pleat; and thermo-fixing.
- d) Connection of the conductive materials with four circuits for each pleat unit – two series circuits of connected conductive threads, one for colour change in the front layer and another for the back; and two series circuits of Nitinol segments linked according to fold up and fold down groups.
- e) Application of an electrical insulating agent; folding of the prototype and setting up in a light box, built with two strips of warm white LEDS (2700K) in the box inner top and bottom;
- f) Definition and manufacturing of the electrical circuit to program the textile activation and programming.

7.4.1 Textile behaviour and light

The prototype dynamic behaviour was analysed with the objective of studying relationships between temporal forms – colour, shape and light – and the expressions of change. A first phase of activation tests has examined the resistive heating properties of the conductive channels one at a time, using a variable power supply, a multimeter and a thermal camera. After, a temporary electrical circuit was developed, linking the 24 conductive channels to an Arduino microcontroller, so the activation could be performed and programmed with more than one heating element at a time. Finally, the prototype was placed on the wall and the analysis included direct observations, photo and video records.

Figure 114 presents the prototype in three different states. From left to right images, the textile pleats change from fold down to fold up in colourized state and then decolorized in the fold up morphology. Through the simultaneously activation of all pleats, colour change created higher light transmittance

variation than shape change, observed by the overall luminosities and tones in the textile surface and the light falling on the wall.

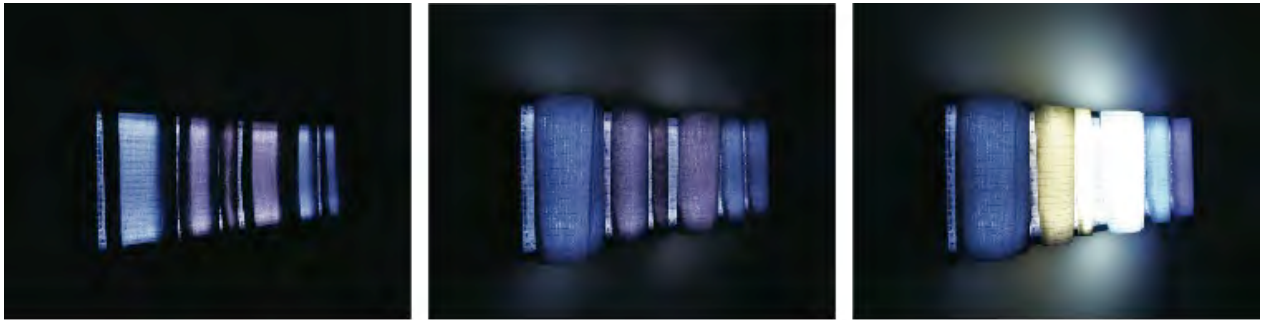


Figure 114. Fold down to fold up in colourized state (1st to 2nd image) and colour change in fold up state (2nd to 3rd image).

With the fold down activation, light reflection on the wall is imperceptible. The textile layers are near and light transmittance is low in comparison to the morphologies attained with fold up, where the pleats unfold and create ‘open pockets’ (Figure 115 right images). During this change, pleat units with larger width (Figure 115 left images, 1st and 4th pleats) attained a larger distance between layers, achieving higher luminosity variation and blur size of light projection on the wall than units with lower widths.

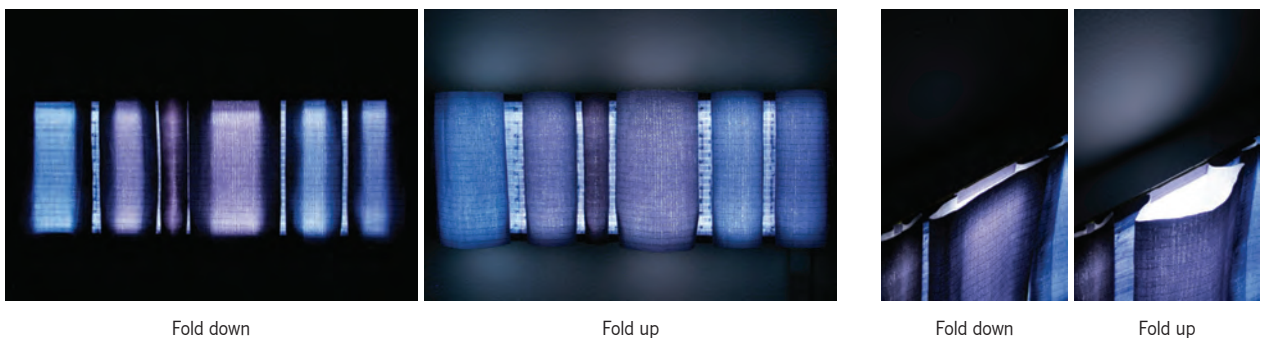


Figure 115. Prototype fold down and fold up activation.

When the prototype was observed at different viewing angles, shape change expressions also differed. This relationship was analysed through Kleins’ shape transformation types (Nefs, 2008). When observed at a frontal view, change of shape produced through the pleats fold down and fold up can be defined as dilation, a similarity change where shape angles and distance ratios are maintained. The textile movement was perceived as very subtle, even at the faster pace with the larger width pleats. It was light transmittance variation that appeared to create a noticeable dynamic expression.

At a side or perspective view, the movement was clearer. The shape transformation was observed with different distance ratios – strain transformation – enabling a greater awareness of the shape change as well as the relation between the textile and light variation.

The importance of textile movement in the intensity levels of change is demonstrated through different viewing angles. This relation identifies morphology, transformation type and positioning as design variables in the dynamic qualities and expressions of textile behaviour.

Through the shape change analysis, it was observed that folded states attained lower angles than the memorized geometries of the Nitinol alloys. Textile substrate and morphology have constrained the Shape Memory Effect (SME), in particular with the lower width pleat, where movements were barely perceived although the Nitinol wires were above their activation temperature, as confirmed with a thermal camera.

Fold up and fold down paces were analysed through electrical current variation. At an ambient temperature of approximately 20°C, mean values attained for each circuit were 14 seconds with 0,6 A, 10 seconds with 0,7 A, 7 seconds with 0,8 A and 5 seconds with 0,9 A. Movements performed appeared organic along the different paces. Although, as demonstrated in test F of section 7.2, the final activation phase with the lower electrical current values is barely perceived by direct observation.

For a comparison between the scale of change and different paces, a larger pleat unit was programmed to fold up more slowly than a medium pleat unit. The changes with the larger pleat were perceived to last slightly long, but the movements were calm in both pleats. The scale of change from one state to another appeared to be small for a comparison between paces of the textile morphology. Instead, consecutive cycles of fold down and fold up movements appeared to enhance the differences. Movements in the medium pleat were perceived as faster and the larger pleat accomplished slower changes but with higher movement amplitudes. The change of the movement direction added a new variable in the analysis, emphasizing the differences of the movements' qualities.

Through the sequential shape change activation, the actuators temperature increased faster in particular in the pleat activated with high current values for faster movements and few cycles were performed until an activation pause was required for cool down. Time for the Nitinol to cool down was tested. As previously discussed, the alloys temperature is not homogeneous and their cool down depends on several variables such as previous activation time, temperatures attained with the electrical current supplied and textile substrate characteristics. With the prototype activated at an ambient temperature of 20°C, values varied between 5 and 20 seconds.

The relationship of shape change and light also depended on the textile colour state and dynamic qualities of chromic behaviour. At the fold up morphology, textile colour change in all pleats is depicted in Figure 116. Light transmittance variation with the colour change effect, created a hierarchy of luminosity differences as targeted: an increase from the first to the third pleat (6 to 12 a.m.); similarities in third and fourth pleat (12 to 2 p.m.); followed a decrease until the sixth pleat (3 to 6 p.m.). Light measurements with one layer of each colour sample confirmed the observations, percentual luminosity differences varied from 13% to 76, 93, 88, 58 and 30%, in respect to the above-mentioned sequence.

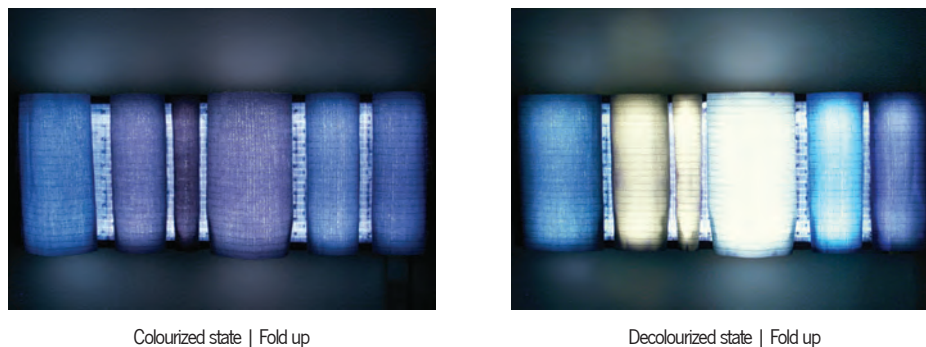


Figure 116. Prototype without and with colour change activation in fold up state (left and right, respectively).

Colour tones perceived by direct observation of textile samples without light transmittance and with the textile placed in a light box have differed (Figure 117). Colour measurements conducted below 27°C in a reflectance spectrophotometer have confirmed colour similarities. CIELAB differences attained values between 0,8 to 1,3 dE*, which can be considered reasonable for colour matching. In the light box, samples screen-printed with pastes that combined TC pigment blue (2nd, 3rd and 4th pleat units) instead of conventional pigment blue, presented a violet nuance. Paste recipe adjustments were conducted, although a subtle violet tone remained.

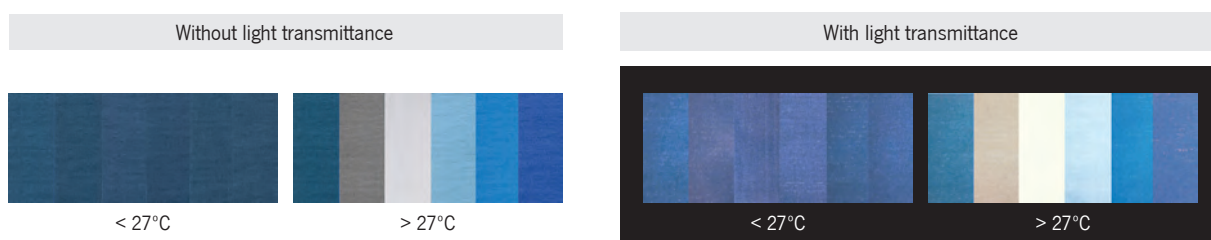


Figure 117. Colour samples below and above 27°C, without and with light transmittance.

From similar to different, colour changes varied light transmittance heterogeneously and affected the luminous relationships attained with shape change. For example, shape and light changes were more evident with pleats of larger width (1st and 4th) in colourized state (Figure 117 left image). In colourless state

it was observed that luminous changes with lighter colours pleats were more obvious, even with smaller pleats (Figure 117 right image). Reversibly, textile morphology also affected how colours were perceived. The smaller pleat (3rd) changed to white, but due to the lower textile layer distance, light shadows made it appear darker than the light blue pleat (4th), thus establishing a relation between the scale of colour change, morphology and light transmittance variations.

Paces of colour change were analysed in all pleats. At an ambient temperature of 20°C and with 1,2 A, mean values to attain full colour change in the front textile layer activation was approximately 2'30'' and 1' for colour return. Through simultaneous activation of the front and back layers the change to colourless was faster (2') and colour return slower (1'20''). The temperature inside the folded layers increased, enhancing the textile thermal expansion and, due to the vertical positioning of the prototype, the upper area of the pleat units also heated up faster than in the bottom (Figure 118). With both layers activation, time variation in heating and on cooling is emphasized when consecutive cycles are run, also changing the textile expressions in particular with less sharp definition of the colour change stripes.

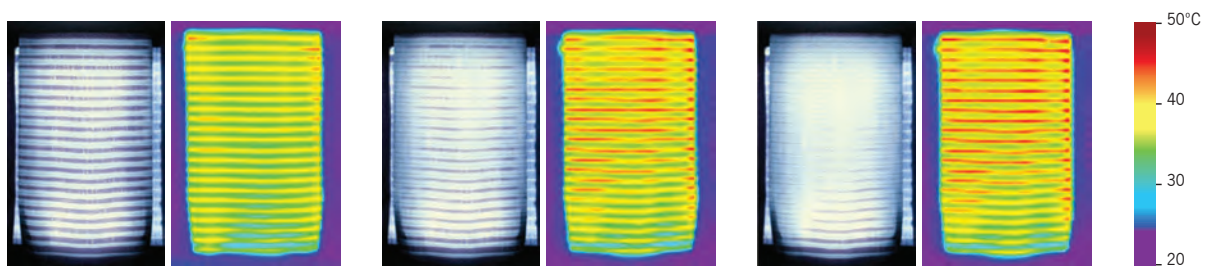


Figure 118. Photos and IR images during colour change.

The rise of temperature in between the textile layers can also interfere with shape change activation and even induce changes in the fold up and fold down Nitinol groups without power supply, assuming a morphology between states. It was observed that these changes were more evident in the upper area of the pleats, also resultant from the vertical position. Colour and shape analyses highlighted the importance of the relation between textile morphology and positioning in the dynamic qualities of thermo-responsive textiles.

Colour change in light transmittance was also investigated in respect to colour differences in the colourless state. From colorized to the striped pattern, changes between hues are not necessarily more obvious than changes between colour tones. Colour lightness appeared to have a more relevant impact in the intensity levels of how the changes were perceived. From the linear pattern to colourless areas, textile colours are

more clearly distinguished and also reflected in the tone of light on the wall, also according to textile morphology.

7.4.2 Colour, shape and light responsive environments

The prototype was presented and analysed in a spatial context, exploring colour, shape and light as dynamic variables of responsive environments. The objective was to display expressive possibilities of change through the textile behaviour and dynamic local lighting and create visual *Narratives of Winter Daylight*. Considering the day observed, the rhythms studied and programmed focused on predominant calm expressions and punctual more intense changes.

An interaction diagram was defined, establishing a relation between the spectator(s) and the dynamic behaviour of the prototype. As illustrated in Figure 119, three ultrasonic sensors were used to detect the presence of the spectators near the prototype. The sensors were connected to a microcontroller and transmitter to communicate via wireless receiver and microcontroller set connected to the prototype. According to the visitor's proximity to the textile, sensors' combination input defined a programmed sequence that activated the textile behaviour.

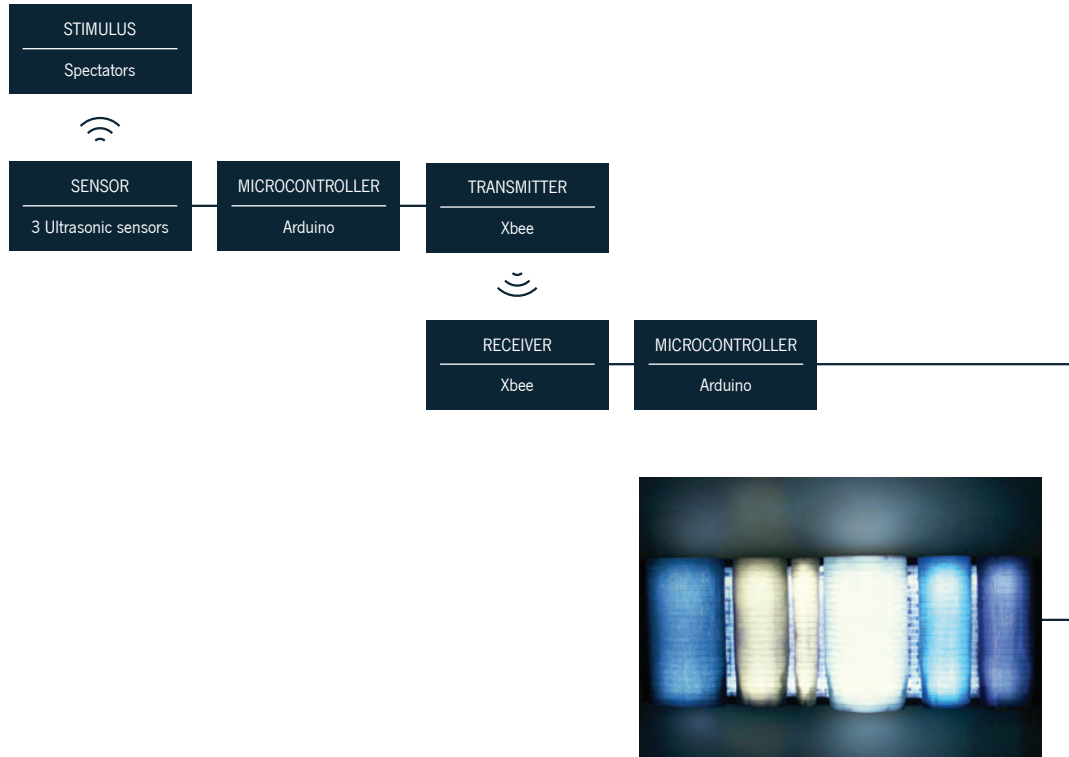


Figure 119. Interaction diagram.

The definition of activation sequences built in the previous studies conducted with the prototype and focused on textile and light dynamic qualities expressed in subtle ways. To depict the textile activation within the 24 conductive channels and guide the respective programming, a graphical setup was developed. Figure 120 presents an activation sequence setup that displays a repeated pattern of change from left to right pleats with a delay of 40'' between them. Colour change in the front layer starts in fold down state and in the last phase of the textile thermal expansion, back layer is also activated and until full colourless, the textile also folds up. On cooling, gradual colour return occurs approximately during 1' in each pleat. The defined sequence explored smooth transitions between lower and higher luminosities in each pleat and lower to higher and lower again in the pleats sequence.

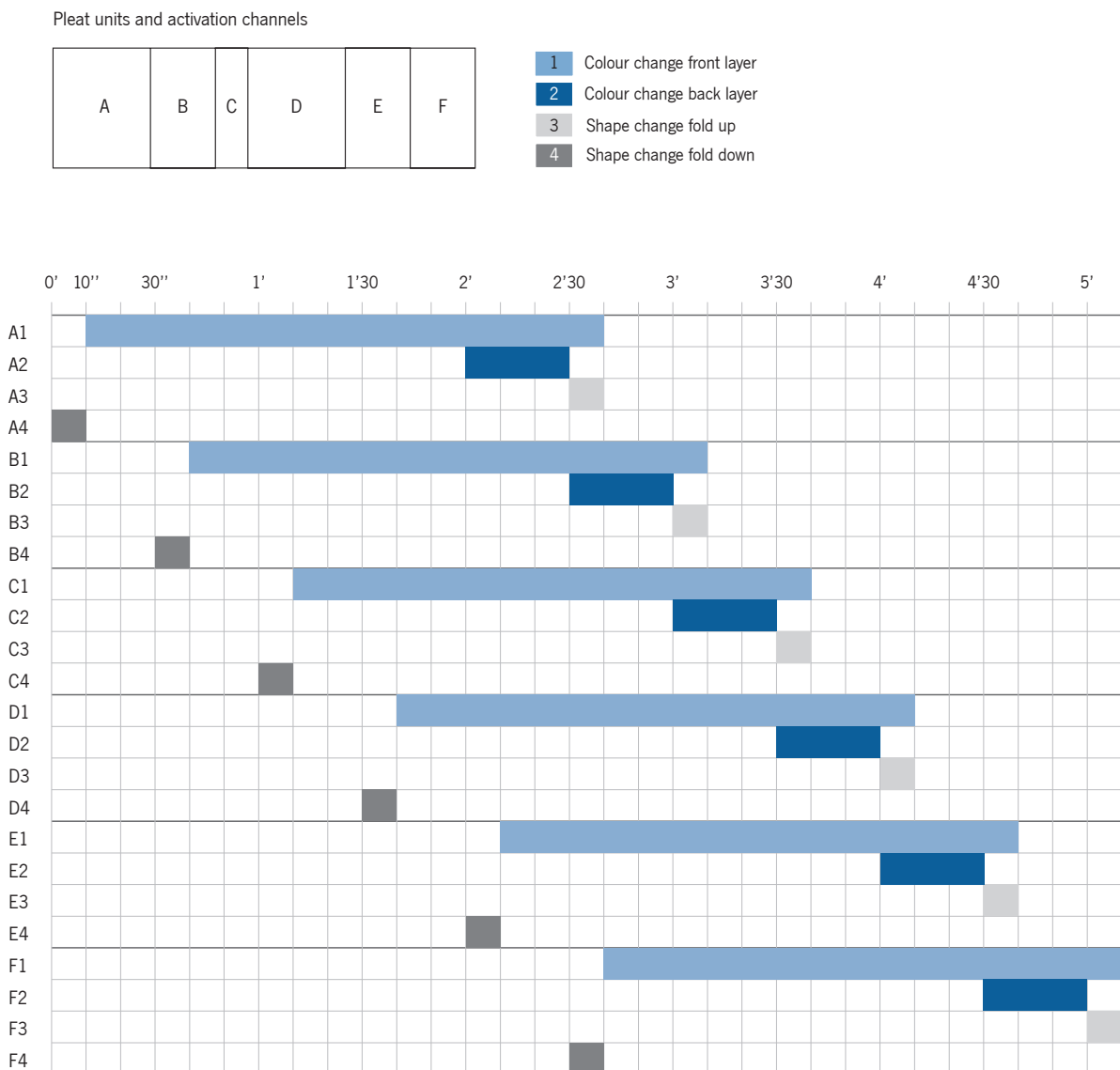


Figure 120. Activation sequence setup.

The prototype presentation took place at Smart Textiles Salon 2016 in Ghent, Belgium. The interactive and dynamic scenario built up through the prototype performance was perceived as slow and calm. Within

mostly discreet changes, colour change in pleats with lighter colours in colourless areas enabled to vary the intensity levels of the changes perception, in particular through the linear pattern of colour change, as well as light transmittance variation with larger width pleats when completing the chromic behaviour. Nevertheless, the slow paces defined have still conferred a calm expression to the more evident perceived changes.

Moreover, the active role of the visitors was also discreet. Depending on the proximity with the prototype and positioning, an activation sequence was triggered. Although, the subtle changes did not become obvious at the beginning or the end of the interaction, they appeared to gradually blur within the still phases. The organic movements and subtle rhythms defined a statement of the textile behaviour and light expressions.

Designing smart textiles in interaction with light that express subtle changes, reveal possibilities to seamlessly integrate the tangible and immaterial aspects of the smart textiles in the environment, their rhythms and contexts of use. This relation draws on the line of calm technology, a concept introduced by Mark Weiser and John Seeley Brown in 1995, which describes possibilities of information technology moving between the periphery and the centre of our attention (Weiser and Brown, 1995; Benitez, 2016). When designing textile behaviour and light, dynamic qualities of smart textiles can be explored as an integral and unobtrusive element of the environment, in which functional and expressive behaviour evolves without necessarily engaging or requiring attention.

In the *Narratives of Winter Daylight* prototype, dynamic qualities and expressions of change were explored through a textile interface with a discreet presence in the surroundings. Design decisions encompassed working with dynamic local lighting, defining the textile horizontal frame with dimensions that enabled its perception with a close spatial relationship and the textile morphologies and colour ratio. With the objective further study the relation of the textile interface definition and design possibilities of intensity levels of change, a second prototype was developed.

7.5 Research prototype II: Dialogues

With the *Dialogues* prototype, dynamic qualities and expressions of change were explored through a textile interface with an obvious presence in the surroundings. Textile colour and shape were studied with the objective to transform ambient light. A natural light and colour phenomena commonly observed in the northern and southern hemispheres have inspired the prototype development: the polar lights, also named auroras.

Aurora borealis (north) or aurora australis (south) are night skylights that display colour and pattern changes, as a result of chemical and physical interactions in the atmosphere. Visual manifestations of the auroras involve possibilities to vary between forms, such as 'curtains' or 'arcs', display intense or dim luminosities, perform rapid modification or steady glows and change between different colours, according to the altitude that the interactions occur. From lower to higher altitudes, light colours are blue and violets; greens; and ruby reds (Yahnin et al., 1997; Hall et al., 2002).

The parameters identified in the colourful skylight phenomena established a framework to explore textile colour and shape behaviour in interaction with light. Considerations included the relation of colours with altitude and changes of form within the colour pattern; scale, direction and rhythms of change within varying light intensities.

Focusing on dynamic ambient light in interior spaces, textile morphology studies included folded surface pattern and the layout of the textile structure. The textile layout explored connections between scale, positioning and viewpoint possibilities. The prototype was defined with three textile modules that compose a geometric configuration in two adjacent vertical planes of an interior space and one horizontal plane (Figure 121).

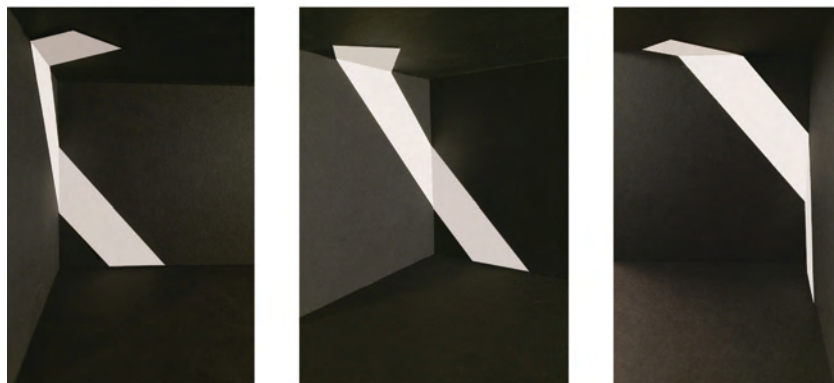


Figure 121. Prototype geometric layout.

Each textile module was defined with an intricate pattern of squaretwists. The selection of this origami tessellation base-fold took into consideration the morphology transformation type through the direction shift of the square tabs folding up and down; the colour effects created through the textile layered morphology in light transmittance. Figure 122 depicts the origami morphology in folded state with the three modules aligned, distinguished through the thicker lines. From the prototype bottom to top, squaretwist dimensions decrease and the direction of the folded pattern varies among modules 1 and 2 (M1 and M2), as depicted through the grey shades. The shades also define the squaretwist tabs that perform shape change. M1 and M2 will be placed in vertical positioning and module 3 (M3) in horizontal.

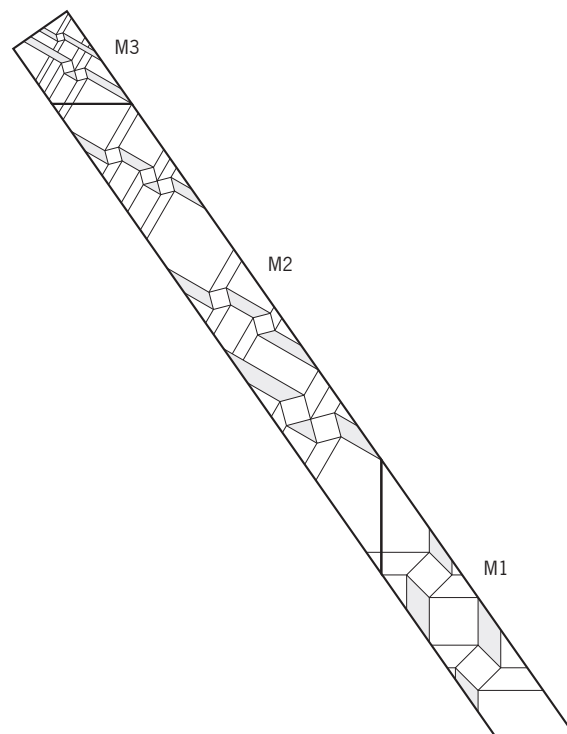


Figure 122. Prototype folded pattern.

Nitinol alloys integration in the woven structure and respective geometries were defined through the origami crease pattern of each module and respective shape change set. Figure 123 presents M3 crease pattern with Nitinol fold up group depicted with light green lines and fold down group with dark green. To apply the origami crease pattern in the weaving plan, particular attention was required in respect to the textile shape change direction. Considering the Nitinol alloys integration in the weft, the axis of the moving tabs required to be in vertical position in the weaving plan and given the loom 150 cm width, the rotated crease pattern had to fit within this dimension.

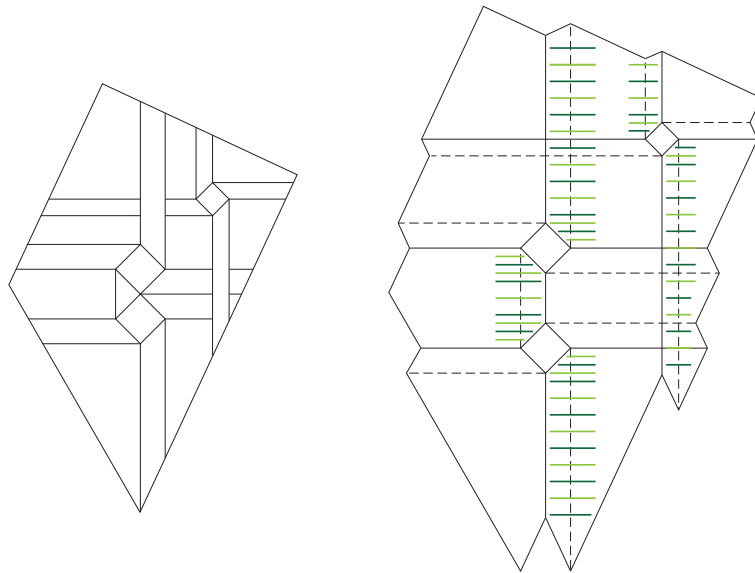


Figure 123. M3 folded pattern (left) and crease pattern (right).

With the objective to explore dynamic coloured light and changes through luminous nuances, textile colour ratio defined was from different to similar with temperature increase. The relation of auroras' colours according to altitude inspired the studies of textile colour and screen printed pattern. Colour experiments included analysis of folded samples in light transmittance. Figure 124 displays a set of study samples developed comprising violet, blue, green and red colours below the TC pigment activation temperature (left image) and yellow after heating (right image).

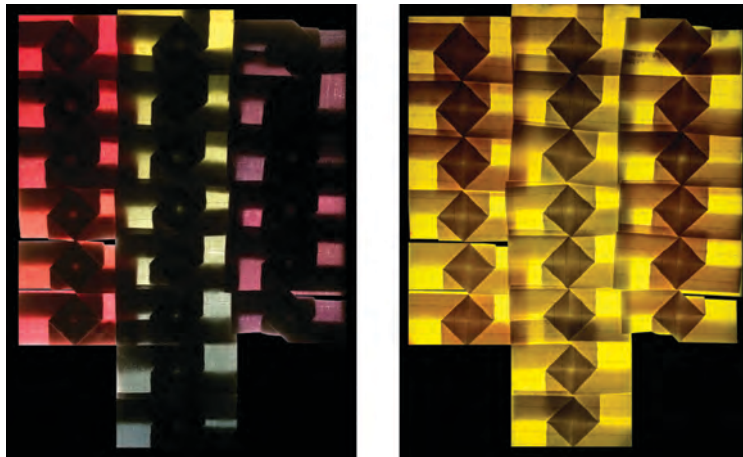


Figure 124. Colour studies with folded samples in light transmittance, below and above 27°C (left and right, respectively).

The screen-printing pattern was defined with the surface in unfolded state, where geometric areas of solid colour were delineated along the flat structure. When the surface was folded, the origami morphology created a new geometric composition that presented areas of piled up layers with more than one colour, thus slightly changing tones when revealed in light transmittance.

Figure 125 presents a section of the textile pattern unfolded (left), folded (centre) and as revealed in light transmittance (right).



Figure 125. Colour and pattern studies.

The prototype activation was defined with 45 channels. For shape change, 2 squaretwist pairs are activated simultaneously and the remaining 8 squaretwist individually, totalizing 20 channels (10 fold up and 10 fold down). For colour change, the conductive threads were connected in series into 25 circuits. In some areas, the connections were carried out in consecutive threads and other areas with intercalated threads. This decision took in consideration the possibility to create gradual colour and pattern change transitions, starting with the 2 cm distance lines and activating the conductive threads in the middle, to display colour change lines with different thicknesses.

The prototype production is summarized as follows:

- a) Definition of textile shapes and respective weaving plan for Nitinol wires integration; definition of Nitinol geometries; drawing and production of dies; optimization of the annealing parameters followed by Nitinol heat treatment; and sandblasting of Nitinol wires' ends.
- b) Weaving of the textile substrate in a plain weave structure with cotton yarns in the warp and polyester yarns in the weft, with Nitinol integration according to the crease pattern defined for each module.
- c) Elaboration of the pastes, according to the colour samples selected with constant concentration of the conventional pigment yellow (1,5%); screen-printing of the textile substrate and thermo-fixing.
- d) Connection of the conductive materials according to the defined layout for colour and shape change.
- e) Application of an electrical insulating agent; folding of the prototype and setting up in a light box, built with two strips of warm white LEDS (2700K) in the box inner top and bottom;
- f) Definition and manufacturing of the electrical circuit to program the textile activation and programming.

7.5.1 Textile behaviour and dynamic lighting

An initial phase of activation tests involved the individual analysis of the conductive circuits' properties and the development of an electrical circuit to program and study textile behaviour and dynamic light.

With the objective to present and analyse the prototype in a spatial context, a contact was established with House of Music – Porto. The House of Music produces an open house event with an invited country every year, being Great Britain in 2017. A relation between the prototype behaviour with the work of a British composer was proposed for the creation of a responsive environment. The connection between sound and visual dimensions were explored through the expressive qualities of the temporal forms.

This section presents the textile behaviour and dynamic lighting analysis conducted at House of Music. The variables proposed to explore textile and light expressions focused on colour and pattern effects, varying luminosities, scale, direction and rhythms of changes. In addition, parameters of the prototype physical context were also analysed. Figure 126 presents the prototype at a view distance with the overall appearance of the textile light transmittance through the layered morphology and colours along the printed and folded patterns.



Figure 126. *Dialogues* prototype.

In colorized state, the light transmittance pattern is built up by colours composition and folded structure, while during colour change activation, the heating lines add a geometric element to the pattern (Figure 127). In the majority of prototype surface, each conductive circuit heats up areas with more than one

colour, displaying the colour ratio from different to similar along the linear forms. Simultaneous colour change activation displayed this effect in adjacent or separated areas.

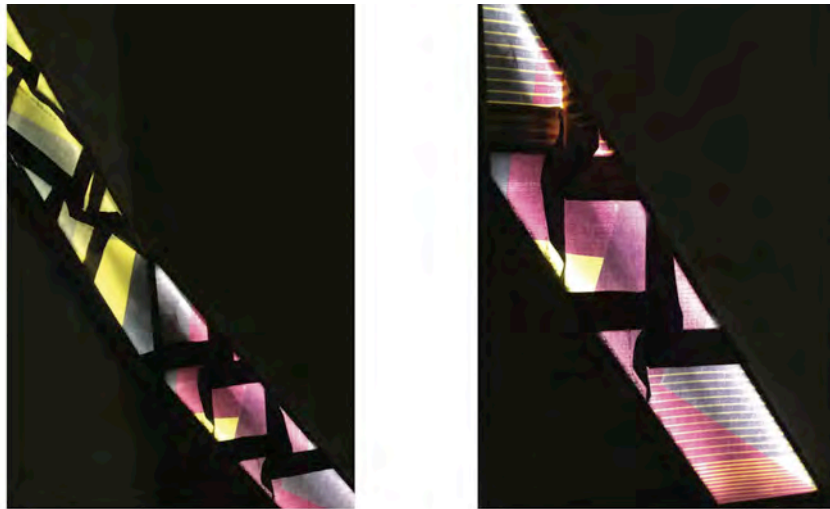


Figure 127. Prototype section in colorized state (left) and changing colour (right).

When complete colour change was attained, solid colour areas were defined with higher luminosities. Figure 128 depicts the influence of colour lightness in the intensity levels of colour change, similarities in light green and yellow areas (image bottom right) and contrast with darker greens (image top left). The transition to a lighter colour has enabled a more obvious distinction between light transmittance in the tabs, which have three pile-up layers and the squares with five. In areas with darker colours, this effect was barely perceived in particular when observed at a distance, appearing to compose a similar dark pattern (Figure 127 left image).

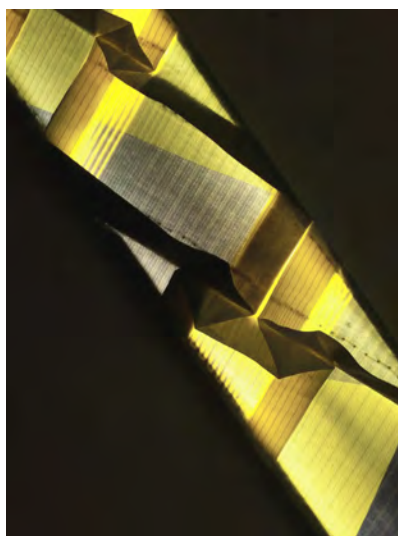


Figure 128. Colour change activation with areas with complete decolorization.

The linear pattern of colour change was also studied according to heating circuits' parameters and the prototype placement. The integration of conductive threads in the weft of the woven substrate was conducted at 1 cm distance each, whereas in some areas the connection of two series circuits was intercalated, accomplishing 2 cm distance between each linked thread. Left image of Figure 129 displays a section of the prototype with colour change stripes at the two different distances, where a squaretwist area activated with the lower distance lines being in complete colourless. In addition, the two modules of the prototype presented (M2 and M3) had the same angle rotation of the crease pattern in the weaving plan but the line direction was transformed by the modules vertical and horizontal positioning.

Right image of Figure 129 presents M1 and M2, which crease pattern had different directions and their positioning in two vertical planes also accomplishes different angles, thus affecting the geometry of the colour change stripes. As discussed in 2.4.1 section, conductive threads are mostly woven in the weft (Eichhoff et al., 2013; Stoppa and Chiolerio, 2014). Textile direction and positioning variables can be explored to design TC textiles with variations in the geometry of the colour change pattern.

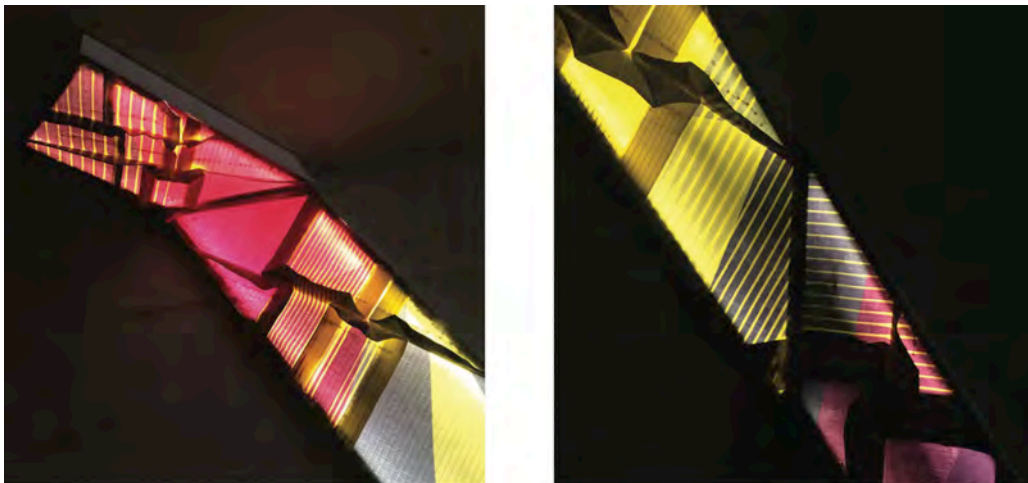


Figure 129. Colour change linear patterns.

Shape change of squaretwist morphologies was previously discussed with a light colour sample. In the prototype, darker colour squaretwists presented dim shades in the square and tabs, which have influenced how movement and shapes were perceived. For example, at a front view, perception of the textile morphology is reduced, namely the folded square depth (Figure 130).

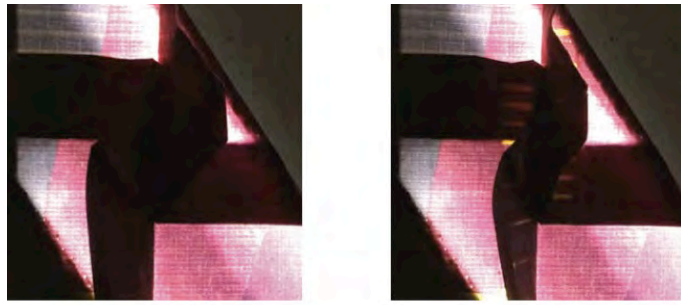


Figure 130. Shape change in a dark colour squarewrist.

In this prototype, shape change activation also changed the textile colour, given all screen printing pastes were elaborated with TC pigments. As a result, heat variation in the Nitinol alloys also introduced a linear colour change pattern particularly perceived during fold up at a side view (Figure 131 left image). In fold up and fold down activation cycles, the thickness of colour change stripes varied, being able to attain areas with full colour change, increasing luminosities and the perception of the textile folded morphology (Figure 131 right image).

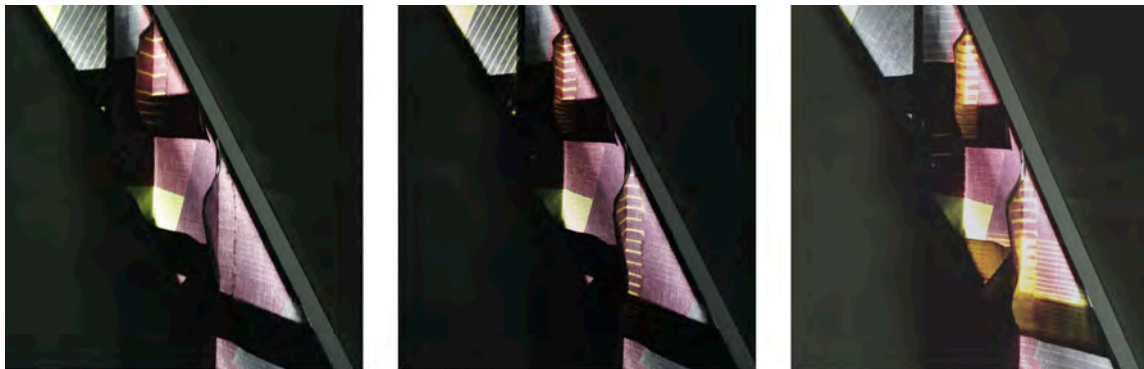


Figure 131. Colour change during shape change activation.

Textile morphology was influenced by squarewrist direction, particularly in larger shapes, after shape change being activated. In horizontal upside down positioning the squarewrist (4 and 6 cm square diagonal) and placement decisions also appeared to have greater relevance after shape change activation.



Figure 132. Shape change

7.5.2 Colour, shape and light responsive environments

For the prototype presentation, an interaction diagram was delineated and a framework that relates sound and visual expressions was studied and defined. The interaction diagram was similar to the previous prototype, as presented in Figure 119. In this case, the sensors intended to detect movement by the visitors at a strategic distance from the prototype, creating possibility to observe the overall dynamic performance from the activation triggering location.

Textile colour and shape change activation was inspired by British composer Fredrick Delius' Concerto in C minor. A study was conducted to draw a connection between sound and visual expressions based on intensity levels of change. Excerpts of the musical composition were selected considering three parameters: volume intensity, Low Frequency (LF) and High frequency (HF) response (bass and treble, respectively) and rhythm. These parameters delineated a framework for the textile activation sequence variables.

High intensity sound levels and faster rhythms defined higher number of simultaneous activations of chromic behaviour, attaining high luminosity changes. Low volume intensity and slower paces defined more subtle light transmittance variations either with shape change and/or colour change in few textile areas.

The relation between HF and LF levels established activation areas. HF levels guided activation definition in the uppermost part of the prototype and LF in the lower part. Level variation defined a direction of the circuits' sequential activation. For example, when the music excerpts had a predominant change from LF to HF, textile activation sequences encompassed a direction of changes from bottom to top areas.

These relations established a conceptual matrix exploring expression of textile behaviour and dynamic light. A visual interpretation of the music was not the goal. Furthermore, textile heating and cooling paces were very slow in comparison to the music rhythms.

In the responsive environment created, the beginning of the activation sequences was obviously perceived via sound. Visitors' movement and location in the space triggered the selection of a sequence, which initiated the playing of a music excerpt and the programmed activation. The definition of the interaction parameters has emphasized the link between sound and visual performances, as occurring and stopping at the same time.

Variables of the physical context had played a crucial role on the prototype qualities and how the changes were perceived. The interior space structure has influenced the textile positioning, defining its final configuration in relation to the angle of the vertical planes in M1 and M2, while the ceiling height set the

distance of M3 from the floor. In addition, the prototype scale was augmented through the reflex of coloured lights on the floor, which geometry depended on the viewpoint. Figure 133 displays the left, front and right perspectives, respectively.

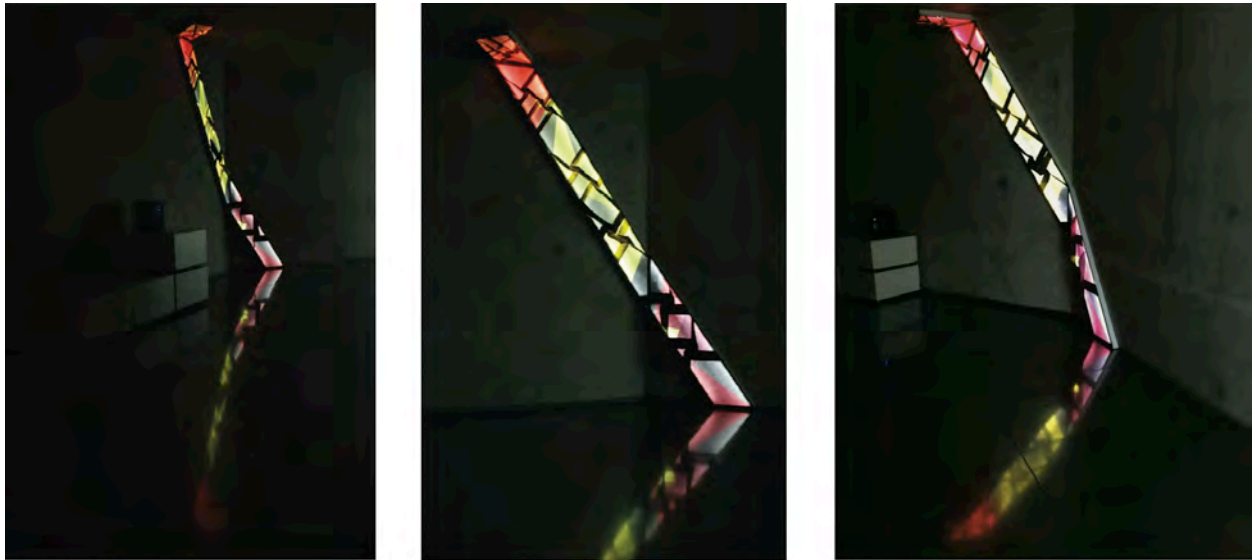


Figure 133. Prototype and light reflection at left, front and right perspectives, respectively.

This effect has captured attention and movement around the prototype. Depending on the viewpoint and distance, changes could also be perceived through the reflection, more comprehensively with M1 colour change, as observed in Figure 134 with the colour change pattern in the textile and reflected on the floor.



Figure 134. Light reflection of the colour change pattern.

Exploring colour change behaviour in association with gradual sound volume variation, differences in the heating circuits connections within consecutive or intercalated conductive threads enabled the creation of diverse expressions. Figure 135 depicts a sequence where colour change started in a squaretwist area with

the heating lines at a lower distance and after approximately 20'' of activation, heating lines in the adjacent areas start to occur simultaneously, with conductive threads at higher distances. The chromic behaviour created gradual colour and pattern transitions with higher colour change, attaining more intense luminosities in centre area and more disperse at the sides.

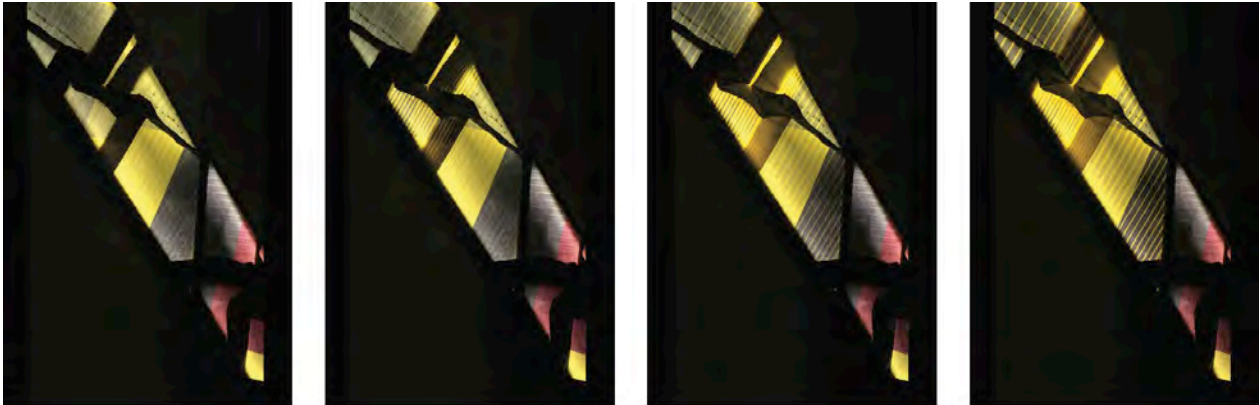


Figure 135. Gradual colour and pattern changes.

Figure 136 displays a combination of colour change expressions, created with a sequence of colour and shape change activations. In the upper area, two squaretwists and tabs changed in a fast pace to full colour change, showing obvious brighter areas. In the area below, colour change through heating elements connected with higher distance displayed a striped pattern in the tabs and in are with one layer, whereas in the square, a spotty colour change pattern is observed. These expressions transformed light within lower luminosities. In the M1 squaretwist, shape change activation combines movement with the linear chromic pattern. From the photo record viewpoint, both changes were obviously perceived and the change of light transmittance has created a brighter area in the tab backside, whereas the overall light transmittance was reduced. The expressions analysed have created a rhythm from higher to lower luminosity changes within a textile direction, occurring from the upper to the bottom areas depicted in the photo.



Figure 136. Dynamic colour and pattern expressions.

Dynamic possibilities explored with textile colour, shape and light have demonstrated the influence of a set of variables in the expressions and intensity levels of change. *Dialogues* prototype established an obvious role in shaping the interior environment and expressively changing ambient light, whereas its dynamic qualities were mostly perceived as subtle and calm.

The geometric light transmittance pattern was build up through different colours and the folded morphology with different pile-up layers. Furthermore, through colour change activation, a linear pattern with similar colour was also introduced, being influenced by the textile positioning. Through these parameters, intensity levels of change were studied.

The visual complexity of the surface appeared to have turned less obvious in how the chromic changes were perceived. Colour and pattern effects were distinguished, although the expressions of change were mostly subtle. The shape change transformation with the squar twists' tabs rotation about a square diagonal was more clearly identified at a side or perspective view. Observed from the front, light transmittance perception was reduced.

Activation sequences definition was explored through a framework that associated sound and visual expressions. The method used has established a guideline for design decisions on textile behaviour activation, namely the definition of simultaneous or sequential activations to explore different intensities of the rhythms and luminosity variations as well as location of changes within the prototype height and changes direction. By focusing on these specific parameters, expression possibilities of textile and light temporal forms were identified and demonstrated.

Physical context parameters were studied through the prototype presentation, namely architectonic structure and scale, as well as surface properties. Expressions of change highlighted have included design possibilities within colour change pattern, scale of changes emphasized by light reflection on the floor and differences in how changes are perceived according to the viewpoint.

Designing for subtle or obvious changes involve a complex relation between design variables. The research conducted through the prototypes demonstrated their importance in the design process of textile behaviour and dynamic light.

7.6 References

- BENITEZ, M. 2016. Sensorial space: responsive interiors through smart textiles. *In: SCHNEIDERMAN, D. & WINTON, A. (eds.) Textile technology and design: from interior space to outer space.* New York: Bloomsbury Academic.
- BRADLEY, S. 2012. *3 Types Of Rhythm You Can Create Visually* [Online]. <http://vansedesign.com/web-design/visual-rhythm/>. 2 october 2014].
- CLARKE, S. 2011. *Textile design*, London, Laurence King.
- CUTTLE, C. 2015. *Lighting design: a perception-based approach*, London and New York, Routledge.
- EICHHOFF, J., HEHL, A., JOCKENHOEVEL, S. & GRIES, T. 2013. Textile fabrication technologies for embedding electronic functions into fibres, yarns and fabrics. *In: KIRSTEIN, T. (ed.) Multidisciplinary know-how for smart textiles developers.* Oxford: Woodhead Publishing.
- HALL, C., PEDERSON, D. & BRYSON, G. 2002. *Northern Lights: The Science, Myth, and Wonder of Aurora Borealis*, Seattle, Sasquatch Books.
- JACKSON, P. 2011. *Folding techniques for designers: from sheet to form*, London, Laurence King Publishing.
- JANSEN, B. 2013. *Composing over time, temporal patterns - in textile design*. Doctoral Thesis, University of Borås.
- LE POIDEVIN, R. 2015. The Experience and Perception of Time. *The Stanford Encyclopedia of Philosophy* [Online].
- LOKE, L., REINHARDT, D. & MCNEILLY, J. Performer-machine scores for choreographing bodies, interaction and kinetic materials. Proceedings of the 2nd International Workshop on Movement and Computing 2015 Vancouver. ACM.
- MOSSÉ, A. 2016. Self-actuated textiles, interconnectivity, and the design of the home as a more sustainable timescape. *In: SCHNEIDERMAN, D. & WINTON, A. (eds.) Textile technology and design: from interior space to outer space.* New York: Bloomsbury Academic.
- NEFS, H. T. 2008. On the visual appearance of objects. *In: SCHIFFERSTEIN, H. & HEKKERT, P. (eds.) Product Experience.* San Diego, CA: Elsevier, 11-39.
- REDSTRÖM, J. 2010. On technology as material in design. *In: REDSTRÖM, M., REDSTRÖM, J. & MAZÉ, R. (eds.) IT+Textiles.* Borås: The Interactive Institute and the Swedish School of Textiles.
- RUTZKY, J. & PALMER, C. K. 2011. *Shadowfolds: surprisingly easy-to-make geometric designs in fabric*, New York, Kodansha International.
- STOPPA, M. & CHIOLERIO, A. 2014. Wearable Electronics and Smart Textiles: A Critical Review. *Sensors*, 14, 11957.
- VALLGÅRDA, A. 2014. Giving form to computational things: developing a practice of interaction design *Personal and Ubiquitous Computing*, 18(3), 577-592.
- WEISER, M. & BROWN, J. S. 1995. *Designing calm technology* [Online]. <http://www.ubiq.com/hypertext/weiser/calmtech/calmtech.htm>. [Accessed 16 february 2017].
- WORBIN, L. 2010. *Designing dynamic textile patterns*. Doctoral Thesis, University of Borås.
- YAHNIN, A. G., SERGEEV, V. A., GVOZDEVSKY, B. B. & VENNERTREM, S. 1997. Magnetospheric source region of discrete auroras inferred from their relationship with isotropy boundaries of energetic particles. *Annales Geophysicae*, 15, 943-958.

FINAL CONCLUSIONS AND FUTURE WORK

CHAPTER 8

CHAPTER 8. FINAL CONCLUSIONS AND FUTURE WORK

This research has studied and developed an integration processes of smart materials in textile substrates, studied light transmittance variation through textile colour and shape change, activated through resistive-heating of conductive materials and has explored and discussed dynamic qualities of thermo-responsive textile in interaction with light, based on selected variables and their influence on the expressions of change.

The conclusions of the developed and discussed research are as follows:

Systematic processes of paste recipe formulation with TC and conventional pigments were developed, demonstrating potential to be applied as an instrumental method for the development of screen printed textiles that change colour according to a predefined colour change ratio.

For textile chromic behaviour from different to similar with temperature increase, it was verified that colour and concentration of the conventional pigment are fixed parameters and they are variable for TC pigments. For textile that changes from similar to different colours, the process developed applied instrumental methods and the results have demonstrated the possibility to create colour change effects as predefined, from similar to different with temperature increase.

Optimization of paste recipe formulation with TC and conventional pigments applied systematic procedures of colour reproduction. The process outlined comprised of development of a database with the colourimetric properties of conventional and TC pigments colours, digital-based formulation of paste recipe considering a pattern colour, visual and instrumental assessing of the results and possible adjustments.

The research on shape memory textiles encompassed a novel approach of Nitinol wires being defined accordingly to a textile geometric morphology and integration of Nitinol segments with different shapes in the same woven textiles. The process developed has produced shape memory textiles with the ability to perform two shapes change behaviour similar to predefined origami morphologies.

The workflow setup proposed consists of defining the origami morphology and shape change transformation, selecting the Nitinol wire and defining geometries according to their integration in the woven substrate; drawing and production of the dies; optimizing the annealing parameters following the Nitinol heat treatment and finishing processes; and integration of Nitinol wires in the weaving process.

The process outlined demonstrated the ability to develop textile shape change with one or two different morphologies based on a bias mechanism, considering resistive heating activation method. The relation between shape change transfer of two Nitinol alloys' groups to the host structure at different times suggested that a compromise on the definition of one memorized morphology was required. Designing shape memory textiles involve a set of relationships between Nitinol and textile parameters, namely morphology, weight and positioning.

The study of conductive threads integration in textiles for electrical activation of colour change observed that resistive heating is not necessarily homogeneous along the conductive threads, influencing the pattern of colour change and demonstrating possibilities to design heterogeneous expressions. Textile thermal variation can also vary in respect to different contact areas between the CT and the textile substrate as a result of the application methods.

Conductive pigments electrical properties are affected by the printing parameters, whereas resistive heating studies with these materials demonstrated that the differences were not significant. In addition, textile folding can vary or damage the materials' electrical conductivity, being an important parameter when designing textiles with colour and shape behaviour.

The preliminary analysis of the chromic effect on light transmittance variation demonstrated the possibilities to change light intensity and tone, considering TC pigments colour, concentration and application processes in the substrate. With the shape change, textile morphology based on origami tessellation techniques to perform layer number variation have attained changes in light transmittance intensity, also displaying a pattern of different luminous on the textile surface.

The research on textile colour and shape behaviour and their interaction with light has demonstrated and discussed how a set of design variables can influence the dynamic qualities and expressions of change. Initial experimental studies focused on temperature as a dynamic design variable and have built up a base understanding on the relationship between activation, physical context and textile parameters in thermal variation, textile behaviour and dynamic light.

Introducing discussion on textile behaviour with different intensity levels of change, the research prototypes demonstrated design possibilities of diverse variables able to influence subtle or evident expressions of change. Variables highlighted through the dynamic examples discussed included: colour ratio, morphology and transformations type, viewpoint, scale of change, positioning, electrical current values, activation and

non-activation time, activation sequences, ambient temperature, architectonic structure, surface properties. These are tools to explore and design thermo-responsive textile behaviour.

Light transmittance variation created through textile colour and shape behaviour can be defined through qualities such as paces of change, rhythms and expressions of the temporal forms. Activation of diverse sequence configurations enable the creation of dynamic and interactive lighting environments, where dynamic qualities can be perceived as obvious or subtle, according to how textile behaviour and light are designed.

Bearing in mind a new generation of textile products with new functional and expressive possibilities, *Dynamic Light Filters* concept can be applied for interior or exterior applications of textile that in interaction with light enable to embed dynamic qualities in our environment.

Emergent possibilities of adaptive and reactive behaviour of colour and shape changing textiles reveal vast potential for the creation of lighting scenarios for functional and expressive purposes. In interior spaces deprived of natural light, design possibilities within subtle intensity levels of change can establish a sense of rhythm through embedded technology in the textiles. For building facades, dynamic qualities of smart textiles can be explored within luminous changes, energy issues and architectural visual aesthetics.

APPENDICES

APPENDIX A

Conductive threads' list:

Bekinox VN 12/1x275/100Z/316 L

Company: Bekaert

Characteristics: Stainless steel filament yarn.

235 Tex, 1 ply, 275 filaments/ply, 100 Z twists per meter.

Linear resistivity approx. $30 \Omega/\text{m} \pm 7\%$.

<http://www.bekaert.com/en/Product%20Catalog/Application/Basic%20materials/Textile.asp>

Bekinox VN 12/4x275/100S/316 L

Company: Bekaert

Characteristics: Stainless steel filament yarn.

1010 Tex, 4 ply, 275 filament/ply, 100 S twists per meter.

Linear resistivity approx. $6,9 \Omega/\text{m} \pm 10\%$

<http://www.bekaert.com/en/Product%20Catalog/Application/Basic%20materials/Textile.aspx>

Bekintex BK 50/2

Company: Bekaert

Characteristics: 20% Stainless steel and 80% PES spun yarn.

40 Tex, 2 ply (50 Nm/ply)

<http://www.bekaert.com/en/products/basic-materials/textile>

Bekintex BK 50/1

Company: Bekaert

Characteristics: Steel and PES spun yarn

20 Tex, 1 ply (50 Nm/ply)

<http://www.bekaert.com/en/products/basic-materials/textile>

Bekintex VN 14/2X90/175S/HT/PFA

Company: Bekaert

Characteristics: PFA (white) insulated stainless steel filament yarn.

2 ply, 90 filament/ply, 175 S twists per meter

<http://www.bekaert.com/en/Product%20Catalog/Application/Basic%20materials/Textile.aspx>

Bekiflex CA 63/8X7/80S/0.245/PFA

Company: Bekaert

Characteristics: PFA (transparent) insulated steel core filament yarn with a

copper outer layer.

<http://www.bekaert.com/en/Product%20Catalog/Application/Basic%20materials/Textile.aspx>

High Flex 3981 7X1 Silver

Company: Karl Grimm

Characteristics: Silver plated, copper and PA thread, 233 Tex, 7 ply.

Linear resistivity approx. $2,3 \Omega/\text{m}$.

<http://www.karl-grimm.com/navi.swf>

High Flex 3981 7x1 Kupfer Blank

Company: Karl Grimm

Characteristics: Copper and PA thread, 7ply.

<http://www.karl-grimm.com/navi.swf>

Constantan High-Flex 8394 7×1

Company: Karl Grimm
Characteristics: Copper, nickel and PA thread, 7ply.
<http://www.karl-grimm.com/navi.swf>

Elitex 235/f34 PA/Ag

Company: Imbut GmbH
Characteristics: Silver coated PA thre, 23,5 Tex / 34 filaments
Linear resistivity 20 Ω /m \pm 10 Ω /m
<http://www.imbut.de/en/special-threads/>

Elitex Garn Art I TPU 667_235/f34 PA/Ag

Company: Imbut GmbH
Characteristics: Insulated silver coated PA thread (235/f34 PA/Ag)
<http://www.imbut.de/en/special-threads/>

Elitex 110/f34/2ply PA/Ag

Company: Imbut GmbH
Characteristics: Silver coated PA thread, 22 Tex / 68 filaments
Linear resistivity 20 Ω /m \pm 10 Ω /m
<http://www.imbut.de/en/special-threads/>

Elitex Lycra

Company: Imbut GmbH
Characteristics: 94 Tex (Limited material description)

Shieldex 235/34x4 HC+E

Company: Statex
Characteristics: Silver plated 6.6 PA thread
Linear resistivity approx. 50 Ω /m \pm 20%
<http://www.statex.de/en/shieldex-yarns/>

Shieldex 110/34 2ply HC+B

Company: Statex
Characteristic: Silver plated 6.6 PA thread
Linear resistivity approx. 500 Ω /m \pm 20%
<http://www.statex.de/en/shieldex-twisted-yarn/>

Elinox SPP 35 300Z

Company: Soeries Elite
Characteristics: PES thread plied with stainless steel, 300 Z twists/m.
<http://www.soerieselite.com>

Elinox PES HT 1100 + VN 60 400 t S/Z

Company: Soeries Elite
Characteristics: PES thread double plied with stainless steel
PES 110 Tex; Stainless steel (2x 60 μ m) 400 S/Z twists/m.
<http://www.soerieselite.com>

LessEmf silver plated nylon

Company: LessEmf
Characteristics: PA silver plated thread, 35 tex, 180 μ m, 3ply.
Linear resistivity approx. 1 K Ω /m
<http://www.lessemf.com/fabric.html>

Lamé LifeSaver

Company: Lamé LifeSaver
Characteristics: (Unknown material description)
Linear resistivity approx. 66 Ω /m
<http://members.shaw.ca/ubik/thread/thread.html>

Linex

Company: Bart Francis
Characteristics: Linnen and stainless steel thread, 56 tex
https://www.bart-francis.be/index.php?item=linex&action=page&group_id=59&lang=EN

Stainless steel 2ply

Company: Sparkfun
Characteristics: Stainless steel
<https://www.sparkfun.com/products/10118>

Stainless steel 4ply

Company: Sparkfun
Characteristics: Stainless steel
<https://www.sparkfun.com/products/10516>

Copper monofilament 100 μ m

Company: (Unknown)
Characteristics: Copper monofilament 100 μ m.

Insulated Copper monofilament 160 μ m

Company: (Unknown)
Characteristics: Insulated copper monofilament 160 μ m.

Stainless steel monofilament 50 μ m

Company: (Unknown)
Characteristics: Stainless steel monofilament 50 μ m.

Nichrome monofilament 200 μ m

Company: Resel
Characteristics: Nickel and chrome alloy 200 μ m.
http://resel.pt/online/index.php?route=product/product&path=59_81&product_id=53

Nm10/3 conductive yarn

Company: Plug and Wear
Characteristics: 80% PES, 20% stainless steel, 43 tex, 3 ply.
http://www.plugandwear.com/default.asp?mod=product&cat_id=105&product_id=213

SilverSpun

Company: Feel Good yarn company
Characteristics: 87% Combed CO, 5% Silver, 5% PA, 3% Spandex
<http://feelgoodyarnco.com/yarns.html>

APPENDIX B

Colour coordinates of study samples presented in 4.5.2 section, comprising concentration ranges from 0,5 to 5% for conventional pigments (magenta, blue, black, yellow, red and orange) and from 5 to 10% for TC pigments (magenta, blue, black, red and orange).

Conventional pigment magenta	Samples' concentration	L*	a*	b*	C*	h
	Cm 0,5%	66,66	39,93	-18,61	44,05	335,01
	Cm 1%	61,03	43,44	-17,11	46,69	338,51
	Cm 2%	52,99	47,90	-13,92	49,88	343,79
	Cm 3%	52,36	44,52	-12,46	46,23	344,36
	Cm 4%	46,90	47,96	-10,15	49,02	348,05
	Cm 5%	42,04	53,11	-9,17	53,89	350,21

Conventional pigment blue	Samples' concentration	L*	a*	b*	C*	h
	Cb 0,5%	58,06	-10,06	-38,07	39,37	255,19
	Cb 1%	51,53	-8,05	-38,42	39,26	258,16
	Cb 2%	44,23	-6,05	-37,67	38,15	260,87
	Cb 3%	40,48	-4,46	-36,99	37,26	263,12
	Cb 4%	37,83	-3,29	-35,29	35,44	264,68
	Cb 5%	30,91	1,34	-37,10	37,13	272,07

Conventional pigment black	Samples' concentration	L*	a*	b*	C*	h
	Ck 0,5%	30,86	1,04	0,81	1,32	37,92
	Ck 1%	24,15	0,62	0,49	0,79	38,31
	Ck 2%	20,79	0,33	0,25	0,42	36,99
	Ck 3%	20,01	0,25	0,22	0,33	41,70
	Ck 4%	20,15	0,30	0,32	0,44	46,47
	Ck 5%	20,15	0,25	0,34	0,42	52,99

Conventional pigment yellow	Samples' concentration	L*	a*	b*	C*	h
	Cy 0,5%	83,15	12,25	80,82	81,74	81,38
	Cy 1%	81,25	17,13	90,69	92,29	79,31
	Cy 2%	79,16	22,50	95,22	97,84	76,71
	Cy 3%	77,51	25,93	95,06	98,54	74,74
	Cy 4%	76,48	27,74	94,18	98,18	73,59
	Cy 5%	75,77	28,91	92,51	96,92	72,64

Conventional pigment red	Samples' concentration	L*	a*	b*	C*	h
	Cr 0,5%	55,71	54,20	8,68	54,89	9,09
	Cr 1%	51,96	57,29	14,23	59,03	13,95
	Cr 2%	47,32	59,80	22,28	63,81	20,44
	Cr 3%	43,78	61,08	29,61	67,88	25,86
	Cr 4%	42,72	60,42	30,91	67,87	27,10
	Cr 5%	41,96	59,61	31,26	67,31	27,67

Conventional pigment orange	Samples' concentration	L*	a*	b*	C*	h
	Co 0,5%	65,76	47,99	54,20	72,40	48,48
	Co 1%	60,96	53,97	58,90	79,89	47,50
	Co 2%	56,19	56,93	57,53	80,94	45,30
	Co 3%	54,18	56,93	54,92	79,10	43,97
	Co 4%	52,43	56,51	52,20	76,93	42,73
	Co 5%	51,51	55,87	50,71	75,46	42,23

TC pigment magenta	Samples' concentration	L*	a*	b*	C*	h
	TCm 5%	60,67	40,57	-19,24	44,90	334,62
	TCm 6%	59,10	41,76	-19,23	45,97	335,27
	TCm 7%	57,83	42,63	-18,96	46,65	336,02
	TCm 8%	56,07	43,97	-19,27	48,01	336,02
	TCm 9%	54,11	45,22	-18,82	48,98	337,41
	TCm 10%	53,60	45,29	-18,50	48,92	337,78

TC pigment blue	Samples' concentration	L*	a*	b*	C*	h
	TCb 5%	66,00	-5,48	-26,47	27,03	258,30
	TCb 6%	64,98	-5,59	-26,69	27,27	258,17
	TCb 7%	63,22	-5,83	-27,17	27,79	257,88
	TCb 8%	61,45	-5,80	-27,86	28,45	258,24
	TCb 9%	60,38	-5,82	-27,94	28,54	258,23
	TCb 10%	59,38	-5,84	-28,39	28,99	258,38

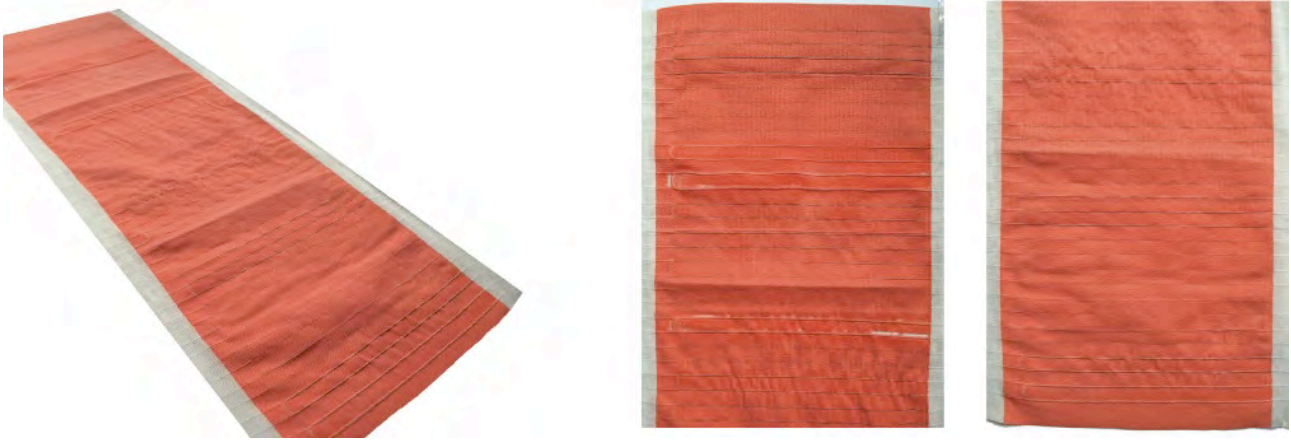
TC pigment black	Samples' concentration	L*	a*	b*	C*	h
	Tck 5%	48,58	-1,15	-0,49	1,25	203,05
	Tck 6%	43,23	-1,12	0,26	1,15	167,18
	Tck 7%	41,11	-1,07	0,45	1,16	159,97
	Tck 8%	38,73	-0,90	0,49	1,03	151,62
	Tck 9%	38,21	-0,86	0,30	0,91	160,78
	Tck 10%	36,66	-0,76	0,50	0,91	146,53

TC pigment red	Samples' concentration	L*	a*	b*	C*	h
	TCr 5%	70,27	39,24	13,06	41,36	18,41
	TCr 6%	69,12	41,79	14,38	44,19	18,98
	TCr 7%	68,08	43,58	15,42	46,23	19,49
	TCr 8%	67,13	45,04	16,45	47,95	20,07
	TCr 9%	66,13	46,15	17,30	49,29	20,55
	TCr 10%	64,88	47,36	18,37	50,80	21,20

TC pigment orange	Samples' concentration	L*	a*	b*	C*	h
	TCo 5%	67,86	49,54	30,73	58,30	31,81
	TCo 6%	66,48	51,97	34,23	62,23	33,37
	TCo 7%	65,14	54,14	38,01	66,15	35,07
	TCo 8%	64,55	54,97	39,21	67,52	35,50
	TCo 9%	64,51	54,82	41,89	67,11	35,22
	TCo 10%	63,20	56,60	42,08	70,53	36,63

APPENDIX C

Image of sample A (chapter6) and results of conductive threads' study presented in 6.3.2 section.



Sample A: from CT1 to CT 14 left image, from CT15 to CT28 right image.

Observations: In most conductive threads' experiments, three voltage stages were conducted with fifteen seconds each, to attain a maximum temperature below or approximately 45°C. Conductive threads that present less voltage stages were due: high temperatures detected through the Infrared camera or voltage limit of the power supplied used – 30 V.

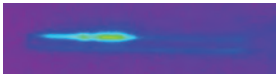

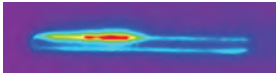



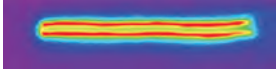



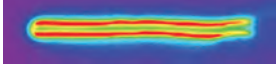





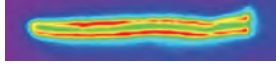



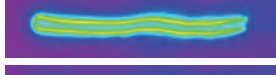

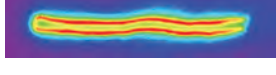



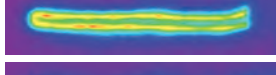

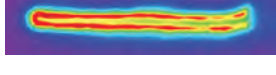





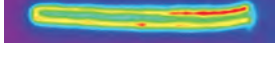

CT1	V (V)	I (A)	R (Ω)	Tmax.(° C)	IR image	Photo
	1,60	0,16	10,00	34,2		15"
	1,80	0,18	10,00	35,8		30"
	2,00	0,19	10,53	38,6		45"
CT2	V (V)	I (A)	R (Ω)	Tmax.(° C)	IR image	Photo
	0,80	0,28	2,86	36,9		15"
	1,00	0,31	3,23	40,5		30"
	1,20	0,38	3,16	41,7		45"
CT3	V (V)	I (A)	R (Ω)	Tmax.(° C)	IR image	Photo
	10,00	0,01	1000,00	29,7		15"
	15,00	0,01	1500,00	33,2		30"
	20,00	0,02	1000,00	42,4		45"

45 °C
40
35
30
25

CT4	V (V)	I (A)	R (Ω)	Tmax.(°C)	IR image	Photo
	15,00	0,01	1500,00	30,1		15"
	20,00	0,01	2000,00	34,4		30"
	25,00	0,02	1250,00	41,6		45"
CT5	V (V)	I (A)	R (Ω)	Tmax.(°C)	IR image	Photo
	1,00	0,09	11,11	28,8		15"
	2,00	0,17	11,76	33,6		30"
	3,00	0,25	12,00	42,0		45"
CT6	V (V)	I (A)	R (Ω)	Tmax.(°C)	IR image	Photo
	0,20	2,16	0,09	33,2		15"
CT7	V (V)	I (A)	R (Ω)	Tmax.(°C)	IR image	Photo
	0,30	0,56	0,54	32,2		15"
	0,40	0,73	0,55	35,1		30"
	0,50	0,87	0,57	40,1		45"
CT8	V (V)	I (A)	R (Ω)	Tmax.(°C)	IR image	Photo
	0,40	0,60	0,67	33,8		15"
	0,50	0,70	0,70	37,0		30"
	0,60	0,78	0,70	40,3		45"
CT9	V (V)	I (A)	R (Ω)	Tmax.(°C)	IR image	Photo
	2,00	0,11	18,18	32,7		15"
	2,50	0,13	19,23	35,6		30"
	3,00	0,16	18,75	39,5		45"

CT10	V (V)	I (A)	R (Ω)	Tmax.(° C)	IR image	Photo
	1,40	0,13	10,77	35,0		15"
	1,60	0,16	10,00	37,0		30"
	1,80	0,18	10,00	40,4		45"
CT11	V (V)	I (A)	R (Ω)	Tmax.(° C)	IR image	Photo
	1,00	0,63	1,59	38,5		15"
CT12	V (V)	I (A)	R (Ω)	Tmax.(° C)	IR image	Photo
	1,00	0,17	5,88	32,4		15"
	1,50	0,25	6,00	38,6		30"
	2,00	0,33	6,06	48,1		45"
CT13	V (V)	I (A)	R (Ω)	Tmax.(° C)	IR image	Photo
	1,50	0,06	25,00	32,4		15"
	2,00	0,08	25,00	38,0		30"
	2,50	0,11	22,73	43,3		45"
CT14	V (V)	I (A)	R (Ω)	Tmax.(° C)	IR image	Photo
	4,00	0,08	50,00	38,9		15"
	5,00	0,11	45,45	46,2		30"
CT15	V (V)	I (A)	R (Ω)	Tmax.(° C)	IR image	Photo
	4,00	0,02	200,00	37,4		15"
	5,00	0,03	166,67	42,0		30"
	6,00	0,04	150,00	49,2		45"

CT16	V (V)	I (A)	R (Ω)	Tmax.(° C)	IR image	Photo
	8,00	0,03	266,67	34,2		15"
	9,00	0,03	300,00	36,3		30"
	10,00	0,04	250,00	38,9		45"
CT17	V (V)	I (A)	R (Ω)	Tmax.(° C)	IR image	Photo
	4,00	0,08	50,00	35,3		15"
	5,00	0,10	50,00	40,4		30"
CT18	V (V)	I (A)	R (Ω)	Tmax.(° C)	IR image	Photo
	20,00	0,01	2000,00	37,1		15"
	25,00	0,01	2500,00	41,4		30"
	30,00	0,01	3000,00	45,7		45"
CT19	V (V)	I (A)	R (Ω)	Tmax.(° C)	IR image	Photo
	3,00	0,11	27,27	37,7		15"
	4,00	0,15	26,67	47,3		30"
CT20	V (V)	I (A)	R (Ω)	Tmax.(° C)	IR image	Photo
	6,00	0,04	150,00	33,5		15"
	7,00	0,05	140,00	36,1		30"
	8,00	0,06	133,33	39,5		45"
CT21	V (V)	I (A)	R (Ω)	Tmax.(° C)	IR image	Photo
	4,00	0,04	100,00	34,1		15"
	5,00	0,04	125,00	37,7		30"
	6,00	0,05	120,00	43,4		45"

CT22	V (V)	I (A)	R (Ω)	Tmax.($^{\circ}$ C)	IR image	Photo
	2,00	0,04	50,00	34,6		
	3,00	0,07	42,86	44,9		
CT23	V (V)	I (A)	R (Ω)	Tmax.($^{\circ}$ C)	IR image	Photo
	0,50	0,60	0,83	34,5		
	0,70	0,78	0,90	42,2		
CT24	V (V)	I (A)	R (Ω)	Tmax.($^{\circ}$ C)	IR image	Photo
	0,30	1,03	0,29	34,6		
	0,40	1,43	0,28	42,9		
CT25	V (V)	I (A)	R (Ω)	Tmax.($^{\circ}$ C)	IR image	Photo
	8,00	0,03	266,67	33,5		
	10,00	0,04	250,00	38,0		
	12,00	0,04	300,00	43,0		
CT26	V (V)	I (A)	R (Ω)	Tmax.($^{\circ}$ C)	IR image	Photo
	1,00	0,21	4,76	32,7		
	1,20	0,24	5,00	35,7		
	1,50	0,30	5,00	41,0		
CT27	V (V)	I (A)	R (Ω)	Tmax.($^{\circ}$ C)	IR image	Photo
	7,00	0,04	175,00	34,2		
	8,00	0,05	160,00	39,3		
	9,00	0,06	150,00	44,2		
CT28	V (V)	I (A)	R (Ω)	Tmax.($^{\circ}$ C)	IR image	Photo
	5,00	0,05	100,00	33,6		
	6,00	0,06	100,00	37,2		
	7,00	0,07	100,00	41,3		

APPENDIX D

Description of samples X and Y used in experimental work presented in 7.2.1 section

Sample X was used in the colour change tests A to D and sample Y in test E. They were woven in the loom Jacquard Vamatex with 41,2 tex CO warp and 14,7 tex PES weft, integrating the conductive thread Karl Grimm High Flex 3981 in the weft of a plain weave structure at 1 cm distance each (13 picks PES and 1 pick conductive thread per cm). Conductive threads insertion in the weaving was programmed through the loom software and did not display a continuous integration in between each pick.

With objective to connect the conductive threads into a series circuit, a complementary sample was developed for analysis of three connection alternatives: silver solder, crimp bead and double knot. The soldering process appeared to have weakened the conductive threads and during the textile handling and power supply, some connections broken near the solder point. Both crimp bead and double knot appeared stable, they did not overheat during power supply and electrical resistance of the threads connected by each process were similar. With crimp bead connection a slightly flatter shape was attained and it was relatively faster to do, being the connection alternative selected.

Previously to the conductive threads connection, samples X and Y were screen-printed with 10% TC red. Additionally, sample Y was folded with a squar twist pattern.